TRACING LEGACY MERCURY SOURCES IN AQUATIC ECOSYSTEMS USING MERCURY STABLE ISOTOPES

by

Patrick Michael Donovan

A dissertation submitted in partial fulfillment
of the requirements for the degree of
Doctor of Philosophy
(Earth and Environmental Sciences)
in the University of Michigan
2015

Doctoral Committee:

Professor Joel D. Blum, Chair
Professor Allen Burton
Associate Professor Gregory J. Dick
Professor Donald R. Zak

© Patrick Michael Donovan
2015

ACKNOWLEDGEMENTS

I would first like to thank my wife, Alison, for the constant support and inspiration over the past five years. I'd also like to thank my dog, Stella, as some of the most important intellectual progress in this dissertation was achieved with a leash in my hand.

I would like to acknowledge my advisor Dr. Joel Blum, who has always encouraged big ideas. My experience at the University of Michigan has been aided by support from the Department of Earth and Environmental Sciences. I thank the department staff for guiding me through the hurdles of graduate school and scientific research. I would also like to thank Rackham Graduate School for their generosity in funding research and travel that has allowed for a truly enriching experience.

I have learned many lessons from the outstanding scientists I have been able to collaborate with during my research. Specifically, I would like to thank Dr. Jason Demers, Dr. Martin T.K. Tsui, and Dr. Michael Singer. These individuals have taught me countless lessons in the field and pushed me to become a better scientist. I would also like to thank current and former members of BEIGL who have tirelessly provided laboratory and fieldwork support. Particularly, I'd like to acknowledge Marcus Johnson for his attention to detail and expert operation of the CV-MC-ICP-MS. I could not have survived without the support of fellow graduate students Sae Yun Kwon, Laura Sherman, Spencer Washburn, and Laura Motta. They have provided a sounding board for good and bad ideas and helped me embrace the highs and lows of graduate school.

Lastly, I'd like to thank my parents who have always provided love, encouragement, and keen editorial assistance throughout my entire educational career.

TABLE OF CONTENTS

LIST OF FIGURES

LIST OF TABLES

ABSTRACT

Mercury (Hg) is a neurotoxic pollutant that exists in both inorganic (Hg^0, Hg^{2+}) and organo-metallic (monomethyl mercury: MMHg) chemical forms. Inorganic Hg (IHg) has been released to aquatic environments during its historical use in mining and industry. In these environments IHg can be converted to MMHg, a potent developmental neurotoxin that bioaccumulates in the food web and can pose a risk to humans and wildlife. Therefore, identifying the distribution of legacy IHg sources, and understanding their transformation to MMHg is of great interest. In this dissertation, we report Hg stable isotope ratios in sediment and food webs from North American streams contaminated by legacy Hg sources. In Chapter 2 and 3, we use Hg isotopes in stream and estuarine sediment to fingerprint multiple Hg sources and trace their transport and deposition. In Chapters 4 and 5, we measure Hg isotopes in both sediment and aquatic food webs to identify MMHg formation, degradation and exposure pathways in streams and wetlands contaminated by historical gold and mercury mining. This work demonstrates that Hg stable isotope measurements can be used to trace the spatial and temporal distribution of legacy Hg sources and identify relevant biogeochemical processes and exposure pathways leading to MMHg bioaccumulation in aquatic environments.

CHAPTER 1: Introduction

1.1 Mercury as a Global Pollutant

Mercury (Hg) is a neurotoxic pollutant that exists in inorganic (Hg^0, Hg^{2+}) and organo-metallic (monomethyl mercury: MMHg) chemical forms. Humans and wildlife can be exposed to inorganic Hg (IHg) from consumer products (e.g.,, fluorescent lights, thermometers, dental amalgams) or occupational activities (e.g., mining or industry). The primary route of MMHg exposure is from fish consumption because MMHg biomagnifies in organisms and bioaccumulates in food webs. Human MMHg exposure in utero and during early childhood can lead to permanent developmental impairment while significant exposure in adults results in neurologic symptoms (e.g., sensory impairment, motor skills, coordination).[1] Wildlife such as mammals, birds and fish are exposed to high levels of MMHg through their diets resulting in behavioral, reproductive and physiological effects.[2] Therefore, identification of Hg sources and exposure pathways in aquatic environments is of great interest.

Mercury undergoes dynamic biogeochemical cycling in the environment after being emitted from natural and anthropogenic sources. In geologic materials, Hg is typically associated with sulfide minerals and natural Hg emissions result from volcanic and hydrothermal activity.[3] Human activities, such as mining and fossil fuel combustion, have mobilized geologic reservoirs of Hg and significantly increased the quantity of Hg actively

cycling in the environment.[4, 5] For example, humans have long mined cinnabar ore (HgS) to produce metallic Hg^0 for use in precious metal mining, industrial processes (e.g., chloralkali process), and consumer products. [3, 6] Although Hg use has decreased throughout North America in the past few decades, Hg released during historical mining and industrial use (i.e., "legacy Hg") persists in aquatic environments. In these environments Hg is subject to a variety of biotic and abiotic reactions (e.g., oxidation, photochemical reduction, degradation) including microbial methylation, which converts a fraction of IHg to the more neurotoxic and bioaccumulative MMHg.[7] This dissertation reports on measurements of natural Hg stable isotope ratios in sediments and biota from aquatic environments to advance our understanding of the transport and transformation of legacy Hg sources in the San Francisco Bay watershed (CA) and in streams near Oak Ridge, TN.

1.2 Mercury Stable Isotopes

In the past decade there have been significant analytical advances for the measurement of Hg stable isotope ratios in environmental matrices. This has allowed researchers to fingerprint diffuse and point sources of Hg and elucidate biogeochemical processes in the environment. Mercury has seven stable isotopes (^{204}Hg, ^{202}Hg, ^{201}Hg, ^{200}Hg, ^{199}Hg, ^{198}Hg, ^{196}Hg) and Hg isotope ratios are measured by multi collector inductively coupled plasma mass spectrometer (MC-ICP-MS), using a cold vapor generation system to introduce Hg as a gas to the inlet of the mass spectrometer. Specific analytical details are outlined in Chapters 2, 3, 4, and 5 and general information can be found elsewhere.[8] Mercury isotopic compositions are typically reported in units of permil (‰) using delta notation ($\delta^{xxx}Hg$) relative to NIST SRM 3133 (eq. 1). Mercury undergoes mass dependent

fractionation (MDF) following the kinetic mass fractionation law, however odd isotopes also exhibit mass independent fractionation (MIF), which is a deviation from the $\delta^{xxx}Hg$ value predicted by MDF alone. Throughout this dissertation, MDF is reported using the $^{202}Hg/^{198}Hg$ ratio ($\delta^{202}Hg$) whereas MIF is reported using capital delta notation ($\Delta^{xxx}Hg$) for ^{199}Hg and ^{201}Hg with $\beta = 0.252$ for $\Delta^{199}Hg$ and $\beta = 0.752$ for $\Delta^{201}Hg$ in eq. 2.[8]

$$\text{Equation [1]: } \delta^{xxx}Hg\ (‰) = \{[(^{xxx}Hg/^{198}Hg)_{sample}/(^{xxx}Hg/^{198}Hg)_{NIST3133}]\text{-}1\} * 1000$$

$$\text{Equation [2]: } \Delta^{xxx}Hg = \delta^{xxx}Hg - (\delta^{202}Hg * \beta)$$

MDF has been observed experimentally during biotic methylation,[9, 10] mer-mediated MMHg degradation,[11] Hg^{2+} reduction,[12-14] and sorption and binding reactions.[15, 16] Variation in Hg isotopic composition has been reported in a number of environmental Hg reservoirs including coal and HgS ores,[17-24] sediment,[25, 26] soil,[18, 27-29] precipitation,[19, 27, 30-32] vegetation[24, 27] and lichens.[33-35] Large magnitude MIF (>0.5‰) occurs for the odd mass isotopes (^{199}Hg and ^{201}Hg) due to the magnetic isotope effect, where differences in the magnetic spin result in differences in reaction rates between odd and even mass isotopes.[36-38] Lesser magnitude MIF can occur from the nuclear volume effect (i.e., due to differences in nuclear radii between odd and even mass isotopes)[39] during kinetic or equilibrium reactions and there is evidence for MIF of even mass Hg isotopes (of ^{200}Hg and ^{204}Hg), although the mechanism remains unknown.[40] Large magnitude MIF has been demonstrated experimentally during photochemical MMHg degradation and photoreduction of Hg^{2+}, [36, 37, 41] and MIF is generally not believed to occur during bioaccumulation or trophic transfer.[42, 43] Therefore, the isotopic composition of Hg in

sediment and aquatic organisms reflects Hg sources and biogeochemical processes prior to bioaccumulation.

1.3 Dissertation Narrative

In this dissertation, we report Hg stable isotope ratios in sediment and food webs from North American streams contaminated by legacy mining and industrial Hg sources. In Chapter 2, 3, 4 and 5 we use the Hg isotopic composition of sediment to fingerprint Hg sources and trace their transport and deposition. In Chapters 4 and 5, we also use Hg isotopes in stream and wetland biota (e.g., benthic macroinvertebrates and fish) to estimate the MMHg isotopic composition and better understand MMHg formation, degradation and exposure pathways. In Chapter 6, the key findings are summarized and we develop questions to direct future research on the fate of Hg in aquatic environments.

In Chapter 2, published in *Environmental Science & Technology*,[44] we investigated Hg in sediment upstream and downstream of the Y-12 National Security Complex (Y12). The use of metallic Hg at Y12 in the 1950's and 1960's, released hundreds of thousands kg of Hg to the surrounding environment.[45] We characterized the isotopic composition of high concentration sediment directly downstream of Y12 in East Fork Poplar Creek, and traced this Hg source to locations 40 km downstream. We also characterized low concentration sediment upstream of Y12. In large streams, the low THg sediment isotopic composition reflected Hg accumulated from geogenic and atmospheric sources across the watershed. In small streams located nearby, but unaffected by Y12, we identified an additional Hg source likely derived from local atmospheric deposition. This work established the use of Hg isotopes as a conservative tracer in stream sediment and laid the foundation for future

investigation of Hg isotopes in water, floodplain soils, benthic macroinvertebrates and fish in the region.

In Chapters 3, 4, and 5 we investigated legacy Hg sources and their fate in the San Francisco Bay (SF Bay) and its surrounding watersheds. Hg in the SF Bay watershed is uniquely tied to its upstream mining history. Since the mid-19th century, HgS ores were mined and processed in the CA Coast Range in watersheds that drain to the Sacramento Valley and eventually SF Bay. The metallic Hg produced was used for hydraulic gold mining in the Sierra Nevada, which mobilized large sediment volumes downstream towards SF Bay. Consequently, there are two distinct sediment sources of Hg entering SF Bay.

Chapter 3, published in *Chemical Geology*,[46] follows up on an earlier study of Hg sources to SF Bay intertidal sediment.[25] We measured Hg in subtidal sediment cores to identify the pre-mining sediment isotopic composition and investigate temporal changes in the delivery of Hg sources to SF Bay. Using Hg isotopic compositions, we quantified the relative contribution of various Hg sources to subtidal locations at different time periods: pre-mining, circa 1960 and present day. The spatial variation of Hg sources observed in c.1960 sediment was consistent with intertidal surface sediment, and we attributed this to the historical delivery of mining sources to SF Bay. This study further demonstrated the utility of Hg isotopes to trace sediment Hg sources and to assess spatial and temporal trends when multiple Hg sources are present.

In Chapter 4, which we plan to submit for publication,[47] we investigated the sources and processes leading to MMHg bioaccumulation in the lower Yuba River. The lower Yuba River is located downstream of former gold mining districts and contains a large anthropogenic sediment fan with elevated THg concentrations. We measured THg, MMHg

and Hg stable isotope ratios in sediment and biota to estimate the isotopic composition of IHg and MMHg. The MMHg isotopic composition was compared to a variety of Hg sources in the watershed. Based on these comparisons, we proposed two plausible explanations for the origin of MMHg. Either (1) the MMHg is derived from upstream and not sourced from the local contaminated sediment or (2) in situ Hg methylation results in negative MDF between IHg and MMHg. We argue that in situ methylation is the most plausible explanation for the origin of MMHg and speculate on possible mechanisms to explain the net negative MDF.

In Chapter 5, which we also plan to submit for publication,[48] we investigated Hg sources and biogeochemical transformations in Cache Creek and wetlands in Yolo Bypass. Cache Creek drains multiple Hg mining districts that contain HgS mine wastes (HgS ore, calcine, etc.). Yolo Bypass is an engineered flood bypass for the Sacramento River that receives inputs from the Yuba River (Chapter 4) and Cache Creek. We measured THg, MMHg and Hg isotope ratios in sediment and biota to estimate the isotopic composition of IHg and MMHg. Variation in the Hg isotopic composition of biota suggests the presence of multiple MMHg sources or exposure pathways. The isotopic composition of MMHg was compared with different Hg sources in each location. In Cache Creek we found net negative MDF between IHg and MMHg, which is consistent with observations in the Yuba River. In contrast, the Yolo Bypass wetlands had net positive MDF between IHg and MMHg similar to previous studies in lakes and coastal ocean environments. Consequently, we hypothesize that differences in net biotic MDF might result from ecosystem level differences in MMHg degradation processes between streams (Cache Creek,[48] Yuba River[47] and Eel River[49]) and wetland (Yolo Bypass)[48], lake[50, 51] or coastal ocean environments.[52-54]

References

1. Mergler, D.; Anderson, H. A.; Chan, L. H. M.; Mahaffey, K. R.; Murray, M.; Sakamoto, M.; Stern, A. H., Methylmercury Exposure and Health Effects in Humans: A Worldwide Concern. *AMBIO: A Journal of the Human Environment* **2007,** *36*, (1), 3-11.

2. Scheuhammer, A. M.; Meyer, M. W.; Sandheinrich, M. B.; Murray, M. W., Effects of Environmental Methylmercury on the Health of Wild Birds, Mammals, and Fish. *Ambio* **2007,** *36*, (1), 12-8.

3. Parsons, M. B.; Percival, J. B., *Mercury : sources, measurements, cycles and effects*. Mineralogical Association of Canada: Ottawa, 2005; Vol. 34.

4. Selin, N. E., Global Biogeochemical Cycling of Mercury: A Review. *Annu. Rev. Environ. Resour.* **2009,** *34*, (1), 43-63.

5. Turner, R. R.; Southworth, G. R., Mercury-Contaminated Industrial and Mining Sites in North America: an Overview with Selected Case Studies. In *Mercury Contaminated Sites*, Ebinghaus, R.; Turner, R.; Lacerda, L.; Vasiliev, O.; Salomons, W., Eds. Springer Berlin Heidelberg: 1999; pp 89-112.

6. UNEP *Global Mercury Assessment 2013: Sources, Emissions, Releases and Environmental Transport*; UNEP Chemicals Branch: Geneva, Switzerland, 2013; p 42.

7. Hsu-Kim, H.; Kucharzyk, K. H.; Zhang, T.; Deshusses, M. A., Mechanisms Regulating Mercury Bioavailability for Methylating Microorganisms in the Aquatic Environment: A Critical Review. *Environ. Sci. Technol.* **2013,** *47*, (6), 2441-2456.

8. Blum, J. D.; Bergquist, B. A., Reporting of variations in the natural isotopic composition of mercury. *Anal. Bioanal. Chem.* **2007,** *388*, (2), 353-359.

9. Perrot, V.; Bridou, R.; Pedrero, Z.; Guyoneaud, R.; Monperrus, M.; Amouroux, D., Identical Hg Isotope Mass Dependent Fractionation Signature during Methylation by Sulfate-Reducing Bacteria in Sulfate and Sulfate-Free Environment. *Environ. Sci. Technol.* **2015,** *49*, (3), 1365-1373.

10. Rodriguez-Gonzalez, P.; Epov, V. N.; Bridou, R.; Tessier, E.; Guyoneaud, R.; Monperrus, M.; Amouroux, D., Species-Specific Stable Isotope Fractionation of Mercury during Hg(II) Methylation by an Anaerobic Bacteria (Desulfobulbus propionicus) under Dark Conditions. *Environ. Sci. Technol.* **2009,** *43*, (24), 9183-9188.

11. Kritee, K.; Barkay, T.; Blum, J. D., Mass dependent stable isotope fractionation of mercury during mer mediated microbial degradation of monomethylmercury. *Geochim. Cosmochim. Acta* **2009,** *73*, (5), 1285-1296.

12. Kritee, K.; Blum, J. D.; Barkay, T., Mercury Stable Isotope Fractionation during Reduction of Hg(II) by Different Microbial Pathways. *Environ. Sci. Technol.* **2008,** *42*, (24), 9171-9177.

13. Kritee, K.; Blum, J. D.; Johnson, M. W.; Bergquist, B. A.; Barkay, T., Mercury stable isotope fractionation during reduction of Hg(II) to Hg(0) by mercury resistant microorganisms. *Environ. Sci. Technol.* **2007,** *41*, (6), 1889-1895.

14. Yang, L.; Sturgeon, R., Isotopic fractionation of mercury induced by reduction and ethylation. *Anal. Bioanal. Chem.* **2009,** *393*, (1), 377-385.

15. Jiskra, M.; Wiederhold, J. G.; Bourdon, B.; Kretzschmar, R., Solution Speciation Controls Mercury Isotope Fractionation of Hg(II) Sorption to Goethite. *Environ. Sci. Technol.* **2012,** *46*, (12), 6654-6662.

16. Wiederhold, J. G.; Cramer, C. J.; Daniel, K.; Infante, I.; Bourdon, B.; Kretzschmar, R., Equilibrium Mercury Isotope Fractionation between Dissolved Hg(II) Species and Thiol-Bound Hg. *Environ. Sci. Technol.* **2010,** *44*, (11), 4191-4197.

17. Lefticariu, L.; Blum, J.; Gleason, J., Mercury Isotopic Evidence for Multiple Mercury Sources in Coal from the Illinois Basin. *Environ. Sci. Technol.* **2011,** *45*, (4), 1724-1729.

18. Biswas, A.; Blum, J. D.; Bergquist, B. A.; Keeler, G. J.; Xie, Z. Q., Natural Mercury Isotope Variation in Coal Deposits and Organic Soils. *Environ. Sci. Technol.* **2008,** *42*, (22), 8303-8309.

19. Sherman, L. S.; Blum, J. D.; Keeler, G. J.; Demers, J. D.; Dvonch, J. T., Investigation of Local Mercury Deposition from a Coal-Fired Power Plant Using Mercury Isotopes. *Environ. Sci. Technol.* **2011,** *46*, (1), 382-390.

20. Yin, R.; Feng, X.; Chen, J., Mercury Stable Isotopic Compositions in Coals from Major Coal Producing Fields in China and Their Geochemical and Environmental Implications. *Environ. Sci. Technol.* **2014,** *48*, (10), 5565-5574.

21. Sun, R.; Heimburger, L.-E.; Sonke, J. E.; Liu, G.; Amouroux, D.; Berail, S., Mercury stable isotope fractionation in six utility boilers of two large coal-fired power plants. *Chem. Geol.* **2013,** *336*, (0), 103-111.

22. Smith, C. N.; Kesler, S. E.; Blum, J. D.; Rytuba, J. J., Isotope geochemistry of mercury in source rocks, mineral deposits and spring deposits of the California Coast Ranges, USA. *Earth Planet. Sci. Lett.* **2008,** *269*, (3-4), 398-406.

23. Stetson, S. J.; Gray, J. E.; Wanty, R. B.; Macalady, D. L., Isotopic Variability of Mercury in Ore, Mine-Waste Calcine, and Leachates of Mine-Waste Calcine from Areas Mined for Mercury. *Environ. Sci. Technol.* **2009,** *43*, (19), 7331-7336.

24. Wiederhold, J. G.; Smith, R. S.; Siebner, H.; Jew, A. D.; Brown, G. E.; Bourdon, B.; Kretzschmar, R., Mercury Isotope Signatures as Tracers for Hg Cycling at the New Idria Hg Mine. *Environ. Sci. Technol.* **2013,** *47*, (12), 6137-6145.

25. Gehrke, G. E.; Blum, J. D.; Marvin-DiPasquale, M., Sources of mercury to San Francisco Bay surface sediment as revealed by mercury stable isotopes. *Geochim. Cosmochim. Acta* **2011,** *75*, (3), 691-705.

26. Foucher, D.; Ogrinc, N.; Hintelmann, H., Tracing Mercury Contamination from the Idrija Mining Region (Slovenia) to the Gulf of Trieste Using Hg Isotope Ratio Measurements. *Environ. Sci. Technol.* **2009,** *43*, (1), 33-39.

27. Demers, J. D.; Blum, J. D.; Zak, D. R., Mercury isotopes in a forested ecosystem: Implications for air-surface exchange dynamics and the global mercury cycle. *Global Biogeochem. Cycles* **2013,** *27*, (1), 222-238.

28. Zhang, H.; Yin, R.-s.; Feng, X.-b.; Sommar, J.; Anderson, C. W.; Sapkota, A.; Fu, X.-w.; Larssen, T. r., Atmospheric mercury inputs in montane soils increase with elevation: evidence from mercury isotope signatures. *Scientific reports* **2013,** *3*.

29. Estrade, N.; Carignan, J.; Donard, O. F. X., Tracing and Quantifying Anthropogenic Mercury Sources in Soils of Northern France Using Isotopic Signatures. *Environ. Sci. Technol.* **2011,** *45*, (4), 1235-1242.

30. Sherman, L. S.; Blum, J. D.; Dvonch, J. T.; Gratz, L. E.; Landis, M. S., The use of Pb, Sr, and Hg isotopes in Great Lakes precipitation as a tool for pollution source attribution. *Sci. Total Environ.* **2015,** *502*, 362-374.

31. Gratz, L. E.; Keeler, G. J.; Blum, J. D.; Sherman, L. S., Isotopic Composition and Fractionation of Mercury in Great Lakes Precipitation and Ambient Air. *Environ. Sci. Technol.* **2010,** *44*, (20), 7764-7770.

32. Chen, J.; Hintelmann, H.; Feng, X.; Dimock, B., Unusual fractionation of both odd and even mercury isotopes in precipitation from Peterborough, ON, Canada. *Geochim. Cosmochim. Acta* **2012,** *90*, (0), 33-46.

33. Blum, J. D.; Johnson, M. W.; Gleason, J. D.; Demers, J. D.; Landis, M. S.; Krupa, S., Chapter 16 - Mercury Concentration and Isotopic Composition of Epiphytic Tree Lichens in the Athabasca Oil Sands Region. In *Developments in Environmental Science*, Kevin, E. P., Ed. Elsevier: 2012; Vol. Volume 11, pp 373-390.

34. Estrade, N.; Carignan, J.; Donard, O. F. X., Isotope Tracing of Atmospheric Mercury Sources in an Urban Area of Northeastern France. *Environ. Sci. Technol.* **2010,** *44*, (16), 6062-6067.

35. Carignan, J.; Estrade, N.; Sonke, J. E.; Donard, O. F. X., Odd Isotope Deficits in Atmospheric Hg Measured in Lichens. *Environ. Sci. Technol.* **2009,** *43*, (15), 5660-5664.

36. Bergquist, B. A.; Blum, J. D., Mass-dependent and -independent fractionation of Hg isotopes by photoreduction in aquatic systems. *Science* **2007,** *318*, (5849), 417-420.

37. Zheng, W.; Hintelmann, H., Mercury isotope fractionation during photoreduction in natural water is controlled by its Hg/DOC ratio. *Geochim. Cosmochim. Acta* **2009,** *73*, (22), 6704-6715.

38. Buchachenko, A. L., Magnetic Isotope Effect: Nuclear Spin Control of Chemical Reactions. *The Journal of Physical Chemistry A* **2001,** *105*, (44), 9995-10011.

39. Estrade, N.; Carignan, J.; Sonke, J. E.; Donard, O. F. X., Mercury isotope fractionation during liquid-vapor evaporation experiments. *Geochim. Cosmochim. Acta* **2009,** *73*, (10), 2693-2711.

40. Blum, J. D.; Sherman, L. S.; Johnson, M. W., Mercury Isotopes in Earth and Environmental Sciences. *Annu. Rev. Earth Planet. Sci.* **2014,** *42*, (1), 249-269.

41. Zheng, W.; Hintelmann, H., Isotope Fractionation of Mercury during Its Photochemical Reduction by Low-Molecular-Weight Organic Compounds. *J. Phys. Chem. A* **2010,** *114*, (12), 4246-4253.

42. Kwon, S. Y.; Blum, J. D.; Chirby, M. A.; Chesney, E. J., Application of mercury isotopes for tracing trophic transfer and internal distribution of mercury in marine fish feeding experiments. *Environ. Toxicol. Chem.* **2013,** *32*, (10), 2322-2330.

43. Kwon, S. Y.; Blum, J. D.; Carvan, M. J.; Basu, N.; Head, J. A.; Madenjian, C. P.; David, S. R., Absence of Fractionation of Mercury Isotopes during Trophic Transfer of Methylmercury to Freshwater Fish in Captivity. *Environ. Sci. Technol.* **2012,** *46*, (14), 7527-7534.

44. Donovan, P. M.; Blum, J. D.; Demers, J. D.; Gu, B.; Brooks, S. C.; Peryam, J., Identification of Multiple Mercury Sources to Stream Sediments near Oak Ridge, TN, USA. *Environ. Sci. Technol.* **2014,** *48*, (7), 3666-3674.

45. Brooks, S. C.; Southworth, G. R., History of mercury use and environmental contamination at the Oak Ridge Y-12 Plant. *Environ. Pollut.* **2011,** *159*, (1), 219-228.

46. Donovan, P. M.; Blum, J. D.; Yee, D.; Gehrke, G. E.; Singer, M. B., An isotopic record of mercury in San Francisco Bay sediment. *Chem. Geol.* **2013,** *349-350*, (0), 87-98.

47. Donovan, P. M.; Blum, J. D.; Singer, M. B.; Marvin-Di Pasquale, M.; Tsui, M., Isotopic composition of inorganic mercury and methylmercury downstream of historical gold mining. **In Prep**.

48. Donovan, P. M.; Blum, J. D.; Singer, M. B.; Marvin-Di Pasquale, M.; Tsui, M. T. K., Comparison of mercury degradation and exposure pathways in streams and wetlands impacted by historical mining. **In Prep**.

49. Tsui, M. T. K.; Blum, J. D.; Kwon, S. Y.; Finlay, J. C.; Balogh, S. J.; Nollet, Y. H., Sources and Transfers of Methylmercury in Adjacent River and Forest Food Webs. *Environ. Sci. Technol.* **2012,** *46*, (20), 10957-10964.

50. Sherman, L. S.; Blum, J. D., Mercury stable isotopes in sediments and largemouth bass from Florida lakes, USA. *Sci. Total Environ.* **2013,** *448*, (0), 163-175.

51. Kwon, S. Y.; Blum, J. D.; Nadelhoffer, K. J.; Timothy Dvonch, J.; Tsui, M. T.-K., Isotopic study of mercury sources and transfer between a freshwater lake and adjacent forest food web. *Sci. Total Environ.* **2015,** *532*, (0), 220-229.

52. Kwon, S. Y.; Blum, J. D.; Chen, C. Y.; Meattey, D. E.; Mason, R. P., Mercury Isotope Study of Sources and Exposure Pathways of Methylmercury in Estuarine Food Webs in the Northeastern US. *Environ. Sci. Technol.* **2014,** *48*, (17), 10089-10097.

53. Gehrke, G. E.; Blum, J. D.; Slotton, D. G.; Greenfield, B. K., Mercury Isotopes Link Mercury in San Francisco Bay Forage Fish to Surface Sediments. *Environ. Sci. Technol.* **2011,** *45*, (4), 1264-1270.

54. Balogh, S. J.; Tsui, M. T. K.; Blum, J. D.; Matsuyama, A.; Woerndle, G. E.; Yano, S.; Tada, A., Tracking the Fate of Mercury in the Fish and Bottom Sediments of Minamata Bay, Japan, Using Stable Mercury Isotopes. *Environ. Sci. Technol.* **2015**.

CHAPTER 2: Identification of multiple mercury sources to stream sediments near Oak Ridge, TN, USA

Authors: Patrick M. Donovan, Joel D. Blum, Jason D. Demers, Baohua Gu, Scott C. Brooks, John Peryam

Citation: Donovan, P. M.; Blum, J. D.; Demers, J. D.; Gu, B.; Brooks, S. C.; Peryam, J., Identification of Multiple Mercury Sources to Stream Sediments near Oak Ridge, TN, USA. Environ. Sci. Technol. **2014,** 48, (7), 3666-3674.

Abstract: Sediments were analyzed for total Hg concentration (THg) and isotopic composition from streams and rivers in the vicinity of the Y-12 National Security Complex (Y12) in Oak Ridge, TN (USA). In the stream directly draining Y12, where industrial releases of mercury (Hg) have been documented, high THg (3.26 to 60.1 μg/g) sediments had a distinct Hg isotopic composition (δ^{202}Hg of 0.02 ± 0.15‰ and Δ^{199}Hg of -0.07 ± 0.03‰; mean ± 1SD, n=12) compared to sediments from relatively uncontaminated streams in the region (δ^{202}Hg = -1.40 ± 0.06‰ and Δ^{199}Hg of –0.26 ± 0.03‰; mean ± 1SD, n=6). Additionally, several streams that are nearby but do not drain Y12 had sediments with intermediate THg (0.06 to 0.21 μg/g) and anomalous δ^{202}Hg (as low as -5.07‰). We suggest that the low δ^{202}Hg values in these sediments provide evidence for the contribution of an additional Hg source to sediments, possibly derived from atmospheric deposition. In

sediments directly downstream of Y12 this third Hg source is not discernible and the Hg isotopic composition can be largely explained by the mixing of low THg sediments with high THg sediments contaminated by Y12 discharges.

2.1 Introduction

Mercury (Hg) is a toxic pollutant that is widely distributed in most aquatic and terrestrial ecosystems. Anthropogenic activities such as coal fired power generation, waste incineration, mining and industrial processes have increased the amount of Hg actively cycling in the environment.[1] The region surrounding Oak Ridge, TN (USA) contains both current and historic anthropogenic Hg sources including coal fired power generation and industrial discharges to the atmosphere and waterways. In the mid-20th century, liquid elemental Hg (Hg^0) was utilized for an amalgam exchange process to isolate Lithium-6 for thermonuclear weapons at the Y-12 National Security Complex (Y12) near Oak Ridge, TN.[2, 3] The Y12 facility was built at the headwaters of the East Fork of Poplar Creek (EFPC) and discharged process water and storm sewer effluent directly into the stream. As a result, the watershed was contaminated by a variety of pollutants used at Y12, including Hg.[3] During operations at Y12, liquid Hg was spilled onsite (166,000 to 242,000 kg of Hg lost) and remains in Y12 soils and building foundations.[2, 4] At that time, large quantities of Hg (128,000 ± 35,000 kg of Hg) were discharged to EFPC in Y12 effluents, mainly as dissolved or particulate Hg^{2+} species,[2] which were eventually deposited in riparian sediments and soils[5, 6]. Active use of Hg at Y12 ceased in the mid-1960's and since then, remedial actions have lowered dissolved Hg concentrations in upper EFPC surface waters[7] and have removed contaminated soils (THg of >400 μg/g) at two EFPC floodplain sites outside of the

Y12 boundary. However, a significant quantity of Hg persists in soils and sediments and the majority of Hg exported from EFPC (>80%) is believed to result from streambank erosion and streambed sediment resuspension.[5, 8]

In addition to industrial Hg discharges, the study region also contains multiple significant (>1 kg/yr) atmospheric Hg emission sources (Figure 2.1).[9, 10] The Oak Ridge, TN area typically has prevailing winds out of the southwest or the northeast following the valley and ridge topography[11] and atmospheric Hg concentrations are elevated above background levels[10, 12, 13]. In the past, Y12 released large quantities of vapor phase Hg (33,000 ± 13,000 kg) to the atmosphere from process gas venting and during the recovery of Hg from contaminated soils.[2] Recently, estimated total Hg emissions from the Tennessee Valley Authority (TVA) Kingston Fossil Plant and Bull Run Fossil Plant, both located less than 20 km from Y12, were 274 kg/yr and 25 kg/yr, respectively.[9] In 2008 waste incineration and coal fired steam generation at Department of Energy facilities (Y12 and K25, a former uranium enrichment facility; Figure 2.1) were estimated to emit a combined ~4.5 kg Hg/yr,[9] although since then coal has been replaced by natural gas and biomass fuel for steam generation. Additionally, Hg contaminated EFPC floodplains have been estimated to re-emit between 1 and 10 kg Hg/yr to the atmosphere.[12] Thus, the Oak Ridge, TN region has multiple sources of atmospheric Hg emissions both past and present.

Mercury has seven stable isotopes and can undergo both mass dependent and mass independent isotope fractionation (MDF and MIF) during its cycling in the environment. MDF has been shown to occur during biotic and abiotic processes (e.g.,[14-16]) while MIF takes place primarily during photochemical reactions such as Hg^{2+} photoreduction and monomethyl mercury (MMHg) photodegradation (e.g., [17, 18]). The measurement of Hg

isotopes in environmental reservoirs (i.e., soils, sediments, and the atmosphere) has proven useful for the identification of anthropogenic Hg sources and can help trace Hg pathways through the environment[19-29] and into biota[30-33]. However, the utility of Hg isotopes as source tracers in regions with multiple atmospheric and aquatic Hg sources has not been extensively tested. Although studies have assessed the spatial distribution of Hg in EFPC soils and sediments[5, 34-36] and estimated the speciation and mobility of sediment-bound Hg[6, 37-40], the Hg isotope composition of sediments in EFPC and its tributaries have not been extensively studied. In this study we measured the Hg isotopic composition of streambed sediments in the vicinity of Oak Ridge, TN to identify relevant Hg sources in the region and help elucidate their fate in nearby biota and downstream environments. Specifically, we (1) determined the Hg isotope composition of Y12 contaminated streambed sediments and (2) isotopically characterized sediments in the region that are not directly impacted by Y12 discharges. Lastly, we (3) employed Hg isotopes to quantify the contribution of Y12 derived Hg to sediments downstream in the Clinch River.

2.2. Materials and Methods

2.2.1. Regional Setting

The study was carried out in a network of streams and rivers in the vicinity of Oak Ridge, TN (Figure 2.1). EFPC originates as a storm drain inside the Y12 facility that outflows into a channelized ditch at a location known as "Outfall 200", approximately 26 km upstream of its confluence with Poplar Creek.[2] After EFPC exits the Y12 boundary, 23 km upstream of Poplar Creek (EFK23.4; also termed Station 17), it flows for 6 km nearby the town of Oak Ridge through a mixture of channelized and non-channelized flow

pathways.[3] Beyond Oak Ridge, EFPC follows a relatively natural sinuous channel for the next 18 km through residential areas and woodlands. Three small tributaries (drainage area of 5.6 to 6.6 km^2) enter EFPC during this stretch at 20, 16 and 10 km upstream of Poplar Creek. EFPC enters the main stem of Poplar Creek 8 km upstream of the Clinch River. Poplar Creek has no headwater Hg point sources,[34] however its western tributaries drain portions of the Appalachian Plateau where historic coal mining has taken place.[41] The stretch of Poplar Creek downstream of EFPC, known as the Poplar Creek Embayment of the Watts Bar Reservoir, is the first reach influenced by Y12 discharges that exhibits widespread sediment deposition and accumulation.[42] The Poplar Creek Embayment flows into the Clinch River ~31 km downstream of the Y12 facility and the Clinch River flows for another 19 km, becoming increasingly lacustrine and depositional, to the Tennessee River.[42] The reference stream for this study, Hinds Creek, enters the Clinch River ~116 km upstream of the Tennessee River and has no headwater Hg point sources. This sampling location is ~25 km northeast of the Y12 facility (Figure 2.1). Streams sampled in this study have a range of watershed sizes. The EFPC watershed area is 76.9 km^2 at its confluence with Poplar Creek whereas the Poplar Creek watershed drains 352 km^2 at its confluence with the Clinch River. The Clinch River watershed is much larger, draining an area of 6,669 km^2.

2.2.2 Sediment Collection, Processing and Analysis

We collected streambed sediments from EFPC, EFPC tributaries, Poplar Creek, Hinds Creek and the Clinch River. All sampling locations were assigned an identification code based on the stream sampled (East Fork (EF), Poplar Creek (PC), Clinch River (CR), Hinds

Creek (HC)) and the distance in river km (i.e., distance following the river channel) from the confluence with the next largest stream (Figure 2.S1). EFPC tributary sampling sites were identified similarly (distance in km upstream of Poplar Creek) and were termed Trib20, Trib16 and Trib10. Sampling locations in these tributaries were 2.9, 4.0, and 6.9 km from the Y12 facility, respectively. Sediments in Poplar Creek and the Clinch River were sampled using either a stainless steel petite ponar grab sampler or a polycarbonate core between June 2011 and April 2012. With each sampling method, the top 10-15 cm of bed sediment was collected from depositional locations within the stream channel. Sediments from EFPC, EFPC tributaries, and Hinds Creek were collected between October 2011 and April 2012. At these locations, 3-5 grab samples of surface sediment (0-6 cm) from the mid-channel were composited and then sieved through acid-cleaned mesh to obtain two size fractions. The first size fraction included all sediment less than 2 mm (<2 mm; hereafter referred to as bulk sediment). The second size fraction included only sediments that passed through a 125 μm mesh (<125 μm; hereafter referred to as fine sediment or fines). All sediments were immediately placed on ice in the field, transferred back to the laboratory and frozen at -18°C for storage.

Prior to analysis, sieved sediments were dewatered by centrifugation, freeze-dried, and homogenized. Sediment samples were combusted in an offline two-stage furnace to isolate Hg for isotope analysis.[32, 43] Between 30 and 2500 mg of sediment was placed in the first stage of the furnace and slowly heated to 750°C over 6 hours while the second stage of the furnace was held at 1000°C. The Hg released from the sediment matrix was carried in Hg-free O_2 through the second furnace and into a 1%$KMnO_4$/1.8 M H_2SO_4 oxidizing solution (1%$KMnO_4$ trap). The recovery of Hg during offline combustion averaged 105 ± 16%

(mean ± 1SD, n=17; minimum = 86%) for a subset of the samples, based on independent concentration analysis by online combustion (Nippon MA-2000). Prior to isotopic analysis, Hg in the original 1%$KMnO_4$ trap was transferred into a secondary 1%$KMnO_4$/1.8M H_2SO_4 oxidizing solution (secondary 1%$KMnO_4$ trap) to avoid any potential matrix effects from combustion residues.[33] The recovery of Hg during this process averaged 97 ± 5% (mean ± 1SD, n= 41; minimum = 88%). The Hg isotope composition of the secondary trap solution was then measured using cold-vapor multi-collector inductively-coupled-plasma mass-spectrometry (CV-MC-ICP-MS; Nu Plasma). The secondary trap solution was pre-reduced by adding 2% (w/w) of 30% hydroxylamine hydrochloride (NH_2OH•HCl) and diluted to THg between 3.6 and 5.0 ng/g. The Hg^{2+} in solution was reduced online to Hg^0 by addition of $SnCl_2$ and then separated from solution using a frosted tip gas-liquid phase separator and transported in Hg-free Ar gas to the MC-ICP-MS. Instrumental mass bias was corrected by the introduction of an internal Tl standard (NIST 997) as a dry aerosol to the Ar gas stream and by sample-standard bracketing using NIST 3133.[44] Here we report mercury isotope compositions in delta notation, relative to the National Institute of Standards and Technology (NIST) Standard Reference Material (SRM) 3133 using Equation [1] with MDF based on the $^{202}Hg/^{198}Hg$ ratio ($\delta^{202}Hg$).[44] MIF is the deviation from the theoretically predicted $\delta^{xxx}Hg$ and is reported with capital delta notation ($\Delta^{xxx}Hg$) using Equation [2]. In the text we use $\Delta^{199}Hg$ to denote MIF and calculate $\Delta^{199}Hg$ using $\beta = 0.2520$ in Eq. [2].[44] All β values and $\Delta^{xxx}Hg$ and $\delta^{xxx}Hg$ values for samples and standards are presented in the supporting information.

Equation [1]: $\delta^{xxx}Hg\ (‰) = [[(^{xxx}Hg/^{198}Hg)_{sample}/(^{xxx}Hg/^{198}Hg)_{NIST3133}]-1] * 1000$

Equation [2]: $\Delta^{xxx}Hg = \delta^{xxx}Hg - (\delta^{202}Hg * \beta)$

Procedural blanks and sediment SRMs (NRC MESS-3 and NIST 1944) were combusted and processed with samples in an identical manner. Procedural blanks yielded between 0.08 and 0.21 ng of Hg (n=6), which was less than 0.3% of the Hg in the final trap solutions. The THg of sediment SRMs measured by offline combustion agreed within 10% of certified values. The yield for the secondary purge and trap procedure for sediment SRMs averaged 95 ± 4% (1SD; n=9; min = 88%) and their Hg isotope composition was consistent with previously reported measurements of the same materials (Table 2.S2).[23, 27, 33, 45] We estimated the long-term analytical uncertainty of Hg isotope measurements using the standard deviation (2SD) of the analytical session mean Hg isotopic composition of UM-Almaden. We estimated external reproducibility from the standard error (2SE) of Hg isotope measurements on replicate processing of SRMs. The 2SD of UM-Almaden was always less than the 2SE of replicate SRMs, therefore we use the 2SE of SRMs to represent the uncertainty associated with Hg isotope measurements in this study: ±0.11‰ for δ^{202}Hg and ±0.06‰ for Δ^{199}Hg.

2.3 Results and Discussion

2.3.1 Mercury Concentrations in Sediments near Oak Ridge, TN

Total Hg concentrations (THg) in the sampled sediments varied over more than three orders of magnitude between relatively uncontaminated streams and streams directly affected by Y12 discharges (Figure 2.2). Sediments in EFPC, directly downstream of Y12, had THg between 3.26 and 60.1 μg/g (mean = 24.4 μg/g) whereas nearby streams that do not receive Y12 effluents had variable but relatively low THg (0.011 to 0.212 μg/g; mean = 0.07 μg/g). Although unaffected by Y12 effluents, intermediate THg was measured in fine

sediments from EFPC tributaries (THg between 0.077 and 0.212 μg/g) and sediments from Poplar Creek (THg of 0.062 and 0.118 μg/g). In contrast, sediments from the Clinch River not influenced by Y12 had a maximum THg of 0.051 μg/g and mean of 0.028 μg/g (±0.016 μg/g, 1SD; n=4) and bulk and fine Hinds Creek sediments had THg of 0.011 and 0.031 μg/g, respectively. Consistently low THg sediments in Hinds Creek and the Clinch River are comparable to uncontaminated terrestrial soils and non-point source impacted stream sediments from across the United States (median THg of 0.030 μg/g; n=259).[13, 46]

Sediments downstream of EFPC, and therefore impacted by Y12 effluents, had elevated THg compared to sediments in the same streams that were not affected by Y12 (Figure 2.2). Poplar Creek embayment sediments had THg between 2.16 and 3.87 μg/g and relatively high concentrations persisted downstream into the Clinch River where THg was between 0.242 and 0.763 μg/g. Measured THg was similar to previous studies of the Y12 influence on downstream sediments[26, 34, 47, 48] and is consistent with the export of sediment-bound Hg from EFPC[5]. However, multiple Hg sources exist in the region and their influence on the sampled sediments, both upstream and downstream of Y12 influence, cannot be quantified by THg alone.

2.3.2 Mercury Isotopic Variation in Sediments near Oak Ridge, TN

Sediments from the Oak Ridge region have a large range of δ^{202}Hg (-5.07 to +0.26‰) and a small but significant range of Δ^{199}Hg (-0.28 to -0.01‰). This isotopic variation could result entirely from the mixing of multiple Hg sources, but only if in-situ environmental processes did not significantly alter sediment Hg isotope ratios. Hg isotopes in sediment can be fractionated only if a significant mass of Hg with a contrasting isotopic

composition, is preferentially lost from (or added to) the sediments. Although Hg isotope fractionation occurs during Hg binding with solids[49,19] and redox transformations of dissolved Hg^{2+} [18, 50] or liquid Hg^0,[51] fractionation of Hg bound to sediments has not been directly demonstrated. Hypothetically, to produce a shift in $\delta^{202}Hg$ of 1‰ from Hg^{2+} reduction (and complete removal of Hg^0), using typical fractionation factors for microbial or photochemical reduction and a Rayleigh-type fractionation model,[16] on the order of 50% of the Hg in sediment would have to be removed. In EFPC sediments and soils the majority of Hg is strongly bound to organic matter or solid phases such as sulfides, and typically only a small fraction of Hg (<5%) is thought to be labile or volatile.[5, 37, 39, 40] It has been estimated that EFPC floodplains soils emit 1-10 kg Hg/yr to the atmosphere,[12] yet this annual flux is less than 0.02% of the total Hg stored in floodplain soils (70,000-80,000 kg)[52]. Thus, floodplain evasion is unlikely to measurably alter Hg isotope ratios of floodplain soils even if the evaded Hg has a highly contrasting Hg isotopic composition. A nearby study in the Clinch and Emory Rivers further demonstrated the stability of Hg isotope values over multiple months of sediment sampling.[26] Therefore, we expect that in situ fractionation is not likely to appreciably alter sediment Hg isotopic compositions in our study.

In the absence of significant environmental fractionation, we suggest that the best explanation for the variation in sediment Hg isotope values in the study area is the input of multiple Hg sources. Sediments directly downstream of Y12 have a narrow range of $\delta^{202}Hg$ and $\Delta^{199}Hg$ that is distinct from the low THg sediments in the Clinch River and Hinds Creek (Figure 2.3). Sediments located downstream of Y12 in the Clinch River have Hg isotope values between these two endmember Hg isotope compositions (Figure 2.4). However, intermediate THg sediments from EFPC tributaries and Poplar Creek have more variable

and sometimes much lower δ^{202}Hg than either reference sediments or Y12 impacted sediments. Therefore, we suggest that there is a third Hg source to sediments in the study area that is characterized by low δ^{202}Hg and Δ^{199}Hg near zero. Below we examine the origin of each of the three proposed Hg isotope endmembers required to explain the distribution of data on Figures 2.3 and 2.4.

2.3.2.1 Regional Background Hg

Sediments from the Clinch River and Hinds Creek that were not affected by Y12 discharges have consistently low THg (0.026 ± 0.014 μg/g;) and a narrow range in Hg isotopic composition with δ^{202}Hg of -1.40 ± 0.06‰ and Δ^{199}Hg of -0.26 ± 0.03‰ (mean ± 1SD, n=6). Streambed sediments are a mixture of geogenic mineral particles, soil particles and terrestrial organic matter derived from the watershed. Similar Hg isotope values (low δ^{202}Hg and negative Δ^{199}Hg) have previously been measured in soils, coal and terrestrial foliage[43, 53, 54] and are characteristic of a mixture of geogenic and atmospheric Hg accumulation in terrestrial environments.[43] Consequently, we interpret these sediments from the Clinch River to be a reasonable representation of a mixture of background Hg sources in the region (i.e., geogenic Hg and long-range atmospheric Hg deposition) that have accumulated in the watershed. Low THg (0.021 ± 0.008 μg/g) sediments from the Emory River, a similarly sized watershed (~2250 km^2) that is partially located within our study area (Figure 2.1), had comparable δ^{202}Hg of -1.17 ± 0.13‰ and Δ^{199}Hg of -0.21 ± 0.06‰ (mean ± 1SD, n=6).[26] This supports our interpretation of a regionally integrated background Hg isotope signal in Clinch River sediments when not directly impacted by Hg point sources.

2.3.2.2 Y12 Derived Hg

EFPC streambed sediments were directly contaminated by discharges of high THg effluents from Y12 and these sediments are isotopically distinct from all non-Y12 impacted sediments in the region. There is some variation between Hg isotopes in fine and bulk sediment, yet combined they exhibit a small range in δ^{202}Hg (-0.28 to +0.26 ‰) and Δ^{199}Hg (-0.03 to -0.13 ‰). We cannot rule out the possibility that processes within Y12, such as evaporation or oxidation, might fractionate Hg between the liquid Hg source and Hg in sediments. Nonetheless, the Hg isotope values in EFPC sediments are generally comparable to measured values for liquid metallic Hg from a variety of sources[51, 55, 56] and consistent with sediments contaminated by industrial Hg discharges[19, 23, 27, 31]. Moreover, the Hg isotope values display no systematic longitudinal changes in δ^{202}Hg or Δ^{199}Hg (δ^{202}Hg was independent of the sampling distance downstream of Y12; distance vs. δ^{202}Hg for bulk and fine sediments had $r^2 = 0.03$, $p = 0.74$, $n=6$ and $r^2 = 0.01$, $p = 0.85$, $n=6$, respectively; Figure 2.S2) and thus our data provide no evidence of in-situ fractionation between the furthest upstream sampling location (EFK22.3) and Poplar Creek. Therefore, we use the mean Hg isotopic composition of all EFPC sediments (both fine and bulk fractions) to approximate the Y12 derived Hg endmember: δ^{202}Hg of 0.02 ± 0.15‰ and Δ^{199}Hg of -0.07 ± 0.03‰ with mean sediment THg of 24.4 ± 18.6 μg/g (mean ± 1SD, n=12).

As mentioned above, there are slight variations in the Hg isotopic composition between EFPC sediment size fractions (Figure 2.S2). The THg of fines at each location was between 1.8 and 18 times higher (mean difference = 28.3 μg/g, $p=0.010$, $n=6$) than the co-occurring bulk sediment (Figure 2.2). This is consistent with other studies, which have

demonstrated that Hg in EFPC is primarily bound to fine sediments and fine sediments constitute a significant but variable proportion of the streambed sediment.[5, 8] In this study we did not measure the mass proportion of sediment in the <125 μm fraction, but it is possible that the variable THg enrichment between fine and bulk sediments could largely be explained by dilution with a varying mass of coarse materials. Nonetheless, the difference in δ^{202}Hg between fine and bulk sediments, expressed as an isotope enrichment factor: $\varepsilon^{202}_{\text{fine-bulk}}$ ($\varepsilon^{202}_{\text{fine-bulk}} = \delta^{202}\text{Hg}_{\text{fine}} - \delta^{202}\text{Hg}_{\text{bulk}}$ and $E^{199}_{\text{fine-bulk}} = \Delta^{199}\text{Hg}_{\text{fine}} - \Delta^{199}\text{Hg}_{\text{bulk}}$), was significant at the uppermost (EFK22.3) and lowermost (EFK5) sampling sites ($\varepsilon^{202}_{\text{fine-bulk}}$ of +0.45‰ and +0.33‰, respectively; Figure 2.S2). At midstream locations (EFK9.8, EFK13.8, EFK17.8, and EFK18.2), the $\varepsilon^{202}_{\text{fine-bulk}}$ values (0.18, 0.00, -0.10 and 0.07‰, respectively) were close to the limits of analytical uncertainty. Overall, the magnitude of $\varepsilon^{202}_{\text{fine-bulk}}$ at EFPC locations was not dependent on the degree of THg enrichment in the co-occurring fine sediments and the $E^{199}_{\text{fine-bulk}}$ was insignificant at all locations.

There are at least two possible explanations for significant differences in δ^{202}Hg between sediment size fractions. First, it is possible that Hg released from Y12 was preferentially associated with and retained in solids of a specific particle size (i.e., Hg sorbed to fine clays, surfaces of oxides or in Hg-sulfide particles). For example, experimental studies suggest that during Hg precipitation with sulfides[19], sorption to organic matter[57], or sorption to goethite[49] the solid phases would be initially enriched with light Hg isotopes. If these solids were preferentially retained in the fine sediments, then fines would exhibit lower δ^{202}Hg. However, when $\varepsilon^{202}_{\text{fine-bulk}}$ is significant (at EFK22.3 and EFK5) the fine sediments exhibit higher δ^{202}Hg than the bulk sediments ($+\varepsilon^{202}_{\text{fine-bulk}}$) rather than the lower δ^{202}Hg ($-\varepsilon^{202}_{\text{fine-bulk}}$) that would be expected if fines contained Hg

fractionated during initial sorption or coprecipitation reactions alone. Alternatively, differences in the input of isotopically distinct Hg sources (e.g., riparian streambanks or soils) that contribute to sediment size fractions at each location could influence the $\varepsilon^{202}_{\text{fine-bulk}}$. In EFPC a significant portion of entrained fine sediments in the streambed are derived from streambank erosion with minor contributions from floodplain soils.[5, 8] Streambank and floodplain soils in EFPC have not been isotopically characterized but may contain different Hg species or geochemical constituents [4, 37, 39, 40]. If, for example, the <125 μm floodplain soils have higher δ^{202}Hg than the bulk streambed, then variable contributions of floodplain Hg to the streambed at each location could explain the observed $\varepsilon^{202}_{\text{fine-bulk}}$ variation. At the present time, we are unable to mechanistically explain the variable $\varepsilon^{202}_{\text{fine-bulk}}$ in EFPC. However, future work to investigate the isotopic composition of specific Hg forms in these sediments (e.g., Hg-sulfides or organic bound Hg) or additional Hg reservoirs in the watershed (e.g., floodplain soils) may better elucidate Hg isotope differences between sediment size fractions.

2.3.2.3 Origin of Low δ^{202}Hg Endmember

Very low δ^{202}Hg, and Δ^{199}Hg near zero, is observed in stream sediments in the Oak Ridge region that have intermediate THg (0.062 to 0.212 μg/g) and no headwater Hg point sources. As discussed above, environmental isotope fractionation might potentially alter Hg isotope ratios in sediments, but we have argued that this is unlikely to shift isotope values significantly because such a large fraction of Hg in sediments would have to be removed. The location of low δ^{202}Hg sediments is scattered within the study area and in some cases, low δ^{202}Hg is only apparent in the fine sediments. Therefore, if very low δ^{202}Hg results from

fractionation in the environment, such processes must also be unique to a small subset of streams. Alternatively, we suggest that low δ^{202}Hg values in sediments represent input from an additional Hg source with a distinct Hg isotopic composition (Figures 2.3, 2.4). This putative endmember is evident in sediments from Poplar Creek and EFPC tributaries; both of which have no headwater Hg point sources but are in close proximity to airborne Hg emissions from Department of Energy facilities (Y12 and K25) and TVA coal fired power plants. Therefore, although speculative, we suggest that one possible explanation for the low δ^{202}Hg signal observed in sediments is the input of Hg from nearby atmospheric sources.

Fine and bulk sediment from EFPC tributaries and bulk sediments from Poplar Creek upstream of EFPC had a much larger range in δ^{202}Hg (-5.07 to -0.84‰) and Δ^{199}Hg (-0.20 to -0.01‰) than other non-Y12 influenced sediments in the region (Figure 2.3). The isotopic composition of these sediments cannot be explained by Y12 or regional background Hg sources. In EFPC tributaries, fine sediments had δ^{202}Hg of -1.32 to -3.22‰ and Δ^{199}Hg of -0.01 to -0.16‰, whereas bulk tributary sediments had higher δ^{202}Hg of -0.84 to -1.71‰. Thus, at each tributary location, there was a significant negative $\varepsilon^{202}_{\text{fine-bulk}}$ that was in contrast to the significant positive $\varepsilon^{202}_{\text{fine-bulk}}$ observed at two EFPC sampling locations. The δ^{202}Hg values for Poplar Creek (as low as -5.07‰) and one EFPC tributary (-3.22‰; Trib16) are among the lowest yet reported for stream sediments. For comparison, other low δ^{202}Hg stream sediments (δ^{202}Hg of -2.75‰ to -4.00‰) were collected in relatively uncontaminated tributaries (THg of 0.09 to 0.14 μg/g) that were near, but not directly receiving effluent from, Hg contaminated mine tailings in New Brunswick, Canada.[19] Similarly low δ^{202}Hg (as low as -3.8‰) was also observed in sediments of

shallow lakes in NW Quebec (Canada) that were in close proximity (21 km or less) to smelting operations and had THg of 0.05 to 0.38 μg/g.[58] However, low δ^{202}Hg values (-2.50‰ to -2.91‰) have also been reported for lake sediments near Seattle, Washington (USA) that were deposited prior to the presence of nearby anthropogenic Hg sources.[59]

It is likely that all streambed sediments have some contribution from atmospheric Hg deposition. However, if nearby point source emissions are the dominant source of Hg deposition to a watershed, then incorporation of this Hg into sediments could lead to low δ^{202}Hg values. It has been demonstrated that precipitation collected in close proximity to a coal fired utility boiler (CFUB) had much lower δ^{202}Hg than precipitation not directly adjacent to the CFUB (and presumably containing long-range transported Hg).[60] In that study, precipitation collected within 11 km of a single large CFUB (~300 kg Hg/yr) in Florida (USA) had very low δ^{202}Hg (-2.56 ± 1.10‰; mean ± 1SD, with a minimum value of -4.37‰) and slightly positive Δ^{199}Hg (0.09 to 0.62‰).[60] Changes in the source of feed coal and emission control technologies likely influence the isotopic composition of CFUB residues and emissions.[60, 61] Feed coal combusted at TVA Kingston and TVA Bull Run in 2011 was primarily sourced from the Appalachian region,[62] which is similar to feed coals for the Florida CFUB study[60]. Combustion residues (fly ash slurry) stored at the TVA Kingston CFUB also had relatively low δ^{202}Hg and negative Δ^{199}Hg (δ^{202}Hg of -1.78 ±0.35‰ and Δ^{199}Hg of -0.21 ± 0.03‰; mean ± 1SD).[26] Therefore, we would expect a similarly low δ^{202}Hg in precipitation collected in close proximity to the TVA CFUBs. Thus, the proximity of sampling locations to coal fired utilities may be important when interpreting Hg isotope values in stream sediments in this region.

Historical vapor phase Hg emissions from Y12 are well documented[2] and gaseous Hg (Hg^0_g) emissions from the EFPC floodplains are significant[12]. Therefore, an alternative explanation for anomalous $\delta^{202}Hg$ in stream sediments could be the incorporation of anthropogenic Hg^0_g with distinctly low $\delta^{202}Hg$. For example, vapor phase Hg displayed significantly lower $\delta^{202}Hg$ ($\delta^{202}Hg$ of -0.58 ± 0.12‰) adjacent to Hg emission sources near Chicago, IL (USA) when compared to rural locations.[29] Low $\delta^{202}Hg$, between -2.32 to -1.88‰ (with $\Delta^{199}Hg$ between -0.24 and -0.34‰), was also measured in ambient gaseous Hg collected above (and presumably reemitted from) Hg contaminated rice fields.[63] We would expect that if historical vapor phase Hg emissions from Y12 were from liquid Hg evaporation, then atmospheric Hg^0 would have lower $\delta^{202}Hg$ than the primary liquid Hg source.[51] Additionally, flue gas Hg^0 from CFUBs would be expected to have $\delta^{202}Hg$ that is similar to or slightly higher (+0.3‰) than the feed coal.[61] If atmospheric Hg^0, either from EFPC floodplain reemissions, Y12 emissions or CFUB flue gas, was incorporated into foliage through leaf stomata (with additional negative MDF of up to 2.9‰)[43] then Hg with extremely low $\delta^{202}Hg$ could be deposited to the forest floor and incorporated into soils or sediments.

The anomalous low $\delta^{202}Hg$ values measured in sediments from Poplar Creek and EFPC Tributaries, which we hypothesize are derived from an atmospheric Hg source, were not discernable in sediments from the Clinch River that were likewise collected close to atmospheric Hg emission sources. It is possible that regional background Hg stored in Clinch River sediments, which is partially derived from long range transported Hg deposited across the watershed, effectively dilutes the isotopically anomalous, local atmospheric Hg source that was deposited across a very small portion of the watershed

area. In contrast, if atmospheric Hg from local emissions (such as Hg^0 reemission or CFUB-derived Hg in precipitation) were deposited across an entire small watershed its isotopic composition could overwhelm the background Hg isotope signal in sediments. Thus, the Hg isotope composition of sediments from streams with no direct aquatic Hg inputs and small watersheds could be more sensitive to inputs from atmospheric Hg emissions than larger streams in the same region.

2.3.3 Hg Endmember Mixing Downstream of Y12

Poplar Creek and Clinch River sediments located downstream of EFPC, and therefore directly affected by Y12, had Hg isotope ratios similar to sediments from EFPC (Figure 2.3; Figure 2.S3). The isotopic composition of Poplar Creek embayment sediments (δ^{202}Hg of 0.00 ± 0.09‰ and Δ^{199}Hg of -0.11 ± 0.04‰; mean ± 1SD, n=4) is within analytical uncertainty of EFPC sediments, suggesting that sediment bound Hg is not fractionated significantly during transport to Poplar Creek. Thus, Hg isotopes are a sensitive tracer of sediment-bound Hg that was derived from Y12, resuspended, and transported downstream. The stepwise decrease in sediment THg between Poplar Creek and the Clinch River coincides with a small shift towards lower δ^{202}Hg (Figure 2.4). Although we propose three Hg isotope endmembers for the region, the isotopic composition of Clinch River sediments downstream of Y12 indicates that the third, low δ^{202}Hg endmember is either not present or is overwhelmed by other Hg sources. Assuming that the Hg isotope composition and THg of Clinch River sediments is relatively stable over time,[26] the Hg in downstream Clinch River sediments can be most simply explained by the mixing of two Hg source endmembers: regional background Hg and Y12 derived Hg.

Consequently, we employed a binary mixing model to quantify the contribution of these Hg sources to downstream Clinch River sediments. Propagation of analytical errors and consideration of endmember variability resulted in uncertainties of less than ±6% (1SE) for these estimates. At CRK0 and CRK15, the Hg in sediments is 76% and 78% attributable to Y12, whereas at CRK2 and CRK7, δ^{202}Hg was much lower (-0.80‰ and -0.85‰, respectively) and Hg in sediments was only 41% and 38% attributable to Y12, respectively. The CRK2 and CRK7 sampling sites are the two locations nearest to the Clinch River-Emory River confluence. This confluence was the site of a December 2008 spill of 4 million m^3 of coal ash from the TVA Kingston Fossil Plant.[64] The materials from this spill were dispersed upstream to Clinch River Mile 5 (CRK8) and downstream to the Tennessee River (CRK0).[64] Therefore, it is likely that sediments sampled downstream of CRK8 (CRK0, CRK2 and CRK7) consisted of Y12 derived Hg that was diluted with both regional background Hg and Hg in fly ash wastes. The fly ash slurry had THg of 0.133 ± 0.023 μg/g and its isotope composition was previously measured as δ^{202}Hg of -1.78 ± 0.35‰ and Δ^{199}Hg of -0.21 ± 0.03‰ (mean ± 1SD, n=4).[26] We suspect that additional dilution with either Emory River sediments or recently released fly ash slurry may partially explain the lower contribution of Y12 derived Hg at CRK2 and CRK7. Nonetheless, it is clear that at downstream Clinch River locations, Y12 derived Hg exported from EFPC and Poplar Creek is a significant source of Hg to the sediments.

2.3.4 Implications for Future Work

This study demonstrates that sediments in EFPC that were contaminated by industrial discharges of Hg from Y12 have a unique Hg isotopic composition when

compared to sediments that were not influenced by Y12. Fish from EFPC have THg that are elevated above the EPA recommended water quality criterion threshold.[7, 65] Therefore, ongoing work to measure the isotopic composition of specific Hg species in sediments (e.g., Hg-sulfides, organic-bound, etc.) and the isotopic composition of Hg in biota, may provide a greater understanding of Hg bioavailability and bioaccumulation in this chronically contaminated stream. Downstream in the Clinch River, the origin of Hg in sediments can be best explained by the binary mixing of high and low THg (Y12 derived and regional background, respectively) sediment. However, to explain the variation in Hg isotopic composition of sediments throughout the study area, we must infer the presence of a third Hg endmember with extremely low δ^{202}Hg. Although the origin of this third, low δ^{202}Hg Hg source is highly speculative, we hypothesize that it is derived from atmospheric Hg deposition. Future measurement of Hg isotopes in additional environmental reservoirs (i.e., precipitation, foliage or floodplain soils), coupled with sediment Hg isotopes from this study, may clarify the relative importance of various Hg inputs to stream sediments in this region.

Acknowledgements

We thank Marcus Johnson for expert assistance in the operation of the CV-MC-ICP-MS and Carrie Miller, Ami Ricassi, Balaji Anandha Rao, and David Kocman for their valuable assistance with field sampling. This manuscript was improved by the constructive comments of three anonymous reviewers. The research was supported by the Office of Science (BER), U. S. Department of Energy under grant DE-SC0007042. ORNL is managed by UT-Battelle LLC for DOE under contract DE-AC05-000R22725.

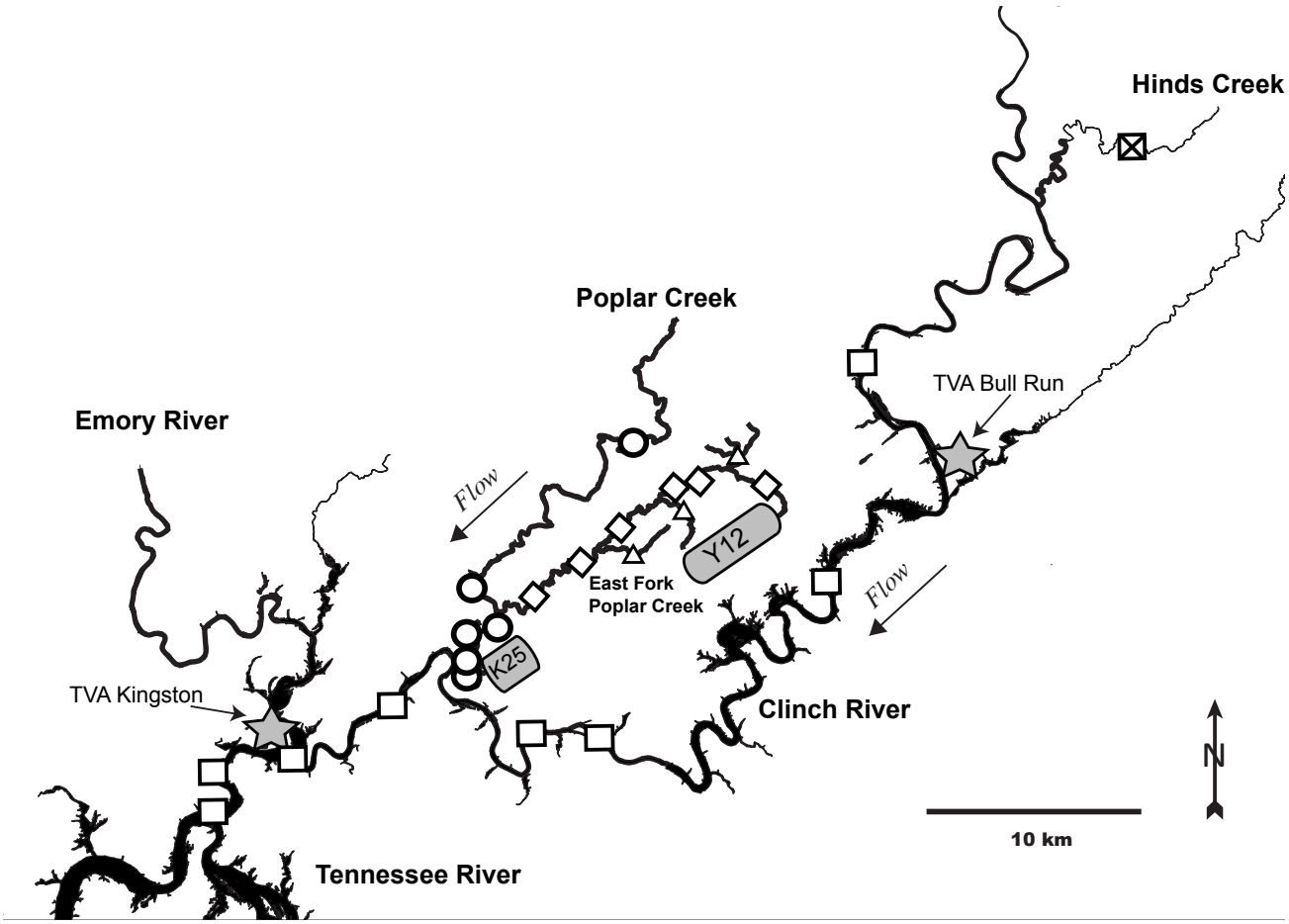

Figure 2.1 Streambed sediment sampling locations
Streambed sediment sampling locations are denoted by open squares (Clinch River), circles (Poplar Creek), diamonds (East Fork Poplar Creek), triangles (EFPC tributaries) and an inset X (Hinds Creek). Arrows parallel to the streams indicate the direction of stream flow. Atmospheric Hg emission sources greater than 1 kg Hg/year (Y12, K25, TVA Bull Run and TVA Kingston) are located on the map with shaded symbols.[9]

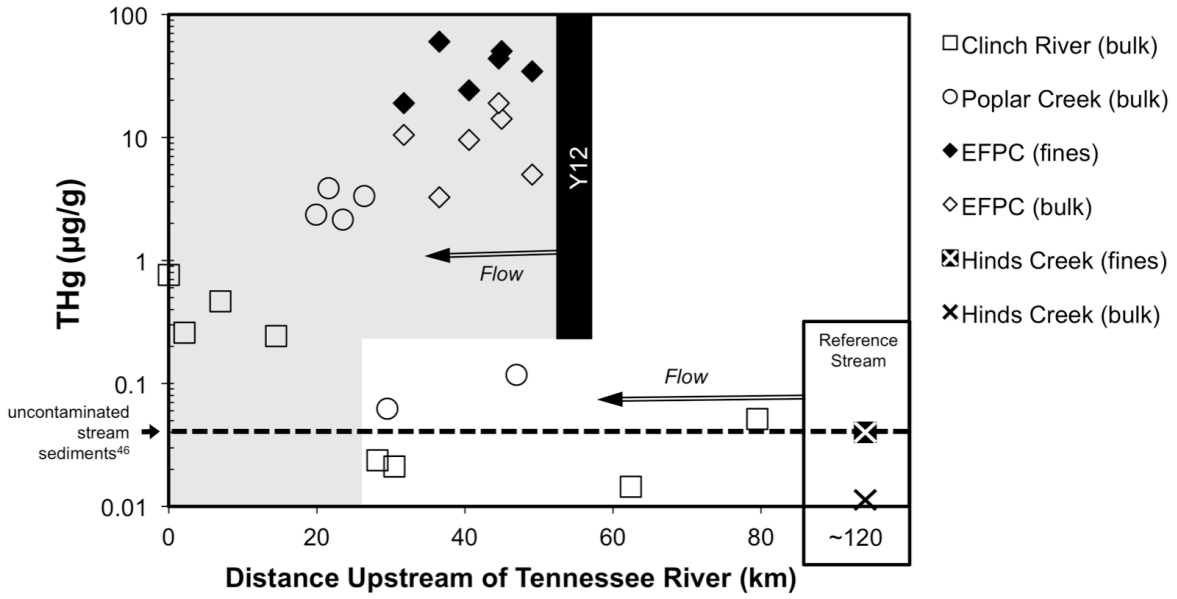

Figure 2.2: Location vs. THg for all streambed sediment
Location (distance upstream from the Tennessee/Clinch River confluence) vs. THg for sediments from the region. The dashed line denotes the median THg for streambed sediments from the United States that are not downstream of Hg point sources (0.03 µg/g)[46]. Streamflow in all watersheds is directed towards the Tennessee River as indicated by the double-line arrows. The gray background represents locations downstream of Y12.

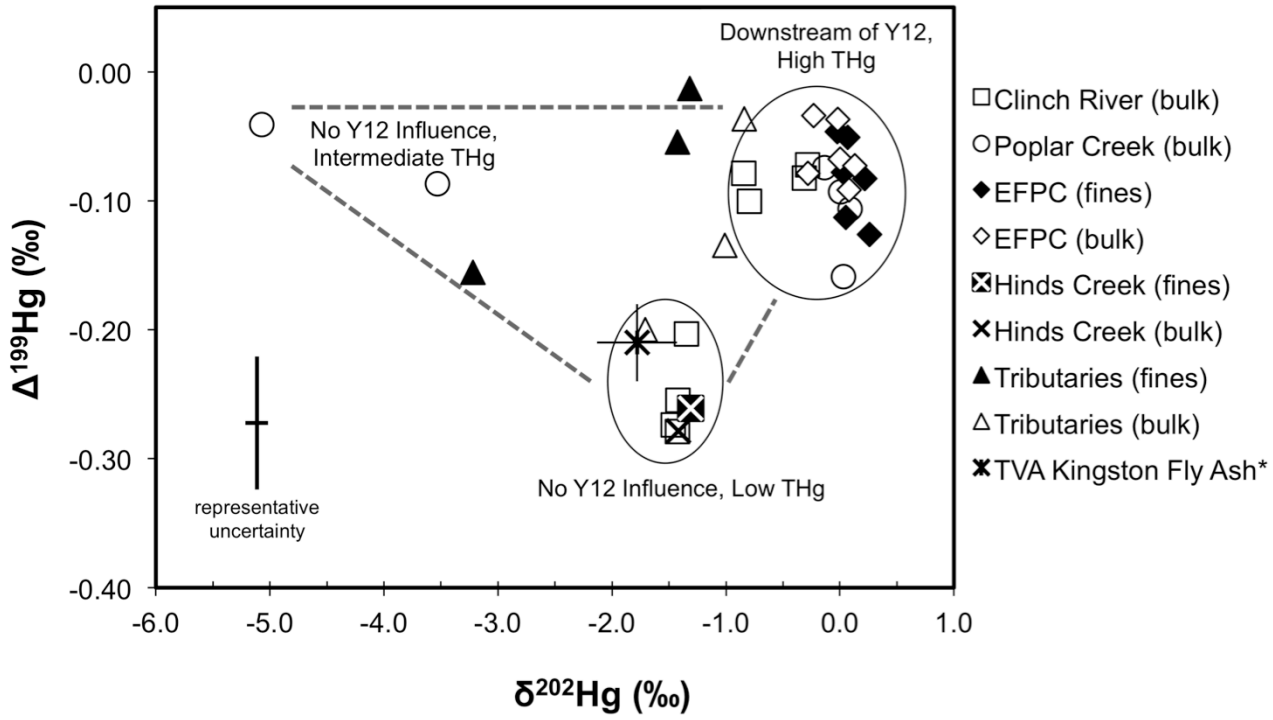

Figure 2.3: The Hg isotope composition (δ^{202}Hg vs. Δ^{199}Hg) of fine and bulk sediment from EFPC, EFPC tributaries, Hinds Creek, Poplar Creek and the Clinch River
The relative THg (low, intermediate, high) for all samples is indicated. Representative uncertainty (±0.11‰ for δ^{202}Hg, ±0.06‰ for Δ^{199}Hg) is the 2SE of replicate measurements of sediment standard reference materials. Fly ash slurry from the Kingston, TN coal ash spill (* from [26]) has been plotted and error bars represent the reported 1SD of ±0.35‰ for δ^{202}Hg and ±0.03‰ for Δ^{199}Hg.

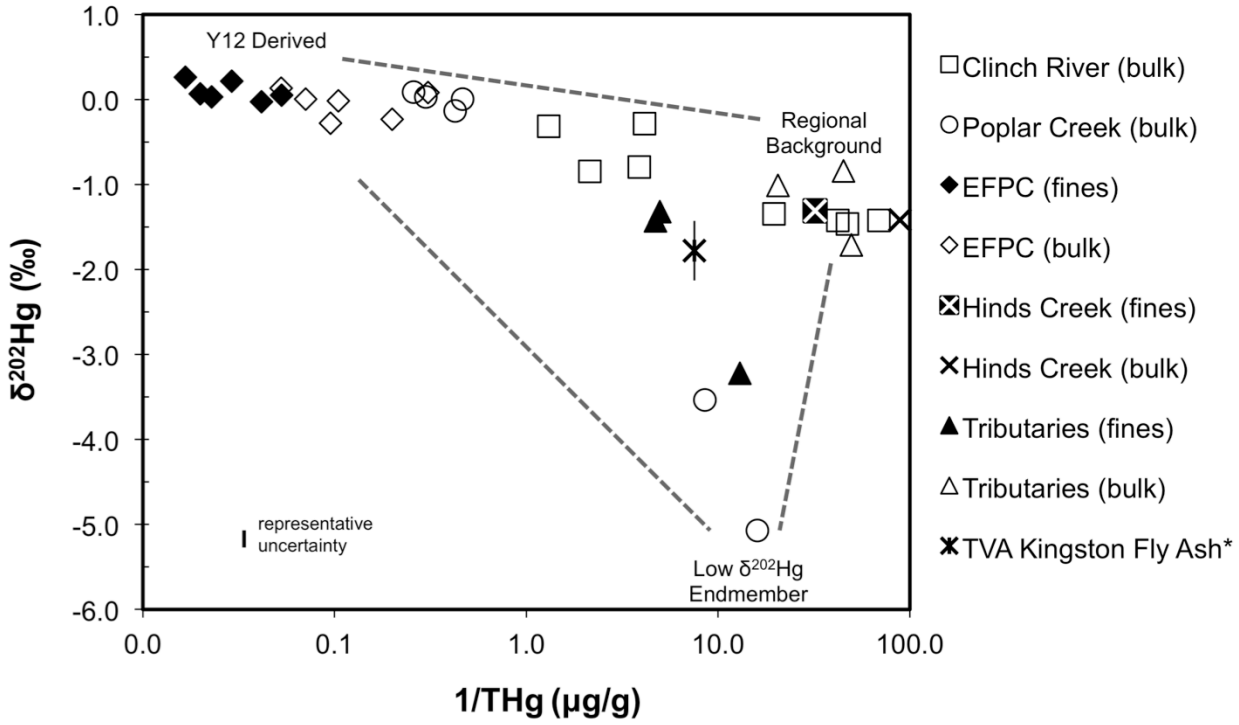

Figure 2.4: Inverse THg vs. δ^{202}Hg for fine and bulk streambed sediment from all sampling locations

The dashed lines approximate mixing between the endmember Hg sources (Y12 derived Hg, Regional Background Hg and the Low δ^{202}Hg Endmember). Representative uncertainty for δ^{202}Hg (± 0.11‰) is the 2SE of replicate measurements of standard reference materials. Fly ash slurry from the Kingston, TN coal ash spill (* from[26]; error bars are reported 1SD of ±0.35‰) is included for reference.

References

1. Selin, N. E., Global Biogeochemical Cycling of Mercury: A Review. *Annu. Rev. Environ. Resour.* **2009,** *34*, (1), 43-63.

2. Brooks, S. C.; Southworth, G. R., History of mercury use and environmental contamination at the Oak Ridge Y-12 Plant. *Environ. Pollut.* **2011,** *159*, (1), 219-228.

3. Loar, J. M.; Stewart, A. J.; Smith, J. G., Twenty-Five Years of Ecological Recovery of East Fork Poplar Creek: Review of Environmental Problems and Remedial Actions. *Environ. Manage.* **2011,** *47*, (6), 1010-1020.

4. Miller, C. L.; Watson, D. B.; Lester, B. P.; Lowe, K. A.; Pierce, E. M.; Liang, L., Characterization of soils from an industrial complex contaminated with elemental mercury. *Environ. Res.* **2013,** *125*, (0), 20-29.

5. Southworth, G.; Greeley, M.; Peterson, M.; Lowe, K.; Ketelle, R., *Sources of Mercury to East Fork Poplar Creek Downstream from the Y-12 National Security Complex: Inventories and Export Rates*; Publication 21460. Oak Ridge National Laboratory: Oak Ridge, TN, 2010. http://info.ornl.gov/sites/publications/files/Pub21460.pdf.

6. Barnett, M. O.; Harris, L. A.; Turner, R. R.; Stevenson, R. J.; Henson, T. J.; Melton, R. C.; Hoffman, D. P., Formation of Mercuric Sulfide in Soil. *Environ. Sci. Technol.* **1997,** *31*, (11), 3037-3043.

7. Mathews, T. J.; Southworth, G.; Peterson, M. J.; Roy, W. K.; Ketelle, R. H.; Valentine, C.; Gregory, S., Decreasing aqueous mercury concentrations to meet the water quality criterion in fish: Examining the water-fish relationship in two point-source contaminated streams. *Sci. Total Environ.* **2013,** *443*, (0), 836-843.

8. Southworth, G., Sources of mercury in a contaminated stream-implications for the timescale of recovery. *Environ. Toxicol. Chem.* **2013,** *32*, (4), 764-772.

9. *National Emissions Inventory for the State of Tennessee.*; U.S. Environmental Protection Agency: Washington, D.C., 2008. http://www.epa.gov/ttn/chief/net/2008inventory.html.

10. Lindberg, S. E.; Turner, R. R.; Meyers, T. P.; Taylor, G. E., Jr.; Schroeder, W. H., Atmospheric concentrations and deposition of Hg to a deciduous forest at Walker Branch watershed, Tennessee, USA. *Water Air & Soil Pollution* **1991,** *56*, (1), 577-594.

11. *Public Health Assessment: TSCA Incinerator, U.S. Department of Energy Oak Ridge Reservation. EPA FACILITY ID: TN1890090003. Oak Ridge, Anderson County, TN*; Agency for Toxic Substances and Disease Registry: Atlanta, GA, 2005. http://www.atsdr.cdc.gov/HAC/pha/PHA.asp?docid=1377&pg=0.

12. Lindberg, S. E.; Kim, K.-H.; Meyers, T. P.; Owens, J. G., Micrometeorological Gradient Approach for Quantifying Air/Surface Exchange of Mercury Vapor: Tests Over Contaminated Soils. *Environ. Sci. Technol.* **1995,** *29*, (1), 126-135.

13. Obrist, D.; Johnson, D. W.; Lindberg, S. E.; Luo, Y.; Hararuk, O.; Bracho, R.; Battles, J. J.; Dail, D. B.; Edmonds, R. L.; Monson, R. K.; Ollinger, S. V.; Pallardy, S. G.; Pregitzer, K. S.; Todd, D. E., Mercury Distribution Across 14 U.S. Forests. Part I: Spatial Patterns of Concentrations in Biomass, Litter, and Soils. *Environ. Sci. Technol.* **2011,** *45*, (9), 3974-3981.

14. Rodriguez-Gonzalez, P.; Epov, V. N.; Bridou, R.; Tessier, E.; Guyoneaud, R.; Monperrus, M.; Amouroux, D., Species-Specific Stable Isotope Fractionation of Mercury during Hg(II) Methylation by an Anaerobic Bacteria (Desulfobulbus propionicus) under Dark Conditions. *Environ. Sci. Technol.* **2009,** *43*, (24), 9183-9188.

15. Zheng, W.; Foucher, D.; Hintelmann, H., Mercury isotope fractionation during volatilization of Hg(0) from solution into the gas phase. *J. Anal. At. Spectrom.* **2007,** *22*, (9), 1097-1104.

16. Kritee, K.; Blum, J. D.; Reinfelder, J. R.; Barkay, T., Microbial stable isotope fractionation of mercury: A synthesis of present understanding and future directions. *Chem. Geol.* **2013,** *336*, (0), 13-25.

17. Zheng, W.; Hintelmann, H., Mercury isotope fractionation during photoreduction in natural water is controlled by its Hg/DOC ratio. *Geochim. Cosmochim. Acta* **2009,** *73*, (22), 6704-6715.

18. Bergquist, B. A.; Blum, J. D., Mass-dependent and -independent fractionation of Hg isotopes by photoreduction in aquatic systems. *Science* **2007,** *318*, (5849), 417-420.

19. Foucher, D.; Hintelmann, H.; Al, T. A.; MacQuarrie, K. T., Mercury isotope fractionation in waters and sediments of the Murray Brook mine watershed (New Brunswick, Canada): Tracing mercury contamination and transformation. *Chem. Geol.* **2013,** *336*, (0), 87-95.

20. Foucher, D.; Ogrinc, N.; Hintelmann, H., Tracing Mercury Contamination from the Idrija Mining Region (Slovenia) to the Gulf of Trieste Using Hg Isotope Ratio Measurements. *Environ. Sci. Technol.* **2009,** *43*, (1), 33-39.

21. Liu, J.; Feng, X.; Yin, R.; Zhu, W.; Li, Z., Mercury distributions and mercury isotope signatures in sediments of Dongjiang, the Pearl River Delta, China. *Chem. Geol.* **2011,** *287*, (1-2), 81-89.

22. Gehrke, G. E.; Blum, J. D.; Marvin-DiPasquale, M., Sources of mercury to San Francisco Bay surface sediment as revealed by mercury stable isotopes. *Geochim. Cosmochim. Acta* **2011,** *75*, (3), 691-705.

23. Sonke, J. E.; Schafer, J.; Chmeleff, J.; Audry, S.; Blanc, G.; DuprÈ, B., Sedimentary mercury stable isotope records of atmospheric and riverine pollution from two major European heavy metal refineries. *Chem. Geol.* **2010,** *279*, (3-4), 90-100.

24. Stetson, S. J.; Gray, J. E.; Wanty, R. B.; Macalady, D. L., Isotopic Variability of Mercury in Ore, Mine-Waste Calcine, and Leachates of Mine-Waste Calcine from Areas Mined for Mercury. *Environ. Sci. Technol.* **2009,** *43*, (19), 7331-7336.

25. Ma, J.; Hintelmann, H.; Kirk, J. L.; Muir, D. C. G., Mercury concentrations and mercury isotope composition in lake sediment cores from the vicinity of a metal smelting facility in Flin Flon, Manitoba. *Chem. Geol.* **2013,** *336*, (0), 96-102.

26. Bartov, G.; Deonarine, A.; Johnson, T. M.; Ruhl, L.; Vengosh, A.; Hsu-Kim, H., Environmental Impacts of the Tennessee Valley Authority Kingston Coal Ash Spill. 1. Source Apportionment Using Mercury Stable Isotopes. *Environ. Sci. Technol.* **2012,** *47*, (4), 2092-2099.

27. Donovan, P. M.; Blum, J. D.; Yee, D.; Gehrke, G. E.; Singer, M. B., An isotopic record of mercury in San Francisco Bay sediment. *Chem. Geol.* **2013,** *349-350*, (0), 87-98.

28. Yin, R.; Feng, X.; Wang, J.; Li, P.; Liu, J.; Zhang, Y.; Chen, J.; Zheng, L.; Hu, T., Mercury speciation and mercury isotope fractionation during ore roasting process and their implication to source identification of downstream sediment in the Wanshan mercury mining area, SW China. *Chem. Geol.* **2013,** *336*, (0), 72-79.

29. Gratz, L. E.; Keeler, G. J.; Blum, J. D.; Sherman, L. S., Isotopic Composition and Fractionation of Mercury in Great Lakes Precipitation and Ambient Air. *Environ. Sci. Technol.* **2010,** *44*, (20), 7764-7770.

30. Gehrke, G. E.; Blum, J. D.; Slotton, D. G.; Greenfield, B. K., Mercury Isotopes Link Mercury in San Francisco Bay Forage Fish to Surface Sediments. *Environ. Sci. Technol.* **2011,** *45*, (4), 1264-1270.

31. Perrot, V.; Epov, V. N.; Pastukhov, M. V.; Grebenshchikova, V. I.; Zouiten, C.; Sonke, J. E.; Husted, S.; Donard, O. F. X.; Amouroux, D., Tracing Sources and Bioaccumulation of Mercury in Fish of Lake Baikal- Angara River Using Hg Isotopic Composition. *Environ. Sci. Technol.* **2010,** *44*, (21), 8030-8037.

32. Tsui, M. T. K.; Blum, J. D.; Kwon, S. Y.; Finlay, J. C.; Balogh, S. J.; Nollet, Y. H., Sources and Transfers of Methylmercury in Adjacent River and Forest Food Webs. *Environ. Sci. Technol.* **2012,** *46*, (20), 10957-10964.

33. Sherman, L. S.; Blum, J. D., Mercury stable isotopes in sediments and largemouth bass from Florida lakes, USA. *Sci. Total Environ.* **2013,** *448*, (0), 163-175.

34. Campbell, K. R.; Ford, C. J.; Levine, D. A., Mercury distribution in poplar creek, Oak Ridge, Tennessee, USA. *Environ. Toxicol. Chem.* **1998,** *17*, (7), 1191-1198.

35. Pant, P.; Allen, M.; Tansel, B., Mercury contamination in the riparian zones along the East Fork Poplar Creek at Oak Ridge. *Ecotoxicol. Environ. Saf.* **2011,** *74*, (3), 467-472.

36. Han, F. X., Mercury distribution and speciation in floodplain soils and uptake into native earthworms (Diplocardia spp.). *Geoderma* **2012,** *170*, 261-268.

37. Liu, G.; Cabrera, J.; Allen, M.; Cai, Y., Mercury characterization in a soil sample collected nearby the DOE Oak Ridge Reservation utilizing sequential extraction and thermal desorption method. *Sci. Total Environ.* **2006,** *369*, (1-3), 384-392.

38. Malek-Mohammadi, S.; Tachiev, G.; Cabrejo, E.; Lawrence, A., Simulation of flow and mercury transport in Upper East Fork Poplar Creek, Oak Ridge, Tennessee. *Remed. J.* **2012,** *22*, (2), 119-131.

39. Han, F.; Shiyab, S.; Chen, J.; Su, Y.; Monts, D.; Waggoner, C.; Matta, F., Extractability and Bioavailability of Mercury from a Mercury Sulfide Contaminated Soil in Oak Ridge, Tennessee, USA. *Water, Air, Soil Pollut.* **2008,** *194*, (1-4), 67-75.

40. Han, F. X.; Su, Y.; Monts, D. L.; Waggoner, C. A.; Plodinec, M. J., Binding, distribution, and plant uptake of mercury in a soil from Oak Ridge, Tennessee, USA. *Sci. Total Environ.* **2006,** *368*, (2-3), 753-768.

41. McMaster, W. M., *Hydrologic Data for the Oak Ridge Area Tennessee*; Water-Supply Paper 1839-N. U.S. Geological Survey; U.S. Department of the Interior: Washington, D.C., 1967. http://pubs.er.usgs.gov/publication/wsp1839N.

42. Cook, R. B.; Suter, G. W.; Sain, E. R., Ecological risk assessment in a large river-reservoir: 1. Introduction and background. *Environ. Toxicol. Chem.* **1999,** *18*, (4), 581-588.

43. Demers, J. D.; Blum, J. D.; Zak, D. R., Mercury isotopes in a forested ecosystem: Implications for air-surface exchange dynamics and the global mercury cycle. *Global Biogeochem. Cycles* **2013,** *27*, (1), 222-238.

44. Blum, J. D.; Bergquist, B. A., Reporting of variations in the natural isotopic composition of mercury. *Anal. Bioanal. Chem.* **2007,** *388*, (2), 353-359.

45. Cooke, C. A.; Hintelmann, H.; Ague, J. J.; Burger, R.; Biester, H.; Sachs, J. P.; Engstrom, D. R., Use and Legacy of Mercury in the Andes. *Environ. Sci. Technol.* **2013,** *47*, (9), 4181-4188.

46. Scudder, B. C.; Chasar, L. C.; Wentz, D. A.; Bauch, N. J.; Brigham, M. E.; Moran, P. W.; Krabbenhoft, D. P., *Mercury in Fish, Bed Sediment, and Water from Streams Across the United States, 1998-2005*; Scientific Investigations Report 2009-5109. U.S. Geological Survey; U.S. Department of the Interior: 2009. http://pubs.usgs.gov/sir/2009/5109.

47. Jones, D. S.; Barnthouse, L. W.; Suter, G. W.; Efroymson, R. A.; Field, J. M.; Beauchamp, J. J., Ecological risk assessment in a large river-reservoir: 3. Benthic invertebrates. *Environ. Toxicol. Chem.* **1999,** *18*, (4), 599-609.

48. Elwood, J. W., *Mercury contamination in Poplar Creek and the Clinch River*; Publication No. 2286. Division, O. R. N. L. E. S.: Oak Ridge, TN, 1984.

49. Jiskra, M.; Wiederhold, J. G.; Bourdon, B.; Kretzschmar, R., Solution Speciation Controls Mercury Isotope Fractionation of Hg(II) Sorption to Goethite. *Environ. Sci. Technol.* **2012,** *46*, (12), 6654-6662.

50. Kritee, K.; Blum, J. D.; Barkay, T., Mercury Stable Isotope Fractionation during Reduction of Hg(II) by Different Microbial Pathways. *Environ. Sci. Technol.* **2008,** *42*, (24), 9171-9177.

51. Estrade, N.; Carignan, J.; Sonke, J. E.; Donard, O. F. X., Mercury isotope fractionation during liquid-vapor evaporation experiments. *Geochim. Cosmochim. Acta* **2009,** *73*, (10), 2693-2711.

52. Turner, R. R.; Southworth, G. R., Mercury-Contaminated Industrial and Mining Sites in North America: an Overview with Selected Case Studies. In *Mercury Contaminated Sites*, Ebinghaus, R.; Turner, R.; Lacerda, L.; Vasiliev, O.; Salomons, W., Eds. Springer Berlin Heidelberg: 1999; pp 89-112.

53. Lefticariu, L.; Blum, J.; Gleason, J., Mercury Isotopic Evidence for Multiple Mercury Sources in Coal from the Illinois Basin. *Environ. Sci. Technol.* **2011,** *45*, (4), 1724-1729.

54. Biswas, A.; Blum, J. D.; Bergquist, B. A.; Keeler, G. J.; Xie, Z. Q., Natural Mercury Isotope Variation in Coal Deposits and Organic Soils. *Environ. Sci. Technol.* **2008,** *42*, (22), 8303-8309.

55. Laffont, L.; Sonke, J. E.; Maurice, L.; Monrroy, S. L.; Chincheros, J.; Amouroux, D.; Behra, P., Hg Speciation and Stable Isotope Signatures in Human Hair As a Tracer for Dietary and Occupational Exposure to Mercury. *Environ. Sci. Technol.* **2011,** *45*, (23), 9910-9916.

56. Sonke, J. E.; Zambardi, T.; Toutain, J.-P., Indirect gold trap-MC-ICP-MS coupling for Hg stable isotope analysis using a syringe injection interface. *J. Anal. At. Spectrom.* **2008,** *23*, (4).

57. Wiederhold, J. G.; Cramer, C. J.; Daniel, K.; Infante, I.; Bourdon, B.; Kretzschmar, R., Equilibrium Mercury Isotope Fractionation between Dissolved Hg(II) Species and Thiol-Bound Hg. *Environ. Sci. Technol.* **2010,** *44*, (11), 4191-4197.

58. Jackson, T. A.; Telmer, K. H.; Muir, D. C. G., Mass-dependent and mass-independent variations in the isotope composition of mercury in cores from lakes polluted by a smelter:

Effects of smelter emissions, natural processes, and their interactions. *Chem. Geol.* **2013,** *352*, (0), 27-46.

59. Gray, J. E.; Pribil, M. J.; Van Metre, P. C.; Borrok, D. M.; Thapalia, A., Identification of contamination in a lake sediment core using Hg and Pb isotopic compositions, Lake Ballinger, Washington, USA. *Appl. Geochem.* **2013,** *29*, (0), 1-12.

60. Sherman, L. S.; Blum, J. D.; Keeler, G. J.; Demers, J. D.; Dvonch, J. T., Investigation of Local Mercury Deposition from a Coal-Fired Power Plant Using Mercury Isotopes. *Environ. Sci. Technol.* **2011,** *46*, (1), 382-390.

61. Sun, R.; Heimburger, L.-E.; Sonke, J. E.; Liu, G.; Amouroux, D.; Berail, S., Mercury stable isotope fractionation in six utility boilers of two large coal-fired power plants. *Chem. Geol.* **2013,** *336*, (0), 103-111.

62. *EIA-923 Schedule 2: Monthly and Annual Fuel Receipts and Costs Data*; United States Energy Information Administration: Washington, D.C., 2011. http://www.eia.gov/electricity/data/eia923/.

63. Yin, R. S.; Feng, X. B.; Meng, B., Stable Mercury Isotope Variation in Rice Plants (Oryza sativa L.) from the Wanshan Mercury Mining District, SW China. *Environ. Sci. Technol.* **2013,** *47*, (5), 2238-2245.

64. *Continuing Investigation of the Nature and Extent of Ash in the Emory, Clinch and Tennessee River Bottoms*; Tennessee Valley Authority: Knoxville, TN, 2009. http://www.tva.gov/kingston/ash_distribution.pdf.

65. Mathews, T. J.; Smith, J. G.; Peterson, M. J.; Roy, W. K., Assessment of Contaminant Bioaccumulation in Invertebrates and Fish in Waters On and Adjacent to the Oak Ridge Reservation - 2010. *ORNL-TM (Oak Ridge National Laboratory)* **2011,** *2011/108*.

2.4 Supporting Information

2.4.1. Materials and Methods

2.4.1.1 Sediment Collection and Sieving Techniques

Poplar Creek and Clinch River sediments were collected between June 2011 and April 2012 in depositional locations that had an overlying water depth between 1 and 11 feet. The top 10-15 cm sediment was collected from each location using a clean stainless steel petite ponar grab or polycarbonate core. When visible, any coarse materials (gravel cobbles and debris) were removed prior to further processing. Sediments from EFPC, Hinds Creek and EFPC tributaries were collected between October 2011 and April 2012. Sediment samples at each location consisted of 3-5 scoops of the top 6 cm of streambed sediment from the main channel that was removed using an acid clean polycarbonate core. The sample was composited and then sieved in the field through either a 2 mm (nominal opening) acid-cleaned nylon mesh or a 125 μm (nominal opening) acid-cleaned polypropylene mesh. The fraction that passed through each mesh was retained for analysis. Thus, we obtained two different size fractions of streambed sediment at each location: the <125 μm fraction (hereafter fine sediments or fines) which by definition contains very fine sand, silt and clay, and the <2 mm fraction (hereafter bulk sediments) which by definition contains fine to coarse sand and gravel, silt and clay. All streambed sediments were retained as a wet slurry in the field and immediately placed on ice then later dewatered by centrifugation for 10 min at 3500 RPM. The overlying water was decanted and the retained sediments were immediately frozen at -18°C for storage prior to further processing.

2.4.1.2 THg Concentration and Hg Isotope Analysis

Prior to analysis, bulk sediment (<2mm) was freeze-dried and then homogenized to a fine powder in an alumina ball mill (SPEX SamplePrep Mixer/Mill). Fine sediment samples (<125μm) were not ground, but instead freeze-dried and manually rehomogenized. All sediment samples were combusted in an offline two stage furnace to isolate Hg for isotopic analyses as has been described elsewhere.[1-3] The amount of sediment combusted depended upon the mass of Hg needed for analysis (typically at least 25 ng Hg). For low THg samples (upstream Clinch River and Hinds Creek samples) between 150 and 2500 mg was combusted. When THg concentrations were extremely high it was necessary to combust enough sediment to minimize potential issues with sample heterogeneity. Therefore, for all high THg concentration samples at least 150 mg and up to 340 mg of sediment was combusted. The only exception to this was the four Poplar Creek samples influenced by Y12 (THg concentrations 2 to 4 μg/g), in which we were sample limited and could only combust 30-60 mg of sediment. For consistency, between 40 and 1100 mg of similarly prepared (dried and sieved) high concentration sediment SRM (NIST 1944; 3.4 μg/g,) and low concentration sediment SRM (NRC MESS-3; 0.091 μg/g) were combusted and analyzed and no measurable differences in Hg isotope composition or THg resulted due to the variable sample mass in the combustion furnace. After sediment was placed in the first furnace (or first stage) the temperature was slowly increased to 750°C over the course of 6 hours while the second furnace (second stage) was held constant at 1000°C. The Hg released from the sediment matrix during this procedure was carried in a flow of Hg-free O_2 (O_2 that was passed through a gold trap immediately prior to entering the combustion furnace) through the second furnace and into a 1%$KMnO_4$/1.8 M H_2SO_4 oxidizing trap solution (1% $KMnO_4$ trap). The 1%$KMnO_4$ trap solutions were then pre-

reduced with 2% (w/w) of 30% hydroxylamine hydrochloride ($NH_2OH•HCl$) and measured by CV-AAS (Nippon MA-2000). Sediment dry weight THg concentrations were calculated based on the mass of Hg in the 1% $KMnO_4$ trap (i.e., the amount of Hg recovered by offline combustion) and the mass of dry sediment placed in the combustion furnace. Dry weight THg concentrations measured by offline combustion are reported in Tables 2.S1 and 2.S2. For a subset of samples (n=17), we completed independent THg concentration analysis by online combustion at 850°C, pre-concentration onto a gold trap, followed by atomic absorption spectrometry (Nippon MA-2000). The dry weight THg concentrations via online combustion were compared to the sediment dry weight THg concentrations determined by offline combustion and for all samples the yield of Hg recovered during offline combustion could be calculated (105 ± 16%, mean ± 1SD; n=17; minimum = 86%).

Prior to isotopic analysis, the contents of the original 1% $KMnO_4$ trap (already pre-reduced with 2% (w/w) of 30% hydroxylamine hydrochloride ($NH_2OH•HCl$)) were distributed evenly in 1-5g aliquots. Each aliquot was treated with 0.3 ml of 20% $SnCl_2$ and 0.3 ml of 50% H_2SO_0 to reduce all Hg to Hg^0 which was then transported into a secondary 1%$KMnO_4$/1.8M H_2SO_4 trapping solution.[4] This pre-concentrates Hg for isotopic analysis and isolates the Hg in the original trap solution from any volatile residues that might have accumulated in the original trap during the combustion process, thereby reducing potential matrix effects during isotopic analysis. An aliquot of the secondary trap solution was analyzed for THg concentration by CV-AAS (Nippon MA-2000) and a transfer yield was calculated based on the mass of Hg in the initial (combustion) and final (post-transfer) trap solutions. The transfer yield for all samples averaged 97 ± 5% (mean ± 1SD; n= 41; minimum = 88%).

The Hg isotope composition of the secondary trap solution was measured using cold-vapor multi-collector inductively-coupled-plasma mass-spectrometry (CV-MC-ICP-MS). The secondary 1% $KMnO_4$ trap solution was pre-reduced with $NH_2OH{\bullet}HCl$ (2% w/w) and diluted to a THg concentration between 3.6 and 5.0 ng/g. The Hg^{2+} in solution was reduced online, by addition of $SnCl_2$, to Hg^0 which was separated from solution using a frosted tip gas-liquid phase separator and transported in Hg-clean Ar gas to the inlet of the MC-ICP-MS. Instrumental mass bias was corrected by the introduction of an internal Tl standard (NIST 997) as a dry aerosol to the Ar gas stream and by strict sample-standard bracketing using NIST 3133 with an identical concentration and solution matrix as that of the sample.[5] In Table 2.S1 and 2.S2 we report $\delta^{xxx}Hg$ and $\Delta^{xxx}Hg$ values for samples and standards for ^{204}Hg, ^{201}Hg, ^{200}Hg and ^{199}Hg based on Equation 2 from the main text [$\Delta^{xxx}Hg = \delta^{xxx}Hg - (\delta^{202}Hg * \beta)$] where β = 1.493, 0.7520, 0.5024 and 0.2520 for ^{204}Hg, ^{201}Hg, ^{200}Hg and ^{199}Hg, respectively.[5]

2.4.1.3 Blanks, Reference Materials and Uncertainty

Sediment standard reference materials (SRMs) NRC MESS-3 (marine sediment reference material) and NIST 1944 (New York/New Jersey waterway sediment) were combusted and processed alongside samples in an identical manner. The THg concentrations measured by offline combustion agreed within 5% of the certified THg concentration of NRC MESS-3 (0.091 μg/g) and within 10% of the reported THg concentration of NIST SRM 1944 (3.40 μg/g). The transfer yield for all sediment SRMs averaged 95 ± 4% (1SD; n=9; min = 88%). We estimate the external reproducibility of Hg isotope measurements based on the standard error (2SE) of process replicates of these sediment reference materials (Table 2.S2). The in-house standard UM-Almaden was

analyzed five times per analytical session, at run concentrations between 3 and 5 ng/g, over the course of 64 analytical sessions between December 2011 and February 2013 during which samples for this study were being analyzed. We estimated the long-term analytical uncertainty of Hg isotope measurements based on the standard deviation (2SD) of the mean Hg isotope values for UM-Almaden from each analytical session (Table 2.S2). The analytical uncertainty of UM-Almaden measurements was always less than the 2SE of the replicate process standards we analyzed. Thus, the most conservative estimate of representative uncertainty for Hg isotope measurements of sediment samples in this study is ±0.11‰ for δ^{202}Hg, ±0.06‰ for Δ^{199}Hg, and ±0.06‰ for Δ^{201}Hg (see Table 2.S2). Procedural combustion blanks were processed alongside each batch of samples and standards in the exact same manner and yielded between 0.08 and 0.21 ng of Hg (mean = 122 pg; n=6) whereas combustion trap solutions contained between 29 and 6,700 ng of Hg. For each batch of samples (6-12 samples), the corresponding blank was never greater than 0.3% of the Hg mass in the final 1% $KMnO_4$ trap solution.

2.4.2 Discussion

2.4.2.1 Comment on $\varepsilon^{202}_{fine\text{-}bulk}$ in Hinds Creek Sediments

The δ^{202}Hg of bulk sediment from Hinds Creek was -1.42‰ and fine sediments had δ^{202}Hg of -1.31‰ thus the $\varepsilon^{202}_{fine\text{-}bulk}$ ($\varepsilon^{202}_{fine\text{-}bulk} = \delta^{202}Hg_{fines} - \delta^{202}Hg_{bulk}$) was within analytical uncertainty (±0.11‰). An insignificant $\varepsilon^{202}_{fine\text{-}bulk}$ in Hinds Creek, and the enrichment of Hg in fine sediments, suggests that Hg was derived from a similar source, with fine sediments containing more Hg per unit mass simply due to their greater surface area. In contrast to the reference site, there was a significant $\varepsilon^{202}_{fine\text{-}bulk}$ at all EFPC tributary

sampling locations with the largest occurring at Trib_16 (-1.51‰) due to the extremely low δ^{202}Hg in the fine sediments at this location (-3.22‰). Sediments from Trib_10 and Trib_20 also had $\varepsilon^{202}_{\text{fine-bulk}}$ in the opposite direction (-0.42‰ and -0.48‰, respectively) of the significant offsets observed in EFPC ($+\varepsilon^{202}_{\text{fine-bulk}}$). As described in the text, this may be explained by differences in Hg binding within certain size classes (e.g., clays vs. sulfides) or isotopic differences in Hg derived from different Hg sources (atmospheric vs. geogenic Hg). For example at the reference or non-Y12 influenced locations, Hg sources to soils (and eventually sediments) include leaf litter and foliage, which can have unique Hg isotope ratios (e.g., [3, 6]). If bulk sediments are a mixture of these components, then the isolation of fine sediments could enrich one size class with a particular Hg source (with unique Hg isotope values), leading to significant δ^{202}Hg differences.

2.4.2.2 Binary Mixing Equations

Here we present concentration weighted isotope mixing equations previously employed by [7] and modified for Hg endmembers in this study: Y12 derived Hg (Y12) and regional background Hg (bk).

$$\delta^{202}Hg_{samp} = F_{Y12} \times \delta^{202}Hg_{Y12} + F_{bk} \times \delta^{202}Hg_{bk}$$

$$1 = F_{Y12} + F_{bk}$$

$$F_{Y12} = 1 - [THg]_{bk} / [THg]_{samp}$$

References

1. Tsui, M. T. K.; Blum, J. D.; Kwon, S. Y.; Finlay, J. C.; Balogh, S. J.; Nollet, Y. H., Sources and Transfers of Methylmercury in Adjacent River and Forest Food Webs. *Environ. Sci. Technol.* **2012,** *46*, (20), 10957-10964.

2. Lefticariu, L.; Blum, J.; Gleason, J., Mercury Isotopic Evidence for Multiple Mercury Sources in Coal from the Illinois Basin. *Environ. Sci. Technol.* **2011,** *45*, (4), 1724-1729.

3. Demers, J. D.; Blum, J. D.; Zak, D. R., Mercury isotopes in a forested ecosystem: Implications for air-surface exchange dynamics and the global mercury cycle. *Global Biogeochem. Cycles* **2013,** *27*, (1), 222-238.

4. Sherman, L. S.; Blum, J. D., Mercury stable isotopes in sediments and largemouth bass from Florida lakes, USA. *Sci. Total Environ.* **2013,** *448*, (0), 163-175.

5. Blum, J. D.; Bergquist, B. A., Reporting of variations in the natural isotopic composition of mercury. *Anal. Bioanal. Chem.* **2007,** *388*, (2), 353-359.

6. Yin, R. S.; Feng, X. B.; Meng, B., Stable Mercury Isotope Variation in Rice Plants (Oryza sativa L.) from the Wanshan Mercury Mining District, SW China. *Environ. Sci. Technol.* **2013,** *47*, (5), 2238-2245.

7. Foucher, D.; Ogrinc, N.; Hintelmann, H., Tracing Mercury Contamination from the Idrija Mining Region (Slovenia) to the Gulf of Trieste Using Hg Isotope Ratio Measurements. *Environ. Sci. Technol.* **2009,** *43*, (1), 33-39.

Sample	Size Fraction	N_1	N_2	THg	$\delta^{204}Hg$	$\delta^{202}Hg$	$\delta^{201}Hg$	$\delta^{200}Hg$	$\delta^{199}Hg$	$\Delta^{204}Hg$	$\Delta^{201}Hg$	$\Delta^{200}Hg$	$\Delta^{199}Hg$
				µg/g	‰	‰	‰	‰	‰	‰	‰	‰	‰
CRK_80	-	1	2	0.051	-2.02	-1.35	-1.24	-0.66	-0.54	-0.01	-0.23	0.02	-0.20
CRK_62	-	1	1	0.015	-2.14	-1.42	-1.29	-0.66	-0.61	-0.02	-0.22	0.05	-0.25
CRK_31	-	1	1	0.021	-2.22	-1.46	-1.33	-0.70	-0.64	-0.04	-0.22	0.03	-0.27
CRK_28	-	1	1	0.024	-2.20	-1.42	-1.34	-0.71	-0.64	-0.08	-0.27	0.00	-0.28
CRK_15	-	1	3	0.242	-0.36	-0.28	-0.25	-0.11	-0.14	0.06	-0.04	0.03	-0.07
CRK_7	-	1	2	0.466	-1.27	-0.85	-0.72	-0.40	-0.29	-0.01	-0.08	0.02	-0.08
CRK_2	-	1	2	0.258	-1.26	-0.80	-0.68	-0.43	-0.30	-0.07	-0.08	-0.03	-0.10
CRK_0	-	1	3	0.763	-0.45	-0.31	-0.33	-0.14	-0.16	0.01	-0.09	0.02	-0.08
PCK_28	-	2	4	0.118	-5.33	-3.53	-2.79	-1.74	-0.98	-0.06	-0.14	0.04	-0.09
PCK_11	-	2	3	0.062	-7.60	-5.07	-3.89	-2.53	-1.32	-0.04	-0.07	0.02	-0.04
PCK_8	-	1	1	3.35	0.13	0.03	-0.03	0.02	-0.15	0.08	-0.06	0.01	-0.16
PCK_5	-	1	2	2.16	0.02	0.01	-0.13	0.00	-0.09	0.01	-0.13	0.00	-0.09
PCK_3	-	1	2	3.87	0.12	0.09	-0.02	0.05	-0.08	-0.01	-0.09	0.01	-0.11
PCK_1	-	1	2	2.35	-0.20	-0.13	-0.18	-0.06	-0.11	-0.01	-0.08	0.00	-0.07
HCK_10	<2mm	1	1	0.011	-2.11	-1.42	-1.37	-0.67	-0.64	0.01	-0.31	0.04	-0.28
HCK_10	<125um	1	2	0.031	-2.00	-1.31	-1.23	-0.66	-0.59	-0.04	-0.25	0.00	-0.26
EFK_22.3	<2mm	1	3	5.01	-0.36	-0.23	-0.23	-0.10	-0.09	-0.01	-0.06	0.02	-0.03
	<125um	1	2	34.4	0.30	0.22	0.11	0.10	-0.03	-0.02	-0.05	-0.01	-0.08
Trib_20	<2mm	1	2	0.022	-1.29	-0.84	-0.72	-0.39	-0.25	-0.03	-0.09	0.03	-0.04
	<125um	1	2	0.201	-2.06	-1.32	-1.06	-0.66	-0.35	-0.09	-0.06	0.00	-0.01
EFK_18.2	<2mm	1	2	14.2	-0.01	0.00	-0.07	0.00	-0.07	-0.01	-0.07	0.00	-0.07
	<125um	1	2	50.3	0.05	0.07	0.02	0.07	-0.03	-0.05	-0.03	0.04	-0.05

EFK_17.8	<2mm	3	8	19.1	0.23	0.13	0.03	0.06	-0.04	0.03	-0.07	-0.01	-0.07
	<125um	3	7	43.8	0.06	0.03	-0.05	0.03	-0.07	0.01	-0.07	0.02	-0.08
Trib_16	<2mm	1	1	0.020	-2.68	-1.71	-1.54	-0.80	-0.63	-0.13	-0.26	0.05	-0.20
	<125um	1	2	0.077	-4.85	-3.22	-2.55	-1.58	-0.97	-0.05	-0.13	0.03	-0.16
EFK_13.8	<2mm	1	2	9.57	-0.03	-0.02	-0.08	0.01	-0.04	0.00	-0.07	0.01	-0.04
	<125um	1	2	24.1	-0.06	-0.02	-0.12	0.00	-0.05	-0.03	-0.10	0.01	-0.05
Trib_10	<2mm	1	2	0.049	-1.53	-1.01	-0.87	-0.48	-0.39	-0.03	-0.11	0.02	-0.13
	<125um	1	2	0.212	-2.10	-1.43	-1.17	-0.70	-0.41	0.03	-0.10	0.02	-0.05
EFK_9.8	<2mm	1	2	3.26	0.04	0.08	-0.04	0.05	-0.07	-0.08	-0.10	0.01	-0.09
	<125um	1	2	60.1	0.34	0.26	0.09	0.13	-0.06	-0.05	-0.11	0.00	-0.13
EFK_5.0	<2 mm	1	2	10.5	-0.42	-0.28	-0.32	-0.14	-0.15	0.00	-0.10	0.00	-0.08
	<125 um	1	2	18.9	0.07	0.05	-0.06	0.07	-0.10	-0.01	-0.10	0.05	-0.11

Table 2.S1: THg concentration and Hg isotope values for all sediment samples

N_1 represents the number of process replicates (i.e. combustion and transfer) whereas N_2 denotes the total number of isotope measurements for the sample during all analytical sessions.

Material	N_1	N_2	THg	$\delta^{204}Hg$	2σ	$\delta^{202}Hg$	2σ	$\delta^{201}Hg$	2σ	$\delta^{200}Hg$	2σ	$\delta^{199}Hg$	2σ	$\Delta^{204}Hg$	2σ	$\Delta^{201}Hg$	2σ	$\Delta^{200}Hg$	2σ	$\Delta^{199}Hg$	2σ
			µg/g	‰	‰	‰	‰	‰	‰	‰	‰	‰	‰	‰	‰	‰	‰	‰	‰	‰	‰
NIST SRM 1944	6	15	3.51	-0.64	0.09	-0.43	0.07	-0.33	0.07	-0.20	0.04	-0.10	0.06	-0.01	0.04	-0.01	0.04	0.01	0.02	0.01	0.06
NRC MESS-3	3	6	0.089	-2.84	0.14	-1.92	0.11	-1.48	0.12	-0.97	0.06	-0.50	0.07	0.03	0.03	-0.03	0.06	-0.01	0.02	-0.02	0.05
UM-Almaden	64			-0.86	0.08	-0.58	0.06	-0.47	0.05	-0.28	0.04	-0.17	0.04	0.00	0.12	-0.04	0.03	0.01	0.06	-0.02	0.03

Table 2.S2: Hg isotope values for UM-Almaden and standard reference materials (SRMs)
For SRMs, N_1 represents the number of process replicates (i.e., combustion and transfer) whereas N_2 denotes the total number of individual isotope measurements during all analytical sessions. For NIST SRM-1944 and NRC MESS-3, σ represents the standard error of the mean values for process replicates. For UM-Almaden, N_1 denotes the number of analytical sessions that UM-Almaden was measured and σ represents the standard deviation of the mean Hg isotope values from 64 analytical sessions between December 2011 and February 2013 during which the run concentrations were between 3 and 5 ng/g.

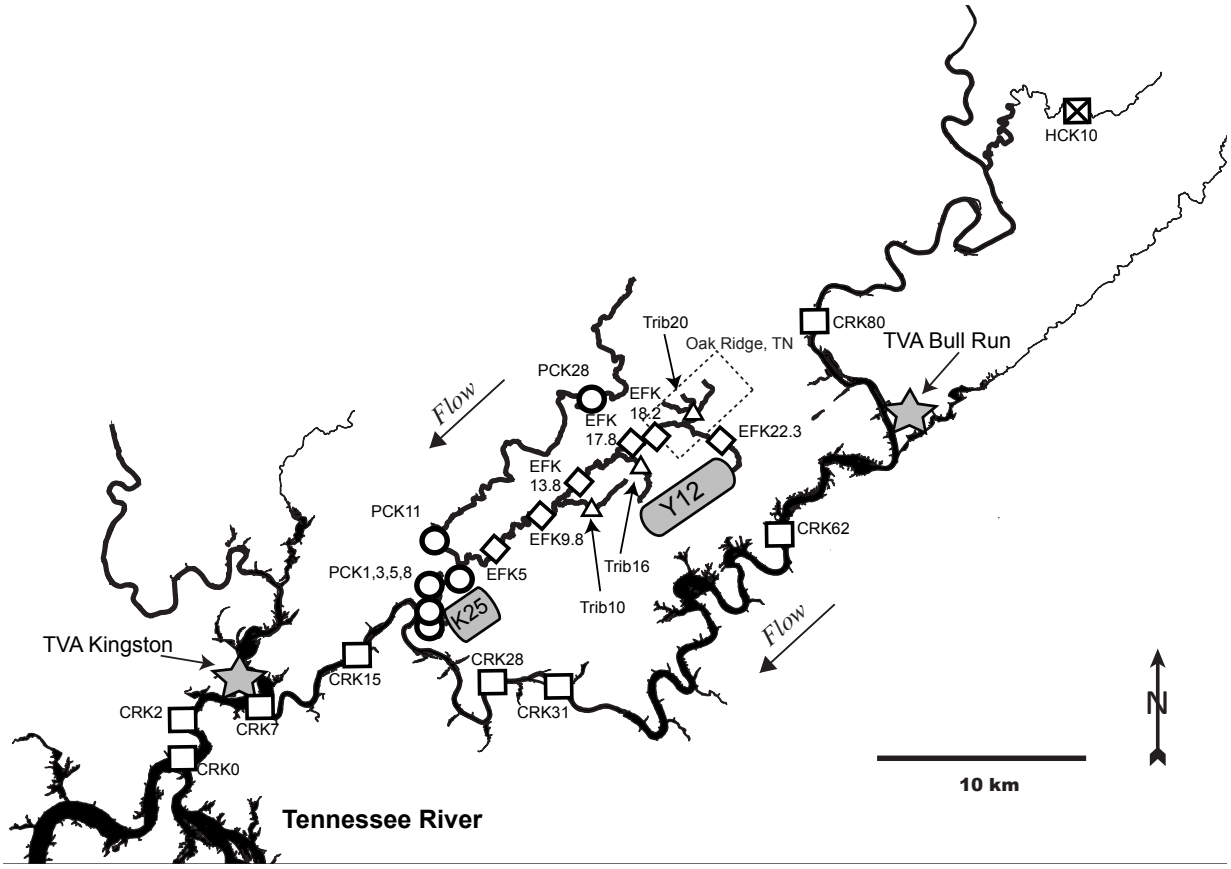

Figure 2.S1: Detailed Sampling Map
The streambed sediment sampling locations are denoted by open squares for Clinch River, circles for Poplar Creek, diamonds for EFPC, triangles for EFPC tributaries and an inset x for Hinds Creek. Sampling site identification codes are denoted next to each symbol according to the naming scheme explained in the main text (Materials and Methods). A dashed-line box denotes the approximate location of the center of the city of Oak Ridge, TN.

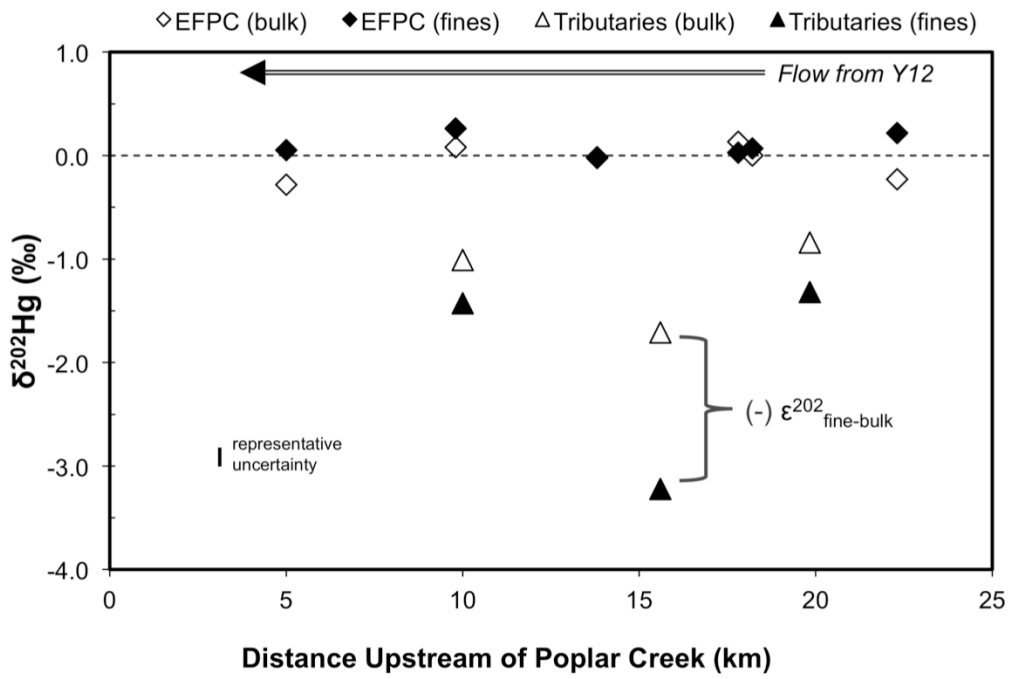

Figure 2.S2: Location vs. δ^{202}Hg for bulk and fine sediment in EFPC and its tributaries
The location (distance upstream of Poplar Creek) vs. δ^{202}Hg for bulk (<2mm) and fine (<125µm) sediments in EFPC and its tributaries. Tributary sediments are plotted at the distance at which the tributary enters EFPC (not the exact distance of the sampling location). Representative uncertainty for δ^{202}Hg (± 0.11‰ or approximately the height of the symbols) is the 2SE of replicate measurements of SRMs. The bracket is an example of the $\varepsilon^{202}_{\text{fine-bulk}}$ for Trib_16.

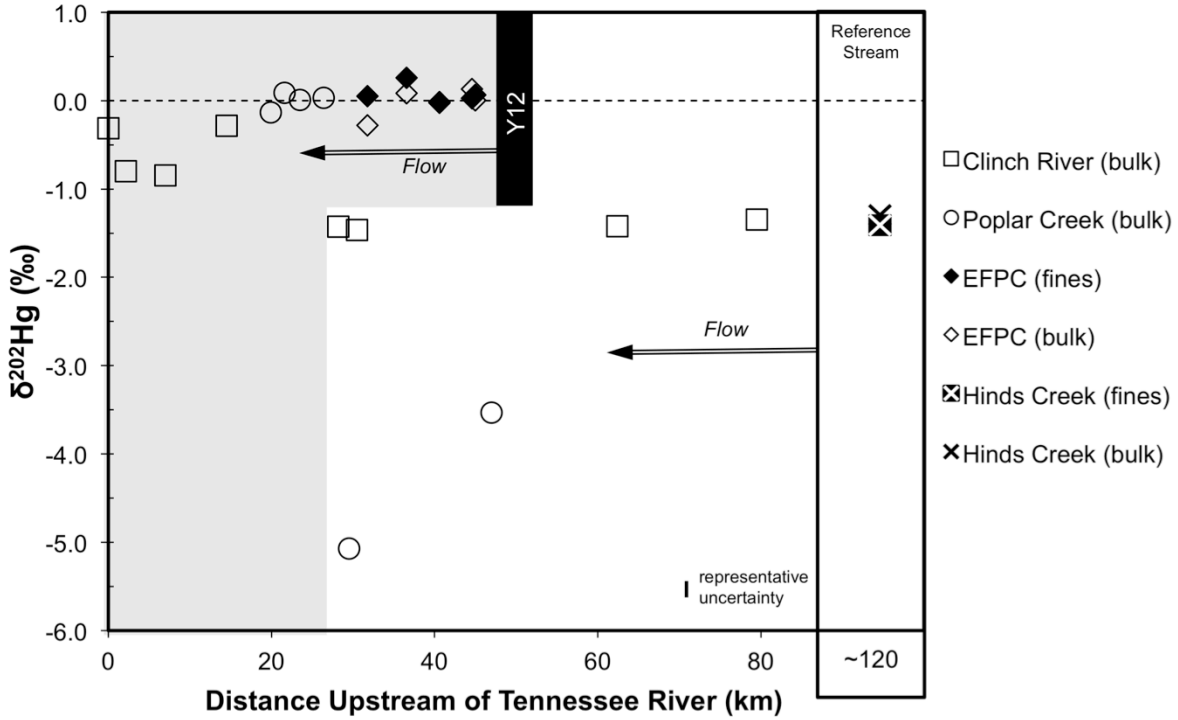

Figure 2.S3: Location vs. δ^{202}Hg for regional sediment
The location (distance upstream from the Tennessee/Clinch River confluence) vs. δ^{202}Hg for sediments from the region. Representative uncertainty for δ^{202}Hg (± 0.11‰ or approximately the height of the symbols) is the 2SE of replicate measurements of SRMs. Streamflow in all watersheds is directed towards the Tennessee River as indicated by the double-line arrows and the gray background denotes locations downstream of Y12.

CHAPTER 3: An Isotopic Record Of Mercury In San Francisco Bay Sediment

Authors: Patrick M. Donovan, Joel D. Blum, Donald Yee, Gretchen E. Gehrke, Michael B. Singer

Citation: Donovan, P. M.; Blum, J. D.; Yee, D.; Gehrke, G. E.; Singer, M. B., An isotopic record of mercury in San Francisco Bay sediment. *Chem. Geol.* **2013,** *349-350*, 87-98.

Abstract

We analyzed eight sediment cores from wetland and subtidal locations around San Francisco (SF) Bay, terrace sediment from the Yuba River, CA and precipitation from the SF Bay region. We defined the Hg isotopic composition of uncontaminated SF Bay sediment, two contributing endmember sediments contaminated by distinct Hg sources, and regional precipitation. Deep subtidal sediments with pre-mining THg concentrations (less than 60 ng/g) have δ^{202}Hg of -0.98 ± 0.06‰ and Δ^{199}Hg of 0.17 ± 0.03‰ (1 s.d.; n = 5). The δ^{202}Hg of subtidal sediment in SF Bay systematically changed between pre-mining, circa 1960, and surface sediment. In circa 1960 sediment δ^{202}Hg ranges from -0.63 to -0.32 ‰ (±0.10‰) with higher δ^{202}Hg in the south and lower δ^{202}Hg in the north; however in surface sediment δ^{202}Hg is nearly constant and averages -0.52 ± 0.04‰ (1 s.d.; n=6). These latter values for SF Bay surface sediment are similar to those for terrace sediment along the Yuba River that have δ^{202}Hg of -0.57 ± 0.10‰ and Δ^{199}Hg of 0.05 ± 0.01‰ (1 s.d.; n=2) and is consistent with sediment contaminated by a metallic Hg source that was derived from Hg ore in the

California Coast Ranges and used in Sierra Nevada gold mining. Wetlands adjacent to south and central SF Bay have high THg in deeper sediment layers (>3000 ng/g) that vary by ~0.6‰ in δ^{202}Hg, presumably reflective of various anthropogenic Hg sources. The three sediment endmembers (metallic Hg, Hg mining and background Hg) were defined using δ^{202}Hg and THg concentrations. Based on the estimated contribution of endmember sediment to subtidal and intertidal locations, we suggest that the subtidal Hg stable isotope record in sediment cores is consistent with historical sediment transport to, and deposition in, SF Bay. Thus, Hg stable isotopes can be used to trace sediment transport in locations that are impacted by multiple anthropogenic Hg sources.

3.1 Introduction

A wide variety of contaminants have been delivered to the San Francisco (SF) Bay estuary over the past 150 years.[1-4] Mercury (Hg) appears as one of the first anthropogenic metals present in the sediment record,[2, 5, 6] with Hg mining and gold (Au) mining considered the most likely early sources of Hg in the Bay.[5, 7-11] Rich deposits of the Hg ore mineral cinnabar (HgS) in the California Coast Range allowed the growth of an industry to mine and process Hg ore into metallic elemental Hg (Hg^0), which was widely used to enhance Au recovery through amalgamation during hydraulic mining of placer deposits in the Sierra Nevada Mountains.[9, 10, 12] Although the use of Hg in Au mining decreased in California during the 20th century, especially following the Sawyer decision that stopped hydraulic Au mining in 1884, the use of Hg by other industries (e.g., chloralkali, petrochemical) and in products such as fungicides and slimicides, became more common.[3] Throughout SF Bay, total mercury (THg) concentrations in surface sediment remain

elevated 2 to 8 times pre-mining levels.[5-7, 11, 13, 14] A portion of the Hg in sediment may be converted to neurotoxic monomethyl mercury (MMHg), contributing to elevated Hg concentrations in various trophic levels of aquatic biota and posing a risk to humans and wildlife.[15-20] Estimating the contribution of Hg to sediment in SF Bay from an array of sources is complicated because of its widespread use and changes in sediment transport as a result of watershed modification during the past 150 years.[14, 21-24] This study utilizes Hg stable isotopes to assess the spatial and temporal distribution of anthropogenic Hg in SF Bay sediment and builds on prior work in the region by providing a discriminant tracer of various sediment sources.

Mercury has seven stable isotopes (196, 198, 199, 200, 201, 202, and 204 amu), and the isotopic composition of Hg in environmental matrices can now be determined with high precision.[25, 26] Mercury stable isotopes are becoming a useful tool to characterize sources and identify biogeochemical transformations of Hg in the environment. For example, the isotopic composition of a variety of Hg-bearing ores has been determined[13, 26-31] along with commercially available metallic Hg.[25, 32-34] Stable isotopes of mercury have also been employed to trace geogenic, urban, industrial and atmospheric sources of Hg in the environment[28, 30, 31, 35-39] and estimate the relative contribution of different Hg sources using endmember mixing calculations.[26, 35, 40]

An initial study of Hg stable isotopes in SF Bay sediments was conducted by Gehrke et al. (2011a). These authors measured Hg in intertidal surface sediment throughout SF Bay and investigated the isotopic composition of roasted Hg mine waste (calcine) and unroasted Hg ore from a mine in the California Coast Range. Gehrke et al. (2011a) also documented a present-day spatial gradient in Hg isotopic composition throughout SF Bay

and demonstrated that calcine and unroasted Hg ore have significantly different Hg isotopic compositions. Based on this spatial gradient the authors suggested that Hg in SF Bay intertidal surface sediment is dominated by two regional anthropogenic sources: Hg mining (entering southern SF Bay) and Au mining (entering northern SF Bay). Gehrke et al. (2011) did not constrain the pre-mining sediment Hg isotopic composition, nor did they explore historical variations in the isotopic composition of Hg in SF Bay. In this study, we use eight sediment cores, dated from pre-1900 to 2006, to constrain the pre-mining sediment Hg isotopic composition. We use Yuba River terrace sediment to characterize the Hg isotopic signature of sediment predominantly contaminated by Au mining. To assess the influence of Hg from precipitation on sediment Hg stable isotopes, we analysed precipitation collected at three locations in the SF Bay area. Finally, we use the variation in sediment Hg isotopic composition in sediment cores to estimate the present day and historical contribution of sediment to locations in SF Bay.

3.2 Materials and Methods

3.2.1 Environmental Setting

San Francisco Bay is a large estuary with a surface area of 1240 km^2 and an average water depth of 6 meters.[41] It is separated into two hydrologic regions, the northern reach and the southern reach, which converge and open to the Pacific Ocean in the Central Bay.[4] The northern reach can be divided into three sub-basins: the Sacramento-San Joaquin Delta, Suisun Bay, and San Pablo Bay. The southern reach includes two sub-basins: South Bay and Lower South Bay.[41] The watersheds that contribute to SF Bay are important

because changes in freshwater flow and suspended sediment delivery can significantly alter circulation and sediment dynamics within the Bay.[42-44] The Sacramento-San Joaquin (SSJ) watershed, which flows into north SF Bay, covers nearly 40% of the land area of the state of California and has been the source of up to 90% of freshwater input and 80% of sediment input to SF Bay.[41] However, as a result of water diversion projects, freshwater discharge from the SSJ watershed is now less than 40% of pre-1850 levels[1] and the SSJ delta currently contributes only 40-60% of the total sediment delivered to SF Bay.[42, 45] There is much evidence of large-scale sediment deposition in floodplains and floodways of the Sacramento Valley well upstream of the delta.[22, 24, 46, 47] The south SF Bay watersheds, including Guadalupe River and Coyote Creek, provide less than 10% of freshwater input to SF Bay;[3] however, small tributaries surrounding SF Bay are important sources of sediment to nearby wetlands and near shore locations.[45]

3.2.2 Sample Locations

Six sediment cores from subtidal locations, with overlying water depths between 2.3 and 7.8 meters, and two sediment cores from wetlands adjacent to SF Bay were analyzed for Hg stable isotope composition for this study (Figure 3.1). Additional details on sediment coring and sampling are provided in Yee et al. (2011). One core was obtained from each subtidal site in Lower South Bay (LSB), Central Bay (CB), San Pablo Bay (SPB), and Suisun Bay (SU) and two subtidal cores were obtained from South Bay (SB1, SB2). One wetland core, termed Coyote Creek (CoW), is located in the southern slough region. This wetland is directly downstream of the New Almaden Hg mining district, the largest historical producer of Hg in the United States, which operated between 1847 and the early 1970's.[5, 8,

[48] The second wetland core is located at the outlet of Damon Slough (DaW) and is adjacent to San Leandro Bay, a small tidally influenced sub-embayment in central SF Bay. To characterize the Hg stable isotope composition of sediment associated with Au mining in the Sacramento River watershed, sediment was collected at two locations within a large riverside terrace along the Yuba River. This site is a dissected mine tailings fan from a tributary basin (Dry Creek), which represents an early phase of hydraulic Au mining without subsequent remobilization.[24] The Yuba and Bear Rivers, tributaries of the Feather River, which eventually joins the Sacramento River and north SF Bay (Figure 3.1), were sites of concentrated Au mining activity in the late 19th Century. Hydraulic Au mining in the Yuba River watershed displaced large volumes of Hg-laden sediment into piedmont and lowland valleys, some of which remains upstream behind flood control structures or as debris fans.[7, 21, 22, 24, 49-51] In addition to sediment, bulk precipitation samples were collected at three locations (Moss Beach, Oakland, San Jose) in the SF Bay area between December 2008 and March 2009 (Figure 3.1).

3.2.3 Sample Handling and Analytical Methods

3.2.3.1 Core Sample Dating and Selection for Hg Isotope Analysis

Sediment cores were dated using ^{137}Cs and ^{210}Pb radiometric methods and analyzed for a suite of trace elements (Ag, Al, As, Cd, Cr, Cu, Fe, Mn, Ni, Pb, Se, and Zn) and sediment quality parameters (e.g., moisture content, Total Organic Carbon, Total Nitrogen) as previously described by Yee et al. (2011). In each sediment core, at least three 2.5 cm depth intervals were measured for Hg stable isotopic composition. Typically, the three intervals consisted of surface sediment (0-2.5 cm), sediment at the greatest depth available in the

core (greater than 67 cm), and sediment closest to the first appearance of ^{137}Cs, reflective of bomb (nuclear weapon) testing in the 1950's and 1960's. Because of the non-continuous depositional history of subtidal locations exact ages were not used for subtidal core intervals. However, Yee et al. (2011) suggested that the depth of ^{137}Cs appearance in subtidal locations marks the maximum depth of downward migration of ^{137}Cs, and that sediment below this maximum depth has not been exposed to the surface since at least the mid-1950's, when bomb testing began. Based on this interpretation, the sediment interval analyzed that is closest to the ^{137}Cs appearance in subtidal cores will hereafter be referred to as "circa 1960" sediment or "c. 1960" sediment. For wetland cores there is evidence of a sharp ^{137}Cs peak in subsurface sediment, suggesting little sediment re-suspension or bioturbation. In wetland cores, an approximate age was assigned to each sediment interval by Yee et al. (2011) based on estimated accumulation rates with the ^{137}Cs peak representing deposition in the early 1960's – the period of maximum ^{137}Cs deposition in the SF Bay area.[52]

3.2.3.2 Sediment Processing, Combustion and THg Concentration

Sediment intervals of SF Bay cores were stored frozen in glass containers and prior to Hg analysis, sediment was freeze-dried and ground to a fine powder with a clean agate mortar and pestle. Terrace sediment from the Yuba River, CA was dried and then sieved to <63 μm and stored in glass vials prior to analysis. For each sample analyzed, at least 200 mg of sediment was placed in a two-stage furnace and progressively heated to release all Hg, following previously described methods.[13, 36, 53, 54] In brief, Hg was released from the sample matrix as Hg^0 as the sample was gradually heated to 750°C over six hours. Mobilized Hg^0 was carried in a flow of O_2, through a second furnace held at 1000°C, after

which it was sparged into a 1% $KMnO_4$/1.8M H_2SO_4 trapping solution, thus oxidizing Hg^0 to Hg^{2+}. Sediment THg concentrations were determined using cold vapor atomic absorption spectroscopy (CV-AAS; Nippon MA-2000) based on the concentration of Hg in the trapping solution and the mass of dry sediment placed in the combustion furnace. The sediment THg concentration for subtidal and wetland sediment cores via combustion typically yielded THg concentrations within 30% of reported THg concentrations for sub-samples of the same sediment measured by wet acid digestion at Moss Landing Marine Lab (Yee et al., 2011). The THg concentration of Yuba River sediment measured by combustion, as described here, agreed to within 10% of the THg concentration measured by cold vapor atomic fluorescence spectroscopy (CVAFS; Tekran) by EPA Method 1631 at the USGS in Menlo Park, CA. The sediment standard NRC MESS-3 (marine sediment reference material) was combusted and processed alongside samples in an identical manner. The combustion yield of Hg in NRC MESS-3 averaged 94 ± 4% and was always within error of the certified THg concentration (91 ± 9 ng/g). Prior to isotopic analysis the original trapping solution was reduced with $SnCl_2$ and all Hg was purged from the original solution into a secondary trapping solution (1% $KMnO_4$/1.8M H_2SO_4) to minimize matrix effects during isotopic analysis that might be associated with combustion products. The yield for the secondary trapping procedure was always greater than 92%, and typically greater than 95%. The secondary purge and trap yield was at least 96% for all NRC MESS-3 aliquots that were analyzed.

3.2.3.3 Precipitation Hg Separation and THg Concentration

At each location, precipitation collectors were assembled using a borosilicate glass funnel (collection area of 181 cm^2), Teflon adaptor with glass vapor lock (to prevent

evaporation), and a 1L Teflon bottle.[55] Collectors were located away from overhanging obstacles and funnels were left open for periods of 3 to 33 days, depending on rainfall amount, collecting multiple precipitation events into a single, pre-acidified (1mL trace metal grade hydrochloric acid) 1L Teflon bottle. A total of six bottles were collected at each site between December 2008 and March 2009, and each bottle was preserved to a final concentration of 1% BrCl upon return to the laboratory. A small (5 ml) aliquot from each collection bottle was analyzed by CV- AAS (Nippon MA-2000) to obtain a volume-weighted average THg concentration for each site. Precipitation samples from each site were combined using purge and trap methods, to obtain sufficient Hg for stable isotope measurements, as described elsewhere.[56] Briefly, the combination of precipitation samples required slowly pumping the entire sample into a mixing chamber with 5% $SnCl_2$ to reduce all Hg to Hg^0. The Hg^0 was separated using a frosted tip phase separator and carried into an oxidizing 1% $KMnO_4$/1.8M H_2SO_4 trapping solution. For Oakland and San Jose collection locations, all six 1L samples were combined into a single trap that represented the entire winter 2009 sampling period. Due to greater precipitation volume at Moss Beach, the six 1L samples collected were combined into two separate traps representing the first half (MB1; January – February 2009) and the second half (MB2; March 2009) of the collection period. The THg concentrations of the final trap solutions were measured prior to Hg stable isotope analysis. Although we expect the whole sample THg concentration (in the oxidizing 1% $KMnO_4$ trap) to be the most accurate measurement, an estimated yield was calculated based on the initial volume weighted average and the final trap THg concentrations. Three of the four estimated sample yields were between 86% and 99% (MB-1, San Jose and Oakland), however one sample (MB-2) had an estimated yield of 152%. The high apparent

yield suggests that the initial 5mL aliquot measured had a lower THg concentration than the entire sample after processing, which can occur from incomplete reduction of Hg in the CV-AAS due to interferences in the original sample matrix.

3.2.3.4 Hg Stable Isotope Analysis

The Hg isotopic composition of the trap solution for each sample was measured using Cold Vapor-Multi Collector-Inductively Coupled Plasma–Mass Spectrometry (CV-MC-ICP-MS; Nu-Instruments). Solutions were partially neutralized with NH_2OH then diluted to a concentration between 1 and 5 ng/g. Hg^{2+} was reduced on-line by the addition of $SnCl_2$ and Hg^0 was separated from the solution using a frosted tip liquid-gas separator. Instrumental mass bias was corrected by the introduction of an internal Tl standard (NIST 997) as a dry aerosol to the Ar gas stream and by sample-standard bracketing using NIST 3133 with the same concentration and solution matrix as that of the sample.[25] The Hg stable isotope composition is reported in delta notation in units of permil (‰) and referenced to the NIST 3133 standard.[25] Mass dependent fractionation (MDF) is calculated by comparing the $^{202}Hg/^{198}Hg$ ratio of the sample to the $^{202}Hg/^{198}Hg$ ratio of the NIST 3133 bracketing standards and is reported as $\delta^{202}Hg$ using equation [1].[25] Mass independent fractionation (MIF) is a measurement of the deviation from the theoretical MDF and is reported in permil (‰) as $\Delta^{199}Hg$ and $\Delta^{201}Hg$ using equations [2] and [3]:[25]

1. $\delta^{202}Hg = 1000 * ([(^{202}Hg/^{198}Hg)_{sample}]/[(^{202}Hg/^{198}Hg)_{NIST3133}] - 1)$.
2. $\Delta^{199}Hg = \delta^{199}Hg - (\delta^{202}Hg * 0.2520)$
3. $\Delta^{201}Hg = \delta^{201}Hg - (\delta^{202}Hg * 0.7520)$

Procedural blanks and replicates of NRC MESS-3 (n=4) were processed alongside sediment samples in an identical manner. Procedural blanks averaged 0.285 ng Hg per 24 gram trap solution (n=5) whereas samples contained between 80 and 250 ng Hg. Total recovery of the NRC MESS-3 process replicates averaged 95 ± 4% (n=4) and the Hg isotopic composition of NRC MESS-3 was δ^{202}Hg = -1.93 ± 0.10‰, Δ^{201}Hg = -0.02 ± 0.07‰ and Δ^{199}Hg = 0.01 ± 0.02‰ (mean ± 2 s.d.; n=4). A procedural standard (NIST-3133) of similar Hg concentration as precipitation samples demonstrated no measureable fractionation upon pre-concentration into the trapping solution (1% $KMnO_4$/1.8M H_2SO_4) with an 85% process yield (δ^{202}Hg of 0.02‰ and Δ^{199}Hg of 0.02‰). Precipitation procedural blanks never accounted for more than 1% of Hg in the final trap solution.

The in-house standard UM-Almaden was monitored over the course of 46 analytical sessions during which sediment analyses were completed and had a long-term average isotopic composition of δ^{202}Hg = -0.58 ± 0.05‰, Δ^{201}Hg = -0.03 ±0.04‰ and Δ^{199}Hg =-0.02 ± 0.04‰ (mean ± 2 s.d.; n=46). The uncertainty associated with sediment Hg stable isotope measurements is reported as the greater of either the uncertainty of replicate analysis of NRC MESS-3 or the long-term analytical uncertainty associated with UM-Almaden. Therefore, the 2 s.d. analytical uncertainty for sediment Hg stable isotope measurements in this study is δ^{202}Hg = ±0.10‰, Δ^{201}Hg = ±0.07‰, and Δ^{199}Hg = ±0.04 ‰. UM-Almaden was analyzed multiple times at identical Hg concentrations as the precipitation samples that were analyzed (1.7 and 3.1 ng/g) during the same session. UM-Almaden at a Hg concentration of 1.7 ng/g had an average isotopic composition of δ^{202}Hg = -0.56 ± 0.14‰, Δ^{201}Hg = -0.12 ±0.15 ‰ and Δ^{199}Hg =-0.03 ± 0.11‰ (mean ± 1 s.d.; n=4). UM-Almaden at a

concentration of 3.1 ng/g had an average isotopic composition of δ^{202}Hg = -0.57 ± 0.05‰, Δ^{201}Hg = -0.04 ±0.05 ‰ and Δ^{199}Hg = 0.00 ± 0.04‰ (mean ± 1 s.d.; n=5).

3.3 Results and Discussion

3.3.1 Mercury Isotopic Composition of Subtidal Sediment

In five of six subtidal sediment cores the THg concentration is between 28 and 58 ng/g at sediment depths greater than 100 cm (Figure 3.2; Table 3.1). The THg concentration in these five subtidal cores agrees with established pre-mining THg concentrations from north SF Bay sediment cores (60 ± 10 ng/g)[6] , San Pablo Bay sediment cores (30 to 80 ng/g)[7] and in wetland sediment cores from south SF Bay (80± 30 ng/g).[5] In the five subtidal cores with THg less than 60 ng/g, δ^{202}Hg is -0.98 ± 0.06‰ and Δ^{199}Hg is 0.17 ± 0.03‰ (1 s.d.; n = 5) with no measureable difference in Hg isotopic composition among the five different locations. The δ^{202}Hg of pre-mining sediment is within error of pre-anthropogenic Mediterranean sapropels (-0.91 ± 0.15‰; 1s.d., n=5)[36] and off-shore sediment from the Gulf of Mexico (-1.00 ± 0.11‰; 1s.d., n=6)[37] In the subtidal sediment core from Suisan Bay (SU), the THg concentration is greater than 140 ng/g throughout the core (Figure 3.2) and there is uncertainty in depositional age estimates.[52] Due to lack of age control, and because THg does not reach a pre-mining concentration at depth, results from this core are not included in further discussion.

In c. 1960 and surface sediment intervals from subtidal locations, the THg concentration is enriched 2 to 6 times over that of pre-mining THg (Figure 3.2; Table 3.1). There is no obvious spatial trend in THg concentrations, and THg concentration is

independent of %TOC (r^2 = 0.09, p= 0.33). The Hg stable isotope composition of subtidal sediment systematically changes between pre-mining, c. 1960 and surface sediment. In c. 1960 sediment, δ^{202}Hg has a range between –0.63 and -0.32‰ with the highest δ^{202}Hg in LSB and lower δ^{202}Hg in SPB and CB (Figure 3.3), following the same geographic trend as observed in intertidal surface sediment.[13] The spatial and temporal variation in sediment δ^{202}Hg is not correlated with %TOC (r^2 = 0.02, p=0.53) or other ancillary sediment chemistry parameters. Interestingly, subtidal surface sediment does not exhibit any spatial variation in δ^{202}Hg. Rather, subtidal surface sediment has consistent δ^{202}Hg (-0.52 ± 0.04‰) and Δ^{199}Hg (0.07 ± 0.03‰; 1 s.d.; n = 6) regardless of location or THg concentration.

3.3.2 Mercury Isotopic Composition of Wetland Sediment

3.3.2.1 Coyote Creek Wetland

In the deepest core samples from the Coyote Creek wetland (CoW), in sediment deposited pre-1943, the THg concentration is 660 ng/g, which is significantly higher than the pre-mining THg concentration throughout SF Bay (<110 ng/g). In sediment deposited between the early 1940's (98.75 cm) and the mid 1950's (78.75 cm), THg increases from 720 ng/g to a maximum of 3,200 ng/g and then decreases to 330 ng/g near the surface (Figure 3.4). The elevated THg concentration in CoW subsurface sediment is consistent with other wetlands in south SF Bay, such as Alviso Slough and Triangle Marsh.[5, 13, 57] In Triangle Marsh, peak THg (~1,200 ng/g) also occurs in mid-20th century sediments and has been attributed to a combination of increased Hg mining activity, changes in watershed hydrology, and land subsidence in the area.[5] In CoW sediment, the THg peak coincides with

a 0.4‰ shift in δ^{202}Hg from -0.20‰ to +0.21‰ (Figure 3.4). The δ^{202}Hg in the highest THg sediment measured in CoW (this study) and in Alviso Slough[13] is ~0.2‰ higher than the only Hg mine waste analyzed from the region (Figure 3.5)[13] During the leaching of Hg mine waste the more soluble byproduct species of Hg are mobilized.[58] Leachates of calcine may contain Hg with up to ~1.2‰ higher δ^{202}Hg than the parent calcine [29]. Soluble Hg will associate quickly with particles, such as iron oxyhydroxides, and travel downstream via the particulate phase.[58] As a result, the δ^{202}Hg of sediment in CoW can be explained by the isotopic variation of the calcine and its leachates that have been mobilized and transported to downstream wetlands. Thus, we suggest that the subsurface sediment in the Coyote Creek wetland is most representative of the isotopic composition of sediment heavily impacted by Hg mine waste that has been transported to SF Bay.

3.3.2.2 Damon Slough Wetland

Sediment at 69 cm depth, and with THg of 23 ng/g, in Damon Slough Wetland (DaW) corresponds to deposition before 1911 and has δ^{202}Hg of -1.08 ‰ and Δ^{199}Hg of -0.24‰ (Figure 3.6), which is nearly identical to subtidal sediments with similar THg concentrations (Figures 3.5 & 3.7). An indistinguishable Hg isotopic composition for low THg (23 ng/g) wetland sediment and low THg (<60 ng/g) subtidal sediment suggests a similar origin for pre-mining Hg in sediment. Sediment is enriched above pre-mining THg concentrations at depths shallower than 40 cm, with the highest THg concentration in DaW (3,100 ng/g) occurring at 19 cm (~1940's), followed by a decrease up-core to 600 ng/g in near-surface sediment (Figure 3.6). The THg maximum in DaW coincides with a shift in δ^{202}Hg; the highest THg sediment (1440 and 3140 ng/g) has the highest δ^{202}Hg (-0.39 and -0.42‰, respectively; Figure 3.6). Subsurface sediments with high THg concentration in

DaW is consistent with previously reported high concentration subsurface sediment in nearby San Leandro (SL) Bay[59] and the δ^{202}Hg of DaW surface sediment (-0.50‰) is within error of previously measured intertidal surface sediment in San Leandro Bay (-0.53‰ and -0.59‰; [13]

Although peak THg concentrations in DaW and CoW are observed in similar age sediment (between 1940 and 1960), and peak THg concentrations are similar (3140 and 3220 ng/g, respectively), the δ^{202}Hg of high THg DaW sediment is ~0.6‰ lower than high THg sediment in CoW (-0.42‰ and +0.21‰, respectively; Table 3.1). The lower δ^{202}Hg of DaW subsurface sediment could be the result of the accumulation of Hg from a discrete Hg source in DaW at the same time as Hg accumulation in CoW. Alternatively, the δ^{202}Hg of DaW sediment could be explained by the mixing of regional Hg sources, with significantly different δ^{202}Hg, emanating from north and south SF Bay, followed by rapid deposition in wetlands adjacent to SF Bay. If rapid deposition of regional Hg sources is responsible for the high THg wetland sediment, we would expect high THg in similarly aged sediment in other wetlands adjacent to SF Bay. However, sediment THg peaks are small or not observable in the other wetlands sampled for this study.[52] Comparatively high THg concentration in intertidal sediments from SL Bay,[13] coupled with high subsurface THg in DaW (this study) and SL Bay,[59] suggests that at some time a local Hg source may have contributed Hg to sediment in SL Bay and DaW.

No Au or Hg mines are present in the four small watersheds that contribute to San Leandro Bay. Instead, most of the surrounding land use is urban or industrial and a variety of industries that use Hg have been present since the mid-19th century. For example, the Oakland, CA Clorox plant, located ~0.6 km from San Leandro Bay, used an electrolytic Hg

cell (containing Hg^0) to produce chlorine and caustic soda from 1919 to 1957.[3, 60] Although the Hg-cell process ceased operation in 1957, Hg contamination of a perched groundwater zone exists below the facility and high THg concentrations persist in the surrounding soil.[60] The Oakland Clorox facility is one example of the possible remnant industrial Hg sources that surround San Leandro Bay, however we do not have evidence that this is the primary source of Hg in San Leandro Bay.

If the Hg in DaW is from the industrial use of metallic Hg then DaW sediment should reflect the Hg isotopic composition of the metallic Hg source plus any additional MIF or MDF that might have been imparted by biogeochemical transformation and loss of Hg from the sediment (e.g., volatilization). When the recovery of Hg^0 from Hg ore is efficient, the isotopic composition of the metallic Hg product will be indistinguishable from the Hg ore itself.[31] The isotopic composition of Hg ores from across California is -0.64 ± 0.84‰ (1s.d., n=91)[27] and Hg ore specifically from the New Idria Hg mine has $\delta^{202}Hg$ of -0.38 ± 0.07‰ (1s.d., n=2).[13] Thus, the high THg subsurface sediment in DaW (with $\delta^{202}Hg$ of -0.4‰) is consistent with metallic Hg recovered from California Coast Range Hg ore. The DaW wetland sediment core is an example of the challenge in tracing Hg in sediment when local Hg sources are present but regional Hg sources have been spatially distributed.

3.3.3 Mercury Isotopic Composition of Yuba River Sediment

The Yuba River is the tributary basin of the Sierra Nevada foothills most heavily impacted by Au mining.[61] We analyzed two sediment samples from a riverside terrace along the Yuba River, CA. In Yuba River terrace sediment the THg concentration is 3180 and 5440 ng/g, $\delta^{202}Hg$ is -0.50‰ and -0.64 ‰ and $\Delta^{199}Hg$ is 0.04‰ and 0.05‰,

respectively (Figure 3.5; Table 3.1). Metallic Hg was used for placer Au mining in the Sierra Nevada and most of the Hg used came from California Coast Range Hg ore.[9] The Hg stable isotope composition of Yuba River sediment is similar to the average isotopic composition of Hg ore deposits from throughout the California Coast Range (δ^{202}Hg of -0.64 ± 0.84‰; 1 s.d., n= 91).[27] As mentioned, efficient recovery of Hg^0 from Hg ore would result in no difference in δ^{202}Hg between the Hg^0 product and the Hg ore.[31] Mercury released to the environment as Hg^0 during Au mining will undergo biogeochemical transformations (i.e. vaporization, dissolution, evaporation, oxidation, etc.) as it becomes particle bound and is incorporated into sediment. The Hg stable isotope composition of sediments contaminated by Au mining could therefore be affected by fractionation during loss of mercury from sediments. Nonetheless, the Hg stable isotope composition of Yuba River sediments is consistent with what can be expected of metallic Hg^0 recovered from California Coast Range Hg ore that was used in Sierra Nevada placer Au mining and became well mixed with displaced hydraulic mining sediments.

Sediment from the Cosumnes River, a tributary of the Mokelumne River that flows into the Sacramento/San Joaquin Delta farther south, was previously used to estimate the stable isotope composition of Hg used during Au mining in the Sierra Nevada foothills,[13] but this system was far less impacted by hydraulic mining. Surface sediment from the Cosumnes River has THg between 65 and 419 ng/g and δ^{202}Hg between -0.75 and -0.91‰ (Gehrke et al., 2011a). Although THg in sediment from marshes adjacent to the Cosumnes River is elevated (303 and 419 ng/g), streambed sediment THg is much lower (65 and 114 ng/g). Yuba River terrace sediment THg concentrations are at least seven times higher (3180 and 5440 ng/g) than any Cosumnes River sediment previously analyzed. The δ^{202}Hg

of Cosumnes River streambed sediment has lower δ^{202}Hg (-0.88 and -0.91‰) when compared to the marsh sediment (-0.75‰) and δ^{202}Hg is significantly lower than Yuba River terrace sediment (-0.57 ± 0.10‰; 1 s.d., n=2). Only the Cosumnes River marsh sediment is enriched above pre-mining THg concentration, and the δ^{202}Hg of Cosumnes River streambed sediment resembles pre-mining sediment in subtidal SF Bay (Figure 3.5). Therefore, Consumes River sediment is not an ideal representation of highly contaminated sediment predominantly impacted by Au mining. Instead, we suggest that Yuba River terrace sediment is consistent with, and a better representation of, the Hg stable isotope composition of sediment contaminated by metallic Hg that was used for Au mining.

3.3.4 Mass Independent Fractionation in SF Bay Sediment

The Δ^{199}Hg observed in sediment is the sum of the Hg isotopic composition of Hg released to the environment and any additional MIF that has occurred in the environment. The magnitude of Δ^{199}Hg is directly proportional to the amount of photochemical reduction that has taken place during environmental exposure.[62, 63] The Δ^{199}Hg observed in pre-mining, low THg (<60 ng/g), downcore (>100 cm) SF Bay sediment (0.17 ± 0.03‰; 1s.d, n=5) is similar to open ocean sediment on the Central Portuguese Margin (0.09 ± 0.04‰; 1s.d., n=8)[64] and mid-Pleistocene sapropels from the Mediterranean Sea (0.11 ± 0.03‰; 1s.d., n=5),[36] neither of which is impacted by anthropogenic Hg sources. We suggest that the isotopic composition of Hg in deep, pre-mining SF Bay sediment is consistent with Hg in seawater that has undergone significant photoreduction (>10%), enriching the odd isotopes of Hg in the residual Hg^{2+} pool such that positive Δ^{199}Hg is preserved in sediment.[36, 64]

In all sediment from CoW, Δ^{199}Hg is between -0.03 and 0.07‰ and consistent with adjacent sediment in Alviso Slough and upstream mine waste. In DaW, however, all sediment has significant positive Δ^{199}Hg (0.11 to 0.24 ‰; Figure 3.7). Metallic Hg used in industrial processes and Au mining around SF Bay is likely derived from CA Coast Range Hg ore that has not previously been exposed at the Earth's surface and is, therefore, unlikely to exhibit significant Δ^{199}Hg. However, Δ^{199}Hg has been observed in some Hg-bearing ore minerals[29] and spahlerite ores[28] and we cannot rule out the possibility that a metallic Hg source, with positive Δ^{199}Hg, contributes Hg to DaW. The photochemical cycling of Hg in SF Bay wetlands likely varies in response to tidal resuspension, periodic drying, variable sunlight exposure and changing chemical conditions. If the Δ^{199}Hg in DaW sediments is purely the result of photochemical reduction then, based on experimental data (Bergquist and Blum, 2007), we infer that 10 to 25% of the Hg^{2+} pool has been photochemically reduced and evaded. It is plausible that significant photochemical reduction of Hg occurs during transport to the wetland, during resuspension within the wetland or during seasonal drying that increases sunlight exposure to wetland surfaces. Although both CoW and DaW likely experience similar periodic sunlight exposure, there is a much higher sediment accretion rate in CoW,[52] which may reduce the time that sediment remains in the photochemically active zone prior to burial. Additionally, DaW sediment has a smaller proportion of fine (<63μm) sediment and a greater %TOC compared to CoW.[52] The presence of DOC can facilitate Hg photoreduction[65, 66] and differences in the type or amount of organic material could lead to enhanced photochemical cycling in DaW. Although it is unclear whether the significant Δ^{199}Hg in DaW is inherited from the Hg source or a result of photochemical reduction in the environment, the Damon Slough wetland demonstrates

that significant Δ^{199}Hg can be present in sediment with high THg concentration (>1000 ng/g).

3.3.5 Mercury Concentration and Stable Isotopes in SF Bay Precipitation

The precipitation samples analyzed for Hg stable isotopes represent Hg from multiple events that were combined to integrate over one to three-month periods. The THg concentration of the precipitation samples for each site ranged from 4.7 to 9.0 ng/L and did not correlate with precipitation volume, distance from the Pacific Ocean, or site elevation. The narrow range in THg concentrations are consistent with previously reported measurements of Hg in SF Bay precipitation (6.6 to 9.7 ng/L)[67] and similar to the average THg concentration of precipitation events from coastal California and south SF Bay (6 to 12 ng/L).[68] Precipitation from the three sites, integrated over the entire winter sampling period, had an average δ^{202}Hg of 0.06 ± 0.11‰ and an average Δ^{199}Hg of 0.30 ± 0.05‰ (mean ± 1s.d.; n=3). The individual samples had a range for δ^{202}Hg between -0.01‰ and 0.19‰ and for Δ^{199}Hg between 0.16‰ and 0.35‰ (Table 3.2; Figure 3.7). The two Moss Beach samples represent Hg deposited on the California coast where a portion of the Hg is likely derived from long range transport over the Pacific Ocean.[68] Collection locations at San Jose and Oakland are in the SF Bay area and likely incorporate a mixture of long range and locally derived Hg. The Hg concentration and isotopic composition of precipitation from the coastal and SF Bay area sampling locations are similar, indicating that the long-term average Hg in precipitation at these locations is not greatly influenced by local Hg sources with distinct Hg stable isotope ratios. Thus, we interpret the range of δ^{202}Hg and Δ^{199}Hg to be a reasonable estimate of the Hg stable isotope composition of precipitation

during the winter season in the SF Bay region. A similar value for δ^{202}Hg (0.13 ± 0.13‰) and Δ^{199}Hg (0.35 ± 0.10‰) has been reported for precipitation collected on the west coat of Florida that was transported inland from the Gulf of Mexico and is believed not to have been impacted by local Hg emission sources.[69] Subtidal surface sediments in SF Bay have δ^{202}Hg (-0.52 ± 0.04‰) and Δ^{199}Hg (0.07 ± 0.03‰) values that are significantly different from the SF Bay area precipitation signal (δ^{202}Hg of 0.06 ± 0.11‰ and Δ^{199}Hg of 0.30 ± 0.05‰). In addition, precipitation Hg stable isotope ratios display no consistent spatial relationship with surface or subsurface sediments in SF Bay (Figure 3.7). Mass balance calculations suggest that atmospheric inputs of Hg are a very minor source of the total Hg flux to sediments[70] and that sediment input contributes up to 100 times more Hg to SF Bay than precipitation.[3, 67] The Hg stable isotope measurements of SF Bay area precipitation provide confirmation that Hg in precipitation is a relatively small input of Hg to sediments in SF Bay.

3.3.6 Sediment endmembers in SF Bay from δ^{202}Hg and THg

Based on the results of sediment from subtidal, wetland and terrace locations, we have characterized three sediment endmembers present in SF Bay using Hg isotopic compositions and THg concentrations (Figure 3.8). The proposed endmembers are:

1) Background sediment (Bk) represented by the average δ^{202}Hg and THg concentration of five, low THg (<60 ng/g) subtidal sediment intervals (δ^{202}Hg = -0.98‰, 1/THg = 18.0). The THg concentration is consistent with pre-mining sediment THg concentration in SF Bay[5-7] and based on the isotopic composition we interpret the Hg to be of marine or background geologic origin.

2) Sediment contaminated by metallic Hg used during Au mining (Met) represented by the average δ^{202}Hg and THg of terrace sediment from the Yuba River (δ^{202}Hg = -0.57‰, 1/THg = 0.23). The Yuba River had significant historical Au mining activity that used Hg^0 and mobilized large volumes of Hg-laden sediment. The Yuba River bulk sediment δ^{202}Hg is most consistent with metallic Hg recovered from Hg ore in the California Coast Range that was later incorporated into sediment.

3) Sediment contaminated by Hg mine waste (HM) represented by subsurface sediment from the Coyote Creek wetland (δ^{202}Hg = 0.21‰, 1/THg = 0.27), which is directly downstream of the New Almaden Hg mining district.[5, 8]

Most of the Hg transported to SF Bay is associated with sediment and delivered during high flow conditions.[71] Here we assume that Hg remains attached to sediment during river transport[58, 72, 73] and that, within SF Bay, Hg is transported primarily adsorbed to suspended sediment.[74] Based on this assumption, we have calculated the relative contribution of each endmember to subtidal locations using equations 4-6 modified from Yin et al., (2012):

Equation 4: $\delta^{202}Hg_{SED} = F_{Bk}\delta^{202}Hg_{Bk} + F_{Met}\delta^{202}Hg_{Met} + F_{HM}\delta^{202}Hg_{HM}$

Equation 5: $1/Hg_{Sed} = F_{Bk}/Hg_{Bk} + F_{Met}/Hg_{Met} + F_{HM}/Hg_{HM}$

Equation 6: $1 = F_{Bk} + F_{Met} + F_{HM}$

We acknowledge that the calculation of the percent contribution of each endmember is only a rough approximation. Here we assume that the THg concentration and Hg isotopic composition of each endmember is invariant, however the concentration of

the contaminated sediment endmembers delivered to SF Bay is likely influenced by variable amounts of dilution with uncontaminated sediment during transport to SF Bay. Nonetheless, the estimated mixtures of the sediment endmembers explain the Hg isotopic variation in all of the subtidal and intertidal sediments in this study and trends in the relative contribution of endmembers to all sediment samples appear robust.

In five subtidal cores, background sediment predominates in downcore (100-160 cm) sediment (Figure 3.9C). In c. 1960 sediment in subtidal locations, there was a small proportion (<22%) of background sediment, and sediment contaminated by metallic Hg accounted for 80% of the sediment deposited in Central Bay and San Pablo Bay locations. In c. 1960 sediment in South Bay and Lower South Bay there was a significant contribution of sediment contaminated by Hg mining (up to 37%; Figure 3.9B). In surface sediment from subtidal locations, the proportion of each sediment endmember is relatively constant and dominated by metallic Hg contaminated sediment (57% or greater contribution; Figure 3.9A). A significant contribution from both Hg mining and metallic Hg endmembers in surface sediment is evidence of a homogenous surface sediment pool in open water locations. The application of the sediment endmembers proposed here to intertidal surface sediment reported by Gehrke et al. (2011a) suggests that in intertidal locations, sediment contaminated by Hg mining is present in South SF Bay (up to 40%) with a transition to sediment contaminated by a metallic Hg source(s) in Central Bay and northward. Thus, intertidal surface sediment and subtidal c. 1960 sediment appear to have the same spatial trend in sediment endmember contribution.

3.3.7 Insight Into Sediment Transport from Hg Stable Isotopes

The Hg isotopic gradient in c. 1960 sediment is consistent with two Hg sources entering SF Bay and, based on the proposed endmembers in SF Bay sediment, the two sediment sources are similarly distributed in c. 1960 subtidal sediment and intertidal surface sediment from [13] Erosion, deposition and sediment distribution in SF Bay is controlled by the amount of sediment delivered from surrounding watersheds.[44] In addition, it is expected that the intertidal area would increase during periods of increased sediment supply and decrease when sediment supply decreased.[43, 75]

Historical changes in sediment supply have changed erosional and depositional patterns in SF Bay. In brief, in the late 1800's large volumes of sediment were mobilized in the rivers leading to the Sacramento-San Joaquin delta due to hydraulic mining operations.[61] As a result, a pulse of sediment was delivered to SF Bay and initially deposited in San Pablo Bay.[7, 11, 43] The sediment in SPB provided a large and easily eroded sediment pool[44] and gradual dispersion of the sediment pool led to net deposition in Central SF Bay between 1895–1947,[76] and in South SF Bay between 1858-1898 and 1931-1956.[77] Beginning in the early 1900's, land use changes, water diversion projects and flood control projects reduced the sediment discharge from SF Bay tributaries including the Sacramento-San Joaquin Delta.[22, 41, 42, 45, 78] Sub-basins within SF Bay shifted from depositional to erosional after depletion of the sediment pool and San Pablo Bay, Central Bay and South Bay all became erosional by the late 1950's.[43, 76, 77]

Because intertidal area growth is dependent on sediment supply[43, 75] it is likely that the intertidal area in SF Bay generally increased until the mid 1950's. Since the 1950's SPB, CB and SB became erosional, and surface sediment in subtidal regions became well

homogenized with respect to Hg isotopic composition. As a result, only the c. 1960 subtidal sediment, and not subtidal surface sediment, retained the spatial trend in δ^{202}Hg that was observed in intertidal surface sediment by Gehrke et al. (2011a). Therefore, we suggest that the sediment remaining in intertidal zones throughout SF Bay, and measured by Gehrke et al. (2011a), was likely deposited during the last period of intertidal growth in SF Bay, probably in the mid-20th century or earlier.

3.4 Conclusion

This study documents the Hg isotopic composition and THg concentration of eight sediment cores around SF Bay, Yuba River terrace sediment and precipitation from the San Francisco Bay region. We propose three sediment endmembers with distinct Hg sources, based on Hg isotopic composition and THg concentration, to explain the distribution of sediment within SF Bay. In wetlands adjacent to SF Bay in two separate locations, high subsurface THg concentrations correlate with shifts in δ^{202}Hg. In the Coyote Creek wetland, we interpret the high THg sediment, deposited in the 1950's, to be the result of Hg that was leached and transported from calcine located upstream. In the Damon Slough wetland, high THg sediment, deposited in the 1940's, is consistent with sediment contaminated by metallic Hg used in industry, but we have not attempted to identify the specific industrial source(s). We use low THg (<60 ng/g) subtidal sediment to identify the Hg isotopic composition of uncontaminated, downcore sediment. The positive Δ^{199}Hg of pre-mining sediment is consistent with Hg that has undergone significant photoreduction. We suggest that at least some of the pre-mining Hg in SF Bay sediment is of marine origin; however the contribution of marine Hg relative to geogenic Hg is unknown.

We have calculated the contribution of three sediment endmembers to subtidal and intertidal locations using a mixing model. The estimated contribution of sediment endmembers to c. 1960 subtidal sediments and present day intertidal surface sediments is similar, suggesting that intertidal sediment was deposited in the mid 20th century or earlier. The sediment endmember mixing calculations suggest that sediment contaminated by metallic Hg was delivered to SF Bay via the SSJ delta and was gradually transported throughout SF Bay, possibly supplemented with sediment contaminated by metallic Hg of industrial, non-Au mining, origin. In south SF Bay the metallic Hg contaminated sediment mixed with sediment contaminated by Hg mining (with higher δ^{202}Hg) that had been delivered to south SF Bay. The relative homogeneity of surface sediment in all subtidal locations is interpreted as the result of continual mixing of the subtidal surface sediment pool. From this study, we suggest that Hg stable isotopes can be a useful tool to assess spatial and temporal trends in sediment deposition when multiple, isotopically distinct Hg sources are present.

Acknowledgements

We thank Marcus Johnson for invaluable instruction and assistance in the operation of the CV-MC-ICP-MS. We also thank Nicole David, Connie Liao, Eric Dunlavey, Sue Hasselwander and Katie Harrold for assistance with precipitation collection. We appreciate the training, assistance and support provided by current and former members of the Michigan Biogeochemistry and Environmental Isotope Geochemistry Laboratory. This project was funded by grants to JDB and MBS from the NSF (EAR-1226741) and to JDB from the John D MacArthur Professorship.

References

1. Nichols, F. H.; Cloern, J. E.; Luoma, S. N.; Peterson, D. H., The Modification of an Estuary. *Science* **1986,** *231*, (4738), 567-573.

2. van Geen, A.; Luoma, S. N., The impact of human activities on sediments of San Francisco Bay, California: an overview. *Mar. Chem.* **1999,** *64*, (1-2), 1-6.

3. Conaway, C. H.; Black, F. J.; Grieb, T. M.; Roy, S.; Flegal, A. R., Mercury in the San Francisco estuary. In *Reviews of Environmental Contamination and Toxicology, Vol 194*, Springer: New York, 2008; Vol. 194, pp 29-54.

4. Conomos, T. J.; American Association for the Advancement of, S.; American Society of, L.; Oceanography, *San Francisco Bay: the urbanized estuary: investigations into the Natural History of San Francisco Bay and Delta with reference to the influence of man: fifty-eighth annual meeting of the Pacific Division/American Association for the Advancement of Science held at San Francisco State University, San Francisco, California, June 12-16, 1977*. The Division: San Francisco, Calif., 1979; p 493 p. : [1] leaf of plates.

5. Conaway, C. H.; Watson, E. B.; Flanders, J. R.; Flegal, A. R., Mercury deposition in a tidal marsh of south San Francisco Bay downstream of the historic New Almaden mining district, California. *Mar. Chem.* **2004,** *90*, (1-4), 175-184.

6. Hornberger, M. I.; Luoma, S. N.; van Geen, A.; Fuller, C.; Anima, R., Historical trends of metals in the sediments of San Francisco Bay, California. *Mar. Chem.* **1999,** *64*, (1-2), 39-55.

7. Bouse, R. M.; Fuller, C. C.; Luoma, S.; Hornberger, M. I.; Jaffe, B. E.; Smith, R. E., Mercury-Contaminated Hydraulic Mining Debris in San Francisco Bay. *San Francisco Estuary and Watershed Science* **2010,** *8*, (1).

8. Thomas, M. A.; Conaway, C. H.; Steding, D. J.; Marvin-DiPasquale, M.; Abu-Saba, K. E.; Flegal, A. R., Mercury contamination from historic mining in water and sediment, Guadalupe River and San Francisco Bay, California. *Geochemistry* **2002,** *2*, (3), 211.

9. Alpers, C. N.; Hunerlach, M. P.; May, J. T.; Hothem, R. L., Mercury contamination from historical gold mining in California. *Fact Sheet - U. S. Geological Survey* **2005,** *1*.

10. Nriagu, J. O., Mercury pollution from the past mining of gold and silver in the Americas. *Sci. Total Environ.* **1994,** *149*, (3), 167-181.

11. Marvin-DiPasquale, M. C.; Agee, J. L.; Bouse, R. M.; Jaffe, B. E., Microbial cycling of mercury in contaminated pelagic and wetland sediments of San Pablo Bay, California. *Environmental Geology* **2003,** *43*, (3), 260-267.

12. Rytuba, J. J., Mercury from mineral deposits and potential environmental impact. *Environmental geology (Berlin)* **2003,** *43*, (3), 326-338.

13. Gehrke, G. E.; Blum, J. D.; Marvin-DiPasquale, M., Sources of mercury to San Francisco Bay surface sediment as revealed by mercury stable isotopes. *Geochim. Cosmochim. Acta* **2011,** *75*, (3), 691-705.

14. Conaway, C. H.; Ross, J. R. M.; Looker, R.; Mason, R. P.; Flegal, A. R., Decadal mercury trends in San Francisco Estuary sediments. *Environ. Res.* **2007,** *105*, (1), 53-66.

15. Greenfield, B. K.; Jahn, A., Mercury in San Francisco Bay forage fish. *Environ. Pollut.* **2010,** *158*, (8), 2716-2724.

16. Greenfield, B. K.; Davis, J. A.; Fairey, R.; Roberts, C.; Crane, D.; Ichikawa, G., Seasonal, interannual, and long-term variation in sport fish contamination, San Francisco Bay. *Sci. Total Environ.* **2005,** *336*, (1-3), 25-43.

17. Davis, J. A.; Greenfield, B. K.; Ichikawa, G.; Stephenson, M., Mercury in sport fish from the Sacramento-San Joaquin Delta region, California, USA. *Sci. Total Environ.* **2008,** *391*, (1), 66-75.

18. Gehrke, G. E.; Blum, J. D.; Slotton, D. G.; Greenfield, B. K., Mercury Isotopes Link Mercury in San Francisco Bay Forage Fish to Surface Sediments. *Environ. Sci. Technol.* **2011,** *45*, (4), 1264-1270.

19. OEHHA. *HEALTH ADVISORY AND SAFE EATING GUIDELINES FOR SAN FRANCISCO BAY FISH AND SHELLFISH*; California, E. P. A.: 2011. http://oehha.ca.gov/fish/nor_cal/2011SFbay.html.

20. Davis, J. A.; Looker, R. E.; Yee, D.; Marvin-Di Pasquale, M.; Grenier, J. L.; Austin, C. M.; McKee, L. J.; Greenfield, B. K.; Brodberg, R.; Blum, J. D., Reducing methylmercury accumulation in the food webs of San Francisco Bay and its local watersheds. *Environ. Res.* **2012,** *119*, (Special Issue), 3-26.

21. James, L. A.; Singer, M. B.; Ghoshal, S.; Megison, M., Historical channel changes in the lower Yuba and Feather Rivers, California: Long-term effects of contrasting river-management strategies. *Management and Restoration of Fluvial Systems with Broad Historical Changes and Human Impacts: Geological Society of America Special Paper* **2009,** *451*, 57-81.

22. Singer, M. B.; Aalto, R.; James, L. A., Status of the lower Sacramento Valley flood-control system within the context of its natural geomorphic setting. *Natural Hazards Review* **2008,** *9*, (3), 104-115.

23. James, L. A.; Singer, M. B., Development of the lower Sacramento Valley flood-control system: Historical perspective. *Natural Hazards Review* **2008,** *9*, (3), 125-135.

24. Singer, M. B.; Aalto, R.; James, L. A.; Kilham, N. E.; Higson, J. L.; Ghoshal, S., Enduring legacy of a toxic fan via episodic redistribution of California gold mining debris. *Proceedings of the National Academy of Sciences* **2013**.

25. Blum, J. D.; Bergquist, B. A., Reporting of variations in the natural isotopic composition of mercury. *Anal. Bioanal. Chem.* **2007,** *388*, (2), 353-359.

26. Foucher, D.; Ogrinc, N.; Hintelmann, H., Tracing Mercury Contamination from the Idrija Mining Region (Slovenia) to the Gulf of Trieste Using Hg Isotope Ratio Measurements. *Environ. Sci. Technol.* **2009,** *43*, (1), 33-39.

27. Smith, C. N.; Kesler, S. E.; Blum, J. D.; Rytuba, J. J., Isotope geochemistry of mercury in source rocks, mineral deposits and spring deposits of the California Coast Ranges, USA. *Earth Planet. Sci. Lett.* **2008,** *269*, (3-4), 398-406.

28. Sonke, J. E.; Schafer, J.; Chmeleff, J.; Audry, S.; Blanc, G.; DuprÈ, B., Sedimentary mercury stable isotope records of atmospheric and riverine pollution from two major European heavy metal refineries. *Chem. Geol.* **2010,** *279*, (3-4), 90-100.

29. Stetson, S. J.; Gray, J. E.; Wanty, R. B.; Macalady, D. L., Isotopic Variability of Mercury in Ore, Mine-Waste Calcine, and Leachates of Mine-Waste Calcine from Areas Mined for Mercury. *Environ. Sci. Technol.* **2009,** *43*, (19), 7331-7336.

30. Feng, X. B.; Foucher, D.; Hintelmann, H.; Yan, H. Y.; He, T. R.; Qiu, G. L., Tracing Mercury Contamination Sources in Sediments Using Mercury Isotope Compositions. *Environ. Sci. Technol.* **2010,** *44*, (9), 3363-3368.

31. Yin, R.; Feng, X.; Wang, J.; Li, P.; Liu, J.; Zhang, Y.; Chen, J.; Zheng, L.; Hu, T., Mercury speciation and mercury isotope fractionation during ore roasting process and their implication to source identification of downstream sediment in the Wanshan mercury mining area, SW China. *Chem. Geol.* **2013,** *336*, (0), 72-79.

32. Laffont, L.; Sonke, J. E.; Maurice, L.; Monrroy, S. L.; Chincheros, J.; Amouroux, D.; Behra, P., Hg Speciation and Stable Isotope Signatures in Human Hair As a Tracer for Dietary and Occupational Exposure to Mercury. *Environ. Sci. Technol.* **2011,** *45*, (23), 9910-9916.

33. Estrade, N.; Carignan, J.; Sonke, J. E.; Donard, O. F. X., Mercury isotope fractionation during liquid-vapor evaporation experiments. *Geochim. Cosmochim. Acta* **2009,** *73*, (10), 2693-2711.

34. Sonke, J. E.; Zambardi, T.; Toutain, J.-P., Indirect gold trap-MC-ICP-MS coupling for Hg stable isotope analysis using a syringe injection interface. *J. Anal. At. Spectrom.* **2008,** *23*, (4).

35. Liu, J.; Feng, X.; Yin, R.; Zhu, W.; Li, Z., Mercury distributions and mercury isotope signatures in sediments of Dongjiang, the Pearl River Delta, China. *Chem. Geol.* **2011,** *287*, (1-2), 81-89.

36. Gehrke, G. E.; Blum, J. D.; Meyers, P. A., The geochemical behavior and isotopic composition of Hg in a mid-Pleistocene western Mediterranean sapropel. *Geochim. Cosmochim. Acta* **2009,** *73*, (6), 1651-1665.

37. Senn, D. B.; Chesney, E. J.; Blum, J. D.; Bank, M. S.; Maage, A.; Shine, J. P., Stable Isotope (N, C, Hg) Study of Methylmercury Sources and Trophic Transfer in the Northern Gulf of Mexico. *Environ. Sci. Technol.* **2010,** *44*, (5), 1630-1637.

38. Foucher, D.; Hintelmann, H.; Al, T. A.; MacQuarrie, K. T., Mercury isotope fractionation in waters and sediments of the Murray Brook mine watershed (New Brunswick, Canada): Tracing mercury contamination and transformation. *Chem. Geol.* **2013,** *336*, (0), 87-95.

39. Estrade, N.; Carignan, J.; Donard, O. F. X., Tracing and Quantifying Anthropogenic Mercury Sources in Soils of Northern France Using Isotopic Signatures. *Environ. Sci. Technol.* **2011,** *45*, (4), 1235-1242.

40. Yin, R.; Feng, X.; Wang, J.; Li, P.; Liu, J.; Zhang, Y.; Chen, J.; Zheng, L.; Hu, T., Mercury speciation, mercury isotope fractionation during ore roasting process and their implication to source identification of downstream sediment in Wanshan mercury mining area, SW China. *Chemical Geology* **2012**, (0).

41. Conomos, T. J.; Smith, R. E.; Gartner, J. W., Environmental setting of San Francisco Bay. *Hydrobiologia* **1985,** *129*, (1), 1-12.

42. McKee, L. J.; Ganju, N. K.; Schoellhamer, D. H., Estimates of suspended sediment entering San Francisco Bay from the Sacramento and San Joaquin Delta, San Francisco Bay, California. *Journal of Hydrology* **2006,** *323*, (1-4), 335-352.

43. Jaffe, B. E.; Smith, R. E.; Foxgrover, A. C., Anthropogenic influence on sedimentation and intertidal mudflat change in San Pablo Bay, California: 1856,Äì1983. *Estuarine, Coastal and Shelf Science* **2007,** *73*, (1-2), 175-187.

44. Schoellhamer, D. H., Sudden Clearing of Estuarine Waters upon Crossing the Threshold from Transport to Supply Regulation of Sediment Transport as an Erodible Sediment Pool is Depleted: San Francisco Bay, 1999. *Estuaries and Coasts* **2011,** *34*, (5), 885-899.

45. McKee, L. J.; Lewicki, M. *Watershed Specific and Regional Scale Suspended Sediment Load Estimates for Bay Area Small Tributaries*; Oakland, Ca, 12/2009, 2009.

46. Springborn, M.; Singer, M. B.; Dunne, T., Sediment-adsorbed total mercury flux through Yolo Bypass, the primary floodway and wetland in the Sacramento Valley, California. *Sci. Total Environ.* **2011,** *412*, (0), 203-213.

47. Singer, M. B.; Aalto, R., Floodplain development in an engineered setting. *Earth Surface Processes and Landforms* **2009,** *34*, (2), 291-304.

48. Cargill, S.; Root, D.; Bailey, E., Resource estimation from historical data: Mercury, a test case. *Mathematical Geology* **1980,** *12*, (5), 489-522.

49. Fleck, J. A.; Alpers, C. N.; Marvin-DiPasquale, M.; Hothem, R. L.; Wright, S. A.; Ellett, K.; Beaulieu, E.; Agee, J. L.; Kakouros, E.; Kieu, L. H.; Eberl, D. D.; Blum, A. E.; May, J. T., The effects of sediment and mercury mobilization in the south Yuba River and Humbug Creek confluence area, Nevada County, California; concentrations, speciation, and environmental fate; Part 1, Field characterization. *Open-File Report - U. S. Geological Survey* **2011,** *1*.

50. James, L. A., Sediment from hydraulic mining detained by Englebright and small dams in the Yuba basin. *Geomorphology* **2005,** *71*, (1-2), 202-226.

51. Hunerlach, M. P.; Alpers, C. N.; Marvin-DiPasquale, M. C.; Taylor, H. E.; De Wild, J. F. *Geochemistry of mercury and other trace elements in fluvial tailings upstream of Daguerre Point Dam, Yuba River, California, August 2001*; 2004; p 77.

52. Yee, D.; Bemis, B.; Hammond, D.; Heim, B.; Jaffe, B.; Rattonetti, A.; van Bergen, S. *Age Estimates and Pollutant Concentrations of Sediment Cores from San Francisco Bay and Wetlands*; Oakland, CA, 2011; pp 45 + Appendices A, B and C.

53. Blum, J. D., Applications of Stable Mercury Isotopes to Biogeochemistry. In Springer-Verlag Berlin Heidelberg: 2011; pp 229-245.

54. Biswas, A.; Blum, J. D.; Bergquist, B. A.; Keeler, G. J.; Xie, Z. Q., Natural Mercury Isotope Variation in Coal Deposits and Organic Soils. *Environ. Sci. Technol.* **2008,** *42*, (22), 8303-8309.

55. Landis, M. S.; Keeler, G. J., Critical Evaluation of a Modified Automatic Wet-Only Precipitation Collector for Mercury and Trace Element Determinations. *Environ. Sci. Technol.* **1997,** *31*, (9), 2610-2615.

56. Gratz, L. E.; Keeler, G. J.; Blum, J. D.; Sherman, L. S., Isotopic Composition and Fractionation of Mercury in Great Lakes Precipitation and Ambient Air. *Environ. Sci. Technol.* **2010,** *44*, (20), 7764-7770.

57. Marvin-DiPasquale, M.; Cox, M. H., Legacy mercury in Alviso Slough, South San Francisco Bay, California concentration, speciation and mobility. In U.S. Dept. of the Interior, U.S. Geological Survey: [Reston, Va], 2007; p 99 p.

58. Rytuba, J. J., Mercury mine drainage and processes that control its environmental impact. *Sci. Total Environ.* **2000,** *260*, (1-3), 57-71.

59. Daum, T.; Lowe, S.; Toia, R.; Bartow, G.; Fairey, R.; Anderson, J.; Jones, J. *Sediment Contamination in San Leandro Bay, CA*; San Francisco Estuary Institute: Oakland, CA, 2000.

60. Jemison, C., *2008 Annual Inspection Report: Clorox Company Oakland Plant Site*; Control, D. o. T. S.: 2009.

http://www.envirostor.dtsc.ca.gov/regulators/deliverable_documents/2547489762/rpt20090327145101333.pdf.

61. Gilbert, G. K., *Hydraulic-mining debris in the Sierra Nevada*. US Gov't Print. Off.: 1917.

62. Zheng, W.; Hintelmann, H., Mercury isotope fractionation during photoreduction in natural water is controlled by its Hg/DOC ratio. *Geochim. Cosmochim. Acta* **2009,** *73*, (22), 6704-6715.

63. Bergquist, B. A.; Blum, J. D., Mass-dependent and -independent fractionation of Hg isotopes by photoreduction in aquatic systems. *Science* **2007,** *318*, (5849), 417-420.

64. Mil-Homens, M.; Blum, J.; Canario, J. o.; Caetano, M.; Costa, A. M.; Lebreiro, S. M.; Trancoso, M.; Richter, T.; de Stigter, H.; Johnson, M.; Branco, V.; Cesario, R.; Mouro, F.; Mateus, M.; Boer, W.; Melo, Z., Tracing anthropogenic Hg and Pb input using stable Hg and Pb isotope ratios in sediments of the central Portuguese Margin. *Chem. Geol.* **2013,** *336*, (0), 62-71.

65. Ravichandran, M., Interactions between mercury and dissolved organic matter--a review. *Chemosphere* **2004,** *55*, (3), 319.

66. Amyot, M.; Mierle, G.; Lean, D.; Mc Queen, D. J., Effect of solar radiation on the formation of dissolved gaseous mercury in temperate lakes. *Geochim. Cosmochim. Acta* **1997,** *61*, (5), 975-987.

67. Hoenicke, R.; Tsai, P. *San Francisco Bay Atmospheric Deposition Pilot Study Part 1: Mercury*; San Francisco Estuary Institute: Richmond, CA, 2001.

68. Steding, D. J.; Flegal, A. R., Mercury concentrations in coastal California precipitation: Evidence of local and trans-Pacific fluxes of mercury to North America. *Journal of Geophysical Research: Atmospheres* **2002,** *107*, (D24), 4764.

69. Sherman, L. S.; Blum, J. D.; Keeler, G. J.; Demers, J. D.; Dvonch, J. T., Investigation of Local Mercury Deposition from a Coal-Fired Power Plant Using Mercury Isotopes. *Environ. Sci. Technol.* **2011,** *46*, (1), 382-390.

70. MacLeod, M.; McKone, T. E.; Mackay, D., Mass Balance for Mercury in the San Francisco Bay Area. *Environ. Sci. Technol.* **2005,** *39*, (17), 6721-6729.

71. Domagalski, J., Mercury and methylmercury in water and sediment of the Sacramento River Basin, California. *Appl. Geochem.* **2001,** *16*, (15), 1677-1691.

72. David, N.; McKee, L. J.; Black, F. J.; Flegal, A. R.; Conaway, C. H.; Schoellhamer, D. H.; Ganju, N. K., Mercury concentrations and loads in a large river system tributary to San Francisco Bay, California, USA. *Environ. Toxicol. Chem.* **2009,** *28*, (10), 2091-2100.

73. Slowey, A. J.; Rytuba, J. J.; Brown, G. E., Speciation of Mercury and Mode of Transport from Placer Gold Mine Tailings. *Environ. Sci. Technol.* **2005,** *39*, (6), 1547-1554.

74. Schoellhamer, D. H.; Mumley, T. E.; Leatherbarrow, J. E., Suspended sediment and sediment-associated contaminants in San Francisco Bay. *Environ. Res.* **2007,** *105*, (1), 119-131.

75. Jaffe, B.; Foxgrover, A., A history of intertidal flat area in south San Francisco Bay, California; 1858 to 2005. *Open-File Report - U. S. Geological Survey* **2006,** *1*.

76. Fregoso, T. A.; Foxgrover, A. C.; Jaffe, B. E., Sediment deposition, erosion, and bathymetric change in central San Francisco Bay; 1855-1979. *Open-File Report - U. S. Geological Survey* **2008,** *1*.

77. Foxgrover, A. C.; Higgins, S. A.; Ingraca, M. K.; Jaffe, B. E.; Smith, R. E., Deposition, erosion, and bathymetric change in South San Francisco Bay; 1858-1983. *Open-File Report - U. S. Geological Survey* **2004,** *1*.

78. Wright, S. A.; Schoellhamer, D. H., Trends in the Sediment Yield of the Sacramento River, California, 1957 - 2001. *San Francisco Estuary and Watershed Science* **2004,** *2*, (2).

Table 3.1: Sediment THg and Hg Isotope Values.

Location	Latitude (N)	Longitude (W)	Depth Interval	THg[1]	δ^{202}Hg	Δ^{201}Hg	Δ^{199}Hg
			cm	ng/g	‰	‰	‰
Suisun Bay	38.1025	122.0459	0-2.5	145	-0.48	0.00	0.04
			30-32.5	372	-0.45	0.02	0.01
			120-122.5	175	-0.65	0.02	0.09
San Pablo Bay	38.072	122.3871	0-2.5	266	-0.50	0.00	0.05
			15-17.5	329	-0.62	-0.01	0.01
			150-152.5	48.0	-0.95	0.04	0.13
Central Bay	37.8761	122.3619	0-2.5	241	-0.56	0.06	0.07
			20-22.5	347	-0.63	0.03	0.05
			67.5-70	130	-0.72	0.01	0.04
			120-122.5	58.0	-0.91	0.04	0.16
South Bay 2	37.626	122.347	0-2.5	241	-0.57	0.05	0.07
			22.5-25	434	-0.43	0.05	0.06
			100-102.5	44.0	-1.01	0.12	0.19
South Bay 1	37.6121	122.265	0-2.5	220	-0.50	0.03	0.07
			20-22.5	258	-0.40	-0.05	0.04
			100-102.5	31.0	-0.95	0.08	0.20
Lower South Bay	37.4791	122.0785	0-2.5	262	-0.53	0.08	0.13
			30-32.5	405	-0.32	0.05	0.09
			157.5-160	28.0	-1.08	0.11	0.18
Coyote Creek Wetland	37.4624	121.9997	2.5-5	329	-0.39	0.05	0.07
			57.5-60	469	-0.25	0.05	0.06
			77.5-80	3220	0.21	0.00	-0.02
			97.5-100	719	-0.20	0.03	0.06
			162.5-165	657	-0.18	0.02	0.01
Damon Slough Wetland	37.7536	122.2133	2.5-5	533	-0.50	0.14	0.16
			17.5-20	3140	-0.42	0.05	0.11
			22.5-25	1440	-0.39	0.12	0.17
			27.5-30	193	-0.65	0.04	0.11
			37.5-40	71.0	-0.80	0.09	0.17
			67.5-70	23.0	-1.08	0.13	0.24
Yuba River (a)	39.21874	121.29905		5440	-0.64	0.05	0.05
Yuba River (b)	39.21914	121.29875		3180	-0.50	0.01	0.04

[1] THg concentrations reported here are from Yee et al. (2011) except for Yuba River sediment (a/b), which is calculated based on the combustion solution concentration (see Materials and Methods 3.2.3.2.).

Table 3.2: Precipitation THg and Hg isotope values.

Location	Latitude (N)	Longitude (W)	THg[2]	$\delta^{202}Hg$	$\Delta^{201}Hg$	$\Delta^{199}Hg$
			ng/L	‰	‰	‰
Moss Beach 1	37.5316	122.51	6.2	0.02	0.19	0.16
Moss Beach 2	37.5316	122.51	9.0	-0.01	0.31	0.33
Moss Beach Avg.			7.7	0.01	0.25	0.25
San Jose	37.4399	121.958	4.7	-0.01	0.19	0.35
Oakland	37.7416	122.206	7.9	0.19	0.27	0.29

[2]THg concentrations reported are based on the combination of Hg from multiple bottles into a 1% $KMnO_4$ oxidizing trap solution. The Moss Beach Average concentration is the volume weighted mean that represents the entire winter 2009 sampling period.

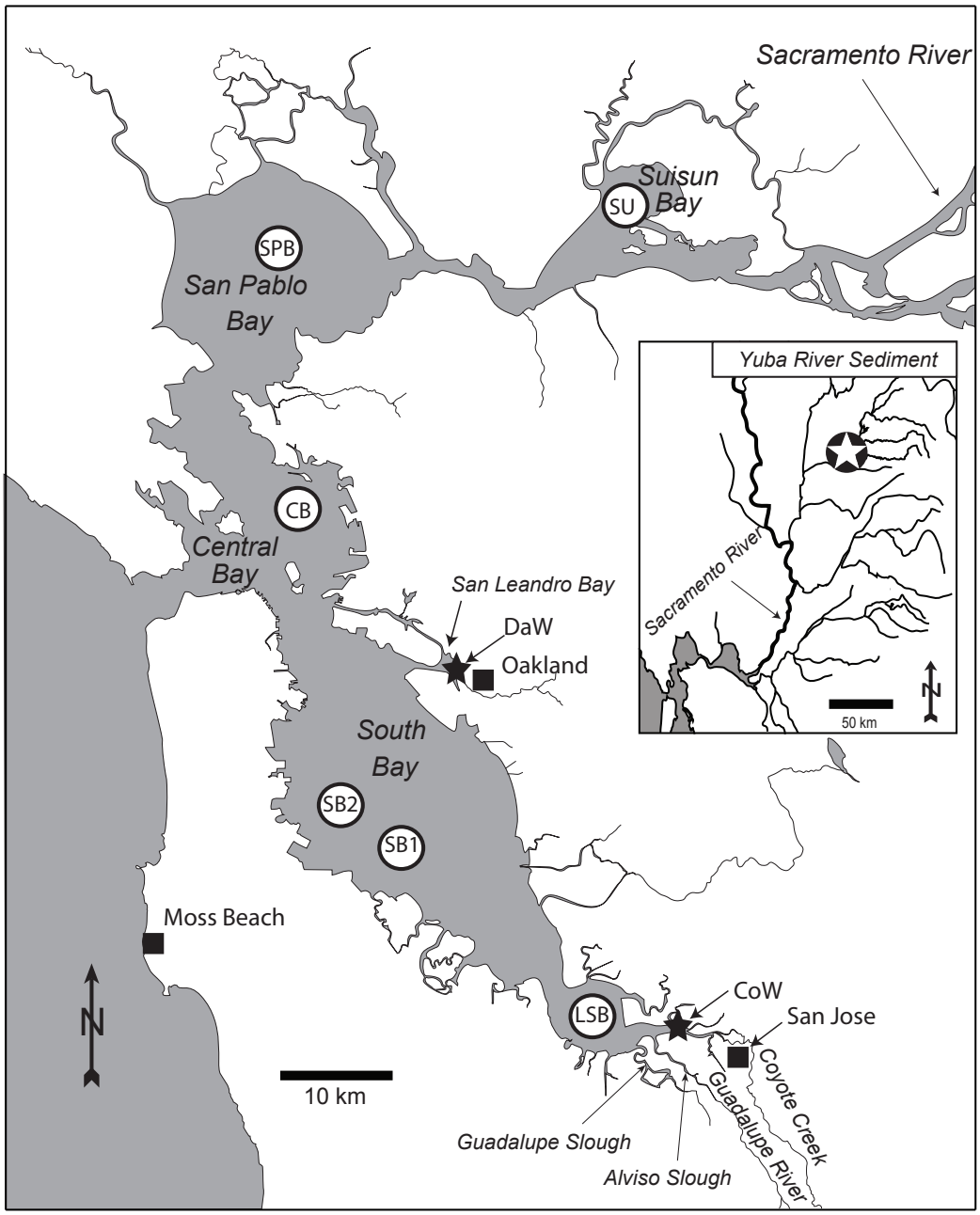

Figure 3.1: Sampling locations for subtidal sediment cores and precipitation
Sampling locations for subtidal sediment cores (open circles), wetland sediment cores (black stars) and precipitation collection stations (black squares). The location of Yuba River terrace sediment (open star) is included on the inset map. Further description of the variety of Hg sources in the SF Bay region can be found in Conaway et al. (2008) and Alpers et al. (2005).

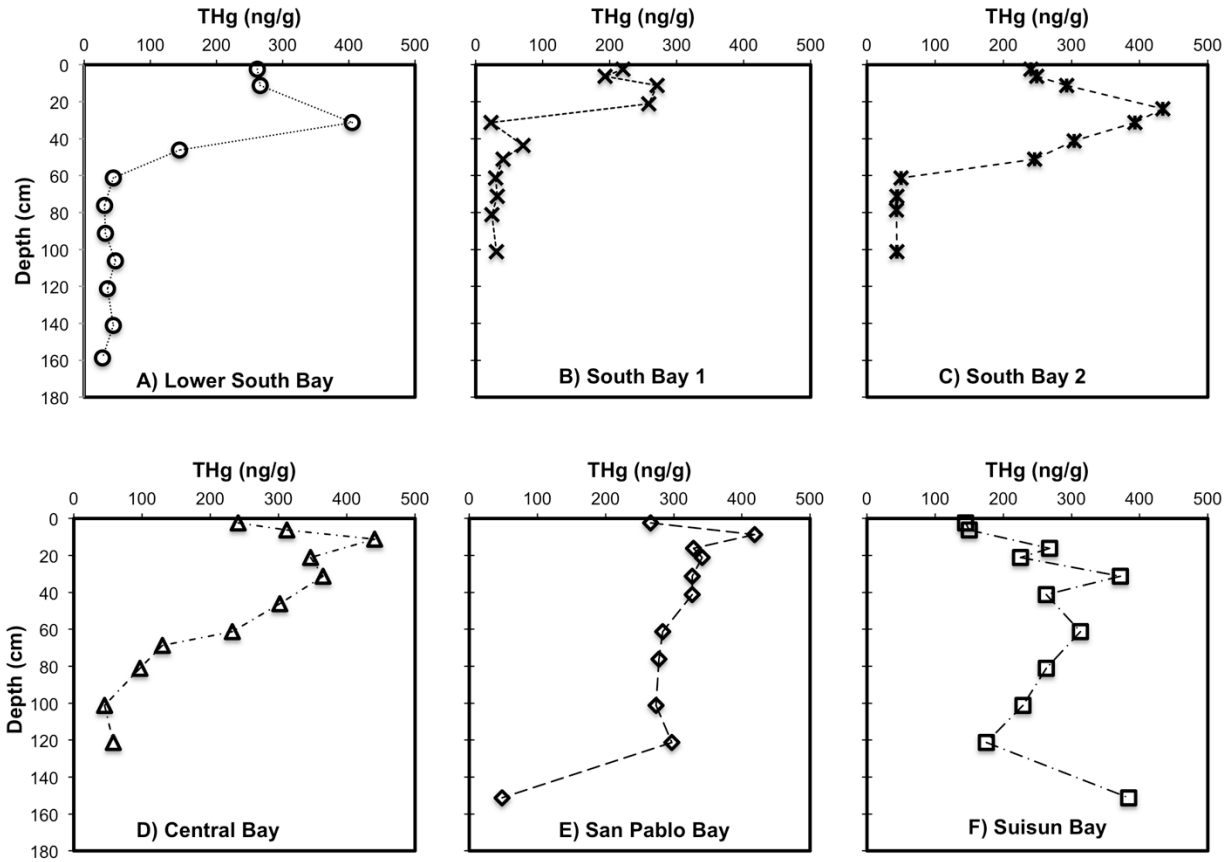

Figure 3.2: Depth vs. THg concentration for six subtidal sediment cores
Depth vs. THg concentration for the six subtidal sediment cores selected for Hg stable isotope analysis (A-F; from Yee et al., 2011). Pre-mining THg concentration is approximately <80 ng/g (Bouse et al., 2010; Hornberger et al., 2009).

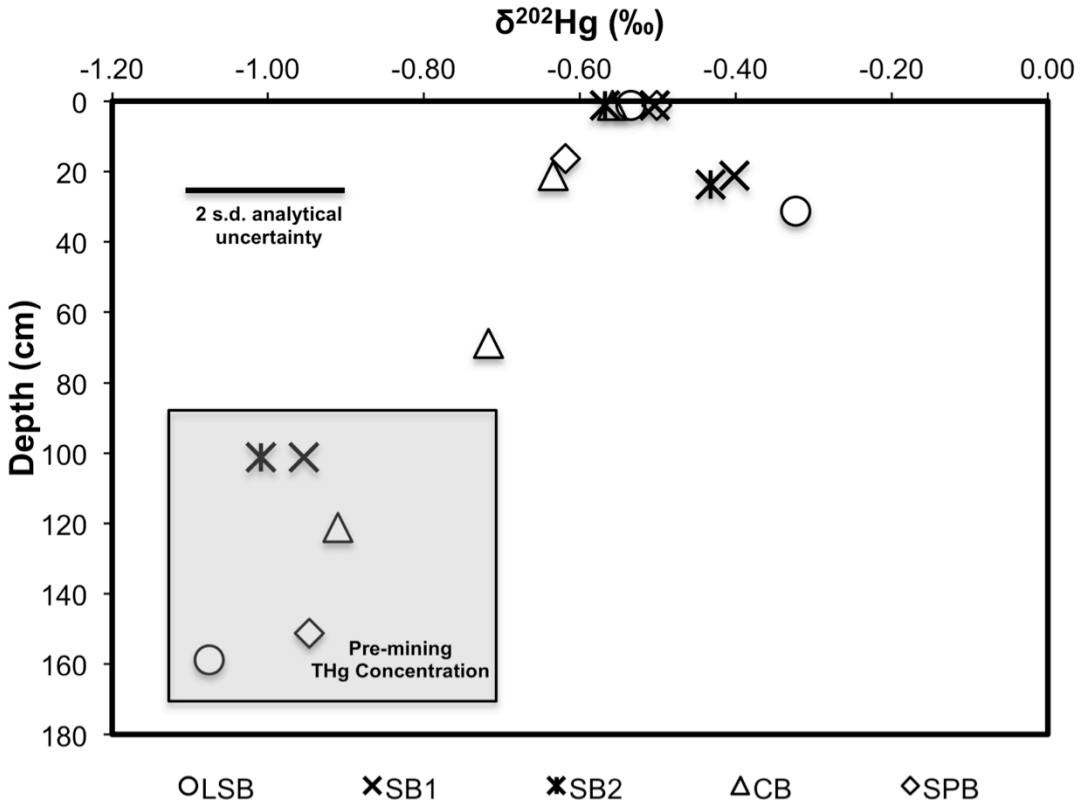

Figure 3.3: Depth vs. δ^{202}Hg for siz subtidal sediment cores
Sediment intervals with pre-mining THg concentration are enclosed by the shaded rectangle.

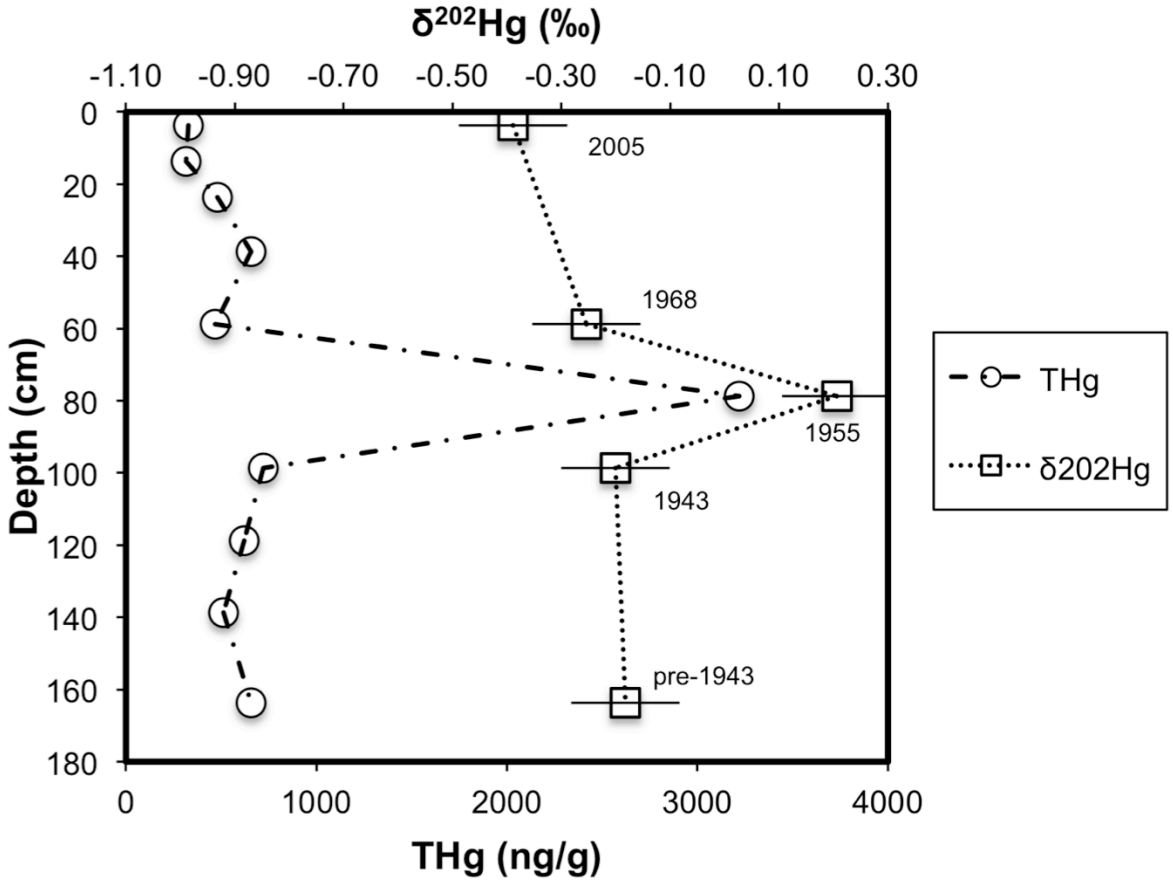

Figure 3.4: THg and δ^{202}Hg vs. Depth for Coyote Creek Wetland sediment core
THg concentration (circles) and δ^{202}Hg (squares) vs. depth for Coyote Creek wetland (CoW) sediment. Approximate radiometric ages are included from Yee et al. (2011) and error bars for δ^{202}Hg represent the 2 s.d analytical uncertainty (±0.10‰)

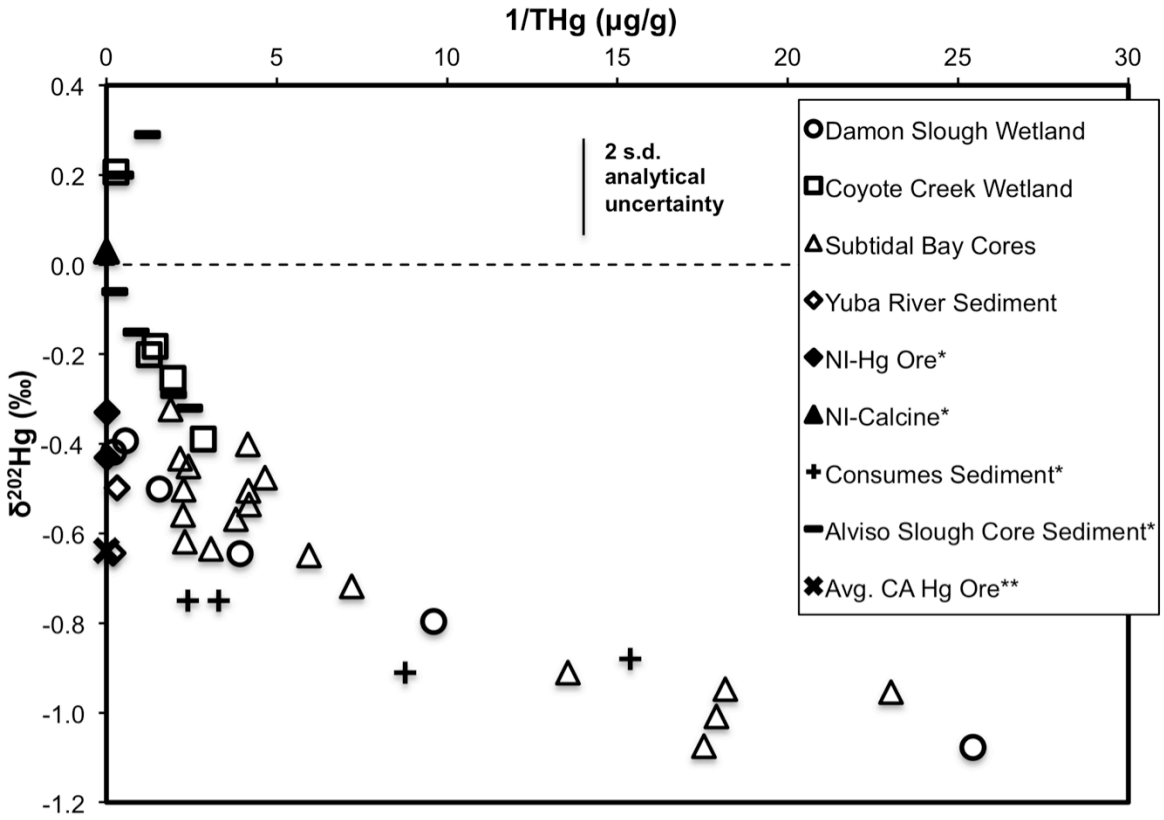

Figure 3.5: δ^{202}Hg vs. 1/THg for SF Bay Sediment
δ^{202}Hg vs. 1/THg for all SF Bay sediment measured in this study. Included is New Idria (NI) Hg ore and calcine, Consumes River surface sediment, Alviso Slough sediment cores (*Gehrke et al., 2011) and California (CA) Hg ore (** Smith et al., 2008).

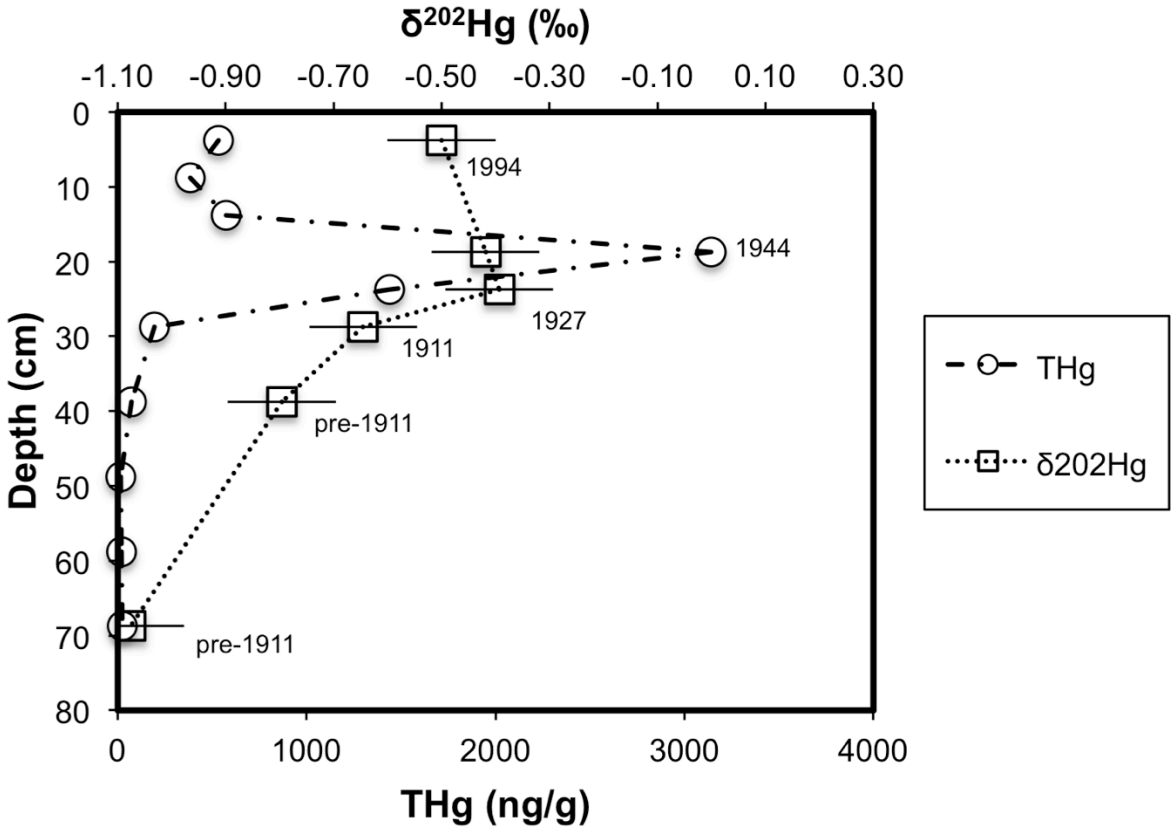

Figure 3.6: THg and δ^{202}Hg vs. depth for Damon Slough wetland sediment core
THg concentration (circles) and δ^{202}Hg (squares) vs. depth for Damon Slough wetland (DaW) sediment. Approximate radiometric ages are included from Yee et al. (2011) and error bars for δ^{202}Hg represent the 2 s.d analytical uncertainty (±0.10‰).

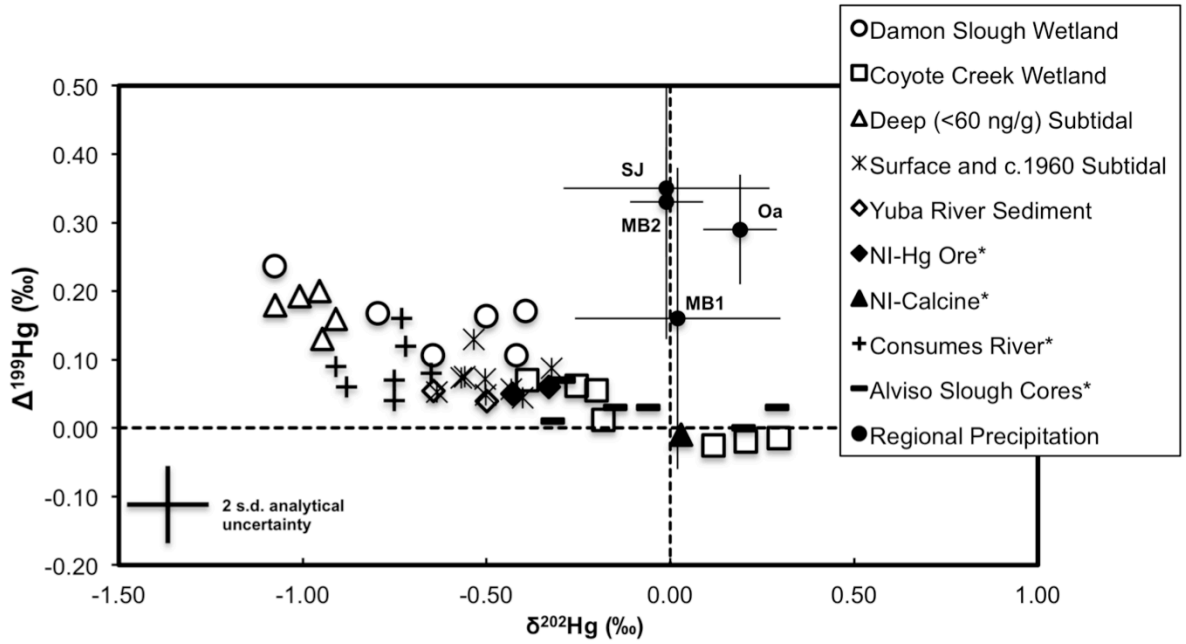

Figure 3.7: Δ^{199}Hg vs. δ^{202}Hg for Yuba River terrace sediment, SF Bay subtidal and wetland sediment and regional precipitation
Precipitation collection sites are denoted by abbreviations (Moss Beach = MB; San Jose = SJ and Oakland = Oa) and precipitation analytical uncertainty is depicted as the 2 s.d. of individual measurements of UM-Almaden as described in Section 2.3.4. Also included is New Idria (NI) ore and calcine, Cosumnes River surface sediment, and Alviso Slough sediment cores (*from Gehrke et al., 2011).

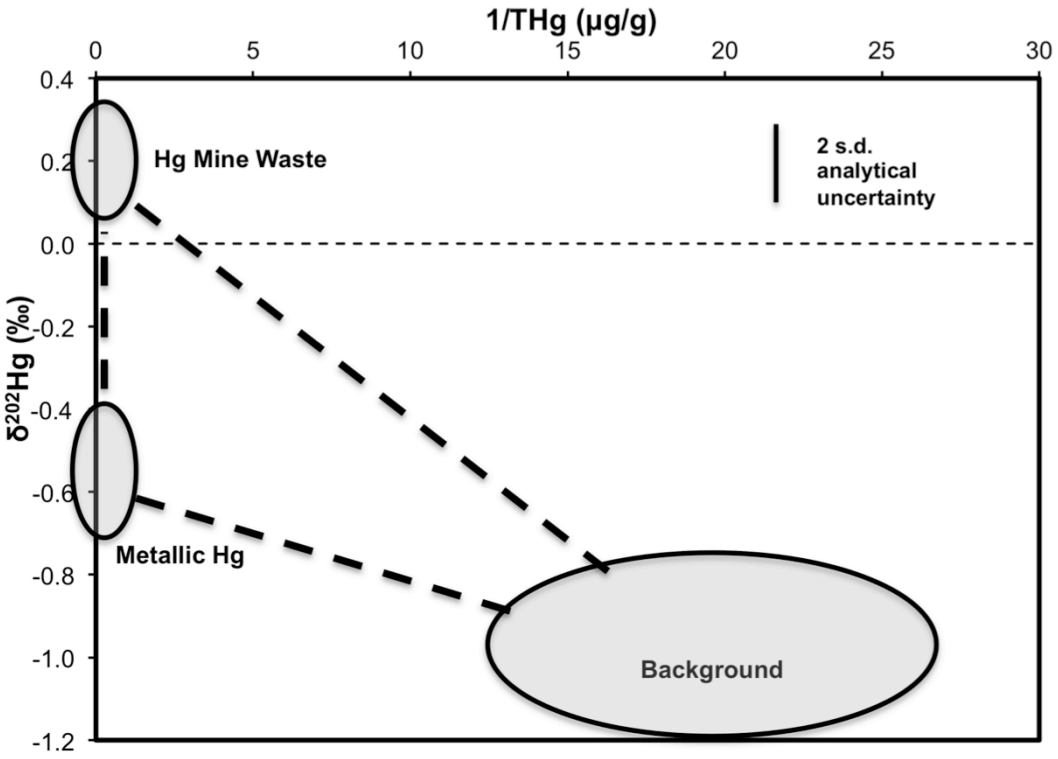

Figure 3.8: δ^{202}Hg vs. 1/THg for three sediment endmembers in SF Bay

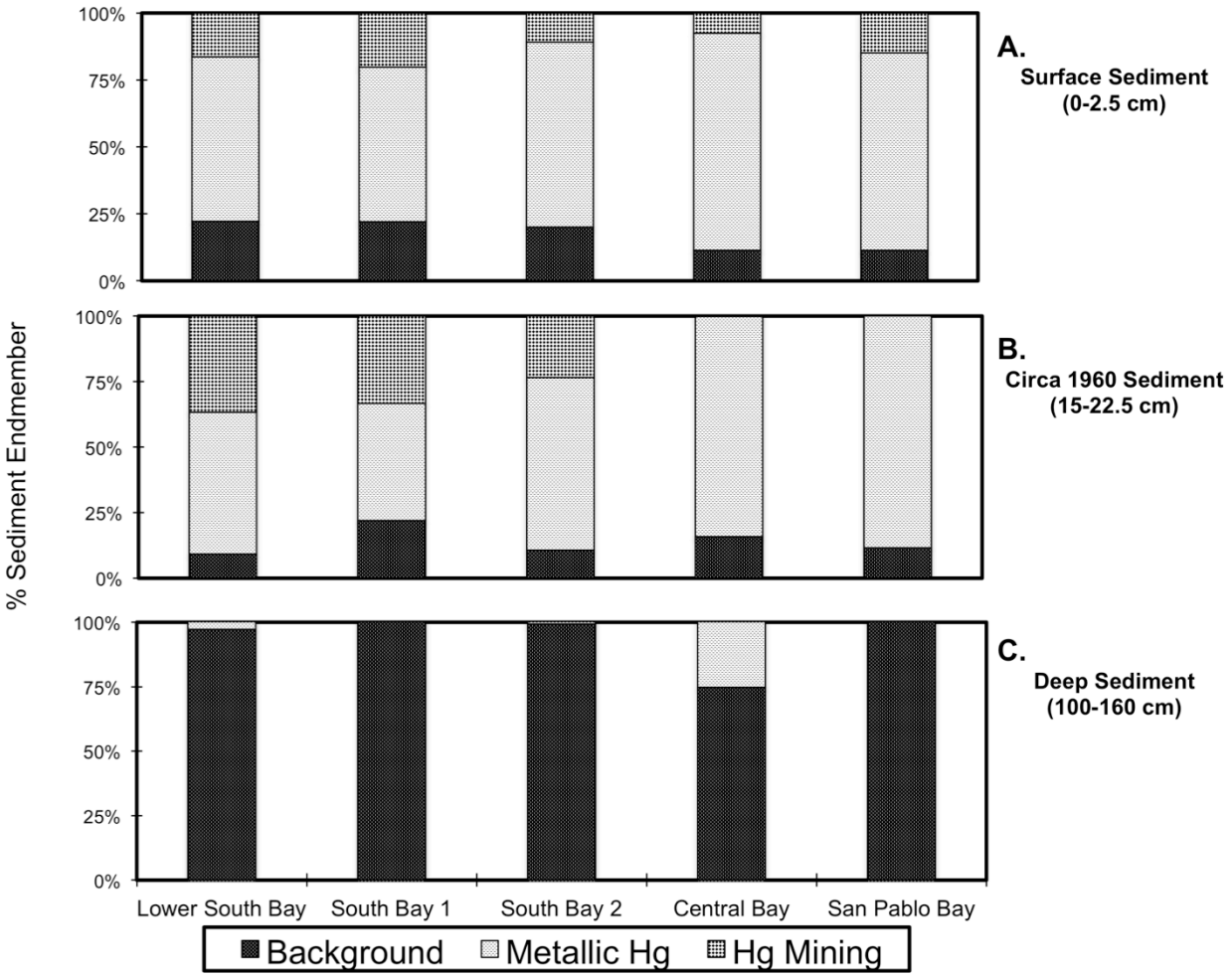

Figure 3.9: Estimated endmember sediment contributions
Estimated endmember sediment contribution to (A) surface, (B) circa 1960, and (C) deep sediment in subtidal locations.

CHAPTER 4: Isotopic composition of inorganic mercury and methylmercury downstream of historical gold mining

Authors: Patrick M. Donovan, Joel D. Blum, Michael B. Singer, Mark Marvin-DiPasquale, Martin T.K. Tsui

Abstract

We measured total mercury (THg) and monomethyl mercury (MMHg) concentrations and Hg isotopic composition in sediment and aquatic organisms in the Yuba River (California, USA) to identify Hg sources and biogeochemical transformations downstream of historical gold (Au) mining. Sediment THg and δ^{202}Hg decreased from the upper Yuba Fan to the lower Yuba Fan and the Feather River. This was consistent with the release of Hg during Au mining followed by mixing, homogenization and dilution. The Hg isotopic composition of Yuba Fan sediment (δ^{202}Hg of -0.38±0.17‰ and Δ^{199}Hg of 0.04±0.03‰; 1SD, n=7) provides a fingerprint of inorganic Hg (IHg) that could be methylated locally or after transport downstream. The isotopic composition of MMHg in the Yuba River food web was estimated from biota with a range of %MMHg (the percent ratio of MMHg to THg) and compared to various IHg sources. The δ^{202}Hg of MMHg prior to photodegradation (−1.29 to −1.07‰) was lower than IHg in Yuba River sediment and algae. We suggest that this results from net negative mass dependent fractionation (MDF) of up to 0.9‰ between IHg and MMHg in this stream. This was in contrast to net positive MDF (+0.4 to 0.8‰) previously observed in lakes, estuaries, coastal oceans and forests. We

hypothesize that this unique relationship could be due to differences in the extent or the pathway of MMHg degradation.

4.1 Introduction

Mercury (Hg) is a globally distributed neurotoxic pollutant that bioaccumulates in food webs as monomethyl mercury (MMHg). The amount of Hg actively cycling in the environment has increased due to anthropogenic activities such as mining, coal combustion, and industrial Hg use.[1] In the 19th century, Hg was widely used to enhance gold (Au) recovery during hydraulic mining of placer deposits throughout the Sierra Nevada, California. During hydraulic mining large volumes of sediment were washed through sluices containing Hg to amalgamate Au, with as much as 30% of the Hg used lost to the environment.[2] The Hg-contaminated sediment was released downstream and deposited in river valleys along the western front of the Sierra Nevada, with significant amounts of sediment affecting lowland channels and reaching San Francisco Bay.[3] Sediment from Au mining persists in large anthropogenic fan deposits evident in terraces and banks alongside rivers draining former mining districts.[4] One of the largest is the Yuba Fan, a massive deposit of mining derived sediment ($252 * 10^6$ m^3)[5] grading from the Sierra Nevada piedmont to the Central Valley. The lower Yuba River, between Englebright Dam and the Feather River, flows through this sediment deposit which has total Hg concentrations (THg) consistently 2-3x higher than pre-mining sediment.[4, 5] The Yuba Fan continues to supply inorganic Hg (IHg) laden sediment to local and downstream environments during major flood events that occur about once a decade.[4]

In sediment, IHg can be transformed by methylating microbes into bioaccumulative MMHg near the oxic-anoxic interface. Conditions that promote IHg methylation are often found in wetlands or estuarine environments,[6] such as in San Francisco Bay where MMHg production in sediment and bioaccumulation in food webs is well documented.[7-9] However, MMHg formation and distribution in rivers is more difficult to predict because it can be a function of both watershed landscape characteristics (i.e., wetland density, land use, etc.)[10, 11] and in-stream processes (i.e., microbial community, hydrology, productivity).[12-14] Thus, in large watersheds with both upstream and local IHg sources it is difficult to identify the origin of bioaccumulated MMHg using MMHg or THg concentrations alone. Nonetheless, MMHg biomagnifies in many riverine food webs[10] and processes governing MMHg production and degradation in streams are of great interest.[13]

In the Yuba River, upstream of Englebright Dam (ED; built in 1941 to trap hydraulic mining sediment) the spatial distribution, speciation and reactivity of Hg in sediment was previously documented,[15, 16] as were fish THg concentrations,[17] and invertebrate THg and MMHg concentrations.[15] Downstream of Englebright Dam, the lower Yuba River flows through the Yuba Fan to the Feather River. Previous work is this reach has shown high THg in sediment within and alongside the river. The THg in bar, bank, terrace, and floodplain sediment has been documented[4], as well as within-channel deposits stored behind Daguerre Point Dam (a 24ft high overflow spillway dam midway between ED and the Feather River).[5] However, no prior studies have investigated MMHg bioaccumulation in the lower Yuba River and the importance of IHg in Yuba Fan sediment to resident biota is unknown. We hypothesized that Yuba Fan IHg could be methylated in situ resulting in MMHg bioaccumulation in the local food web. However, we also considered whether MMHg

might be derived from watershed sources upstream of the Yuba Fan (i.e., upstream of ED). To better understand the processes by which MMHg enters riverine food webs we measured Hg stable isotope ratios in sediment and biota in the lower Yuba River.

Mercury has seven stable isotopes that undergo mass dependent fractionation (MDF) and mass independent fractionation (MIF) in the environment. Hg stable isotope ratios have become a powerful tool for identifying anthropogenic Hg sources and tracing their transport and deposition in stream systems.[18-20] Comparisons of Hg isotopes in sediment (mostly IHg) with fish or other biota (containing MMHg) have been used to infer important transformations between IHg and MMHg such as microbial IHg methylation, microbial MMHg degradation, and photochemical MMHg degradation.[21, 22] Recent studies have measured biota with a range in %MMHg (the percent ratio of MMHg to THg) to identify the isotopic composition of both IHg and MMHg in food webs.[23-25] For example, Kwon et al.[24] measured Hg isotope ratios in estuarine sediment and biota along the U.S. northeast coast. From the isotopic composition of MMHg, the authors were able to determine that organisms were primarily exposed to MMHg from local sediment and not external sources. In another study, MMHg isotopic composition was estimated in the South Fork Eel River (CA) to evaluate Hg exchange across ecosystem boundaries via organismal movement,[26] [25] and longitudinal changes in MMHg photochemical degradation.[27] So far, investigation of MMHg in stream ecosystems using Hg isotopes has been limited to the Eel River (CA), a relatively remote, bedrock-dominated, free flowing river where Hg is derived mainly from atmospheric deposition (i.e., no Hg point sources). In contrast, the lower Yuba River has been anthropogenically modified; it contains large quantities of high THg sediment derived from 19th Century gold mining.

Here we present the first Hg isotope study to investigate Hg sources and biogeochemical transformations in sediment and biota in a river contaminated by historical Au mining. We report THg, MMHg and Hg isotopic compositions of sediment, filamentous algae and aquatic organisms from the lower Yuba River (six sites) and the Feather River (one site; Figure 4.S1). A diverse suite of organisms with a wide range of %MMHg was collected, including five types of benthic macroinvertebrates: stonefly larva (*Perlidae*), caddisfly larva (*Hydropsychidae*), mayfly larva (*Heptageniidae* & *Ephemerellidae*), aquatic worm (*Oligochaeta*), asian clam (*Corbicula fluminea*), and two fish species: riffle sculpin (*Cottus gulosus*) and speckled dace (*Rhinichthys osculus*). We estimated the isotopic composition of both IHg and MMHg in the food web to (1) determine the source of bioaccumulated MMHg and (2) identify important microbial and photochemical processes governing Hg cycling in the lower Yuba/Feather system.

4.2 Materials and Methods

4.2.1 Study Site and Sample Collection

Twelve sediment samples were analyzed from eight locations (five of which correspond to biota sampling locations) in the Yuba and Feather Rivers (Figure 4.1). Nine of the sediment samples had been collected between 2006-2008 from subaerial riverbanks and terraces and analyzed for THg at the USGS (Menlo Park, CA) by Singer et al.[4] Three additional samples were collected in March 2013 from subaerial riverbanks and analyzed for both THg and MMHg at the USGS (Menlo Park, CA). All sediment was dry-sieved to <63μm using a stainless steel sieve, and either air dried (n=9 from Singer et al.) or freeze-dried (n=3 from March 2013), and then homogenized prior to analysis. Filamentous algae

and aquatic organisms were collected from a total of five sites in the lower Yuba River: Rose Bar (RB), Parks Bar (PB), Hammon Grove (HG), Dantoni (Da), and Simpson Bridge (SB), and one site in the Feather River at Star Bend (FR; Figure 4.S1). Organisms were collected during two separate sampling campaigns that occurred during March 2013 (RB, Da and FR) and June 2014 (all sites). Organisms were collected using a kick net, dip net and directly off gravel cobbles, and individual organisms were removed with clean stainless steel tweezers and transferred into a secondary container for identification. Individuals were sorted by family into composite samples, placed in clean centrifuge tubes and immediately put on dry ice in the field. All samples, except for a single riffle sculpin sample, are composites of 5 or more individuals. When organisms were plentiful (i.e., more than ~50 individuals at a single sampling site), these individuals were split into replicate samples and analyzed separately. Biotic samples were freeze-dried and then ground and homogenized, with either an agate mortar and pestle or an alumina ball mixer mill, prior to analysis.

4.2.2 MMHg Concentration Analysis

The concentration of MMHg (expressed as dry wt.) in sediment and biota was measured at the USGS (Menlo Park, CA). Freeze dried sediment was sub-sampled (0.02–0.03 g) and extracted for MMHg using 25% potassium hydroxide in methanol at 60°C for four hours.[16] Freeze dried biota was sub-sampled (3–7 mg) and extracted for MMHg using 30% nitric acid at 60°C (overnight, 12-16 hrs), as adapted.[28] In both cases (sediment and biota), extract sub-samples were diluted, pH adjusted with citrate buffer and assayed for MMHg by aqueous phase ethylation (with sodium tetraethylborate) on an automated

MMHg analyzer (MERX system, Brooks Rand Laboratories).[29] For sediment MMHg (assayed in a single batch), the relative percent deviation (RPD) of analytical duplicates was 8.4% (n=1 pair), matrix spike recovery was 107±1% (n = 2), and certified reference material (CRM) ERM-CC580 (estuarine sediment) recovery was 95% (n=1). For biota, the mean RPD of analytical duplicates was 3.0% (n=12 pairs), matrix spikes recoveries were 105±1% (mean ± SE, n = 26), and CRM recoveries from NRC Tort-3 (lobster hepatopancreas) was 86±2% (mean ± SE, n=7) and from NIST-2967 (marine mussel tissue) was 94±3% (mean ± SE, n=7).

4.2.3 THg and Hg Isotope Analysis

Hg was separated from samples for Hg stable isotope composition and THg concentration by offline combustion, as described elsewhere.[25, 30] Briefly, up to 1 g of homogenized sample was placed in a ceramic boat in the first furnace of a two-stage offline combustion system. The furnace temperature was increased to 750°C over six hours while the second furnace was held at 1000°C. Hg released from the sample was carried in a flow of Hg-free O_2 through the second furnace and sparged into a 1%$KMnO_4$/10%H_2SO_4 solution (1% $KMnO_4$ trap). Trap solutions were partially reduced with 2% w/w hydroxylamine hydrochloride (NH_2OH•HCl) and an aliquot was measured for THg by CV-AAS (Nippon MA-2000) to calculate the sample dry wt. THg concentration (based on THg in the 1% $KMnO_4$ trap and the sample mass combusted). Compared to an independent analysis (a subset of samples measured for THg at USGS-Menlo Park), offline combustion recovered 107 ± 11% (1SD, n=6) of Hg from biotic samples and 97 ± 11% (1SD, n=15 including 3 replicate combustions) of Hg from sediment samples.

Prior to isotopic analysis, contents of the original 1%$KMnO_4$ trap solution were divided into 1-5 g aliquots, treated with 0.3ml of 20% $SnCl_2$ and 0.3ml of 50% H_2SO_4 to reduce Hg to Hg^0, and Hg was purged into a secondary 1%$KMnO_4$ trap to increase Hg concentration and isolate Hg from combustion residues. An aliquot of the secondary trap solution was analyzed by CV-AAS (Nippon MA-2000) and transfer recoveries averaged 98 ± 3% (1SD; n= 36) for biotic samples and 99 ± 2% (1SD; n=15) for sediment samples. Hg isotopic composition of the secondary trap solution was measured by cold vapor multi-collector inductively coupled plasma mass spectrometry (CV-MC-ICP-MS; Nu Instruments). Trap solutions were partially reduced with 2% w/w $NH_2OH{\bullet}HCl$, diluted to a concentration between 0.9 and 5 ng/g, and Hg was reduced online by the continuous addition of 2% $SnCl_2$. The Hg^0 generated was separated from solution using a frosted tip gas-liquid separator and carried in a Hg-free stream of Ar gas to the MC-ICP-MS inlet. Instrumental mass bias was corrected by introduction of an internal Tl standard (NIST 997) as a dry aerosol to the gas stream and by strict sample standard bracketing using NIST 3133 with a matching Hg concentration (±10%) and solution matrix.[31]

4.2.4 Hg Isotopic Composition: Blanks, SRMs and Uncertainty

Mercury stable isotope compositions are reported in permil (‰) using delta notation ($\delta^{xxx}Hg$) relative to NIST SRM 3133 (Eq. 1), with MDF based on the $^{202}Hg/^{198}Hg$ ratio ($\delta^{202}Hg$).[31] MIF is the deviation from theoretically predicted MDF and is reported in permil (‰) using capital delta ($\Delta^{xxx}Hg$) notation (Eq. 2). In this study, we use $\Delta^{199}Hg$ and $\Delta^{201}Hg$ to report MIF with $\beta = 0.252$ for $\Delta^{199}Hg$ and $\beta = 0.752$ for $\Delta^{201}Hg$.[31] All $\delta^{xxx}Hg$ and $\Delta^{xxx}Hg$ values for samples and standards are available in Tables 4.S1, 4.S2, and 4.S3.

Equation [1]: $\delta^{xxx}Hg\ (‰) = ([(^{xxx}Hg/^{198}Hg)_{sample}/(^{xxx}Hg/^{198}Hg)_{NIST3133}]-1) * 1000$

Equation [2]: $\Delta^{xxx}Hg = \delta^{xxx}Hg - (\delta^{202}Hg * \beta)$

Procedural process blanks and two standard reference materials (SRMs; NRC TORT-2–Lobster Hepatopancreas and NIST 1944–New York/New Jersey Waterway Sediment) were processed alongside samples in an identical manner. Process blanks for sediment and biota averaged 95±15 pg (1SD, n=8) and 104±30 pg (1SD, n= 6), respectively, and accounted for between 0.2% to 1.8% of Hg in final trap solutions. Mean THg for SRMs were within 5% of certified values (3.51±0.3 ug/g for NIST SRM 1944 and 276±5 ng/g for NRC TORT-2; Table 4.S3) and recovery during secondary purge and trap was 94±4% (1SD, n=6, minimum = 87%) and 96±7% (1SD, n=11, minimum = 80%), respectively. The Hg isotopic composition of SRMs (Table 4.S3) was consistent with previously reported values for these materials.[18, 21, 24-26, 32-36] The long-term analytical uncertainty of Hg isotope ratio measurements is estimated from the standard deviation (2SD) of analytical session mean Hg isotopic compositions of UM-Almaden with a run concentration of 3-5 ng/g (Table 4.S3). We also estimated external reproducibility using the error (2SD) associated with replicate measurements of SRMs. The 2SD of SRMs was greater than the 2SD associated with the long-term analytical uncertainty of UM-Almaden. Therefore, the uncertainty for sediment and biota in this study is estimated from the SRMs and is ±0.08‰ for $\delta^{202}Hg$ and ±0.05‰ for $\Delta^{199}Hg$.

4.3 Results & Discussion

4.3.1 Sediment THg and Hg Isotopic Composition

Yuba River and Feather River sediment total Hg concentrations (THg) ranged from 170 to 6,821 ng/g, δ^{202}Hg ranged from −0.95 to 0.72‰ and Δ^{199}Hg was near zero (0.04±0.03‰; 1SD n=12; Table 4.S1). Both THg and δ^{202}Hg generally decreased downstream from the upper Yuba Fan (~0 to 20 km downstream of ED) to the lower Yuba Fan (20-36 km downstream of ED) and into the Feather River (>36 km downstream of ED; Figure 4.1). Metallic Hg (Hg^0) was used during the hydraulic mining of placer deposits adjacent to Rose Bar in the upper fan, between 1850 and the early 1900's. Upper fan sediment had high THg (up to 6,820 ng/g) and δ^{202}Hg was variable but near zero (δ^{202}Hg of −0.04 ± 0.52‰; mean ± 1SD, n=4). High THg sediment (3,180 and 5,440 ng/g) previously analyzed from a single tailings pile at Rose Bar had δ^{202}Hg on the low end of this range (−0.50‰ and −0.63‰, respectively),[37] but one sediment sample nearby had δ^{202}Hg of +0.71‰. The δ^{202}Hg of metallic Hg^0 has been reported to vary globally from −1.06 to 0.0‰ (mean of −0.39±0.37‰, 1SD, n=7),[38] and is typically similar to the δ^{202}Hg of Hg ore that it is sourced from.[39] Sierra Nevada Au mining operations obtained metallic Hg from the CA Coast Range[2] where Hg ore deposits have δ^{202}Hg of −0.64±0.84‰ (mean±1SD, n=91).[40] The variable δ^{202}Hg of upper fan sediment indicates that some heterogeneity of sediment bound Hg might have resulted from Hg^0 released from different Au mines or during different mining periods. Nonetheless, although metallic Hg likely underwent complex biogeochemical cycling (i.e., oxidation, dissolution, volatilization, sorption) after release,[41] the mean Hg isotopic composition of Upper Yuba Fan sediment is generally consistent with the δ^{202}Hg of metallic Hg globally and sourced from CA Coast Range ores.[38, 40]

From the lower Yuba Fan into the Feather River, sediment THg concentration decreased to between 170 and 413 ng/g. Sediment from the lower fan had δ^{202}Hg of −0.44±0.16‰ (n=4) and sediment from the Feather River had δ^{202}Hg of −0.66±0.26‰ (n=4). There is less isotopic variability in these stream sections suggesting that various metallic Hg sources within the watershed have been well homogenized. Multiple studies have demonstrated that sediment Hg isotopic composition can be used to conservatively trace downstream Hg transport and mixing in rivers.[18, 20, 42] Pre-mining sediment in subtidal sediment cores from SF Bay, with background THg (less than 60 ng/g), had δ^{202}Hg of −0.98±0.06‰ and Δ^{199}Hg of 0.17±0.03 (1SD, n=5).[37] If we assume this to be the isotopic composition of pre-mining sediment, then the decrease in THg and gradual shift toward lower δ^{202}Hg suggests homogenization of the Au mining sources and potential dilution with uncontaminated background sediment (Figure 4.S3). This is consistent with the model of progressively diluted hydraulic mining sediments being remobilized and redeposited within the fan and exported from it.[4, 43, 44] Thus, the Hg isotope signature of Yuba Fan sediment (δ^{202}Hg of −0.38±0.17‰ and Δ^{199}Hg of 0.04±0.03‰; 1SD, n=7 with one anomalously high δ^{202}Hg sample excluded) provides a fingerprint of the large volume of IHg that could be methylated locally or exported downstream.

4.3.2 Yuba-Feather River Biota

4.3.2.1 Biota THg and MMHg

Biota THg and MMHg concentrations in the Yuba and Feather Rivers were similar to previous surveys downstream of Au mining in the Sierra Nevada (e.g.,[15, 45, 46]) yet overlap with THg and MMHg reported for biota when no Hg point sources are present (e.g, [10, 47]).

MMHg in filamentous algae increased with distance downstream in the Lower Yuba River from 2.4 ng/g at Rose Bar to 17 ng/g at Dantoni and 14.6 ng/g at Simpson Bridge. Similar levels of MMHg were observed in the Eel River (3-34 ng/g) where the authors suggested that in situ methylation of IHg may be mediated by microbial communities associated with the algae.[12, 47] Yuba River algae THg varied between 57 and 186 ng/g likely due to the accumulation of fine sediment with high THg derived from the Yuba Fan. Benthic macroinvertebrate MMHg ranged from 37 to 271 ng/g and there was no systematic change in MMHg or %MMHg between sampling locations. These concentrations were more similar to benthic macroinvertebrates from streams affected by atmospheric deposition (e.g., Eel River[47] and others across the US[10]) than streams with significant Hg point sources (e.g., Cache Creek[48] and streams near Oak Ridge, TN[49]). The highest MMHg and THg values here were measured in asian clam (79 to 271 ng/g and 168 to 426 ng/g, respectively) and forage fish (380 to 406 ng/g and 377 to 436 ng/g, respectively) but these organisms were only collected at downstream sites (downstream of Hammon Grove). Forage fish THg was within the reported range for similar species from US streams unaffected by point sources of Hg.[10] There were consistent differences in %MMHg among the organisms sampled depending on their feeding behavior or presumed trophic position. The %MMHg increased from sediment (<3%) to filamentous algae (6±6%), aquatic worm (30±9%), asian clam (49±20%), caddisfly larva (66±7%), mayfly larva (73±2%), stonefly larva (80±9%), and fish (93-100%). This trend is strongly indicative of the preferential trophic transfer of MMHg via biomagnification in the Yuba River.

4.3.2.2 Biota Hg Isotopic Compositions

Aquatic organisms had a relatively narrow range in δ^{202}Hg (−0.84 to −0.42‰) but a wide range in Δ^{199}Hg (0.06 to 1.17‰; Table 4.S2). We performed linear regressions between %MMHg and biota Hg isotope values (δ^{202}Hg and Δ^{199}Hg) to estimate the isotopic composition of IHg and MMHg in the food web. Sediment was excluded from the regressions to allow comparison of IHg in the food web with IHg in sediment and algae. In biota we observed a significant positive relationship for Δ^{199}Hg (r^2 = 0.78; $p<0.001$) with increasing %MMHg, but not for δ^{202}Hg (r^2 = 0.01 $p=0.61$). The relationship between Δ^{199}Hg and %MMHg strengthened when benthic macroinvertebrates (excluding fish) were grouped by sampling year (r^2 = 0.96 for 2013 and r^2 = 0.94 for 2014). Positive relationships between Δ^{199}Hg and %MMHg have been previously reported in stream, lake and estuarine food webs.[23-25] In contrast, there was no significant positive relationship between δ^{202}Hg and %MMHg in Yuba-Feather River biota. Previous studies of lake, forest and estuary food webs have consistently demonstrated significant positive relationships between δ^{202}Hg and %MMHg,[23-25] although no such relationship was observed in the Eel River.[25]

We estimated the isotopic composition of IHg and MMHg during each sampling campaign by extrapolation to 100% IHg and 100% MMHg for Δ^{199}Hg and δ^{202}Hg (Figure 4.2a,b). Because there was no significant positive relationship for δ^{202}Hg, we also estimated MMHg δ^{202}Hg using the mean δ^{202}Hg of organisms with >70% MMHg (following Tsui et al.[25]) and IHg δ^{202}Hg using the mean δ^{202}Hg of <15% MMHg biota (filamentous algae). The δ^{202}Hg values estimated by high trophic level biota (−0.69±0.12‰ for MMHg) and low %MMHg algae (−0.70±0.08‰ for IHg) are not significantly different than MMHg and IHg estimates from linear regression. Thus, we use MMHg and IHg values estimated by linear

regression in the following discussion. In 2013, MMHg had δ^{202}Hg of −0.72±0.05‰ and Δ^{199}Hg of 0.90±0.04‰ and IHg had δ^{202}Hg of −0.63±0.06‰ and Δ^{199}Hg of 0.05±0.04‰. In 2014, MMHg had a δ^{202}Hg of −0.72±0.04‰ and Δ^{199}Hg of 1.44±0.04‰ while IHg had δ^{202}Hg of −0.70±0.05‰ and Δ^{199}Hg of −0.04±0.05‰. The error reported for these estimates is the ±1SE of the intercept (i.e., at 100% IHg or MMHg). These estimates suggest a significant change in MMHg Δ^{199}Hg between 2013 and 2014 (Figure 4.2a), but a relatively consistent isotopic composition of IHg between years (δ^{202}Hg of −0.70‰ and Δ^{199}Hg of 0.05‰ for 2013 and 2014 combined).

4.3.2.3 MMHg Isotopic Composition

The isotopic composition of MMHg reflects the isotopic composition of Hg source(s) and the sum of fractionation due to biogeochemical processes prior to entering the food web.[50] The Δ^{199}Hg:Δ^{201}Hg ratio in environmental samples such as fish and biota can differentiate between photochemical MMHg degradation (slope of ~1.3) and photochemical Hg^{2+} reduction (slope of ~1.0).[51] Biota from the Yuba-Feather River had a Δ^{199}Hg/Δ^{201}Hg slope of 1.27±0.05 (1SE, n=35; Figure 4.S4), which is comparable to freshwater fish from lakes (1.28±0.01; 1SE, n=135)[52] and consistent with other freshwater food web studies.[23-26] This implies that the Δ^{199}Hg and Δ^{201}Hg values of MMHg result from MIF due to the magnetic isotope effect during photochemical MMHg degradation.[51] During MMHg photodegradation, which is likely occurring in the highly exposed, nearly treeless Yuba-Feather riparian zone, the residual MMHg (with positive Δ^{199}Hg and Δ^{201}Hg) forms the pool of MMHg that can be incorporated into the food web. The magnitude of MIF is directly proportional to the extent of photochemical degradation, and can be quantified

from slopes derived experimentally in 1 mg/L or 10 mg/L DOC conditions.[51] During a 4-year period in the lower Yuba River surface water DOC averaged 1.16±0.05 mg/L (1SE, n=104).[53] Thus, we use 1 mg/L DOC experimental slopes to calculate (±3%) that 24% of MMHg had undergone photodegradation in 2013, while in 2014 35% of MMHg had undergone photodegradation in the Yuba-Feather River.

In aquatic systems, MIF from photochemical MMHg degradation has been shown to vary with water clarity,[21] water depth,[54] or canopy cover.[23, 27] In this study, the extent of MMHg photodegradation was different between March 2013 and June 2014 in the Yuba River. This could result from different environmental conditions between years (e.g., streamflow and water depth, shading) or the timing of sampling (e.g., early spring vs. early summer), which could affect the Δ^{199}Hg of bioaccumulated MMHg. Although we are unable to identify the relative importance of these different factors, fish sampled in 2014 with >90% MMHg have Δ^{199}Hg of 0.79 and 0.84‰; nearly identical to the Δ^{199}Hg of MMHg in 2013 (0.90‰). We suspect this similarity could result because the fish sampled are relatively long lived (1-3 years) and might integrate the MMHg across years compared to seasonal growth and MMHg bioaccumulation in the benthic macroinvertebrates sampled. Regardless, in each year we observed no significant change in the extent of photodegradation (i.e., Δ^{199}Hg) between sampling sites. Thus, although MMHg Δ^{199}Hg changes seasonally or annually, the extent of photodegradation (i.e., Δ^{199}Hg) did not change spatially in the section of the Yuba-Feather River system we sampled.

To isolate photochemical and non-photochemical processes in aquatic environments, we subtract the known MDF and MIF that results from photochemical MMHg degradation from the MMHg isotopic composition. Using experimentally derived

slopes for $\Delta^{199}Hg/\delta^{202}Hg$ (2.43 for 1 mg/L DOC)[51] we can estimate the $\delta^{202}Hg$ of MMHg prior to photodegradation ("pre-photodegraded MMHg"). This approach has been used to isolate MDF between IHg and MMHg in studies of estuaries, the coastal ocean and lakes.[21-24, 55] In these past studies, a consistent positive $\delta^{202}Hg$ offset ($\delta^{202}Hg_{\text{pre-degraded MMHg}} - \delta^{202}Hg_{IHg}$) was found and interpreted to result from biotic MDF (e.g., a combination of biotic methylation and degradation) in the environment. [21, 22, 24] Assuming that pre-photodegraded MMHg has $\Delta^{199}Hg$ near zero, consistent with IHg in Yuba Fan sediment and the food web, the $\delta^{202}Hg$ of pre-photodegraded MMHg in 2013 was −1.07‰ and in 2014 was −1.29‰. These values are much lower than the $\delta^{202}Hg$ of IHg pools in sediment (−0.38±0.17‰) or algae (−0.70±0.08‰) in the Yuba River and results in a negative $\delta^{202}Hg$ offset between IHg and MMHg (Figure 4.3). This negative $\delta^{202}Hg$ offset has not been previously observed and we examine possible explanations for this unique relationship below.

4.3.3 Hg Sources in the Yuba River

The Yuba River contains large quantities of IHg in streambed and stream bank/terrace sediment, which provide a persistent source of Hg to the river. The isotopic composition of two IHg pools were characterized in this study: Yuba Fan sediment with >95% IHg has $\delta^{202}Hg$ of −0.38±0.17‰ and $\Delta^{199}Hg$ of 0.04±0.03‰ (1SD, n=7) and filamentous algae with 85-98% IHg has $\delta^{202}Hg$ of −0.70±0.08‰ and $\Delta^{199}Hg$ of 0.11±0.04‰ (1SD, n=7). We estimated the isotopic composition of IHg in biota and it has $\delta^{202}Hg$ of −0.70±0.04‰ and $\Delta^{199}Hg$ of 0.05±0.07‰, which is similar to in-stream IHg pools (Figure 4.3). Therefore, we suggest the IHg in the food web is directly accumulated from sediment

and algae, likely because these materials are a dietary resource for benthic macroinvertebrates. The isotopic composition of MMHg and pre-photodegraded MMHg in the Yuba River was also estimated. MMHg could have been produced in the stream from in situ methylation in the hyporheic zone or associated with benthic biofilms or filamentous algae.[12, 56-58] If so, then either a bioavailable portion of IHg (with δ^{202}Hg lower than bulk sediment) is preferentially methylated or net negative MDF (of up to −0.9‰) occurs between IHg and pre-photodegraded MMHg (Figure 4.4a). Alternatively, the presence and bioaccumulation of MMHg in some streams is considered a function of watershed characteristics that promote Hg deposition and methylation.[10, 11, 13, 59] If MMHg in the lower Yuba River were derived from upstream watershed Hg sources (not produced in situ) then Yuba Fan sediment might only be a source of IHg, and perhaps not MMHg, to the food web.

We explore possible external Hg sources by comparing known isotopic compositions of these sources with Yuba River MMHg and pre-photodegraded MMHg. In lakes and oceans, atmospheric deposition may provide a readily reactive IHg source that can be methylated and provide MMHg to the food web.[60] [54] Precipitation that was unaffected by local point sources of Hg collected near SF Bay,[37] coastal FL,[61] Ontario, CA[62] and the Midwest US,[30, 63] had δ^{202}Hg of −0.43±0.50‰ and Δ^{199}Hg of 0.37±0.26‰ (mean±1SD; n=62). Significant positive Δ^{199}Hg in precipitation, but not in IHg in the food web (Δ^{199}Hg of 0.05±0.07‰) clearly demonstrate that Yuba biota do not obtain IHg from precipitation. If precipitation Hg were the precursor to MMHg in Yuba River biota, then precipitation Hg must be preferentially methylated despite the presence of high THg Yuba Fan sediment. Furthermore, significant negative MDF of at least 0.6‰ would still be required to link precipitation IHg to pre-photodegraded MMHg in the Yuba River. At

present, there is no evidence to suggest precipitation Hg is a significant input to biota and we think it is highly unlikely to be preferentially methylated in the Yuba River.

It is also possible that IHg accumulated in the upstream watershed (e.g., upstream of Englebright Dam) would be a source of MMHg that could enter the lower Yuba River. Terrestrial soils accumulate Hg from dry deposition, leaf litter, and precipitation.[30, 64] This IHg could then be methylated in wetlands, floodplains or reservoirs and transported to aquatic environments during runoff events.[65] Basal resources (foliage, soil, and submerged leaf litter) from the Eel River in northern California had relatively low δ^{202}Hg (−2.53 to −1.54‰) and negative Δ^{199}Hg (−0.37 to −0.15‰).[25] The isotopic composition of forest floor samples from the upper Midwest (δ^{202}Hg from −1.05 to −1.88 and Δ^{199}Hg from −0.15 to −0.25 ‰) and low THg sediment from TN streams (δ^{202}Hg of −1.40±0.06 and Δ^{199}Hg of −0.26±0.03 ‰) had a similar range.[30] [18] When not impacted by Au mining, we expect the isotopic composition of IHg in the Yuba River watershed might have a similar range to these resources (δ^{202}Hg of −1 to −2.5 ‰ and negative Δ^{199}Hg). Since the δ^{202}Hg of pre-photodegraded MMHg in the Yuba River overlaps with watershed IHg pools (Figure 4.4b), we cannot rule these out as a possible source of MMHg to the Yuba River. However, THg in Yuba Fan sediment is at least ~3X, and up to 2 orders of magnitude, higher than background sediment and is present in locations where methylation is thought to occur (e.g., streambed, floodplains, hyporheic zones, and associated with filamentous algae).[11, 12, 58, 66, 67] Moreover, IHg in biota is directly accumulated from sediment and algae (Figure 4.3), and it follows that MMHg associated with these benthic resources is likely to be derived from nearby IHg pools. Therefore, we suggest that Hg in Yuba River sediment or algae is

the most likely IHg source to be methylated leading to MMHg bioaccumulation in the lower Yuba River food web.

4.3.4 In Stream Processes and MDF

4.3.4.1 Labile Hg in Sediment

Only a fraction of the IHg pool in sediment may actually be available for microbial methylation.[11, 16, 68-70] If this fraction has lower δ^{202}Hg than bulk sediment, then the negative δ^{202}Hg offset between IHg and pre-photodegraded MMHg may be an artifact of the difference between bulk sediment δ^{202}Hg and the δ^{202}Hg of labile IHg. If we assume biotic MDF is consistent with previous studies (δ^{202}Hg offset of +0.4‰ to +0.8‰)[21, 22, 24, 55] from the pre-photodegraded MMHg δ^{202}Hg (−1.29 to −1.07) we would predict labile IHg to have δ^{202}Hg between −1.5 and −2.1‰. Multiple experiments have shown that leachates (water soluble, thiosulfate soluble and weak acid soluble) have consistently higher δ^{202}Hg (up to 1.3‰) than bulk sediment and mine waste.[71-73] In Au mine tailings, HgS species and Hg sorbed to colloids may be susceptible to methylation in the hyporheic zone or inundated floodplains.[74] A few studies have demonstrated that precipitation of HgS, β-HgS and HgO from solution[75, 76] and sorption of Hg to goethite[77] result in a lower δ^{202}Hg for the reaction product (HgS or goethite-Hg). However, a separate investigation of sediment contaminated by metallic Hg suggests that sulfide bound Hg actually has higher δ^{202}Hg (up to 1‰) than bulk sediment.[78] Although these studies demonstrate that Hg fractions in sediment may have different δ^{202}Hg, at present we are unable to identify a specific labile Hg fraction with consistent low δ^{202}Hg that could explain the IHg-MMHg relationship. Thus, we use bulk

material Hg isotopic compositions of sediment and algae to best define the IHg pools in the Yuba River.

4.3.4.2 Net MDF during Biotic Processes

Previous studies have found a net positive $\delta^{202}Hg$ offset ($\delta^{202}Hg_{\text{pre-photodegraded MMHg}} - \delta^{202}Hg_{IHg}$) between bulk sediment (IHg) and pre-photodegraded MMHg. The magnitude of this offset ranges from +0.4 to +0.8‰ in studies of coastal oceans (San Francisco Bay, East Coast estuaries, Minamata Bay) and freshwater lakes in Michigan and Florida.[21, 22, 24, 55] Biotic methylation preferentially methylates light Hg isotopes (MMHg produced has lower $\delta^{202}Hg$ than the IHg substrate),[79, 80] while biotic degradation by the mercury reductase mechanism leads to higher $\delta^{202}Hg$ for the residual MMHg.[81] Therefore, it was previously concluded that during biotic processing of Hg in sediment, methylation is followed by significant MMHg degradation, resulting in a $\delta^{202}Hg$ of residual MMHg that is higher than the original sediment. This residual MMHg is subsequently photodegraded ($+\Delta^{199}Hg$ and $+\delta^{202}Hg$)[51, 82] and bioaccumulated (no additional MIF or MDF)[32, 50]. In contrast, in this study the $\delta^{202}Hg$ of pre-photodegraded MMHg in the Yuba River is significantly lower (at least 0.4‰ in 2013, and at least 0.6‰ in 2014) than either sediment or filamentous algae $\delta^{202}Hg$. Therefore, we suggest that there is a fundamental difference in Hg biogeochemistry, and resulting isotope fractionation, that is related to either the net extent of methylation and degradation or to different biotic MMHg degradation pathways. We note that all of the previous studies we have referred to were in lakes, coastal oceans or estuaries and that this is the first such study to compare IHg and MMHg in a river system.

A number of environmental characteristics (e.g., DOC, redox, turbulence, suspended solids, etc.) that affect MMHg formation and degradation differ between rivers (flowing water) and lake or coastal ocean (non-flowing water) environments and might affect net MDF between IHg and MMHg. In streams, in-situ Hg methylation in sediment, hyporheic zones, benthic biofilms or filamentous algae (e.g.,[12, 56, 58, 66]) would be followed by MMHg advection from the substrate into the water column. Intuitively, we would expect this transport to be greater in flowing water (i.e., rivers) than in non-flowing water environments (i.e., lakes or estuaries). Turbulent diffusion of MMHg has previously been hypothesized to increase MDF during experimental studies of biotic methylation and degradation.[80] Similarly, in-situ methylation in flowing water could lead to continuous removal of the product MMHg from the site of methylation and decrease the quantity of MMHg available for biotic degradation. The result would be MMHg exported to the water column that has not been biotically degraded, and therefore exhibits lower δ^{202}Hg than the original IHg substrate. Conversely, when MMHg resides for a relatively long period of time in sediment, as might be the case in standing water, it could be biotically degraded to a greater extent. Significant biotic MMHg degradation would drive the residual MMHg to higher δ^{202}Hg values than the sediment, as has been observed in lakes and coastal ocean environments. If this is the mechanism, then the δ^{202}Hg offset between IHg and MMHg would suggest that relatively little biotic MMHg degradation occurs in the Yuba River (i.e. photochemical degradation is likely the dominant degradation pathway) compared to standing water environments where biotic MMHg degradation must occur to a greater extent.

It might also be possible that non-*mer* mediated biotic degradation pathways could have different MDF leading to the negative δ^{202}Hg offset observed. Biotic MMHg degradation can occur through either *mer*-mediated degradation or oxidative demethylation pathways.[83, 84] During *mer*-mediated degradation, MMHg is converted to Hg^0 and which can be partially removed from the substrate,[84] resulting in +MDF (residual MMHg with higher δ^{202}Hg).[81] Oxidative demethylation, which is considered a byproduct of microbial metabolism, likely converts MMHg to Hg^{2+} product.[6, 85, 86] Isotopic fractionation during oxidative demethylation has not yet been measured, but during this process the Hg^{2+} product could undergo remethylation. We hypothesize that during biotic cycling, when oxidative MMHg degradation is the dominant pathway, MMHg would become enriched in light Hg isotopes through successive methylation (−MDF), degradation and re-methylation (−MDF). Environmental conditions that determine preferred degradation pathways might differ between flowing and standing water environments. In general, oxidative demethylation is expected to be dominant when bioavailable Hg is not at a high enough concentration to induce *mer*-enzyme expression (i.e., low THg environments).[83, 86] However, in high THg environments geochemical conditions such as redox state, organic matter content and sulfide may control Hg bioavailability and therefore change the dominant degradation pathway.[83] Although we cannot pinpoint the specific mechanism for the observed net negative MDF between IHg and MMHg, the extent or pathway of biotic MMHg degradation are plausible mechanisms for the MMHg to have lower δ^{202}Hg than the IHg source.

4.3.4.3 Annual Variation in MDF and MIF

After comparing IHg and MMHg in the Yuba-Feather River with previously studied environments, we suggest that the δ^{202}Hg offset is driven by differences in net biotic MDF during biotic methylation and degradation. There was a ~0.5‰ difference in Δ^{199}Hg, and thus the extent of MMHg photodegradation, between 2013 and 2014. If a single isotopically distinct pool of MMHg were photodegraded in both 2013 and 2014, then we would expect MMHg to fall along the same experimental photochemical degradation slope each year. However, 2013 MMHg does not fall on the 2014 photochemical degradation line (Figure 4.3). Instead, the δ^{202}Hg of pre-photodegraded MMHg is different between years, which could indicate that the source of bioavailable IHg or the extent of biotic MDF changed between 2013 and 2014. Alternatively, we note that the IHg and MMHg have nearly identical δ^{202}Hg, regardless of sampling year or Δ^{199}Hg value. This could imply that the experimental δ^{202}Hg/Δ^{199}Hg slope (1 mg/L DOC) does not accurately represent Hg isotope fractionation during photochemical MMHg degradation in this location. Experimental work under more environmentally relevant conditions (i.e., DOC content and MMHg:DOC ratios) and in flowing water environments, is required to better understand and differentiate between biotic and photochemical Hg isotope fractionation in river systems.

4.3.5 Implications for Future Work

This study is the first to use Hg isotopes to identify MMHg sources and infer important biogeochemical transformations in a stream contaminated by historical Au mining. We have characterized the isotopic composition of sediment in the Yuba Fan, which will enable future tracing of sediment-bound IHg to downstream floodplains and wetlands

in the Sacramento Valley. We also identified the isotopic composition of Yuba River MMHg, which could be valuable for future studies that investigate whether MMHg from the Yuba River is exported downstream (such as to the Yolo Bypass, a 24000 ha engineered flood bypass downstream)[70, 87] or to the terrestrial food web. Comparison of IHg with MMHg and pre-photodegraded MMHg provided useful insight on Hg biogeochemical processes in the Yuba River. We were unable to rule out the possibility that upstream, watershed Hg sources provide some MMHg to the lower Yuba River food web. However, Hg isotopes demonstrate that filamentous algae and sediment provide IHg to benthic macroinvertebrates through their diet. Thus, we think it likely that MMHg in the lower Yuba River is formed through in situ processes that methylate IHg in sediment or filamentous algae. As a result, the relationship between IHg and MMHg observed in this study is different than in previous studies of lakes, estuaries and forests. We hypothesize that this could be due to differences in net MDF resulting from the extent or the pathway of biotic MMHg degradation in the Yuba River. If changes in biotic MMHg degradation result from characteristic differences between flowing and non-flowing water environments, then we expect similar net negative MDF to be observed between IHg and MMHg in other streams systems.

Acknowledgements

We thank Marcus Johnson (UM-BEIGL) for assistance in the operation of the CV-MC-ICP-MS and Tyler Nakamura and Ka'ai Jensen (San Jose State University) for their valuable assistance with field sampling. We also thank Evangelos Kakouros, Michelle Arias and Le H. Kieu (USGS, Menlo Park, CA) for sediment THg and sediment and biota MMHg analysis. We also acknowledge financial support from the National Science Foundation: EAR-1226741 (to M.B.S.).

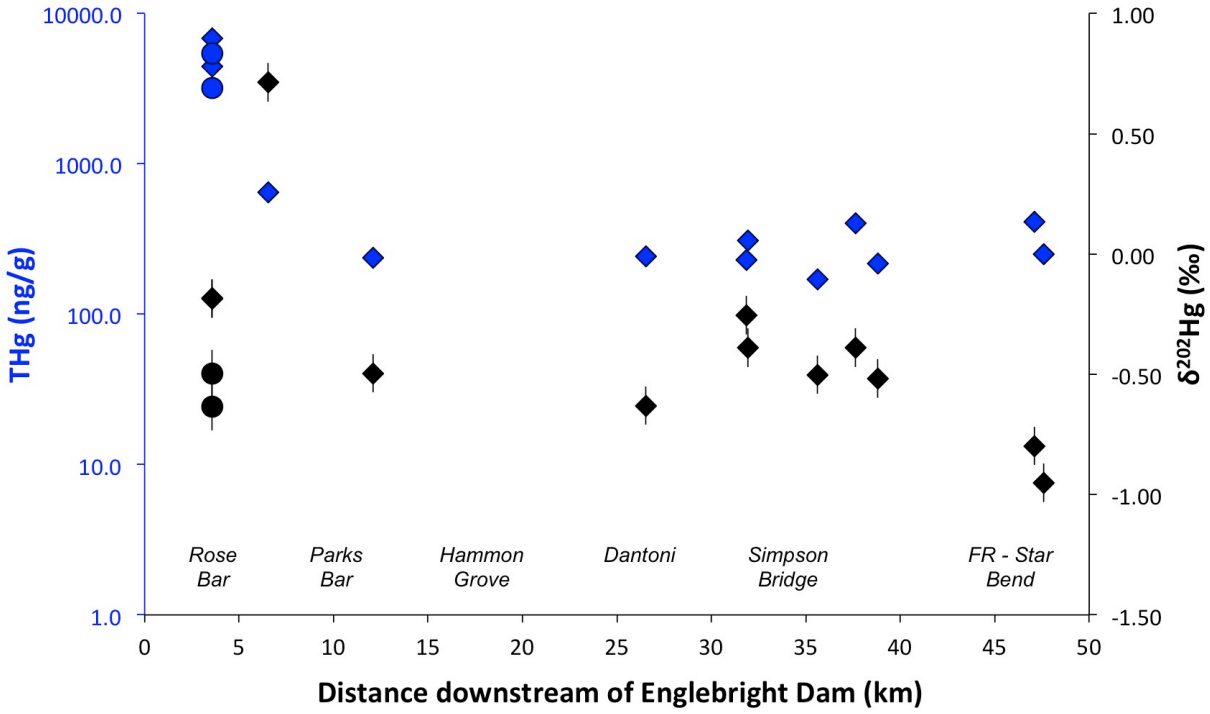

Figure 4.1: Sediment δ^{202}Hg and THg vs. distance downstream of Englebright Dam in the Yuba-Feather river system

Diamonds represent sediment analyzed in this study, with blue indicating THg and black indicating the corresponding δ^{202}Hg values (±0.08‰). Circle symbols represent two sediment samples previously analyzed by Donovan et al.[37] from Rose Bar. Biota sampling sites (RB, PB, HG, Da, SB, FR-Star Bend) are noted at the bottom of the figure in their approximate location along the Yuba and Feather River.

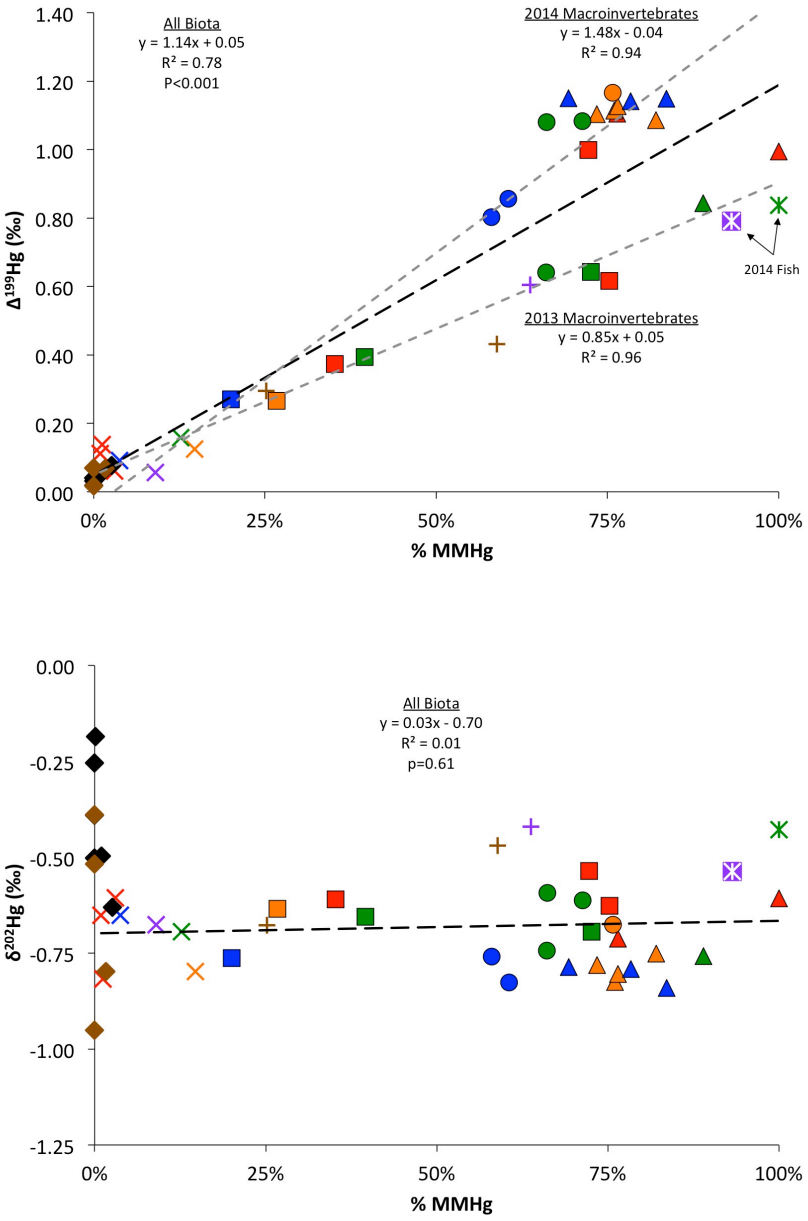

Figure 4.2: %MMHg vs. Δ^{199}Hg (A, top) or δ^{202}Hg (B, bottom) for all biota
Dark dashed lines represent linear relationships for all biota while light gray lines indicate specific sampling year. Biota are colored corresponding to their sampling location (RB = red, PB = orange, HG = blue, Da = green, SB = purple, FR = brown). Symbols represent the sample type (stonefly = triangle, caddisfly = circle, Mayfly and Aq. Worm= square, clam = +, fish = asterisk and filamentous algae = x). Sediment is included and symbols are colored by stream with solid black diamonds representing Yuba River sediment and solid brown diamonds representing Feather River sediment. A detailed legend can be found in Figure 4.S2.

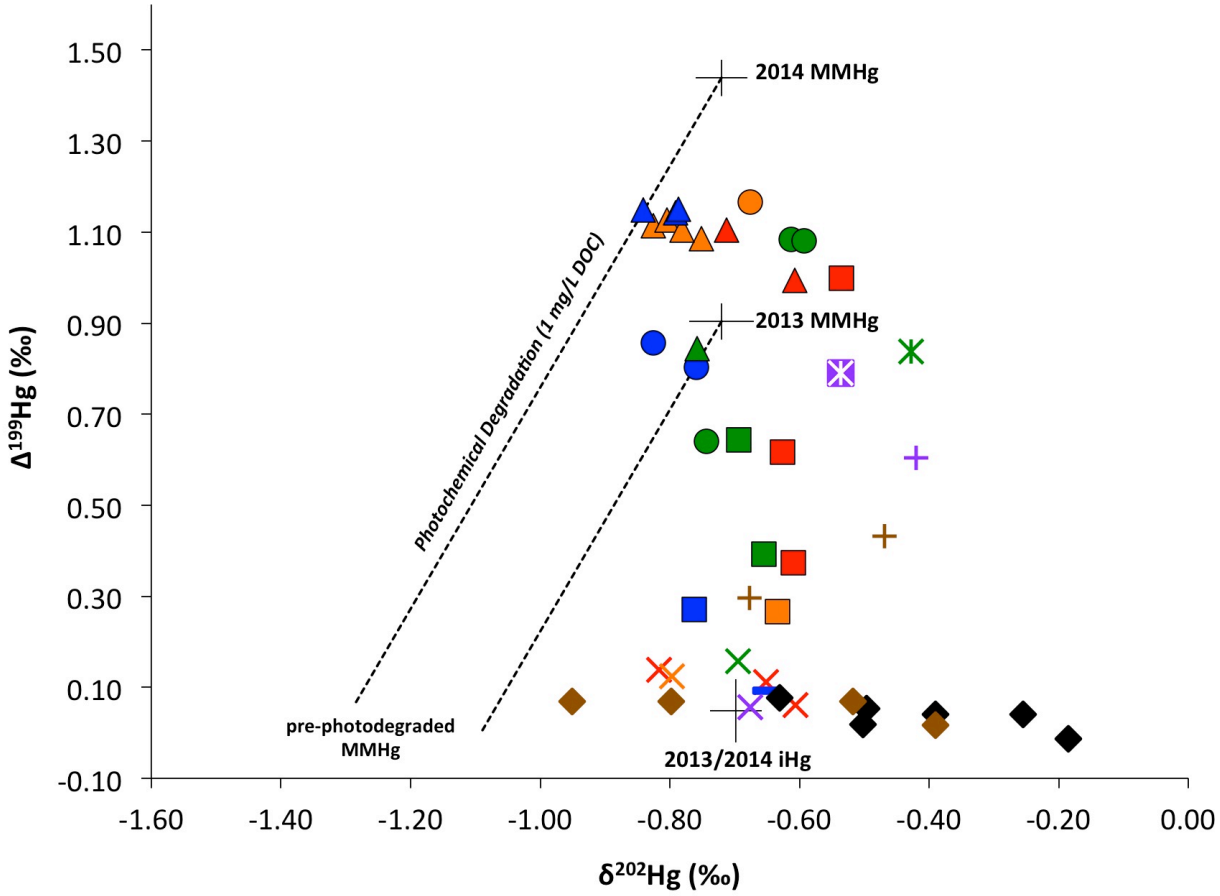

Figure 4.3: Hg isotopic composition (δ^{202}Hg vs. Δ^{199}Hg) for biota and sediment in the Yuba and Feather Rivers

Symbols are identical to Figure 4.2 and approximate 2SD error for biota is ±0.08‰ for δ^{202}Hg and ±0.05 for Δ^{199}Hg. MMHg and IHg isotopic compositions estimated from linear regression are black crosses and their size is representative of the 1SE uncertainty for these estimates. The 1 mg/L MMHg photochemical degradation slope is from Bergquist and Blum.[51]

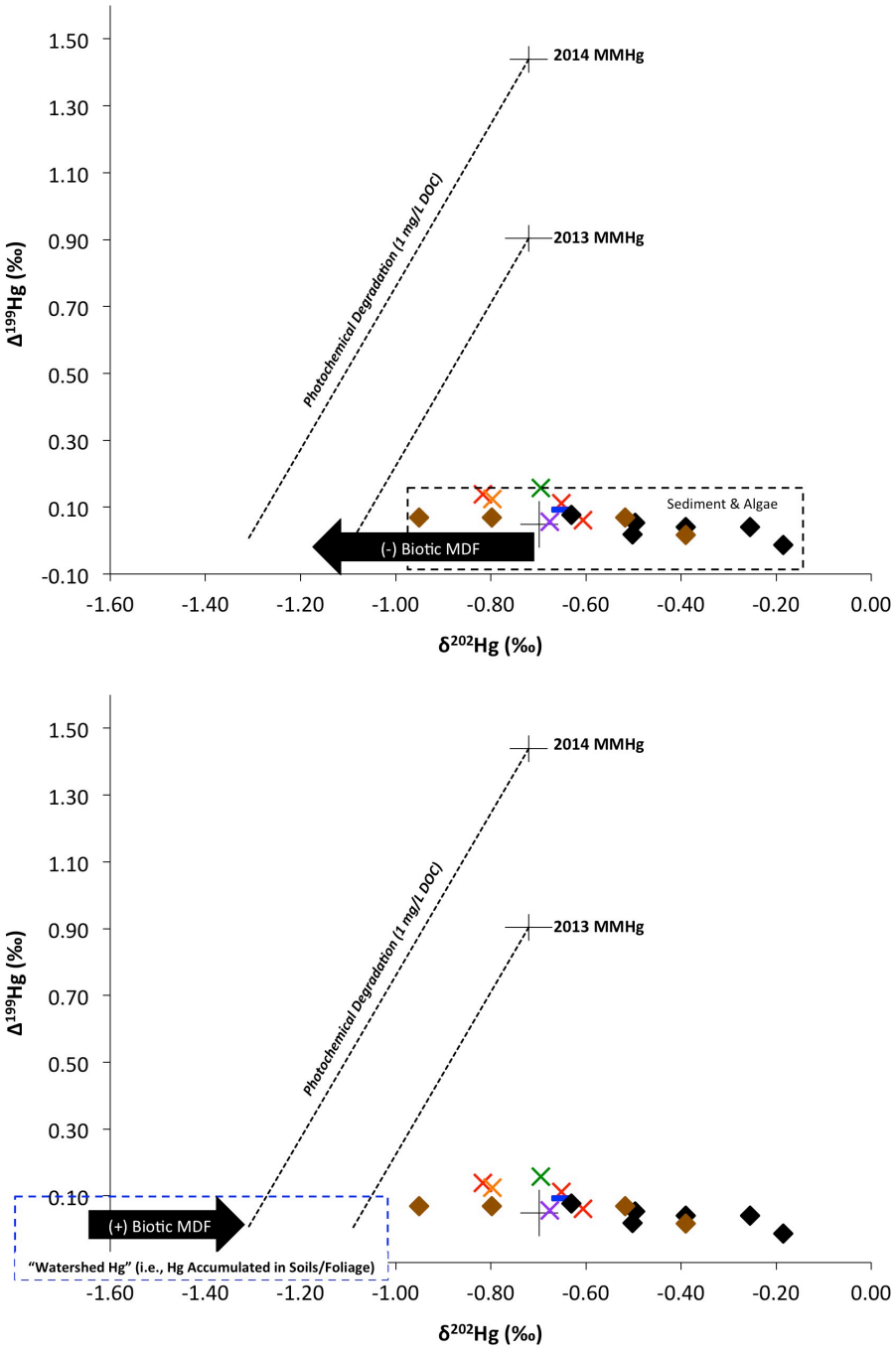

Figure 4.4: Explanations for the origin of MMHg in the Yuba and Feather Rivers
Either (A, top) sediment and algae IHg sources result in net negative biotic MDF or (B, bottom) watershed IHg sources (~δ^{202}Hg of −1 to −2.5‰) are methylated and input to the Yuba-Feather River, with net positive biotic MDF consistent with previous studies.

References

1. Selin, N. E., Global Biogeochemical Cycling of Mercury: A Review. *Annu. Rev. Environ. Resour.* **2009,** *34*, (1), 43-63.

2. Alpers, C. N.; Hunerlach, M. P.; May, J. T.; Hothem, R. L., Mercury contamination from historical gold mining in California. *Fact Sheet - U. S. Geological Survey* **2005,** *1*.

3. Gilbert, G. K., *Hydraulic-mining debris in the Sierra Nevada*. US Gov't Print. Off.: 1917.

4. Singer, M. B.; Aalto, R.; James, L. A.; Kilham, N. E.; Higson, J. L.; Ghoshal, S., Enduring legacy of a toxic fan via episodic redistribution of California gold mining debris. *Proceedings of the National Academy of Sciences* **2013**.

5. Hunerlach, M. P.; Alpers, C. N.; Marvin-DiPasquale, M. C.; Taylor, H. E.; De Wild, J. F. *Geochemistry of mercury and other trace elements in fluvial tailings upstream of Daguerre Point Dam, Yuba River, California, August 2001*; 2004; p 77.

6. Hsu-Kim, H.; Kucharzyk, K. H.; Zhang, T.; Deshusses, M. A., Mechanisms Regulating Mercury Bioavailability for Methylating Microorganisms in the Aquatic Environment: A Critical Review. *Environ. Sci. Technol.* **2013,** *47*, (6), 2441-2456.

7. Marvin-DiPasquale, M.; Agee, J. L., Microbial mercury cycling in sediments of the San Francisco Bay-Delta. *Estuaries* **2003,** *26*, (6), 1517-1528.

8. Davis, J. A.; Looker, R. E.; Yee, D.; Marvin-Di Pasquale, M.; Grenier, J. L.; Austin, C. M.; McKee, L. J.; Greenfield, B. K.; Brodberg, R.; Blum, J. D., Reducing methylmercury accumulation in the food webs of San Francisco Bay and its local watersheds. *Environ. Res.* **2012,** *119*, (Special Issue), 3-26.

9. Marvin-DiPasquale, M. C.; Agee, J. L.; Bouse, R. M.; Jaffe, B. E., Microbial cycling of mercury in contaminated pelagic and wetland sediments of San Pablo Bay, California. *Environmental Geology* **2003,** *43*, (3), 260-267.

10. Chasar, L. C.; Scudder, B. C.; Stewart, A. R.; Bell, A. H.; Aiken, G. R., Mercury Cycling in Stream Ecosystems. 3. Trophic Dynamics and Methylmercury Bioaccumulation. *Environ. Sci. Technol.* **2009,** *43*, (8), 2733-2739.

11. Marvin-DiPasquale, M.; Lutz, M. A.; Brigham, M. E.; Krabbenhoft, D. P.; Aiken, G. R.; Orem, W. H.; Hall, B. D., Mercury Cycling in Stream Ecosystems. 2. Benthic Methylmercury Production and Bed Sediment-Pore Water Partitioning. *Environ. Sci. Technol.* **2009,** *43*, (8), 2726-2732.

12. Tsui, M. T. K.; Finlay, J.; Balogh, S.; Nollet, Y., In Situ Production of Methylmercury within a Stream Channel in Northern California. *Environ. Sci. Technol.* **2010,** *44*, (18), 6998-7004.

13. Ward, D. M.; Nislow, K. H.; Folt, C. L., Bioaccumulation syndrome: identifying factors that make some stream food webs prone to elevated mercury bioaccumulation. *Ann. N. Y. Acad. Sci.* **2010,** *1195*, (1), 62-83.

14. Walters, D. M.; Raikow, D. F.; Hammerschmidt, C. R.; Mehling, M. G.; Kovach, A.; Oris, J. T., Methylmercury Bioaccumulation in Stream Food Webs Declines with Increasing Primary Production. *Environ. Sci. Technol.* **2015,** *49*, (13), 7762-7769.

15. Fleck, J. A.; Alpers, C. N.; Marvin-DiPasquale, M.; Hothem, R. L.; Wright, S. A.; Ellett, K.; Beaulieu, E.; Agee, J. L.; Kakouros, E.; Kieu, L. H.; Eberl, D. D.; Blum, A. E.; May, J. T., The effects of sediment and mercury mobilization in the south Yuba River and Humbug Creek confluence area, Nevada County, California; concentrations, speciation, and environmental fate; Part 1, Field characterization. *Open-File Report - U. S. Geological Survey* **2011,** *1*.

16. Marvin-DiPasquale, M.; Agee, J. L.; Kakouros, E.; Kieu, L. H.; Fleck, J. A.; Alpers, C. N., The effects of sediment and mercury mobilization in the South Yuba River and Humbug Creek confluence area, Nevada County, California; concentrations, speciation, and environmental fate; Part 2, Laboratory experiments. *Open-File Report - U. S. Geological Survey* **2011,** *1*.

17. May, J. T.; Hothem, R. L.; Alpers, C. N.; Law, M. A., Mercury bioaccumulation in fish in a region affected by historic gold mining: the South Yuba River, Deer Creek, and Bear River watersheds, California, 1999. **2000**.

18. Donovan, P. M.; Blum, J. D.; Demers, J. D.; Gu, B.; Brooks, S. C.; Peryam, J., Identification of Multiple Mercury Sources to Stream Sediments near Oak Ridge, TN, USA. *Environ. Sci. Technol.* **2014,** *48*, (7), 3666-3674.

19. Gray, J. E.; Van Metre, P. C.; Pribil, M. J.; Horowitz, A. J., Tracing historical trends of Hg in the Mississippi River using Hg concentrations and Hg isotopic compositions in a lake sediment core, Lake Whittington, Mississippi, USA. *Chem. Geol.* **2015,** *395*, (0), 80-87.

20. Smith, R. S.; Wiederhold, J. G.; Jew, A. D.; Brown, G. E.; Bourdon, B.; Kretzschmar, R., Stable Hg Isotope Signatures in Creek Sediments Impacted by a Former Hg Mine. *Environ. Sci. Technol.* **2015,** *49*, (2), 767-776.

21. Sherman, L. S.; Blum, J. D., Mercury stable isotopes in sediments and largemouth bass from Florida lakes, USA. *Sci. Total Environ.* **2013,** *448*, (0), 163-175.

22. Gehrke, G. E.; Blum, J. D.; Slotton, D. G.; Greenfield, B. K., Mercury Isotopes Link Mercury in San Francisco Bay Forage Fish to Surface Sediments. *Environ. Sci. Technol.* **2011,** *45*, (4), 1264-1270.

23. Kwon, S. Y.; Blum, J. D.; Nadelhoffer, K. J.; Timothy Dvonch, J.; Tsui, M. T.-K., Isotopic study of mercury sources and transfer between a freshwater lake and adjacent forest food web. *Sci. Total Environ.* **2015,** *532*, (0), 220-229.

24. Kwon, S. Y.; Blum, J. D.; Chen, C. Y.; Meattey, D. E.; Mason, R. P., Mercury Isotope Study of Sources and Exposure Pathways of Methylmercury in Estuarine Food Webs in the Northeastern US. *Environ. Sci. Technol.* **2014,** *48*, (17), 10089-10097.

25. Tsui, M. T. K.; Blum, J. D.; Kwon, S. Y.; Finlay, J. C.; Balogh, S. J.; Nollet, Y. H., Sources and Transfers of Methylmercury in Adjacent River and Forest Food Webs. *Environ. Sci. Technol.* **2012,** *46*, (20), 10957-10964.

26. Tsui, M. T. K.; Blum, J. D.; Finlay, J. C.; Balogh, S. J.; Nollet, Y. H.; Palen, W. J.; Power, M. E., Variation in Terrestrial and Aquatic Sources of Methylmercury in Stream Predators as Revealed by Stable Mercury Isotopes. *Environ. Sci. Technol.* **2014,** *48*, (17), 10128-10135.

27. Tsui, M. T. K.; Blum, J. D.; Finlay, J. C.; Balogh, S. J.; Kwon, S. Y.; Nollet, Y. H., Photodegradation of methylmercury in stream ecosystems. *Limnol. Oceanogr* **2013,** *58*, (1), 13-22.

28. Hammerschmidt, C.; Fitzgerald, W., Bioaccumulation and Trophic Transfer of Methylmercury in Long Island Sound. *Arch. Environ. Contam. Toxicol.* **2006,** *51*, (3), 416-424.

29. USEPA *Method 1630: Methyl Mercury in Water by Distillation, Aqueous Ethylation, Purge and Trap, and CVAFS*; U.S. Environmental Protection Agency, Office of Water, Office of Science and Technology, Engineering and Analysis Division: Washington, D.C., 2001.

30. Demers, J. D.; Blum, J. D.; Zak, D. R., Mercury isotopes in a forested ecosystem: Implications for air-surface exchange dynamics and the global mercury cycle. *Global Biogeochem. Cycles* **2013,** *27*, (1), 222-238.

31. Blum, J. D.; Bergquist, B. A., Reporting of variations in the natural isotopic composition of mercury. *Anal. Bioanal. Chem.* **2007,** *388*, (2), 353-359.

32. Kwon, S. Y.; Blum, J. D.; Chirby, M. A.; Chesney, E. J., Application of mercury isotopes for tracing trophic transfer and internal distribution of mercury in marine fish feeding experiments. *Environ. Toxicol. Chem.* **2013,** *32*, (10), 2322-2330.

33. Masbou, J.; Point, D.; Sonke, J. E., Application of a selective extraction method for methylmercury compound specific stable isotope analysis (MeHg-CSIA) in biological materials. *J. Anal. At. Spectrom.* **2013,** *28*, (10), 1620-1628.

34. Cooke, C. A.; Hintelmann, H.; Ague, J. J.; Burger, R.; Biester, H.; Sachs, J. P.; Engstrom, D. R., Use and Legacy of Mercury in the Andes. *Environ. Sci. Technol.* **2013,** *47*, (9), 4181-4188.

35. Biswas, A.; Blum, J. D.; Bergquist, B. A.; Keeler, G. J.; Xie, Z. Q., Natural Mercury Isotope Variation in Coal Deposits and Organic Soils. *Environ. Sci. Technol.* **2008,** *42*, (22), 8303-8309.

36. Sonke, J. E.; Schafer, J.; Chmeleff, J.; Audry, S.; Blanc, G.; DuprÈ, B., Sedimentary mercury stable isotope records of atmospheric and riverine pollution from two major European heavy metal refineries. *Chem. Geol.* **2010,** *279*, (3-4), 90-100.

37. Donovan, P. M.; Blum, J. D.; Yee, D.; Gehrke, G. E.; Singer, M. B., An isotopic record of mercury in San Francisco Bay sediment. *Chem. Geol.* **2013,** *349-350*, (0), 87-98.

38. Laffont, L.; Sonke, J. E.; Maurice, L.; Monrroy, S. L.; Chincheros, J.; Amouroux, D.; Behra, P., Hg Speciation and Stable Isotope Signatures in Human Hair As a Tracer for Dietary and Occupational Exposure to Mercury. *Environ. Sci. Technol.* **2011,** *45*, (23), 9910-9916.

39. Yin, R.; Feng, X.; Wang, J.; Li, P.; Liu, J.; Zhang, Y.; Chen, J.; Zheng, L.; Hu, T., Mercury speciation and mercury isotope fractionation during ore roasting process and their implication to source identification of downstream sediment in the Wanshan mercury mining area, SW China. *Chem. Geol.* **2013,** *336*, (0), 72-79.

40. Smith, C. N.; Kesler, S. E.; Blum, J. D.; Rytuba, J. J., Isotope geochemistry of mercury in source rocks, mineral deposits and spring deposits of the California Coast Ranges, USA. *Earth Planet. Sci. Lett.* **2008,** *269*, (3-4), 398-406.

41. William Miller, J.; Callahan, J. E.; Craig, J. R., Mercury interactions in a simulated gold placer. *Appl. Geochem.* **2002,** *17*, (1), 21-28.

42. Bartov, G.; Deonarine, A.; Johnson, T. M.; Ruhl, L.; Vengosh, A.; Hsu-Kim, H., Environmental Impacts of the Tennessee Valley Authority Kingston Coal Ash Spill. 1. Source Apportionment Using Mercury Stable Isotopes. *Environ. Sci. Technol.* **2012,** *47*, (4), 2092-2099.

43. Kilham, N. E.; Roberts, D.; Singer, M. B., Remote sensing of suspended sediment concentration during turbid flood conditions on the Feather River, California,Äîa modeling approach. *Water Resour. Res.* **2012,** *48*, (1).

44. Higson, J. L.; Singer, M. B., The impact of streamflow hydrographs on sediment supply from terrace erosion. *Geomorphology* **In Press**.

45. Slotton, D. G.; Ayers, S. M.; Reuter, J. E.; Goldman, C. R., Gold Mining Impacts on Food Chain Mercury in Northwestern Sierra Nevada Streams. In University of California Water Resources Center: 1995.

46. Alpers, C. N.; Hunerlach, M. P.; May, J. T.; Hothem, R. L.; Taylor, H. E.; Antweiler, R. C.; De Wild, J. F.; Lawler, D. A., Geochemical characterization of water, sediment, and biota affected by mercury contamination and acidic drainage from historical gold mining, Greenhorn Creek, Nevada County, California, 1999-2001. **2004**.

47. Tsui, M. T. K.; Finlay, J. C.; Nater, E. A., Mercury Bioaccumulation in a Stream Network. *Environ. Sci. Technol.* **2009,** *43*, (18), 7016-7022.

48. Slotton, D. G.; Ayers, S. M.; Suchanek, T. H.; Weyand, R. D.; Liston, A. M., Mercury bioaccumulation and trophic transfer in the Cache Creek watershed of California, in relation to diverse aqueous mercury exposure conditions. *Report to the California Bay Delta Authority, Sacramento* **2004**.

49. Mathews, T. J.; Smith, J. G.; Peterson, M. J.; Roy, W. K., Assessment of Contaminant Bioaccumulation in Invertebrates and Fish in Waters On and Adjacent to the Oak Ridge Reservation - 2010. *ORNL-TM (Oak Ridge National Laboratory)* **2011,** *2011/108*.

50. Kwon, S. Y.; Blum, J. D.; Carvan, M. J.; Basu, N.; Head, J. A.; Madenjian, C. P.; David, S. R., Absence of Fractionation of Mercury Isotopes during Trophic Transfer of Methylmercury to Freshwater Fish in Captivity. *Environ. Sci. Technol.* **2012,** *46*, (14), 7527-7534.

51. Bergquist, B. A.; Blum, J. D., Mass-dependent and -independent fractionation of Hg isotopes by photoreduction in aquatic systems. *Science* **2007,** *318*, (5849), 417-420.

52. Blum, J. D.; Sherman, L. S.; Johnson, M. W., Mercury Isotopes in Earth and Environmental Sciences. *Annu. Rev. Earth Planet. Sci.* **2014,** *42*, (1), 249-269.

53. Chow, A. T.; Dahlgren, R. A.; Harrison, J. A., Watershed sources of disinfection byproduct precursors in the Sacramento and San Joaquin Rivers, California. *Environ. Sci. Technol.* **2007,** *41*, (22), 7645-7652.

54. Blum, J. D.; Popp, B. N.; Drazen, J. C.; Choy, C. A.; Johnson, M. W., Methylmercury production below the mixed layer in the North Pacific Ocean. *Nature Geoscience* **2013,** *6*, (10), 879-884.

55. Balogh, S. J.; Tsui, M. T. K.; Blum, J. D.; Matsuyama, A.; Woerndle, G. E.; Yano, S.; Tada, A., Tracking the Fate of Mercury in the Fish and Bottom Sediments of Minamata Bay, Japan, Using Stable Mercury Isotopes. *Environ. Sci. Technol.* **2015**.

56. Hamelin, S. p.; Planas, D.; Amyot, M., Mercury methylation and demethylation by periphyton biofilms and their host in a fluvial wetland of the St. Lawrence River (QC, Canada). *Sci. Total Environ.* **2015,** *512*, 464-471.

57. Bell, A. H.; Scudder, B. C., Mercury Accumulation in Periphyton of Eight River Ecosystems. *JAWRA Journal of the American Water Resources Association* **2007,** *43*, (4), 957-968.

58. Buckman, K. L.; Marvin-Di Pasquale, M.; Taylor, V. F.; Chalmers, A.; Broadley, H. J.; Agee, J.; Jackson, B. P.; Chen, C. Y., Influence of a chlor-alkali superfund site on mercury bioaccumulation in periphyton and low-trophic level fauna. *Environ. Toxicol. Chem.* **2015,** *34*, (7), 1649-1658.

59. Balogh, S. J.; Nollet, Y. H.; Offerman, H. J., A comparison of total mercury and methylmercury export from various Minnesota watersheds. *Sci. Total Environ.* **2005,** *340*, (1), 261-270.

60. Harris, R. C.; Rudd, J. W.; Amyot, M.; Babiarz, C. L.; Beaty, K. G.; Blanchfield, P. J.; Bodaly, R.; Branfireun, B. A.; Gilmour, C. C.; Graydon, J. A., Whole-ecosystem study shows rapid fish-mercury response to changes in mercury deposition. *Proceedings of the National Academy of Sciences* **2007,** *104*, (42), 16586-16591.

61. Sherman, L. S.; Blum, J. D.; Keeler, G. J.; Demers, J. D.; Dvonch, J. T., Investigation of Local Mercury Deposition from a Coal-Fired Power Plant Using Mercury Isotopes. *Environ. Sci. Technol.* **2011,** *46*, (1), 382-390.

62. Chen, J.; Hintelmann, H.; Feng, X.; Dimock, B., Unusual fractionation of both odd and even mercury isotopes in precipitation from Peterborough, ON, Canada. *Geochim. Cosmochim. Acta* **2012,** *90*, (0), 33-46.

63. Gratz, L. E.; Keeler, G. J.; Blum, J. D.; Sherman, L. S., Isotopic Composition and Fractionation of Mercury in Great Lakes Precipitation and Ambient Air. *Environ. Sci. Technol.* **2010,** *44*, (20), 7764-7770.

64. Demers, J. D.; Driscoll, C. T.; Fahey, T. J.; Yavitt, J. B., Mercury Cycling in Litter and Soil in Different Forest Types in the Adirondack Region, New York, USA. *Ecological Applications* **2007,** *17*, (5), 1341-1351.

65. Balogh, S. J.; Meyer, M. L.; Johnson, D. K., Transport of Mercury in Three Contrasting River Basins. *Environ. Sci. Technol.* **1998,** *32*, (4), 456-462.

66. Stoor, R. W.; Hurley, J. P.; Babiarz, C. L.; Armstrong, D. E., Subsurface sources of methyl mercury to Lake Superior from a wetland,Äìforested watershed. *Sci. Total Environ.* **2006,** *368*, (1), 99-110.

67. Hinkle, S.; Bencala, K.; Wentz, D.; Krabbenhoft, D., Mercury and Methylmercury Dynamics in the Hyporheic Zone of an Oregon Stream. *Water Air Soil Pollut* **2013,** *225*, (1), 1-17.

68. Hall, G. E. M.; Pelchat, P., The design and application of sequential extractions for mercury, Part 2. Resorption of mercury onto the sample during leaching. *Geochemistry: Exploration, Environment, Analysis* **2005,** *5*, (2), 115-121.

69. Bloom, N. S.; Preus, E.; Katon, J.; Hiltner, M., Selective extractions to assess the biogeochemically relevant fractionation of inorganic mercury in sediments and soils. *Anal. Chim. Acta* **2003,** *479*, (2), 233-248.

70. Marvin-DiPasquale, M.; Windham-Myers, L.; Agee, J. L.; Kakouros, E.; Kieu, L. H.; Fleck, J. A.; Alpers, C. N.; Stricker, C. A., Methylmercury production in sediment from

agricultural and non-agricultural wetlands in the Yolo Bypass, California, USA. *Sci. Total Environ.* **2014,** *484*, (0), 288-299.

71. Wiederhold, J. G.; Smith, R. S.; Siebner, H.; Jew, A. D.; Brown, G. E.; Bourdon, B.; Kretzschmar, R., Mercury Isotope Signatures as Tracers for Hg Cycling at the New Idria Hg Mine. *Environ. Sci. Technol.* **2013,** *47*, (12), 6137-6145.

72. Stetson, S. J.; Gray, J. E.; Wanty, R. B.; Macalady, D. L., Isotopic Variability of Mercury in Ore, Mine-Waste Calcine, and Leachates of Mine-Waste Calcine from Areas Mined for Mercury. *Environ. Sci. Technol.* **2009,** *43*, (19), 7331-7336.

73. Yin, R.; Feng, X.; Wang, J.; Bao, Z.; Yu, B.; Chen, J., Mercury isotope variations between bioavailable mercury fractions and total mercury in mercury contaminated soil in Wanshan Mercury Mine, SW China. *Chem. Geol.* **2012,** *336*, (Special Issue), 80-86.

74. Slowey, A. J.; Rytuba, J. J.; Brown, G. E., Speciation of Mercury and Mode of Transport from Placer Gold Mine Tailings. *Environ. Sci. Technol.* **2005,** *39*, (6), 1547-1554.

75. Foucher, D.; Hintelmann, H.; Al, T. A.; MacQuarrie, K. T., Mercury isotope fractionation in waters and sediments of the Murray Brook mine watershed (New Brunswick, Canada): Tracing mercury contamination and transformation. *Chem. Geol.* **2013,** *336*, (0), 87-95.

76. Smith, R. S.; Wiederhold, J. G.; Kretzschmar, R., Mercury isotope fractionation during precipitation of metacinnabar (HgS) and montroydite (HgO). *Environ. Sci. Technol.* **2015,** *49*, (7), 4325-4334.

77. Jiskra, M.; Wiederhold, J. G.; Bourdon, B.; Kretzschmar, R., Solution Speciation Controls Mercury Isotope Fractionation of Hg(II) Sorption to Goethite. *Environ. Sci. Technol.* **2012,** *46*, (12), 6654-6662.

78. Wiederhold, J. G.; Skyllberg, U.; Drott, A.; Jiskra, M.; Jonsson, S.; Bjorn, E.; Bourdon, B.; Kretzschmar, R., Mercury Isotope Signatures in Contaminated Sediments as a Tracer for Local Industrial Pollution Sources. *Environ. Sci. Technol.* **2015,** *49*, (1), 177-185.

79. Rodriguez-Gonzalez, P.; Epov, V. N.; Bridou, R.; Tessier, E.; Guyoneaud, R.; Monperrus, M.; Amouroux, D., Species-Specific Stable Isotope Fractionation of Mercury during Hg(II) Methylation by an Anaerobic Bacteria (Desulfobulbus propionicus) under Dark Conditions. *Environ. Sci. Technol.* **2009,** *43*, (24), 9183-9188.

80. Perrot, V.; Bridou, R.; Pedrero, Z.; Guyoneaud, R.; Monperrus, M.; Amouroux, D., Identical Hg Isotope Mass Dependent Fractionation Signature during Methylation by Sulfate-Reducing Bacteria in Sulfate and Sulfate-Free Environment. *Environ. Sci. Technol.* **2015,** *49*, (3), 1365-1373.

81. Kritee, K.; Barkay, T.; Blum, J. D., Mass dependent stable isotope fractionation of mercury during mer mediated microbial degradation of monomethylmercury. *Geochim. Cosmochim. Acta* **2009,** *73*, (5), 1285-1296.

82. Chandan, P.; Ghosh, S.; Bergquist, B. A., Mercury Isotope Fractionation during Aqueous Photoreduction of Monomethylmercury in the Presence of Dissolved Organic Matter. *Environ. Sci. Technol.* **2015,** *49*, (1), 259-267.

83. Marvin-DiPasquale, M.; Agee, J.; McGowan, C.; Oremland, R. S.; Thomas, M.; Krabbenhoft, D.; Gilmour, C. C., Methyl-mercury degradation pathways: A comparison among three mercury-impacted ecosystems. *Environ. Sci. Technol.* **2000,** *34*, (23), 4908-4916.

84. Benoit, J.; Gilmour, C.; Heyes, A.; Mason, R.; Miller, C., Geochemical and biological controls over methylmercury production and degradation in aquatic ecosystems (Biogeochemistry of Environmentally Important Trace Elements). *ACS Symp. Ser.* **2003,** *835*, 262-297.

85. Ullrich, S. M.; Tanton, T. W.; Abdrashitova, S. A., Mercury in the aquatic environment: A review of factors affecting methylation. *Critical Reviews in Environmental Science and Technology* **2001,** *31*, (3), 241-293.

86. Schaefer, J. K.; Yagi, J.; Reinfelder, J. R.; Cardona, T.; Ellickson, K. M.; Tel-Or, S.; Barkay, T., Role of the bacterial organomercury lyase (MerB) in controlling methylmercury accumulation in mercury-contaminated natural waters. *Environ. Sci. Technol.* **2004,** *38*, (16), 4304-4311.

87. Springborn, M.; Singer, M. B.; Dunne, T., Sediment-adsorbed total mercury flux through Yolo Bypass, the primary floodway and wetland in the Sacramento Valley, California. *Sci. Total Environ.* **2011,** *412*, (0), 203-213.

Figure 4.S1: Yuba R. and Feather R. Sampling Locations and Collection Details.

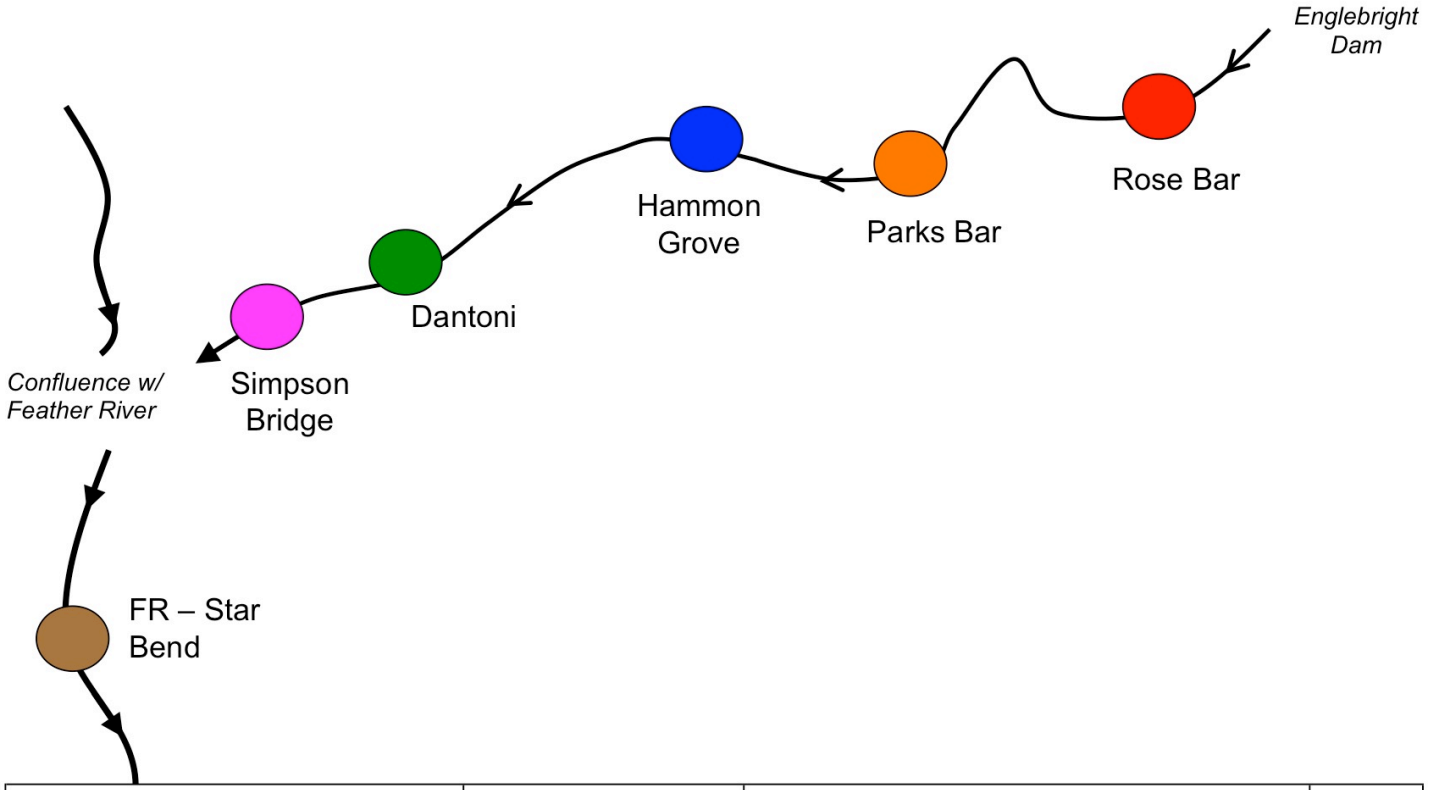

Biota	Feeding Behavior	Yuba River					Feather River
Common Name (*scientific ID*)		RB	PB	HG	Da	SB	Star Bend
Stonefly Larva (*Perlidae*)	Predator (Engulfer)	X	X	X	X		
Net Spinning Caddisfly Larva (*Hydropsychidae*)	Collector/Filterer	X	X	X	X		
Mayfly Larva (*Heptageniidae & Ephemerellidae spp.*)	Collector/Gatherer or Scraper	X			X		
Aquatic Worm (*Oligochaeta*)	Collector/Gatherer	X	X	X	X		
Asian Clam (*Corbicula fluminea*)	Collector/Filterer					X	X
Riffle Sculpin (*Cottus gulosus*)	Forager/Omnivore				X		
Speckled Dace (*Rhinichthys osculus*)	Forager/Omnivore					X	

Figure 4.S2: Detailed Legend for Figure 4.2 and 4.3 and Figure 4.S4.

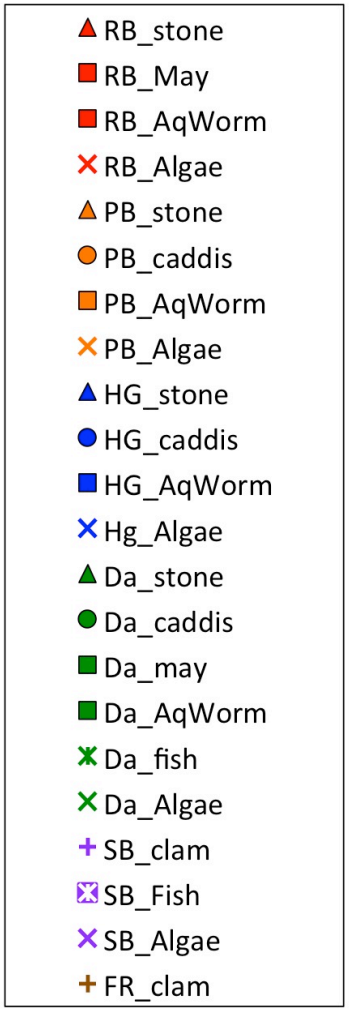

Figure 4.S3: THg concentration (1/THg) vs. δ^{202}Hg for Yuba and Feather River Sediment

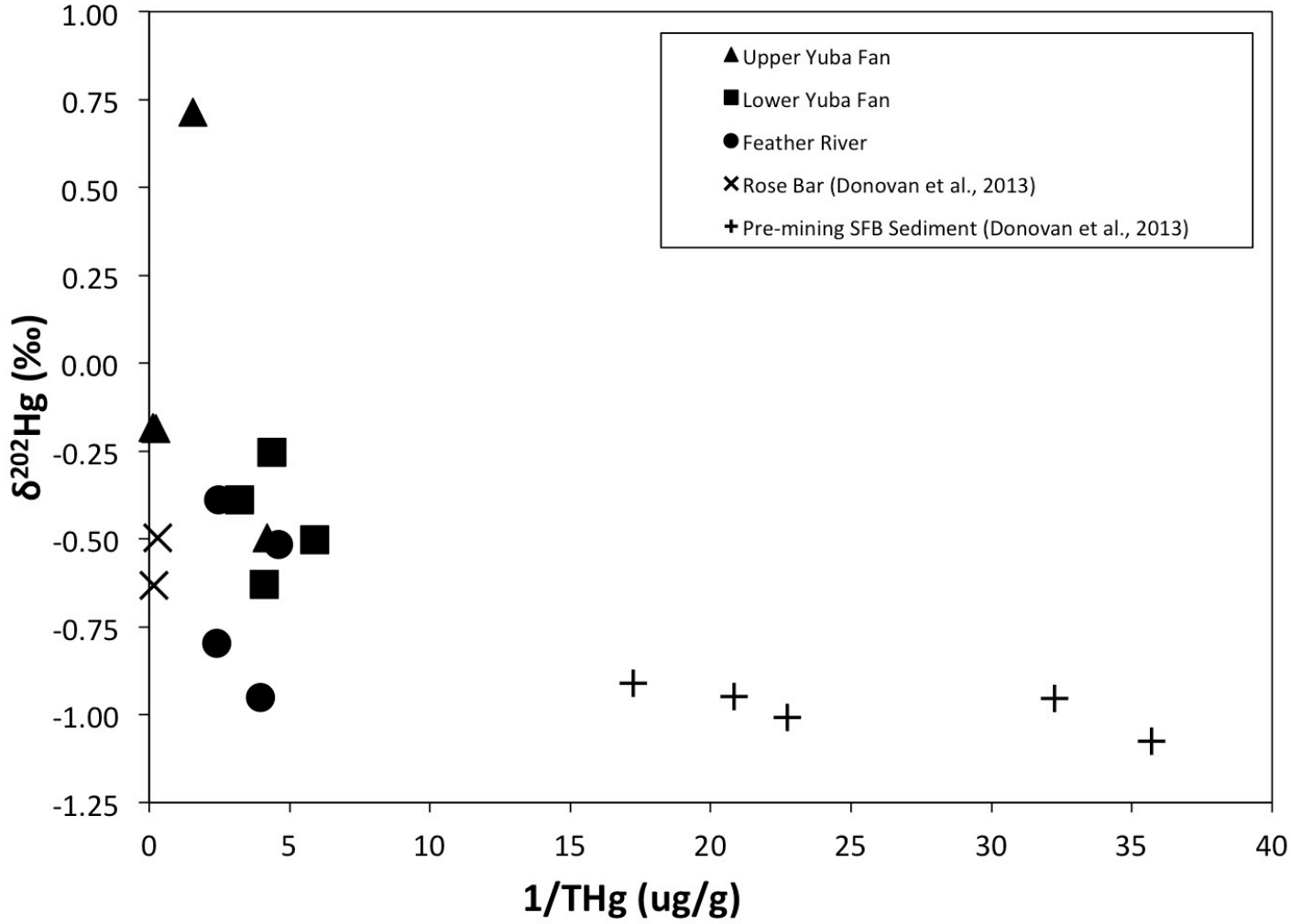

Figure 4.S4: Δ^{201}Hg vs. Δ^{199}Hg for all Yuba-Feather River Biota
Symbols are identical to Figure 4.S2. The linear regression equation is for all biota (sediment excluded).

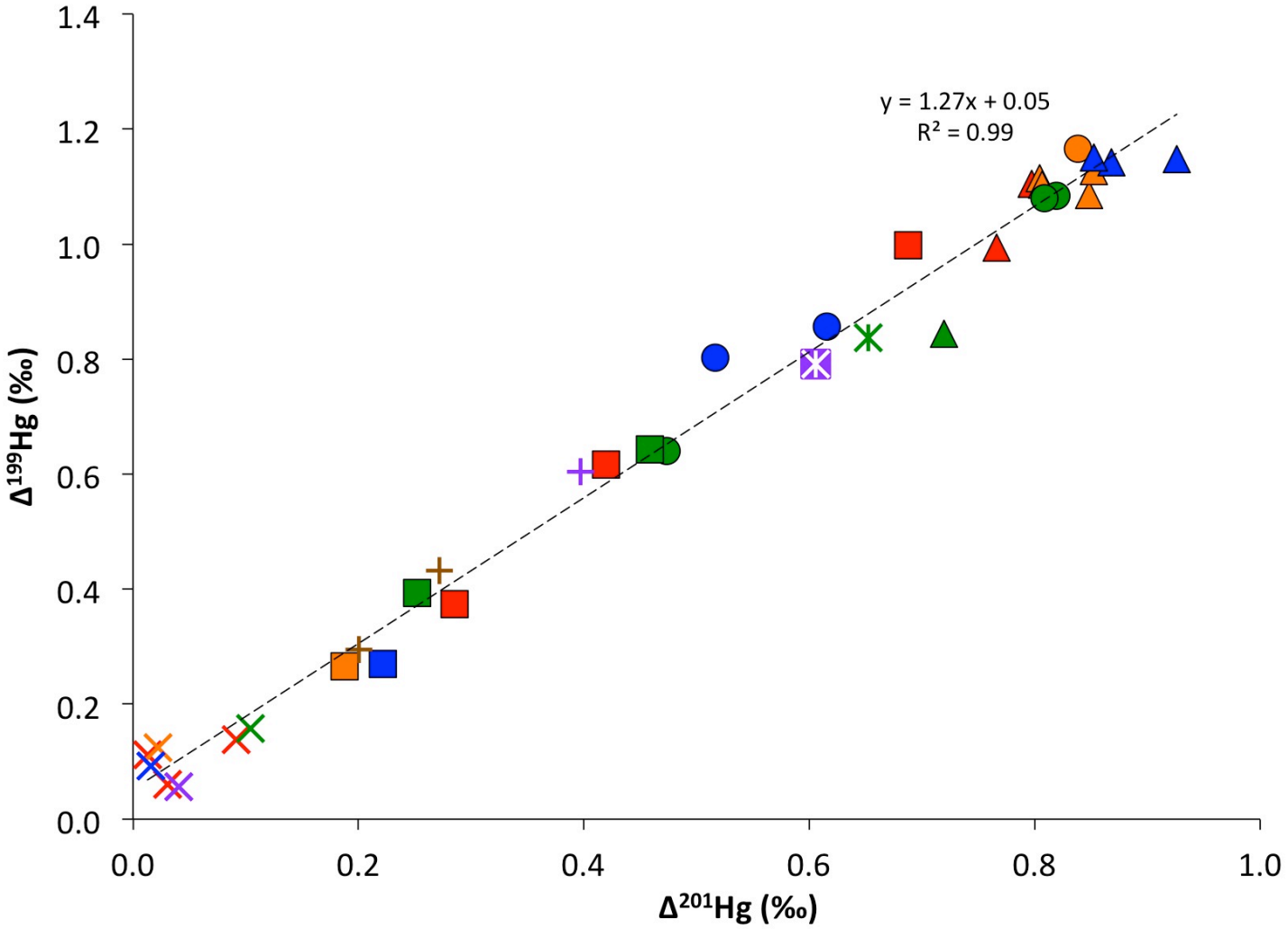

Table 4.S1: Sediment THg, MMHg and Hg isotope values

Location	Dist. Downstream of EB Dam	MMHg	THg	%MMHg	$\delta^{204}Hg$	$\delta^{202}Hg$	$\delta^{201}Hg$	$\delta^{200}Hg$	$\delta^{199}Hg$	$\Delta^{204}Hg$	$\Delta^{201}Hg$	$\Delta^{200}Hg$	$\Delta^{199}Hg$
	km	dw ng/g	dw ng/g	%	‰	‰	‰	‰	‰	‰	‰	‰	‰
Upper Yuba Fan	3.565		6821.2		-0.22	-0.18	-0.11	-0.07	0.00	0.06	0.02	0.02	0.04
	3.565	5.22	4453.2	0.1%	-0.30	-0.19	-0.19	-0.09	-0.06	-0.02	-0.05	0.00	-0.01
	6.53		646.7		1.05	0.71	0.53	0.38	0.21	-0.01	-0.01	0.02	0.03
	12.101	2.36	237.1	1.0%	-0.75	-0.50	-0.38	-0.23	-0.07	-0.01	-0.01	0.02	0.05
Lower Yuba Fan	26.527	6.38	243.5	2.6%	-0.92	-0.63	-0.42	-0.32	-0.08	0.02	0.05	0.00	0.08
	31.849		228.2		-0.38	-0.25	-0.19	-0.10	-0.02	0.00	0.00	0.02	0.04
	31.94		309.0		-0.49	-0.39	-0.29	-0.18	-0.06	0.09	0.00	0.02	0.04
	35.611		170.0		-0.77	-0.50	-0.40	-0.23	-0.11	-0.02	-0.02	0.02	0.02
Lower Feather River	37.623		401.5		-0.51	-0.39	-0.28	-0.23	-0.08	0.07	0.01	-0.04	0.02
	38.803		217.7		-0.80	-0.52	-0.37	-0.22	-0.06	-0.02	0.02	0.04	0.07
	47.117	6.84	413.1	1.7%	-1.24	-0.80	-0.56	-0.42	-0.13	-0.05	0.04	-0.02	0.07
	47.592		251.3		-1.46	-0.95	-0.69	-0.46	-0.17	-0.04	0.02	0.02	0.07

Table 4.S2: THg, MMHg and Hg Isotope Values for Aquatic Organisms

Stream	Location	Sampling Year	Sample Type	MMHg	THg	%MMHg	$\delta^{204}Hg$	$\delta^{202}Hg$	$\delta^{201}Hg$	$\delta^{200}Hg$	$\delta^{199}Hg$	$\Delta^{204}Hg$	$\Delta^{201}Hg$	$\Delta^{200}Hg$	$\Delta^{199}Hg$
				dw ng/g	dw ng/g	%	‰	‰	‰	‰	‰	‰	‰	‰	‰
Yuba River	Rose Bar	2013	Stonefly Larva (*Perlidae*)	76.9	66.8	100%	-0.96	-0.61	0.31	-0.25	0.84	-0.06	0.77	0.05	0.99
			Mayfly Larva (*Heptageniidae & Ephemerellidae spp.*)	36.8	49.0	75%	-1.01	-0.63	-0.05	-0.26	0.46	-0.08	0.42	0.06	0.62
			Filamentous Algae (*Cladophora*)	3.7	122.1	3%	-0.89	-0.61	-0.42	-0.30	-0.09	0.01	0.03	0.00	0.06
			Filamentous Algae (*Cladophora*)	1.8	185.7	1%	-1.03	-0.65	-0.48	-0.33	-0.05	-0.06	0.01	0.00	0.11
		2014	Stonefly Larva (*Perlidae*)	92.9	121.6	76%	-1.13	-0.71	0.26	-0.42	0.92	-0.07	0.80	-0.06	1.10
			Mayfly Larva (*Heptageniidae & Ephemerellidae spp.*)	37.8	52.3	72%	-0.91	-0.54	0.29	-0.22	0.86	-0.11	0.69	0.05	1.00
			Aquatic Worm (*Oligochaeta*)	142.6	404.8	35%	-0.94	-0.61	-0.17	-0.29	0.22	-0.03	0.29	0.02	0.37
			Filamentous Algae (*Cladophora*)	1.6	133.3	1%	-1.28	-0.82	-0.52	-0.38	-0.07	-0.07	0.09	0.03	0.14
	Parks Bar	2014	Stonefly Larva (*Perlidae*)	74.4	97.9	76%	-1.22	-0.83	0.18	-0.41	0.91	0.01	0.80	0.01	1.11
			Stonefly Larva (*Perlidae*)	78.7	95.8	82%	-1.10	-0.75	0.28	-0.36	0.90	0.02	0.85	0.01	1.09
			Stonefly Larva (*Perlidae*)	73.3	95.9	76%	-1.29	-0.80	0.25	-0.39	0.92	-0.09	0.85	0.02	1.13
			Stonefly Larva (*Perlidae*)	61.2	83.3	73%	-1.28	-0.78	0.22	-0.37	0.91	-0.12	0.81	0.02	1.10
			Net Spinning Caddisfly Larva (*Hydropsychidae*)	63.3	83.5	76%	-0.98	-0.68	0.33	-0.31	1.00	0.03	0.84	0.03	1.17
			Aquatic Worm (*Oligochaeta*)	89.9	337.1	27%	-0.99	-0.63	-0.29	-0.30	0.11	-0.05	0.19	0.02	0.27
			Filamentous Algae (*Cladophora*)	8.5	57.4	15%	-1.26	-0.80	-0.58	-0.43	-0.08	-0.07	0.02	-0.03	0.12
	Hammon Grove	2014	Stonefly Larva (*Perlidae*)	76.5	91.5	84%	-1.21	-0.84	0.29	-0.37	0.94	0.04	0.93	0.05	1.15
			Stonefly Larva (*Perlidae*)	64.0	92.4	69%	-1.18	-0.79	0.26	-0.37	0.95	0.00	0.85	0.03	1.15
			Stonefly Larva (*Perlidae*)	71.5	91.3	78%	-1.21	-0.79	0.27	-0.40	0.94	-0.03	0.87	0.00	1.14
			Net Spinning Caddisfly Larva (*Hydropsychidae*)	55.3	95.3	58%	-1.15	-0.76	-0.05	-0.35	0.61	-0.01	0.52	0.03	0.80
			Net Spinning Caddisfly Larva (*Hydropsychidae*)	56.7	93.6	61%	-1.30	-0.83	-0.01	-0.39	0.65	-0.07	0.62	0.02	0.86
			Aquatic Worm (*Oligochaeta*)	73.1	364.9	20%	-1.13	-0.76	-0.35	-0.33	0.08	0.01	0.22	0.05	0.27
			Filamentous Algae (*Cladophora*)	7.0	185.9	4%	-1.02	-0.65	-0.47	-0.33	-0.07	-0.04	0.02	-0.01	0.09
	Dantoni	2013	Stonefly Larva (*Perlidae*)	81.0	91.0	89%	-0.97	-0.76	0.15	-0.34	0.65	0.16	0.72	0.04	0.84
			Net Spinning Caddisfly Larva (*Hydropsychidae*)	60.7	91.9	66%	-1.21	-0.74	-0.09	-0.38	0.45	-0.10	0.47	0.00	0.64
			Mayfly Larva (*Heptageniidae & Ephemerellidae spp.*)	54.6	75.2	73%	-1.17	-0.69	-0.06	-0.36	0.47	-0.14	0.46	-0.01	0.64
		2014	Net Spinning Caddisfly Larva (*Hydropsychidae*)	95.6	134.0	71%	-0.79	-0.61	0.36	-0.28	0.93	0.13	0.82	0.03	1.08
			Net Spinning Caddisfly Larva (*Hydropsychidae*)	90.1	136.2	66%	-0.95	-0.59	0.36	-0.27	0.93	-0.06	0.81	0.03	1.08
			Aquatic Worm (*Oligochaeta*)	127.8	323.1	40%	-0.96	-0.65	-0.24	-0.33	0.23	0.01	0.25	0.00	0.39
			Riffle Sculpin (*Cottus gulosus*; individual)	380.2	377.3	100%	-0.64	-0.43	0.33	-0.19	0.73	-0.01	0.65	0.03	0.84
			Filamentous Algae (*Cladophora*)	16.8	132.0	13%	-1.08	-0.69	-0.42	-0.30	-0.02	-0.05	0.10	0.05	0.16
	Simpson Bridge	2014	Asian Clam (*Corbicula fluminea*)	271.3	425.6	64%	-0.71	-0.42	0.08	-0.20	0.50	-0.08	0.40	0.01	0.60
			Speckled Dace (*Rhinichthys osculus*)	406.7	436.6	93%	-0.82	-0.54	0.20	-0.23	0.66	-0.02	0.61	0.04	0.79
			Filamentous Algae (*Cladophora*)	14.6	162.6	9%	-1.06	-0.68	-0.47	-0.30	-0.11	-0.05	0.04	0.04	0.06
Feather River	Star Bend	2013	Asian Clam (*Corbicula fluminea*)	98.7	167.6	59%	-0.77	-0.47	-0.08	-0.25	0.31	-0.07	0.27	-0.01	0.43
			Asian Clam (*Corbicula fluminea*)	78.6	312.1	25%	-1.07	-0.68	-0.31	-0.30	0.12	-0.05	0.20	0.04	0.30

Table 4.S3: Total Hg concentration and Hg Isotope values for all SRMs

For SRMS's, N1 denotes the number of combustion replicates and N2 denotes the total number of isotope measurements during all analytical sessions. Theta denotes the standard deviation of the mean values for process replicates. For UM Almaden, N1 denotes the number of analytical sessions that UM-Almaden was measured and theta represents the SD of mean Hg isotope values for analytical sessions between January 2013 and December 2014 during which the run concentrations were either between 3 and 5 ng/g, or less than 3 ng/g.

Reference Material	N1	N2	THg (dry wt)	1SD	δ^{204}Hg	2σ	δ^{202}Hg	2σ	δ^{201}Hg	2σ	δ^{200}Hg	2σ	δ^{199}Hg	2σ	Δ^{204}Hg	2σ	Δ^{201}Hg	2σ	Δ^{200}Hg	2σ	Δ^{199}Hg	2σ
			ug.g	ug/g	‰	‰	‰	‰	‰	‰	‰	‰	‰	‰	‰	‰	‰	‰	‰	‰	‰	‰
NRC TORT-2	11	23	0.276	0.005	0.00	0.15	0.06	0.08	0.63	0.07	0.09	0.06	0.76	0.04	-0.08	0.06	0.59	0.03	0.06	0.05	0.75	0.04
NIST SRM 1944	6	14	3.51	0.30	-0.68	0.14	-0.45	0.08	-0.35	0.10	-0.21	0.09	-0.11	0.07	-0.01	0.08	-0.01	0.04	0.01	0.06	0.00	0.05
UM-Almaden (3-5 ppb)	100				-0.86	0.07	-0.57	0.05	-0.47	0.05	-0.28	0.04	-0.16	0.04	-0.01	0.06	-0.04	0.03	0.01	0.03	-0.02	0.03
UM-Almaden (<3 ppb)	24				-0.86	0.17	-0.55	0.11	-0.45	0.13	-0.26	0.09	-0.14	0.11	-0.04	0.12	-0.03	0.07	0.02	0.05	0.00	0.09

CHAPTER 5: Comparison of mercury degradation and exposure pathways in streams and wetlands impacted by historical mining

Authors: Patrick M. Donovan, Joel D. Blum, Michael B. Singer, Mark Marvin-DiPasquale, Martin T.K. Tsui

Abstract

We measured Hg isotopic compositions (δ^{202}Hg and Δ^{199}Hg), along with monomethyl mercury (MMHg) and total mercury (THg) concentrations, in sediment and biota from Cache Creek and Yolo Bypass wetlands, in a region of central California impacted by historical mining activity. Cache Creek sediment had a large range in THg (87 to 3,868 ng/g) and δ^{202}Hg (−1.69 to −0.20‰) reflecting the heterogeneity of Hg sources in sediment downstream of Hg mining. The δ^{202}Hg of high THg Yolo Bypass wetland sediment (−0.5‰) was indistinguishable from gold mining contaminated sediment located upstream. Fish and benthic macroinvertebrates in both locations had trends in %MMHg (the ratio MMHg to THg) consistent with the bioaccumulation and trophic transfer of MMHg. Relationships between %MMHg and Hg isotope values (δ^{202}Hg and Δ^{199}Hg) in food web biota were somewhat variable and high %MMHg biota in Yolo Bypass had a wide range in Δ^{199}Hg (0.34 to 1.81‰). We suggest this is due to the bioaccumulation of isotopically distinct pools of MMHg in the same habitat as a result of distinct feeding

behaviors (e.g., benthic versus planktonic). There were contrasting relationships between the δ^{202}Hg of pre-photodegraded MMHg and co-located sediment IHg in Cache Creek (MMHg δ^{202}Hg was 0.4‰ lower than sediment) and Yolo Bypass (MMHg δ^{202}Hg was 0.2 to 0.5‰ higher than sediment). This supports the hypothesis that −MDF between IHg and MMHg results from a lack of biotic MMHg degradation (+MDF) in rivers (flowing water) compared to standing water environments such as wetlands, lakes or the coastal ocean.

5.1 Introduction

Monomethyl mercury (MMHg) is a developmental neurotoxin that bioaccumulates in food webs and is produced from inorganic Hg (IHg) in aquatic environments.[1, 2] IHg has been released for hundreds of years from the mining of mercury sulfide ores (HgS), contaminating aquatic environments downstream of mining in various locations around the globe.[3] Between the 1850's and 1970's approximately 100,000 Mg of Hg was mined in the California Coast Ranges.[4] Metallic Hg (Hg^0) was concentrated from Hg ores (typically HgS) by heating ('roasting'), volatilizing Hg and then recondensing the Hg^0 vapor.[5] Mine waste tailings and thermally processed ores ("calcine", which contains residual Hg) were commonly disposed of near mining and processing sites.[5, 6] Cache Creek, in the California Coast Range, drains one of the most prolific Hg mining regions in North America with over 30 former Hg mines in the watershed.[7] Studies have reported high concentrations of Hg in Cache Creek sediment and water (IHg),[8] and MMHg bioaccumulation in aquatic[9-12] and terrestrial biota in the watershed.[13] Hg associated with sediment and water can be transported downstream in Cache Creek through the Cache Creek Settling basin (CCSB, a 3,600 acres leveed flood water and sediment containment area) and into the Yolo Bypass, a

larger floodwater conveyance area (Figure 5.S1). The Yolo Bypass drains into the San Francisco Bay-Delta during high flows. Thus, IHg from mining in the Cache Creek watershed is potential source of MMHg to local Cache Creek food webs and also downstream Yolo Bypass and Bay-Delta food webs.

Yolo Bypass is a ~24,000 ha engineered flood bypass that diverts high river flows around the city of Sacramento, CA and uses a network of drainage and water supply channels to support agriculture and wildlife habitat. As mentioned, during floods Yolo Bypass receives water and suspended sediment from Cache Creek but it also receives overflow from the Sacramento River and the Feather River and Sutter Bypass (via the Fremont weir),[14, 15] the latter of which drain multiple Au mining districts in the Sierra Nevada (e.g., Yuba River, Bear River, etc.; Figure 5.S1)[16]. MMHg is thought to be produced in situ in Yolo Bypass wetlands,[17] and bioaccumulation has been documented in aquatic invertebrates, forage fish and salmonids throughout Yolo Bypass.[18-20] Therefore, IHg from upstream mining activities (Cache Creek or the Yuba River), might input a labile source of IHg to Yolo Bypass wetlands[15, 21] and lead to MMHg bioaccumulation. However it is difficult to identify the relative contribution of Coast Range Hg mining and Sierra Nevada Au mining sources and the transformation of these sources to MMHg.[18, 22] To differentiate between Hg sources, biogeochemical transformations (e.g., methylation, degradation) and MMHg exposure pathways we employed Hg stable isotope measurements in sediment and aquatic biota from Cache Creek and Yolo Bypass.

Mercury has seven stable isotopes that are affected by mass dependent fractionation (MDF: δ^{202}Hg) and mass independent fractionation (MIF: Δ^{199}Hg or Δ^{201}Hg) in the environment. Experimental studies of Hg isotope fractionation have demonstrated MDF

during biotic (i.e, Hg^{2+}-methylation, MeHg degradation, Hg^{2+} reduction)[23-26] and abiotic (IHg sorption, coprecipitation, etc.)[27, 28] reactions while large magnitude MIF (>0.5‰) occurs primarily during photochemical reactions.[29, 30] The Hg isotopic composition of sediment has helped to identify anthropogenic Hg sources and trace their transport and deposition in river and estuarine environments.[31-35] Hg isotopes have been measured in different pools of Hg associated with Hg mining activities including calcines and CA Coast Range Hg-ores.[36-40] Although Hg mine wastes can vary widely in isotopic composition over very small spatial scales (δ^{202}Hg range of >5‰),[31, 32] Hg isotopes in sediment downstream of individual mines are thought to be a more integrative tracer of Hg mining sources.[35, 39, 41] We hypothesized that high THg sediment in Cache Creek, downstream of individual mining districts, would provide a fingerprint of IHg that could be methylated in situ or transported downstream in the Sacramento Valley. Since Yolo Bypass receives suspended sediment from both Hg mining (Cache Creek; this study) and Au mining (Yuba River)[42] regions, we hypothesized this fingerprint would help distinguish the contribution of Au and Hg mining sources to Yolo Bypass wetlands.

The Hg isotopic composition of biota with a range of %MMHg (the percent ratio of MMHg to THg) has become a useful tool for estimating the isotopic composition of bioaccumulated MMHg. Fish feeding studies show no isotopic fractionation of MMHg during trophic transfer,[43, 44] and therefore the isotopic composition of MMHg provides insight on Hg sources and biogeochemical transformations prior to bioaccumulation in the food web. From comparisons of MMHg and IHg isotopic compositions, we can infer relevant photochemical (MDF and MIF) and/or microbial (MDF only) transformations between these Hg pools. For example, MMHg isotopic compositions have been used to

evaluate the transfer of MMHg between aquatic and terrestrial ecosystems,[45-47] and changes in MMHg photodegradation between different locations.[45, 48] The only study comparing sediment IHg and MMHg in a stream environment (the Yuba River, CA), unique net negative MDF was observed between IHg and MMHg.[42] This result contrasted with net positive MDF commonly observed in other environments (e.g., [49-51]). The measurement of Hg isotopes in food webs has not yet been applied in streams or wetlands downstream of former Hg mining regions. In both Cache Creek and Yolo Bypass, sediment is thought to be an important source of IHg that can be methylated leading to MMHg bioaccumulation in resident biota.[11, 17] Therefore we hypothesized that the MDF between sediment IHg and MMHg would reflect biogeochemical processes in upstream (Cache Creek) and downstream (Yolo Bypass) environments. To identify biogeochemical processes and MMHg exposure pathways, we measured THg, MMHg, and Hg isotope ratios in sediment, benthic macroinvertebrates and forage fish from five sites in Cache Creek and three wetlands in Yolo Bypass. This is the first study to use Hg isotopes to broadly compare biogeochemical processes between riverine and wetland environments (Cache Creek, Yuba River,[42] and Yolo Bypass) within a regional watershed that contains multiple mining related Hg sources (Au mining vs. Hg mining).

5.2 Methods and Materials

5.2.1 Study Locations and Sample Processing

Sediment was collected in 2013 from bars and terraces at two locations in Cache Creek (Rumsey and Capay; Figure 5.S2) and at two sites upstream in Bear Creek, which is one of three primary tributaries to the Cache Creek (Table 5.S1). Surface sediment (0-10

cm) from Yolo Bypass was collected in 2013 and 2014 from three different wetlands we refer to as Upper Wetland (UW), Permanent Wetland 2 (PW2), and Lower Wetland (LW). UW is located upstream of the CCSB while PW2 and LW are downstream of CCSB (Figure 5.S3). All sediment was freeze-dried and then sieved with a stainless steel sieve to <1mm. A split of <1mm sediment was ground and homogenized while a separate split of <1mm sediment was further sieved to <63µm. The fraction passing <1mm sieve but not the 63µm sieve was retained, ground and homogenized (referred to as the 1mm-63µm fraction). The fraction passing the <63µm sieve was also retained and homogenized but not ground. Thus, multiple sediment fractions (<63µm, 1mm-63µm, and <1mm) were analyzed from two locations in Cache Creek. Similarly, in Yolo Bypass, both the <1mm and <63µm sediment fractions were analyzed in UW and LW. However, the <63µm fraction contained nearly all of this material (>95%, as dry mass) due to the fine-grained nature of this wetland sediment.

Aquatic organisms were collected from Cache Creek and Yolo Bypass wetlands during two separate sampling campaigns in March 2013 and June 2014 (Table 5.S2). Filamentous algae (*Spirogyra* and *Hydrodictyon*) and aquatic organisms were collected at four sites in Cache Creek (Regional Park, Rumsey, Guinda, and Capay; Figure 5.S2). In 2013 we collected macroinvertebrates from riffles (including *Megaloptera*, *Perlidae*, and *Hydropsychidae*), whereas in 2014 we collected macroinvertebrates (including *Libellulidae*, *Gomphidae*, *Coenagrionidae*, etc) and filamentous algae in slow moving water and pools at the same locations. The difference in sampling was due to considerably lower streamflow during June 2014 (<0.1 m^3/s at the Rumsey Bridge NOAA Gauging Station) compared to March 2013 (1.4 to 2 m^3/s). Aquatic organisms in Yolo Bypass were collected at the same

wetlands where sediment was collected during 2013 (UW, LW) and 2014 (UW, PW2; Figure 5.S3). A diverse set of macroinvertebrates was collected, including damselfly larva, dragonfly larva and backswimmers (*Libellulidae*, *Gomphidae*, *Coenagrionidae, and Notonectidae)*. Two types of forage fish were also collected when present in 2013 and 2014: Mosquitofish (*Gambusia affinis)* and Mississippi Silverside (*Menidia beryllina*). The organisms collected in each location and during each sampling campaign are summarized in the Supporting Information (Figures 5.S2 and 5.S3). All aquatic organisms were collected using a kick net, dip net, and by picking directly off of gravel cobbles or sediment. Individual organisms were removed with clean stainless steel tweezers and transferred into a secondary container with native water for identification. Organisms were then composited by family or species (when possible), transferred into clean centrifuge tubes and immediately placed on dry ice in the field. All biotic samples are composites of 10 or more whole body individuals (except for crayfish that contained 1-3 individuals per sample). Biotic samples were freeze-dried and then ground and homogenized with either an agate mortar and pestle or an alumina ball mixer mill prior to analysis.

5.2.2 MMHg Concentration Analysis

The concentration of MMHg (dry wt.) in sediment and biota was measured at the USGS (Menlo Park, CA) simultaneously with samples from a parallel study of the Yuba River. Therefore QA/QC of MMHg analyses are reported here for the entire dataset and can also be found elsewhere.[42] Briefly, freeze dried sediment was sub-sampled (0.02–0.03 g) and extracted for MMHg using 25% potassium hydroxide in methanol at 60°C for four hours.[52] Freeze dried biota was sub-sampled (3–7 mg) and extracted for MMHg using 30%

nitric acid at 60°C (overnight, 12-16 hrs), as adapted.[53] Extract sub-samples were diluted, pH adjusted with citrate buffer and assayed for MMHg by aqueous phase ethylation (with sodium tetraethylborate) on an automated MMHg analyzer (MERX system, Brooks Rand Laboratories).[54] For sediment MMHg, the relative percent deviation (RPD) of analytical duplicates was 8.4% (n=1 pair), matrix spike recovery was 107±1% (n = 2), and certified reference material (CRM) ERM-CC580 (estuarine sediment) recovery was 95% (n=1). For biota, the mean RPD of analytical duplicates was 3.0% (n=12 pairs), matrix spikes recoveries were 105±1% (mean ± SE, n = 26), and CRM recoveries from NRC Tort-3 (lobster hepatopancreas) was 86±2% (mean ± SE, n=7) and from NIST-2967 (marine mussel tissue) was 94±3% (mean ± SE, n=7).

5.2.3 THg and Hg Isotope Analysis

Hg was separated from biota and sediment samples for THg concentration and Hg stable isotope measurements by offline combustion.[47, 55] Briefly, up to 1 g of sample was placed in a ceramic boat in the first furnace of a two-stage combustion system. The first furnace temperature was increased to 750°C over the course of 6 hours while the second furnace was held at 1000°C. Hg released from the sample was carried in a flow of Hg-free O_2 through the second furnace and into a 1%$KMnO_4$/10%H_2SO_4 trapping solution (1% $KMnO_4$ trap). Trap solutions were partially reduced with 2% w/w hydroxylamine hydrochloride (NH_2OH•HCl) and an aliquot was measured for THg by CV-AAS (Nippon MA-2000). The dry weight THg concentration of each sample was calculated based on the mass of Hg in the 1% $KMnO_4$ trap and the sample mass combusted. Compared to independent analysis (hot concentrated acid digestion and CVAFS at the USGS Menlo Park, CA) for a

subset of 2013 biota from Cache Creek and Yolo Bypass, offline combustion recovered 112±17% (1SD; n=17) of THg.

Prior to isotopic analysis, contents of the original 1%$KMnO_4$ trap solution were divided into 1 to 5 g aliquots and treated with 0.3 ml 20% $SnCl_2$ and 0.3 ml 50% H_2SO_4 to reduce Hg^{2+} to Hg^0. All Hg^0 was then purged into a secondary 1% $KMnO_4$ trap and reoxidized to Hg^{2+}, to concentrate Hg and isolate combustion residues. An aliquot of the secondary trap solution was analyzed by CV-AAS (Nippon MA-2000) and transfer recoveries averaged 95±5% (1SD; n= 59, minimum of 81%) for biota and 96±4% (1SD; n=27, minimum of 87%) for sediment. The Hg isotopic composition of the secondary trap solution was measured by cold vapor- multi collector-inductively coupled plasma mass spectrometry (CV-MC-ICP-MS; Nu Instruments). The trap solution was partially reduced with 2% w/w NH_2OH•HCl, diluted to a concentration between 0.9 and 5 ng/g, and Hg was chemically reduced to Hg^0 by the continuous addition of 2% $SnCl_2$. The Hg^0 generated was separated from solution using a frosted tip gas-liquid separator and carried in a Hg-free stream of Ar gas to the MC-ICP-MS inlet. Instrumental mass bias was corrected by the introduction of an internal Tl standard (NIST 997) as a dry aerosol to the gas stream and by strict sample standard bracketing using NIST 3133 with a matching Hg concentration (±10%) and solution matrix.[56]

5.2.4 Blanks, Reference Materials and Uncertainty

Mercury stable isotope composition is reported in permil (‰) using delta notation ($\delta^{xxx}Hg$) relative to the NIST SRM 3133 (Eq. 1), with MDF based on the $^{202}Hg/^{198}Hg$ ratio ($\delta^{202}Hg$). MIF is the deviation from theoretically predicted MDF and is reported in permil

(‰) using capital delta notation ($\Delta^{xxx}Hg$; Eq. 2).[56] In this study, we use $\Delta^{199}Hg$ and $\Delta^{201}Hg$ to report MIF with $\beta = 0.252$ for $\Delta^{199}Hg$ and $\beta = 0.752$ for $\Delta^{201}Hg$.[56] All $\delta^{xxx}Hg$ and $\Delta^{xxx}Hg$ values for samples and SRMs are available in Tables 5.S1, 5.S2, and 5.S3.

Equation [1]: $\delta^{xxx}Hg\ (‰) = [[(^{xxx}Hg/^{198}Hg)_{sample}/(^{xxx}Hg/^{198}Hg)_{NIST3133}]-1] * 1000$

Equation [2]: $\Delta^{xxx}Hg = \delta^{xxx}Hg - (\delta^{202}Hg * \beta)$

Procedural process blanks and two standard reference materials (SRMs; NRC Tort-2 and NIST 1944) were processed alongside samples in an identical manner. Samples and SRMs in this study were run simultaneously with samples from a parallel study of the Yuba River.[42] Therefore, SRM and process blank measurements are reported for the entire dataset and additional details can be found elsewhere.[42] Briefly, process blanks accounted for 0.2% to 1.8% of Hg in the final trap solutions. Mean THg (±1SD) for SRMs was 3.51±0.3 µg/g for NIST SRM 1944 (n=6) and 276±5 ng/g for NRC Tort-2 (n=11; Table 5.S3) and within 5% of certified values. Recovery during secondary purge and trap was 94±4% (1SD, n=6, minimum = 87%) and 96±7% (1SD, n=11, minimum = 80%) for NIST SRM 1944 and NRC Tort-2, respectively. The Hg isotopic composition of sediment and biota SRMs was consistent with previously reported values (Table 5.S3).[32, 44, 46, 47, 51, 57-61] Long-term analytical uncertainty of Hg isotope ratio measurements was estimated from the standard deviation (2SD) of the mean Hg isotopic composition of UM-Almaden during all analytical sessions (Jan. 2013 to Dec. 2014) when analytical run concentrations were between 3 and 5 ng/g (Table 5.S3). We estimated external reproducibility using the error (2SD) associated with replicate measurement of SRMs. The 2SD of SRMs was greater than the 2SD associated

with the long-term analytical uncertainty of UM-Almaden. Therefore, we use SRMs to estimate uncertainty for Hg isotope measurements in this study as ±0.08‰ for δ^{202}Hg and ±0.05‰ for Δ^{199}Hg.

5.3 Results and Discussion

5.3.1 Regional Sediment Sources

Cache Creek sediment had highly variable THg (87 to 3,868 ng/g) and δ^{202}Hg (−1.69‰ to −0.20 ‰) that likely reflects the heterogeneous distribution of Hg from mine waste sources. Bulk sediment (<1mm) and 1mm-63μm sediment had THg (87 to 1,481 ng/g) and δ^{202}Hg (−1.69 to −0.55) that overlapped with replicate analysis of <63μm sediment (98 to 3870 ng/g and δ^{202}Hg from −1.42 to −0.20‰). Overall, sediment δ^{202}Hg and Δ^{199}Hg showed no systematic differences with size class or THg (Figure 5.1, Figure 5.S4). A similar δ^{202}Hg range of more than 1‰ (−0.58 to 0.80‰) was reported for sediment downstream of the New Idria Hg mine in CA.[35] In that study, isotopic variability was attributed to the heterogenous distribution of calcine and cinnabar particles within the sediment.[35] Given the multiple mining districts and Hg point sources in the Cache Creek watershed, we think it is likely that similarly heterogeneous Hg mining products persist in this catchment.[7] For example, sediment from Bear Creek, one of three primary tributaries upstream of our Cache Creek sampling sites, had extremely high THg (23.7 to 468 μg/g). Bear Creek contains both Hg mining districts and hydrothermal inputs,[62 9] and its sediment Hg isotopic composition (δ^{202}Hg of −0.31±0.17‰ and Δ^{199}Hg of 0.08±0.01‰; 1SD, n=3) was comparable to unroasted Hg mine wastes (δ^{202}Hg of −0.43 to +0.16‰)[39-41] and CA coast range Hg ores (−0.64±0.84‰, mean± 1SD, n=91).[38] This is one of multiple possible

tributary Hg sources, but if only a small mass of this sediment was transported downstream it could significantly alter the Hg isotopic composition of downstream sediment. The sediment collected in Cache Creek at Rumsey and Capay was over 14 km (river km) downstream of Bear Creek, and even further from individual mining districts, and has likely integrated multiple mine waste Hg sources. Therefore, its mean isotopic composition (δ^{202}Hg of −0.99±0.45‰; and Δ^{199}Hg of 0.10±0.07‰; mean±1sd, n=11) provides a reasonable estimate of the large quantity of IHg potentially available to the food web at the Cache Creek we sampled.

The Hg isotopic composition of Yolo Bypass wetland surface sediment changes as a function of THg (Figure 5.1), suggesting a mixture of high and low THg sediment from different sources. Yolo Bypass sediment with THg <60 ng/g (typical for pre-mining sediment in the Sierra Nevada)[63] had δ^{202}Hg between −0.67 and −1.03‰; similar to pre-mining sediment in SF Bay (δ^{202}Hg of −0.98±0.06‰).[33] As sediment THg increases, δ^{202}Hg shifts towards −0.5‰ and becomes indistinguishable from Yuba Fan sediment contaminated by Au mining (δ^{202}Hg of −0.38±0.17‰; 1SD, n=7).[33, 42] In the few wetlands sampled, sediment THg and δ^{202}Hg also change in the downstream direction from relatively low THg and δ^{202}Hg in UW to higher THg and δ^{202}Hg in PW2 and LW. Thus, future investigation of Hg isotopes in Yolo Bypass sediment with greater spatial or temporal resolution may be valuable. For example, downstream changes in sediment δ^{202}Hg could reflect local deposition of specific upstream sources, erosional regions within Yolo Bypass or be related to the timing of episodic sediment delivery.[14, 15] Previous work has shown that most floods probably deliver diluted mining sediment from the Sierra, whereas decadal floods produce large volumes of Hg-laden sediment from the Yuba-Feather system.[64] To

link upstream Hg sources to Yolo Bypass sediment, it would be valuable to characterize Hg isotopes in the suspended load transported from Cache Creek and the Yuba River. Regardless, in this study the isotopic composition of all Yolo Bypass wetland sediment is best explained as a mixture of low THg non-mining sediment (with δ^{202}Hg of −1‰) and high THg mining derived sediment (with δ^{202}Hg of −0.5‰).

5.3.2 Biota THg and MMHg

5.3.2.1 Cache Creek

In Cache Creek, aquatic organisms collected in 2014 (n=25) had an overlapping range in THg (151to 889 ng/g) and MMHg (80 to 608 ng/g) with organisms from 2013 (n=7; 104 to 334 ng/g and 45 to 220 ng/g, respectively). Filamentous algae in Cache Creek (*Spirogyra* and *Hydrodicton*; from 2014 only) had generally higher MMHg levels (7 to 83 ng/g, n=4) than *Cladoraphora* measured in other similar CA rivers (Yuba River[42] and Eel River).[65, 66] Among 2014 biota, THg was highest in asian clam (722±182 ng/g; 1SD, n=4), mosquitofish (718±49 ng/g; 1sd, n=3) and predatory invertebrates (mean THg > 370 ng/g, n=9). The %MMHg (percent ratio of MMHg to THg) was relatively high in mosquitofish (82±6%, n=3) and predatory invertebrates (mean >86% MMHg, n=9) and slightly lower in asian clam (62±14% MMHg, n=4). Asian clam %MMHg increased moving downstream (43% at Regional Park to 74% at Capay), but there were no other significant spatial trends in biota THg or MMHg. Instead, %MMHg changed with presumed trophic level from collector/gatherers and filter feeders (low %MMHg) to predatory invertebrates and fish (high %MMHg). This finding is consistent with the preferential trophic transfer of MMHg via biomagnification, as reported previously in Cache Creek (e.g., [11, 13]) and elsewhere.[67]

5.3.2.2 Yolo Bypass

Wetlands in Yolo Bypass contained similar types of macroinvertebrates (e.g., dragonfly larva, damselfly larva, crayfish) and fish (Mississippi silversides and mosquitofish) between sampling years. Across all wetlands and sampling years, macroinvertebrate THg was between 67 and 524 ng/g and forage fish had a similar range (125 to 573 ng/g). The %MMHg in macroinvertebrates ranged between 55% and 100%, with 13 of 16 samples containing >80% MMHg. The highest overall MMHg concentration was measured in a water scavenger beetle sample (426 ng/g; 81% MMHg), although nearly as high MMHg and %MMHg (134 to 426 ng/g and >82% MMHg) was measured in invertebrate predators (backswimmers, creeping waterbugs, and dragonfly larva). Mosquitofish and Mississippi silversides had a large range in MMHg (114 to 630 ng/g, n=6) but consistently high %MMHg (> 87%), which is similar to forage fish from Cache Creek (this study) and the Yuba River.[42] Slightly lower MMHg (71 to 148 ng/g, n=5) was measured in damselfly larva, midge larva and fairy shrimp although %MMHg was still relatively high (55 to 95% MMHg). The range of different aquatic organisms with elevated MMHg and high %MMHg suggests the trophic transfer and bioaccumulation of MMHg in Yolo Bypass wetland food webs and is consistent with previous studies throughout Yolo Bypass.[10, 18-20]

5.3.3 Estimates for IHg and MMHg Isotopic Compositions

Filamentous algae, benthic macroinvertebrates and forage fish from Yolo Bypass and Cache Creek had a wide range in both δ^{202}Hg (−1.23 to +0.52‰) and Δ^{199}Hg (0.20 to

1.81‰). The diverse array of food web biota enabled us to estimate the isotopic composition of MMHg in both locations. In Cache Creek, we use linear relationships between %MMHg and Hg isotope values to estimate both IHg and MMHg isotopic compositions in the food web. In Yolo Bypass we use high %MMHg biota to estimate MMHg isotopic composition in the food web. We did not estimate the isotopic composition of IHg in Yolo Bypass food webs because there were an insufficient number of low %MMHg samples. .

5.3.3.1 Cache Creek

The Δ^{199}Hg of all Cache Creek biota increased with increasing %MMHg (r^2 of 0.34, $p<0.001$; Figure 5.2A) and at the y-intercept of 0% MMHg (i.e., 100% IHg) Δ^{199}Hg (0.19±0.17‰) was within error of bulk sediment (Δ^{199}Hg of 0.10±0.07‰, 1SD, n=11). When biota was separated by sampling year (2013 and 2014; Figure 5.2A), relationship between %MMHg and Δ^{199}Hg strengthened for the 2014 data (r^2=0.51, $p<0.001$) but there was no relationship for 2013 (r^2= 0.05, p = 0.64). This resulted in significant differences for the estimated Δ^{199}Hg of MMHg and IHg between sampling years. The δ^{202}Hg of food web biota did not increase with increasing %MMHg (Figure 5.3A, r^2 of 0.10, p =0.08 for 2013 and 2014). Although significant positive relationships between δ^{202}Hg and %MMHg have been reported in lakes, forests and the coastal ocean[45, 47, 57], our lack of such a relationship is consistent with previous stream studies.[42, 47]

Given these relationships, we extrapolated the linear equations to 100% IHg and 100% MMHg to obtain estimates for Hg isotope values (δ^{202}Hg and Δ^{199}Hg) of IHg and MMHg. Because there was no significant relationship between %MMHg and δ^{202}Hg, for

comparison we estimated MMHg δ^{202}Hg from the mean δ^{202}Hg of organisms with >80% MMHg (n=14 for 2014, n=3 for 2013). The mean δ^{202}Hg of organisms with >80%MMHg (−0.95±0.09‰ for 2014 and −1.11±0.11‰ for 2013) was nearly identical to estimates of MMHg from linear regression (−0.92‰ and −1.16‰, respectively). Therefore, we use linear regression estimates (±1SE) to estimate the isotopic composition of IHg and MMHg in the Cache Creek food web. These estimates are summarized in Table 5.1A.

5.3.3.2 Yolo Bypass

In Yolo Bypass, we evaluated each wetland food web separately because sediment δ^{202}Hg was different in each location, suggesting differing sediment IHg sources. The Δ^{199}Hg and δ^{202}Hg of wetland biota generally increased with increasing %MMHg (Figure 5.2B, 5.3B); however, for each wetland there were very few organisms with less than 80% MMHg. Therefore linear regressions, impoverished in values with low %MMHg, did not provide significant relationships nor reliable estimates for MMHg and IHg. Instead, the isotopic composition of MMHg in each wetland was estimated from mean Hg isotope values (±1SD) for high %MMHg organisms (>80%). These estimates are summarized in Table 5.1B.

5.3.4 Hg Isotope Variation within Food Webs

The isotopic composition of MMHg and IHg estimated from food web biota can be a valuable tool for understanding Hg sources and transformations. The underlying assumption of this method is that Hg isotopic composition of biota across the food web is a mixture of two distinct Hg pools: a single IHg isotopic composition and a single MMHg

isotopic composition. In this study, biota from Cache Creek had significant variation in δ^{202}Hg and Δ^{199}Hg that is not explained by %MMHg alone (i.e., biota vary from the linear mixing of IHg and MMHg). Similarly, the Δ^{199}Hg of high %MMHg biota in Yolo Bypass wetlands varied by ~1.5 ‰ across all wetlands (and a 1SD of ±0.44‰ for a single wetland). Below we consider possible explanations for such variation.

In Cache Creek, samples of Asian clam and filamentous algae exhibit a ~1‰ range in δ^{202}Hg (−1.15 to −0.18‰) Asian clam are filter feeding bivalves that extract particles from the water column or from the benthic substrate.[68] Similarly, filamentous algae can trap suspended sediment moving downstream. Thus, the combination of physical characteristics and feeding behavior likely lead these biota to accumulate IHg directly from Cache Creek sediment, which has variable δ^{202}Hg (~1.5‰ range). Although less obvious, we suspect that the Δ^{199}Hg of certain Cache Creek biota might also vary by feeding behavior. For example, aquatic worm and burrowing mayfly larva, which non-selectively consume benthic detritus and sediment, fall below the linear relationship for %MMHg vs. Δ^{199}Hg (Figure 5.2A). Since large magnitude Δ^{199}Hg is directly proportional to the extent of MMHg photodegradation,[30] it is possible these organisms obtain MMHg from sediment that has been less photochemically degraded than MMHg accumulated by other organisms.

The Δ^{199}Hg of MMHg in Yolo Bypass was also quite variable; across all wetlands high %MMHg biota (>80%) had a 1.5‰ range in Δ^{199}Hg. The lowest Δ^{199}Hg was measured in omnivorous crayfish (0.34 to 0.66‰ from UW and LW), which are opportunistic feeders but often forage near sediment in wetland environments. Conversely, forage fish (mosquitofish and Mississippi silversides) from all wetlands had Δ^{199}Hg between 0.76 and 1.81‰ (n=6). Mosquitofish are forage feeders that consume zooplankton and

macroinvertebrates near the water surface.[69] Mississippi silversides are planktivores whose diet is based solely on zooplankton or other particulates in the water column.[70] Zooplankton in arctic lakes had Δ^{199}Hg (2.2 to 3.4‰) that was much higher than co-located benthic organisms,[71] and high Δ^{199}Hg (1.34±0.27) was also measured in low %MMHg zooplankton from Lake Baikal.[72] Thus, the range in Δ^{199}Hg among high %MMHg organisms suggests exposure to different pools of MMHg that have been more or less photodegraded (i.e., MMHg with higher or lower Δ^{199}Hg). The biota Hg isotope data from Cache Creek and Yolo Bypass wetlands challenges the assumption that MMHg with a single isotopic composition is bioaccumulated by all organisms in a particular location. Furthermore, these data suggest that Hg isotope measurements might aid in separating benthic vs. planktonic exposure pathways, similar to the use of Hg isotopes to understand energy exchanges across the aquatic-riparian interface.[46, 47]. We recommend that future Hg isotope studies carefully consider the feeding behavior of aquatic organisms sampled, whose diets might change with environmental setting, prey availability and age.

5.3.5 Comparison of MMHg Photodegradation

Large magnitude MIF (Δ^{199}Hg) is directly proportional to the extent of photochemical Hg degradation and the Δ^{199}Hg/Δ^{201}Hg ratio can be used to differentiate between inorganic Hg^{2+} reduction (~1.0) and photochemical MMHg degradation (~1.2 to 1.4).[29, 73] Cache Creek and Yolo Bypass biota have Δ^{199}Hg/Δ^{201}Hg ratios of 1.23±0.03 (1SE, n= 32; Figure 5.S5) and 1.16±0.03 (1SE, n=25; Figure 5.S6), respectively. The Cache Creek ratio falls between literature averages for freshwater fish (1.28±0.01, n=135)[30] and marine fish (1.20±0.01, n=60)[30], and is consistent with other riverine food webs in the region

(Yuba River=1.27±0.03 and Eel R.=1.28±0.08).[42, 47] The Yolo Bypass ratio is on the low end of experimental estimates (1.17 to 1.38),[73] but comparable to forest food webs from northern Michigan (1.21±0.03) and northern California (1.15±0.06).[47] [45] In both Cache Creek and Yolo Bypass, these ratios strongly suggest that the Δ^{199}Hg and Δ^{201}Hg of MMHg results from MIF during MMHg photodegradation prior to entering the food web.

The extent of MMHg photodegradation can be quantified from experimental relationships that change with DOC concentration (1 or 10 mg/L).[29] Surface water DOC in Cache Creek below Capay during a 4 year period was 2.8±0.12 mg/L (1SE, n=104),[74] and at the Rumsey site DOC ranges between 1 and 3 mg/L.[75] In non-agricultural Yolo Bypass wetlands, pore water DOC was 12 mg/L (median, n=20)[17] and wetland surface waters range from 6 to 10 mg/L.[21] Therefore, we employ experimental relationships for 1 mg/L DOC for Cache Creek and 10 mg/L for Yolo Bypass wetlands. We estimate that in 2014 ~31±4% of MMHg in Cache Creek had undergone photodegradation, which is substantially higher than what we estimated for MMHg photodegradation in 2013 (~17%±3). These estimates are similar to observations nearby in the Yuba River (24% in 2013 and 35% in 2014)[42] and the South Fork Eel River (27%).[47] For all Yolo Bypass wetland locations and sampling seasons, we estimate that 9–12% of MMHg had undergone photodegradation. This is much less than the extent of photodegradation in Cache Creek, but similar to Florida Lakes where photodegradation was thought to be inhibited by low water clarity and high DOC.[51]

To differentiate between photochemical and non-photochemical processes we subtract the MIF and MDF that occurs during MMHg photodegradation using experimentally derived Δ^{199}Hg vs. δ^{202}Hg slopes (2.43 for 1 mg/L DOC and 4.79 for 10

mg/L DOC).[29] This approach has been used to compare the δ^{202}Hg of IHg and pre-photodegraded MMHg and infer MDF during biogeochemical processes in forests, rivers, lakes, and coastal ocean environments.[49-51, 57] To estimate the δ^{202}Hg of pre-photodegraded MMHg we must assume that all Δ^{199}Hg of MMHg results from photochemical degradaton (i.e., MMHg has Δ^{199}Hg of ~0‰ pre-photodegradation). This assumption is true when MMHg is formed from sediment or basal resources with Δ^{199}Hg near zero, such as Yolo Bypass wetland sediment (Δ^{199}Hg of 0.09±0.03‰) or Cache Creek sediment (Δ^{199}Hg of 0.10±0.07‰). Based on these calculations, pre-photodegraded MMHg in Cache Creek had δ^{202}Hg between −1.40 and −1.45‰, regardless of the sampling year (Figure 5.4). In Yolo Bypass the δ^{202}Hg of pre-photodegraded MMHg was estimated for each wetland individually: −0.51‰, −0.13‰ and −0.37‰ for UW, PW2 and LW, respectively (Figure 5.5).

5.3.6 Hg Sources and Processes in Yolo Bypass

As discussed, sediment in Yolo Bypass wetlands is a mixture of mining-derived (likely Au mining) and background (non-mining) sediment and δ^{202}Hg varies as a function of THg concentration. In each wetland, the δ^{202}Hg of pre-photodegraded MMHg is higher than the δ^{202}Hg of sediment. Thus, there is a positive δ^{202}Hg offset between sediment (>95% IHg) and MMHg ($\delta^{202}Hg_{\text{pre-photodegraded MMHg}} - \delta^{202}Hg_{IHg}$) in each location. The offset is +0.35 ‰, +0.49 ‰ and +0.16 ‰, for UW, PW2 and LW, respectively (Figure 5.5). This is similar in direction and magnitude to positive δ^{202}Hg offsets (+0.4 to +0.8‰) previously reported in lakes, estuaries and the coastal ocean,[49-51, 57] which were suggested to result from net biotic processes (e.g., Hg methylation and MMHg degradation).[49, 51] Biotic Hg^{2+}-

methylation preferentially reacts light Hg isotopes and leads to MMHg with lower δ^{202}Hg than IHg substrate. [25, 26] Biotic *mer*-mediated MMHg degradation also preferentially reacts light Hg isotopes and leads to higher δ^{202}Hg of the residual MMHg.[23] The positive δ^{202}Hg offset in Yolo Bypass wetlands (0.16 to 0.49‰) is consistent with the interpretation that IHg in sediment is biotically methylated and the MMHg formed is then biotically degraded such that the residual MMHg (available for photodegradation and bioaccumulation) has higher δ^{202}Hg than the sediment IHg. Thus, Hg isotopes in sediment and biota from Yolo Bypass wetlands links IHg in sediment to bioaccumulated MMHg and further confirms that MMHg is formed in situ within these wetlands. Therefore the transport of IHg-enriched sediment from upstream, and its deposition in Yolo Bypass, is an important process that supplies IHg to downstream wetlands. This potentially labile IHg, derived from upstream mining sources, could then be methylated leading to MMHg bioaccumulation in Yolo Bypass food webs.

5.3.7 Hg Sources and Processes in Cache Creek

5.3.7.1 Annual Changes in Δ^{199}Hg

Our estimates of Δ^{199}Hg for IHg and MMHg in Cache Creek changed beyond analytical uncertainty between 2013 and 2014. This result could indicate different IHg and/or MMHg pools between years (Figure 5.2A). The estimated Δ^{199}Hg of IHg was higher in 2013 (0.55±0.07‰) than in 2014 (0.06±0.18‰),reflecting the accumulation of an IHg source with positive Δ^{199}Hg only in 2013. Aquatic organisms accumulate IHg from their dietary resources, and so the difference in Δ^{199}Hg may reflect the different types of biota sampled or changes in habitat and/or flow conditions. For example, IHg Δ^{199}Hg in 2014

was similar to sediment, suggesting that sediment is a significant resource at the base of the food web for biota in slower moving water. However in 2013, the Δ^{199}Hg of IHg was higher than all sediment from this study. Organisms sampled in 2013 were mainly from riffle environments where some biota (e.g., *Hydropsychidae*) rely on filtering particulates and detritus that are moving downstream with streamflow. Thus, IHg in 2013 could reflect IHg from upstream resources or suspended sediment that has higher Δ^{199}Hg than bar or terrace sediment. Additionally, changes in Cache Creek flows shift the relative input from upstream tributaries containing different Hg sources (e.g., mine wastes from Clear Lake vs. hydrothermal Hg from Bear Creek).[8, 11] Alternative IHg sources, with slightly positive Δ^{199}Hg, include precipitation (0.37±0.26‰; mean±1SD; n=43),[33, 55, 76-78] or hydrothermal fluids (0.13±0.06‰).[79] Small positive Δ^{199}Hg (<0.4‰) has been observed in some hydrothermal precipitates, Hg ores and sinters,[30] although the majority of these materials have Δ^{199}Hg near zero (<0.2‰).[35, 38, 39] Therefore, we think it is possible that IHg in 2013 organisms might be from an upstream IHg source with high Δ^{199}Hg. However the limited sample collection in 2013 (n=7), with a small number of low %MMHg organisms, limits our ability to identify this IHg source.

Regardless of differences in IHg, the Δ^{199}Hg/Δ^{201}Hg ratios of biota demonstrate that the Δ^{199}Hg and Δ^{201}Hg of MMHg results from MIF during MMHg photodegradation. Therefore, we interpret the change in MMHg Δ^{199}Hg between 2013 and 2014 to result from differences in the extent of MMHg photodegradation. This result is consistent with a parallel study of the Yuba River, where a greater extent of MMHg photodegradation was found in 2014 compared to 2013.[42] The Yuba River and Cache Creek are on opposite sides of the Sacramento Valley (75 km apart) and contaminated by different Hg sources (Au

mining vs. Hg mining) but experience relatively similar environmental conditions (e.g., high sunlight/low shading). Thus, we suggest the change in Δ^{199}Hg between years in both streams might results from large-scale controls on MMHg exposure to sunlight. For example, changes in streamflow could affect MMHg exposure (and thus, photodegradation) by changing water depth, water clarity and MMHg residence time. Both streams had significantly higher flows in 2013 than in 2014 due to progressive drought that is decreasing discharge in many California rivers and streams. Alternatively, the timing of sampling may also be important since both streams were sampled in early spring of 2013 compared to early summer of 2014. Thus, there may have been a greater extent of MMHg photodegradation prior to sampling in June 2014 (during spring) than prior to March 2013 sampling. Whether due to annual or seasonal differences, the consistent trend in MMHg Δ^{199}Hg, between Cache Creek and the Yuba River, demonstrates that MMHg in short-lived aquatic organisms may be useful to identify changes in the extent of MMHg photodegradation.

5.3.7.2 δ^{202}Hg of IHg and MMHg

Although there were differences in MMHg Δ^{199}Hg between years, the δ^{202}Hg of pre-photodegraded MMHg in Cache Creek was always between −1.40 and −1.45‰, indicating a common pool of MMHg was photodegraded each year. Pre-photodegraded MMHg δ^{202}Hg is ~0.7‰ lower than IHg in the food web (−0.59 to −0.68‰) and ~0.4‰ lower than co-located sediment (−0.99 ± 0.45‰; Figure 5.4). This relationship (δ^{202}Hg offset of −0.4 to −0.7‰) is consistent in both direction and magnitude with our previous work in the nearby Yuba River (δ^{202}Hg offset of −0.4 to −0.9‰).[42] The negative δ^{202}Hg offset implies

that either (1) a different IHg source (i.e., not bulk sediment or IHg in the food web) with a δ^{202}Hg of −1.4‰ or lower is preferentially methylated in Cache Creek or (2) in-situ methylation of IHg results in net negative MDF.

The presence of MMHg in streams is often considered a function of point and non-point sources of Hg and drainage basin landscape characteristics that promote Hg deposition and IHg-methylation within the watershed.[67, 80-82] Therefore, Hg accumulated in the watershed and stored in organic matter or soils could be a source of MMHg to Cache Creek. If so, then the negative δ^{202}Hg offset might be an artifact of the difference between the δ^{202}Hg of in stream IHg (from sediment or the food web) and the δ^{202}Hg of watershed IHg sources. If we assume the δ^{202}Hg offset here is consistent with Yolo Bypass or previous studies (i.e., +0.4 to +0.8‰)[49-51, 57], then we would predict the external IHg source to have δ^{202}Hg between −2.2 and −1.4‰. Terrestrial organic matter and soils typically have low δ^{202}Hg and negative Δ^{199}Hg and could provide a substrate for IHg-methylation in upstream floodplains or reservoirs.[83] Forest floor samples from the Midwest US ranged from δ^{202}Hg of −1.05 to −1.88‰,[55] and foliage, soil and leaf litter in northern CA had a similar range (−1.54 to −2.53 ‰).[47] These values are consistent with predicted external IHg sources (−2.2 to −1.4‰) for Cache Creek. However, this steep mountainous catchment has high erosion rates and does not allow for significant accumulation of surface organic matter.[84] The mass of IHg in surface organic matter is likely small relative to Hg from mine wastes in this region, such as the ~100 Mg of Hg stored in Clear Lake (upstream of our sampling sites).[85] Furthermore, MMHg concentrations in Cache Creek biota increases with distance away from these upstream reservoirs.[11] Methylation of sediment IHg is thought to be promoted by local geochemical conditions such as high sulfate in Bear Creek and Cache

Creek.[11, 62] Previous work in streams suggests that IHg can be methylated in situ in hyporheic zones[86] or when associated with epilithic periphyton[87] or filamentous algae.[65] Thus, Cache Creek sediment is the most likely source of labile IHg leading to MMHg in lower Cache Creek.[75]

Only a fraction of IHg in stream sediment might be available for methylation,[17, 82] and the negative δ^{202}Hg offset might be an artifact of the difference between δ^{202}Hg of labile Hg in sediment and the δ^{202}Hg of bulk sediment. The isotopic composition of labile Hg in Hg mine wastes and sediment was estimated from leaching experiments (water soluble, thiosulfate extractable, etc.) and mobilized leachates have been found to have up to 1.3‰ higher δ^{202}Hg than the corresponding bulk material.[31, 37, 88] Additional processes could fractionate Hg mass dependently (–MDF) in mine waste systems, such as co-precipitation or sorption reactions, with lower δ^{202}Hg in the reaction products such as HgS or Hg bound to colloids.[27, 28] Other studies have demonstrated systematic differences in the δ^{202}Hg of different size fractions of sediment,[32, 35] although, as discussed above, we observed no such differences in Cache Creek. Clearly, it is possible for different pools of Hg within sediment to have δ^{202}Hg that is different from the bulk sediment, depending on the source material and transport history. However, neither sediment size-fractions nor experimental estimates of labile Hg in sediment can identify a specific fraction of Hg in Cache Creek sediment that would have consistent δ^{202}Hg of −1.4 to −1.45‰ and be preferentially methylated in this stream. Because the δ^{202}Hg of external Hg sources or labile Hg in sediment cannot explain the pre-photodegraded MMHg δ^{202}Hg, we suggest that the difference in δ^{202}Hg results from net negative MDF of up to 0.7‰ between IHg and MMHg within Cache Creek.

5.3.8 Comparison of MDF in California Streams and Wetlands

In this study, we observed a negative δ^{202}Hg offset in Cache Creek but a positive δ^{202}Hg offset in Yolo Bypass wetlands. Combined with the negative δ^{202}Hg offset previously observed in the Yuba River,[42] we suggest that streams and wetlands within the same drainage can have different relationships between sediment IHg and MMHg. In the Yuba River, the only other study where a negative δ^{202}Hg offset was observed, we proposed that net negative MDF could result from different biotic MMHg degradation pathways or the extent of biotic MMHg degradation.[42] Each of these mechanisms depends upon physical and geochemical conditions that vary between stream and wetland environments. Therefore, we further hypothesized that the net MDF between IHg and MMHg might result from characteristic differences between fast flowing water and standing water environments. The $+\delta^{202}$Hg offset in Yolo Bypass wetlands and $-\delta^{202}$Hg offsets in Cache Creek and Yuba River supports this hypothesis. In light of these results, we reexamine the possible mechanisms for the negative MDF observed in stream systems. .

It was previously speculated that biotic oxidative MMHg degradation, instead of biotic *mer*-mediated degradation, could result in different MDF because these pathways have different reaction products.[42] Oxidative MMHg degradation results in Hg^{2+} and could be remethylated (methylation has a −MDF)[25, 26], whereas Hg^0 is partially lost by evasion during *mer*-mediated degradation (resulting in +MDF of residual MMHg).[23] However, isotope fractionation during oxidative MMHg degradation has not yet been quantified. Oxidative MMHg degradation is thought to be dominant in relatively pristine environments where bioavailable Hg is low.[89, 90] Therefore, we might expect significant *mer*-mediated

degradation (+MDF) and a +δ^{202}Hg offset in relatively contaminated environments and a –δ^{202}Hg offset in low THg environments (or when bioavailable Hg is limited) regardless of the environmental setting. In both the Yuba River and Cache Creek, large quantities of sediment with elevated THg persist yet we observe a –δ^{202}Hg offset between this sediment and MMHg in the food web. In the UW of Yolo Bypass, where sediment THg is closer to pre-mining background values (~60 ng/g), we observed a positive δ^{202}Hg offset (+0.35‰). Although there was a range in sediment THg in Yolo Bypass, the δ^{202}Hg offset did not change as a function of sediment THg. A study in multiple estuaries on the NW coast also reported positive δ^{202}Hg offsets in estuaries, regardless of sediment THg (6 to 2,960 ng/g).[57] Therefore, sediment THg concentrations alone cannot predict the δ^{202}Hg offset. Future characterization of MDF during oxidative degradation, and additional measurements of geochemical parameters that control Hg bioavailability (i.e., DOC, redox, etc.) or *mer*-enzyme activity, might help to explain the observed relationships between IHg and MMHg in aquatic environments.

Instead of different biotic degradation pathways, the negative δ^{202}Hg offset in the Yuba River and Cache Creek might simply indicate that there is a lack of biotic MMHg degradation (no +MDF) in streams prior to MMHg bioaccumulation. An experimental study of biotic IHg-methylation and MMHg degradation suggested that turbulent diffusion of MMHg from the IHg substrate could increase the magnitude of negative MDF.[26] Following this, Donovan et al.[42] proposed that in situ IHg methylation in flowing water might continually advect MMHg to the water column, removing it from the substrate and decreasing the quantity of MMHg available for biotic degradation. This would result in pre-photodegraded MMHg with lower δ^{202}Hg than the IHg substrate because it would have

undergone relatively little biotic degradation (i.e., minimal +MDF). Conversely, in standing water such as the Yolo Bypass wetlands, MMHg may be stored in the sediment for longer periods of time leading to a greater extent of biotic MMHg degradation (and +MDF). In this study, −MDF was observed in Cache Creek and +MDF was observed in Yolo Bypass wetlands. Although we acknowledge Cache Creek flows varied between years, we suggest these results are consistent with the hypothesis that biotic MMHg degradation occurs to a lesser extent in streams than in standing water environments. Therefore, we suggest that biotic MMHg degradation is limited in stream environments while photochemical MMHg degradation is a significant degradation pathway (up to 35% in the Yuba River and Cache Creek). Conversely, in wetland environments biotic degradation must occur to a much greater extent compared to streams, evidenced by positive δ^{202}Hg offset, while MMHg photodegradation is relatively limited (9-12%).

5.3.9 Implications for Future Studies

This study provides valuable new insight that will aid in future tracing of Hg and MMHg in stream and wetland food webs in the Sacramento Valley and elsewhere. Analysis of THg, MMHg and Hg isotopes in benthic macroinvertebrates and forage fish proved valuable to identify the isotopic composition of MMHg. The variety of biota analyzed with different feeding behaviors provided evidence for multiple MMHg isotopic compositions within a single aquatic environment. Thus, we suggest it is important to consider feeding preferences and behavior in future Hg isotope food web studies. This detail could ultimately help to identify benthic and planktonic MMHg exposure pathways in aquatic environments. In this study, Hg isotopes in sediment, and estimates of IHg in the food web,

enabled us to compare the δ^{202}Hg of IHg and pre-photodegraded MMHg in Cache Creek and Yolo Bypass. We found positive (Yolo Bypass Wetlands) and negative (Cache Creek and Yuba River[42]) δ^{202}Hg offsets within the same watershed, indicating that biotic MDF changes between these environments. We think the best explanation for this difference is the absence of biotic MMHg degradation (with +MDF) in streams, which implies that MMHg photodegradation is the primary MMHg degradation pathway in stream environments.

Acknowledgements

We thank Marcus Johnson (UM-BEIGL) for assistance in the operation of the CV-MC-ICP-MS; Tyler Nakamura and Ka'ai Jensen (SJSU) for their valuable assistance with field sampling; and Evangelos Kakouros, Le Kieu and Michelle Arias (USGS, Menlo Park, CA) for sediment and biota Hg analysis. We also acknowledge financial support from the National Science Foundation: EAR-1226741 (to M.B.S.).

(A)		δ^{202}Hg	1SE	Δ^{199}Hg	1SE
		‰	‰	‰	‰
2013	IHg	-0.59	0.15	0.55	0.07
	MMHg	-1.16	0.08	0.60	0.04
2014	IHg	-0.68	0.16	0.06	0.18
	MMHg	-0.92	0.07	1.22	0.08

(B)		δ^{202}Hg	1SD	Δ^{199}Hg	1SD	n
		‰	‰	‰	‰	
Upper Wetland (UW)	MMHg	-0.30	0.16	0.99	0.44	9
Permanent Wetland 2 (PW2)	MMHg	0.08	0.28	0.96	0.18	7
Lower Wetland (LW)	MMHg	-0.22	0.10	0.70	0.21	3

Table 5.1: MMHg and IHg compositions in food webs from (A) Cache Creek and (B) Yolo Bypass Wetlands

Cache Creek estimates are derived from linear relationships between %MMHg and Hg isotope values (either δ^{202}Hg or Δ^{199}Hg). The error (1SE) is the error associated with the intercept of the linear regression. Yolo Bypass MMHg estimates are based on all organisms within each individual wetland with greater than 80%MMHg. The error is the 1SD of the mean value for this group of organisms.

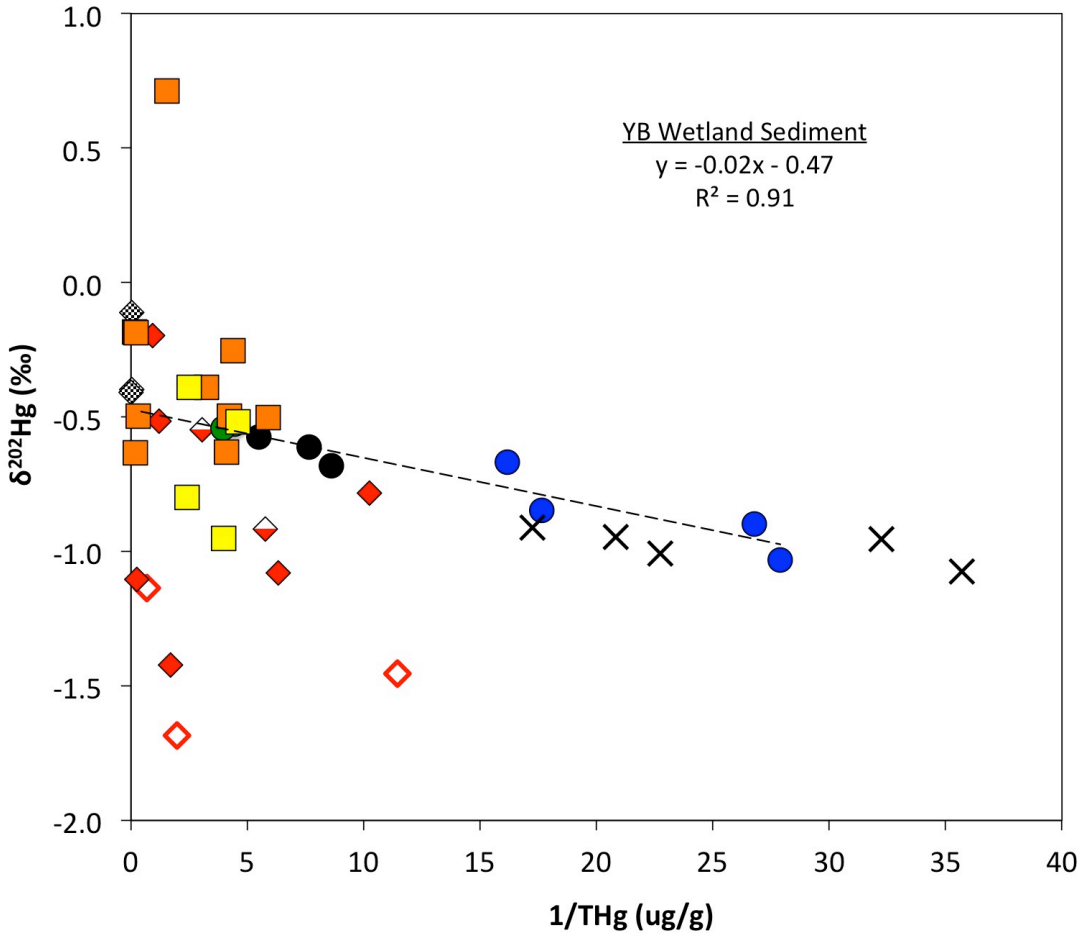

Figure 5.1: THg concentration (1/THg) vs. δ^{202}Hg for regional sediment
Diamonds represent Cache Creek sediment (colors denote size fraction: filled = <63µm, half-filled = 1mm-63µm, empty = <1mm) and checkered diamonds are from Bear Creek. Circles represent Yolo Bypass (colors denote wetland: blue = upper, black = PW2, green = lower) and squares represent the Yuba Feather River (orange for Yuba River and yellow for Feather River)[42]. Pre-mining sediment from San Francisco Bay (x) are included from a previous study of subtidal sediment cores.[33] The dashed line represents the relationship for all samples collected and analyzed in Yolo Bypass wetlands (n=9).

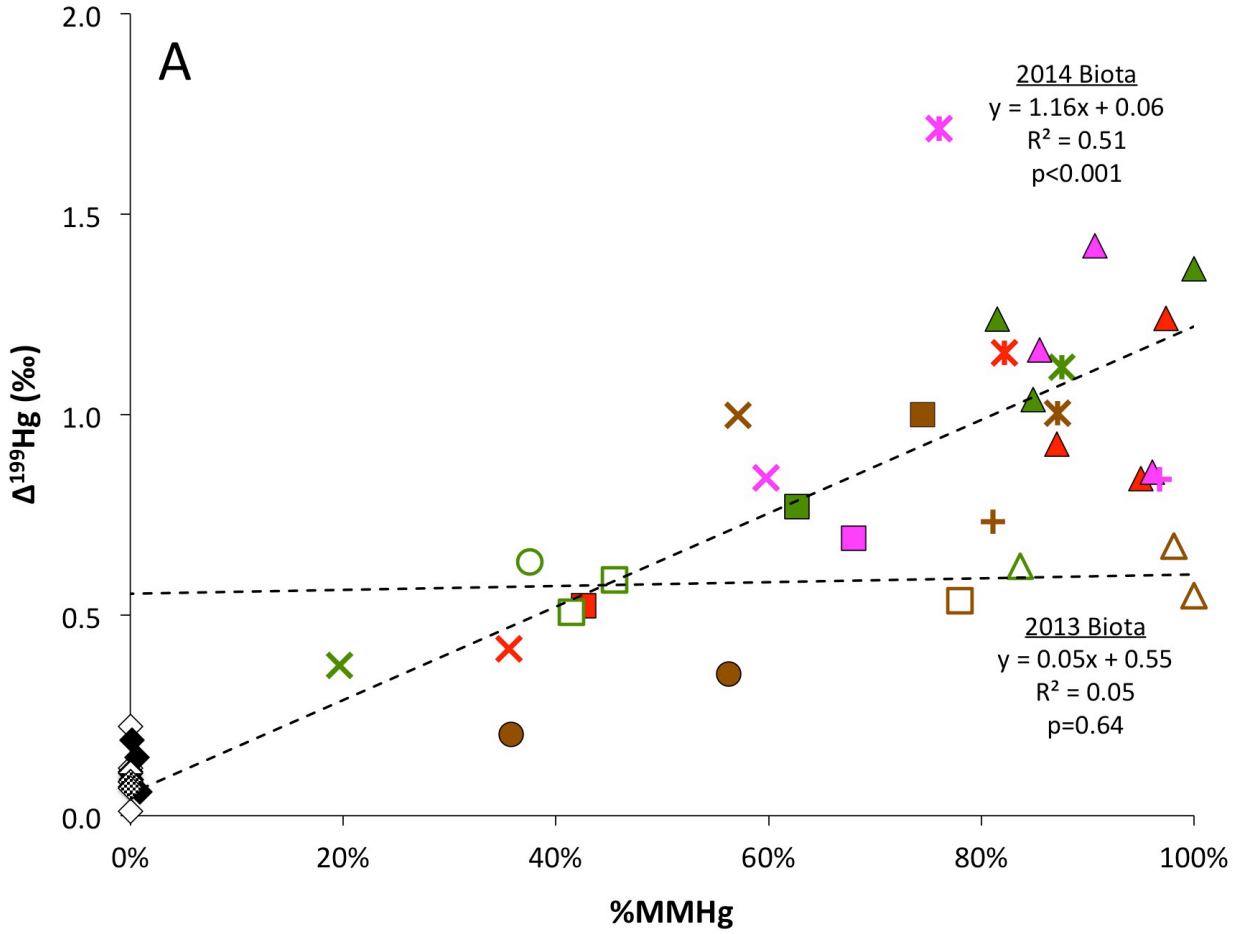
A
2014 Biota
y = 1.16x + 0.06
R² = 0.51
p<0.001
2013 Biota
y = 0.05x + 0.55
R² = 0.05
p=0.64
Δ199Hg (‰)
%MMHg
2.0
1.5
1.0
0.5
0.0
0%
20%
40%
60%
80%
100%

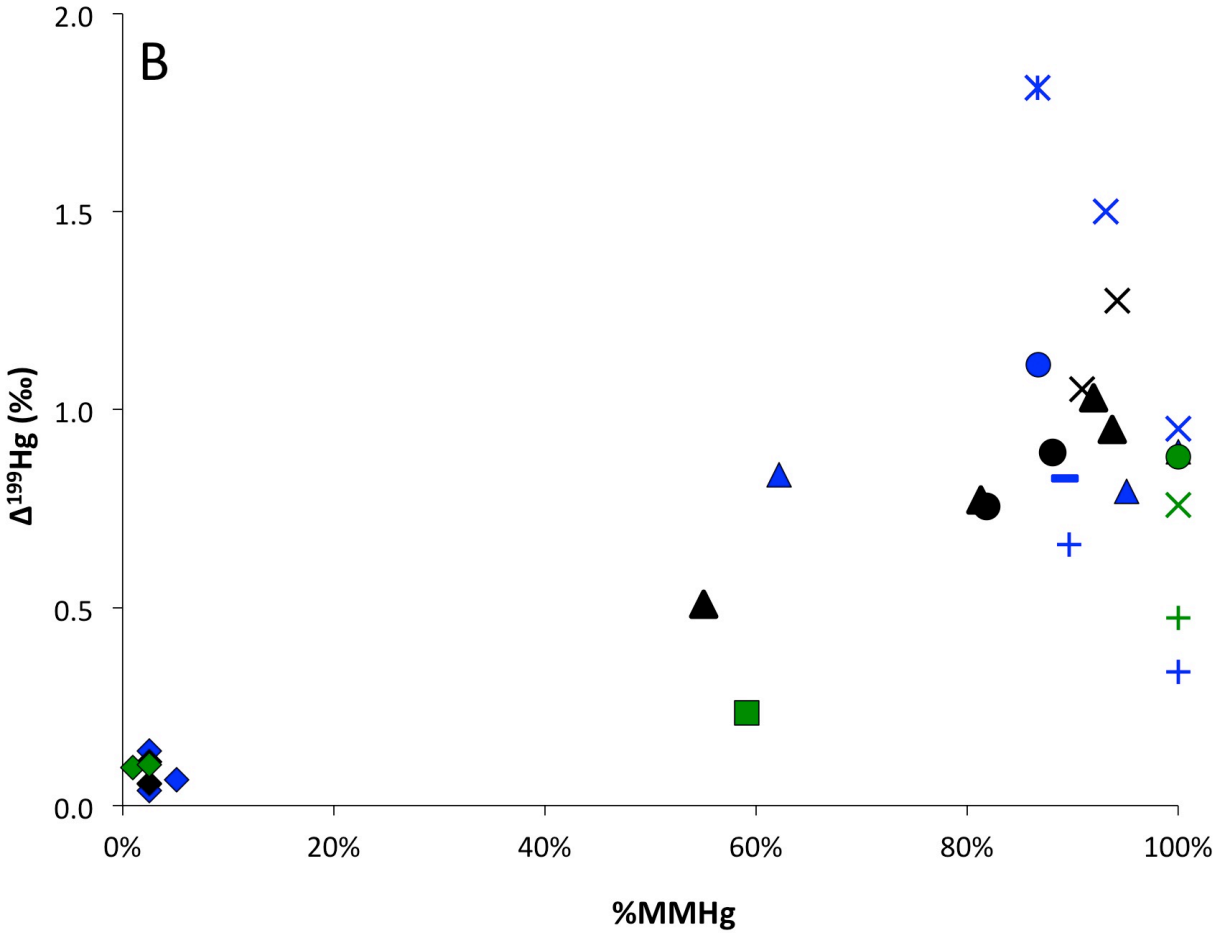

Figure 5.2: %MMHg vs. Δ^{199}Hg for biota from (A) Cache Creek and (B) Yolo Bypass Wetlands

Co-located sediment is included on each figure at approximate %MMHg (<5%) with black and white diamond symbols. Colored symbols for (A) denote location (red = Reg. Park, green = Rumsey, pink = Guinda, and brown = Capay) with open symbols sampled in 2013 and closed symbols from 2014. The type of symbol denotes the sample type (triangle = predators, square = collector-filterer, circle = collector-gatherer, plus sign = crayfish, X = filamentous algae, and star X = fish). Colored symbols in (B) represent different wetlands (blue = UW, black = PW2, green = LW) and different symbols represent different types of biota (triangles = engulfer predator, circles = piercer predator, square = collector gatherer, plus sign = crayfish, dash = fairy shrimp, x= mosquitofish, and star x = mississippi silverside).

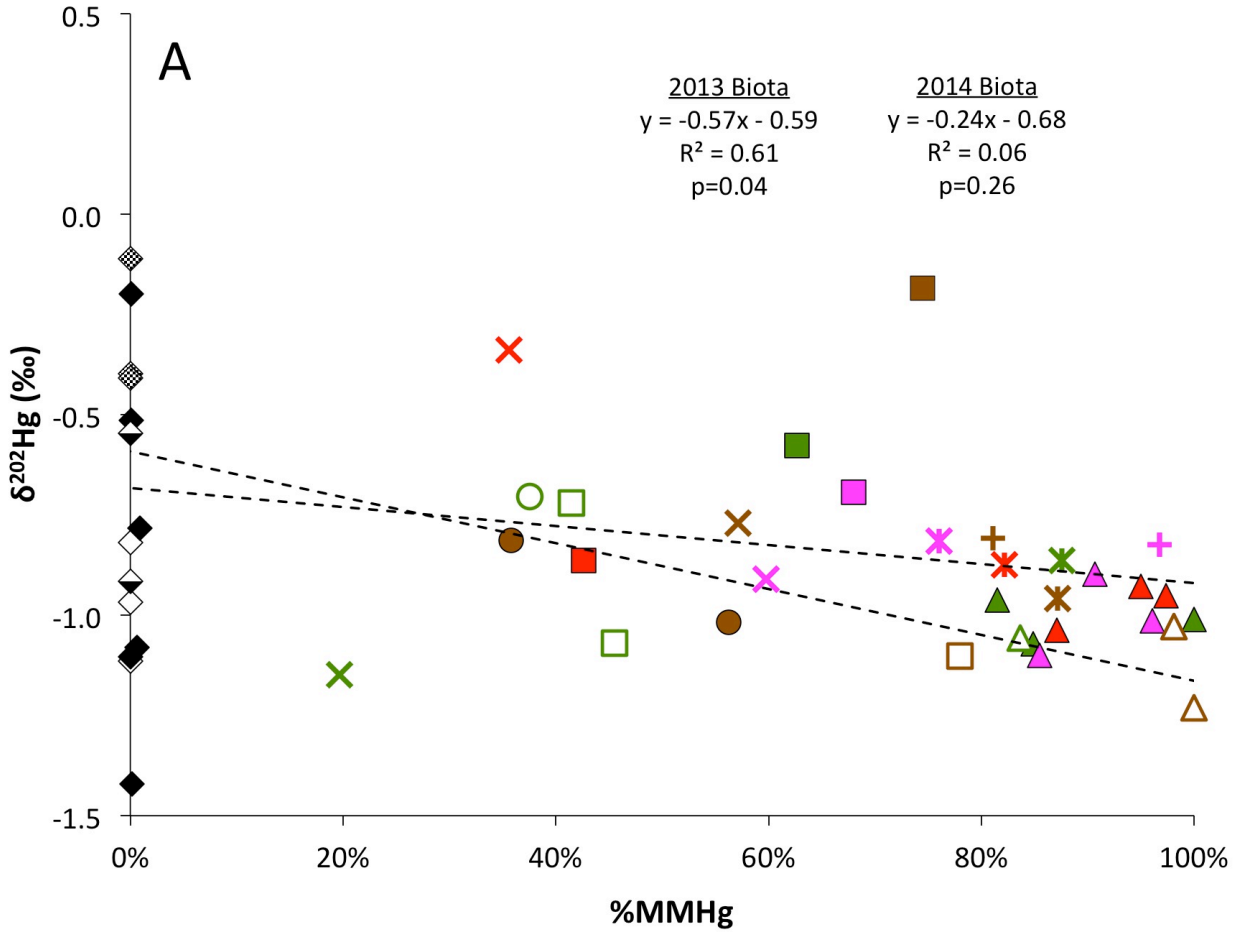
A
2013 Biota
y = -0.57x - 0.59
R² = 0.61
p=0.04
2014 Biota
y = -0.24x - 0.68
R² = 0.06
p=0.26
0.5
0.0
-0.5
-1.0
-1.5
δ202Hg (‰)
0%
20%
40%
60%
80%
100%
%MMHg

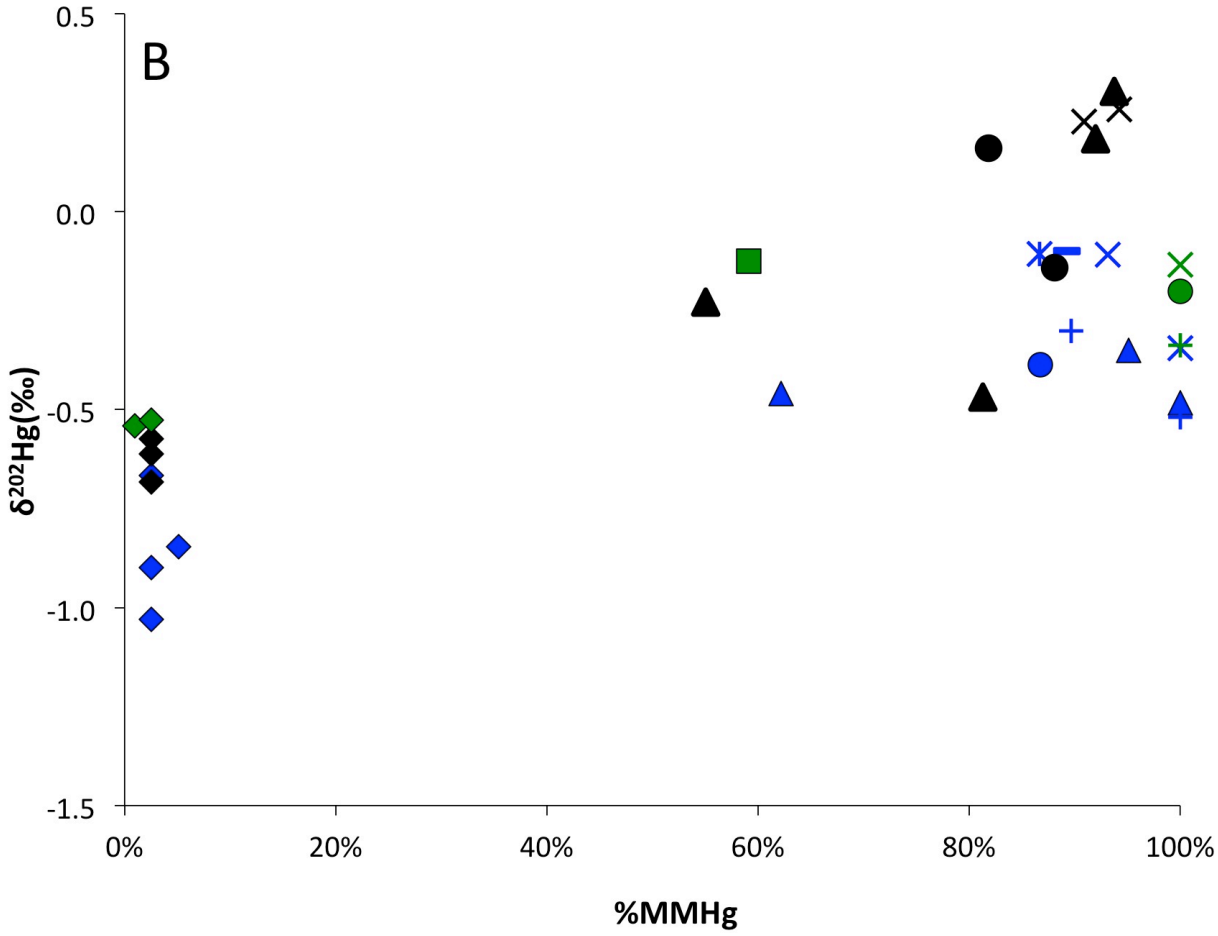

Figure 5.3: %MMHg vs. δ^{202}Hg for biota from (A) Cache Creek and (B) Yolo Bypass Wetlands

Co-located sediment is included on each figure at approximate %MMHg (<5%) with black and white diamond symbols. Colored symbols for (A) denote location (red = Reg. Park, green = Rumsey, pink = Guinda, and brown = Capay) with open symbols sampled in 2013 and closed symbols from 2014. The type of symbol denotes the sample type (triangle = predators, square = collector-filterer, circle = collector-gatherer, plus sign = crayfish, X = filamentous algae, and star X = fish). Colored symbols in (B) represent different wetlands (blue = UW, black = PW2, green = LW) and different symbols represent different types of biota (triangles = engulfer predator, circles = piercer predator, square = collector gatherer, plus sign = crayfish, dash = fairy shrimp, x= mosquitofish, and star x = mississippi silverside).

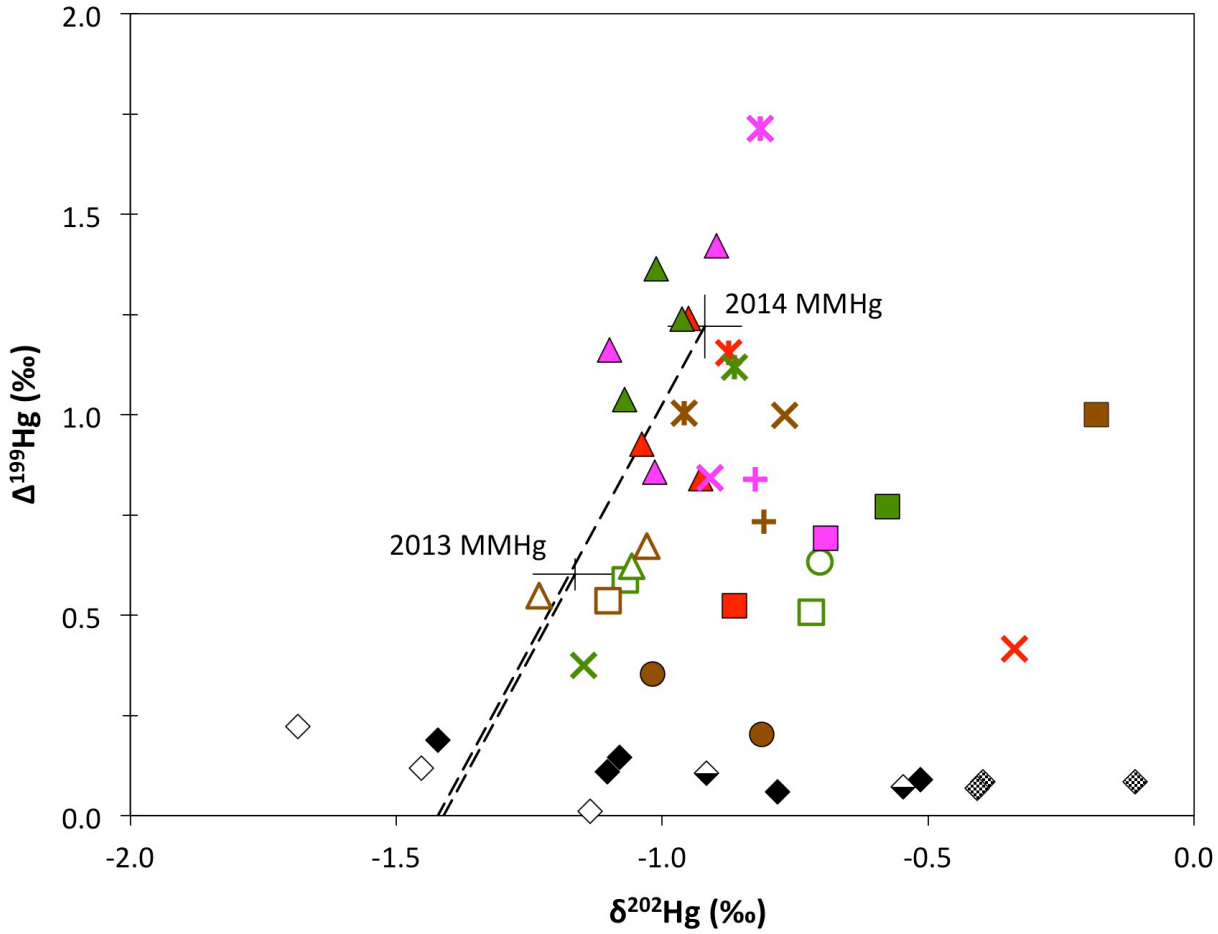

Figure 5.4: Hg isotopic composition (δ^{202}Hg vs. Δ^{199}Hg) of Cache Creek sediment and biota

All types of sediment (black and white) and biota symbols (colored) correspond to the identical samples as explained in Figures 5.2 and 5.3 for Cache Creek. The estimated MMHg isotopic composition for each year is labeled and the size of the cross represents the 1SE error associated with the estimated isotopic composition. The experimental slope for MMHg photodegradation (1 mg/L DOC from[29]) is drawn from estimated MMHg values as a black dashed line, and the pre-photodegraded MMHg is estimated when Δ^{199}Hg is near zero (δ^{202}Hg of −1.4 and −1.45‰).

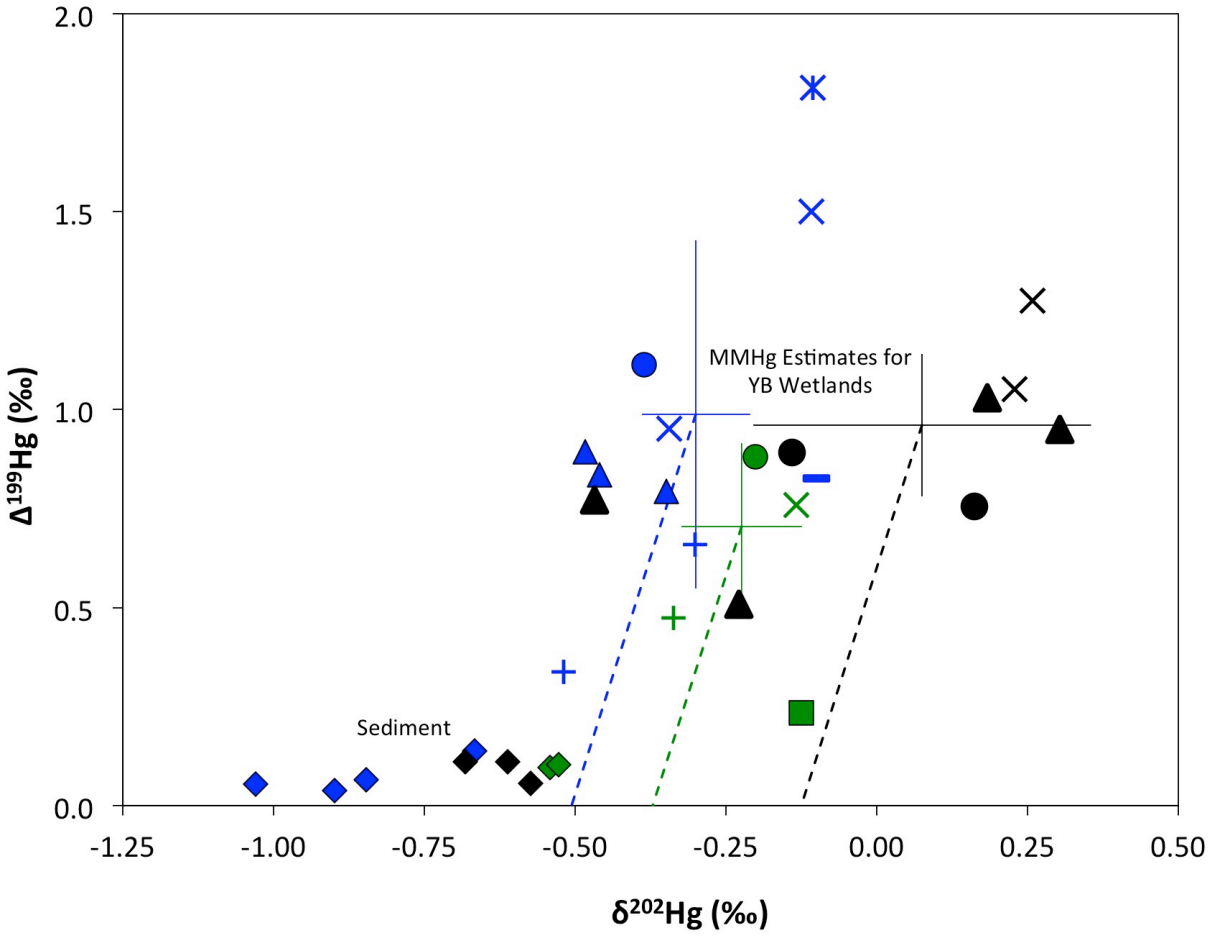

Figure 5.5: Hg isotopic composition (δ^{202}Hg vs. Δ^{199}Hg) of Yolo Bypass sediment and biota

All symbols are colored according to their location (blue = UW, black = PW2 and green = LW). The different types of biota and sediment (diamonds) symbols correspond to the identical samples as explained for Yolo Bypass in Figures 5.2 and 5.3.

Estimates of MMHg isotopic compositions for each wetland are included as large crosses and the size of the cross denotes the 1SE uncertainty of the estimate. Experimental photochemical degradation slopes under 10 mg/L conditions (from[29]) are included as dashed lines (colored according to location) for comparison of pre-photodegraded MMHg δ^{202}Hg with sediment.

References

1. Scheuhammer, A. M.; Meyer, M. W.; Sandheinrich, M. B.; Murray, M. W., Effects of Environmental Methylmercury on the Health of Wild Birds, Mammals, and Fish. *Ambio* **2007,** *36*, (1), 12-8.

2. Mergler, D.; Anderson, H. A.; Chan, L. H. M.; Mahaffey, K. R.; Murray, M.; Sakamoto, M.; Stern, A. H., Methylmercury Exposure and Health Effects in Humans: A Worldwide Concern. *AMBIO: A Journal of the Human Environment* **2007,** *36*, (1), 3-11.

3. UNEP *Global Mercury Assessment 2013: Sources, Emissions, Releases and Environmental Transport*; UNEP Chemicals Branch: Geneva, Switzerland, 2013; p 42.

4. Wiener, J. G.; Suchanek, T. H., THE BASIS FOR ECOTOXICOLOGICAL CONCERN IN AQUATIC ECOSYSTEMS CONTAMINATED BY HISTORICAL MERCURY MINING. *Ecological Applications* **2008,** *18*, (sp8), A3-A11.

5. Rytuba, J. J., Mercury mine drainage and processes that control its environmental impact. *Sci. Total Environ.* **2000,** *260*, (1-3), 57-71.

6. Rytuba, J. J., Mercury from mineral deposits and potential environmental impact. *Environmental geology (Berlin)* **2003,** *43*, (3), 326-338.

7. DTSC, C. *Final Site Discovery Report. Cache Creek Watershed. Lake, Yolo, Colusa Counties, California*; California Department of Toxic Substances Control: 2011; p 87.

8. Domagalski, J. L.; Alpers, C. N.; Slotton, D. G.; Suchanek, T. H.; Ayers, S. M., Mercury and methylmercury concentrations and loads in the Cache Creek watershed, California. *Sci. Total Environ.* **2004,** *327*, (1), 215-237.

9. Hothem, R. L.; Rytuba, J. J.; Brussee, B. E.; Goldstein, D. N., *Assessment of mercury and methylmercury in water, sediment, and biota in Sulphur Creek in the vicinity of the Clyde Gold Mine and the Elgin Mercury Mine, Colusa County, California*; 2013.

10. Hothem, R.; Bergen, D.; Bauer, M.; Crayon, J.; Meckstroth, A., Mercury and Trace Elements in Crayfish from Northern California. *Bull. Environ. Contam. Toxicol.* **2007,** *79*, (6), 628-632.

11. Slotton, D. G.; Ayers, S. M.; Suchanek, T. H.; Weyand, R. D.; Liston, A. M., Mercury bioaccumulation and trophic transfer in the Cache Creek watershed of California, in relation to diverse aqueous mercury exposure conditions. *Report to the California Bay Delta Authority, Sacramento* **2004**.

12. Suchanek, T. H.; Hothem, R. L.; Rytuba, J. J.; Yee, J. L., *Mercury Assessment and Monitoring Protocol for the Bear Creek Watershed, Colusa County, California*; 2010.

13. Hothem, R.; Trejo, B.; Bauer, M.; Crayon, J., Cliff Swallows Petrochelidon pyrrhonota as Bioindicators of Environmental Mercury, Cache Creek Watershed, California. *Arch. Environ. Contam. Toxicol.* **2008,** *55*, (1), 111-121.

14. Singer, M. B.; Aalto, R., Floodplain development in an engineered setting. *Earth Surface Processes and Landforms* **2009,** *34*, (2), 291-304.

15. Springborn, M.; Singer, M. B.; Dunne, T., Sediment-adsorbed total mercury flux through Yolo Bypass, the primary floodway and wetland in the Sacramento Valley, California. *Sci. Total Environ.* **2011,** *412*, (0), 203-213.

16. Alpers, C. N.; Hunerlach, M. P.; May, J. T.; Hothem, R. L., Mercury contamination from historical gold mining in California. *Fact Sheet - U. S. Geological Survey* **2005,** *1*.

17. Marvin-DiPasquale, M.; Windham-Myers, L.; Agee, J. L.; Kakouros, E.; Kieu, L. H.; Fleck, J. A.; Alpers, C. N.; Stricker, C. A., Methylmercury production in sediment from agricultural and non-agricultural wetlands in the Yolo Bypass, California, USA. *Sci. Total Environ.* **2014,** *484*, (0), 288-299.

18. Henery, R. E.; Sommer, T. R.; Goldman, C. R., Growth and methylmercury accumulation in juvenile Chinook salmon in the Sacramento River and its Floodplain, the Yolo Bypass. *Transactions of the American Fisheries Society* **2010,** *139*, (2), 550-563.

19. Ackerman, J. T.; Eagles-Smith, C. A., Agricultural Wetlands as Potential Hotspots for Mercury Bioaccumulation: Experimental Evidence Using Caged Fish. *Environ. Sci. Technol.* **2010,** *44*, (4), 1451-1457.

20. Ackerman, J. T.; Miles, A. K.; Eagles-Smith, C. A., Invertebrate mercury bioaccumulation in permanent, seasonal, and flooded rice wetlands within California's Central Valley. *Sci. Total Environ.* **2010,** *408*, (3), 666-671.

21. Marvin-DiPasquale, M.; Alpers, C. N.; Fleck, J. A., Mercury, methymercury and other constituents in sediment and water from seasonal and permanent wetlands in the Cache Creek Settling Basin and Yolo Bypass, Yolo County, California, 2005-06. In U.S. Dept. of the Interior, U.S. Geological Survey: [Reston, Va], 2009; p 69.

22. Springborn, M.; Singer, M. B.; Dunne, T., Sediment-adsorbed total mercury flux through Yolo Bypass, the primary floodway and wetland in the Sacramento Valley, California. *Sci. Total Environ.* **2011,** *412-413*, 203-213.

23. Kritee, K.; Barkay, T.; Blum, J. D., Mass dependent stable isotope fractionation of mercury during mer mediated microbial degradation of monomethylmercury. *Geochim. Cosmochim. Acta* **2009,** *73*, (5), 1285-1296.

24. Kritee, K.; Blum, J. D.; Johnson, M. W.; Bergquist, B. A.; Barkay, T., Mercury stable isotope fractionation during reduction of Hg(II) to Hg(0) by mercury resistant microorganisms. *Environ. Sci. Technol.* **2007,** *41*, (6), 1889-1895.

25. Rodriguez-Gonzalez, P.; Epov, V. N.; Bridou, R.; Tessier, E.; Guyoneaud, R.; Monperrus, M.; Amouroux, D., Species-Specific Stable Isotope Fractionation of Mercury during Hg(II) Methylation by an Anaerobic Bacteria (Desulfobulbus propionicus) under Dark Conditions. *Environ. Sci. Technol.* **2009,** *43*, (24), 9183-9188.

26. Perrot, V.; Bridou, R.; Pedrero, Z.; Guyoneaud, R.; Monperrus, M.; Amouroux, D., Identical Hg Isotope Mass Dependent Fractionation Signature during Methylation by Sulfate-Reducing Bacteria in Sulfate and Sulfate-Free Environment. *Environ. Sci. Technol.* **2015,** *49*, (3), 1365-1373.

27. Jiskra, M.; Wiederhold, J. G.; Bourdon, B.; Kretzschmar, R., Solution Speciation Controls Mercury Isotope Fractionation of Hg(II) Sorption to Goethite. *Environ. Sci. Technol.* **2012,** *46*, (12), 6654-6662.

28. Smith, R. S.; Wiederhold, J. G.; Kretzschmar, R., Mercury isotope fractionation during precipitation of metacinnabar (HgS) and montroydite (HgO). *Environ. Sci. Technol.* **2015,** *49*, (7), 4325-4334.

29. Bergquist, B. A.; Blum, J. D., Mass-dependent and -independent fractionation of Hg isotopes by photoreduction in aquatic systems. *Science* **2007,** *318*, (5849), 417-420.

30. Blum, J. D.; Sherman, L. S.; Johnson, M. W., Mercury Isotopes in Earth and Environmental Sciences. *Annu. Rev. Earth Planet. Sci.* **2014,** *42*, (1), 249-269.

31. Wiederhold, J. G.; Skyllberg, U.; Drott, A.; Jiskra, M.; Jonsson, S.; Bjorn, E.; Bourdon, B.; Kretzschmar, R., Mercury Isotope Signatures in Contaminated Sediments as a Tracer for Local Industrial Pollution Sources. *Environ. Sci. Technol.* **2015,** *49*, (1), 177-185.

32. Donovan, P. M.; Blum, J. D.; Demers, J. D.; Gu, B.; Brooks, S. C.; Peryam, J., Identification of Multiple Mercury Sources to Stream Sediments near Oak Ridge, TN, USA. *Environ. Sci. Technol.* **2014,** *48*, (7), 3666-3674.

33. Donovan, P. M.; Blum, J. D.; Yee, D.; Gehrke, G. E.; Singer, M. B., An isotopic record of mercury in San Francisco Bay sediment. *Chem. Geol.* **2013,** *349–350*, 87-98.

34. Foucher, D.; Ogrinc, N.; Hintelmann, H., Tracing Mercury Contamination from the Idrija Mining Region (Slovenia) to the Gulf of Trieste Using Hg Isotope Ratio Measurements. *Environ. Sci. Technol.* **2009,** *43*, (1), 33-39.

35. Smith, R. S.; Wiederhold, J. G.; Jew, A. D.; Brown, G. E.; Bourdon, B.; Kretzschmar, R., Stable Hg Isotope Signatures in Creek Sediments Impacted by a Former Hg Mine. *Environ. Sci. Technol.* **2015,** *49*, (2), 767-776.

36. Gray, J. E.; Pribil, M. J.; Higueras, P. L., Mercury isotope fractionation during ore retorting in the Almaden mining district, Spain. *Chem. Geol.*, (0).

37. Stetson, S. J.; Gray, J. E.; Wanty, R. B.; Macalady, D. L., Isotopic Variability of Mercury in Ore, Mine-Waste Calcine, and Leachates of Mine-Waste Calcine from Areas Mined for Mercury. *Environ. Sci. Technol.* **2009,** *43*, (19), 7331-7336.

38. Smith, C. N.; Kesler, S. E.; Blum, J. D.; Rytuba, J. J., Isotope geochemistry of mercury in source rocks, mineral deposits and spring deposits of the California Coast Ranges, USA. *Earth Planet. Sci. Lett.* **2008,** *269*, (3-4), 398-406.

39. Wiederhold, J. G.; Smith, R. S.; Siebner, H.; Jew, A. D.; Brown, G. E.; Bourdon, B.; Kretzschmar, R., Mercury Isotope Signatures as Tracers for Hg Cycling at the New Idria Hg Mine. *Environ. Sci. Technol.* **2013,** *47*, (12), 6137-6145.

40. Gehrke, G. E.; Blum, J. D.; Marvin-DiPasquale, M., Sources of mercury to San Francisco Bay surface sediment as revealed by mercury stable isotopes. *Geochim. Cosmochim. Acta* **2011,** *75*, (3), 691-705.

41. Smith, R. S.; Wiederhold, J. G.; Jew, A. D.; Brown Jr, G. E.; Bourdon, B.; Kretzschmar, R., Small-scale studies of roasted ore waste reveal extreme ranges of stable mercury isotope signatures. *Geochim. Cosmochim. Acta* **2014,** *137*, (0), 1-17.

42. Donovan, P. M.; Blum, J. D.; Singer, M. B.; Marvin-Di Pasquale, M.; Tsui, M., Isotopic composition of inorganic mercury and methylmercury downstream of historical gold mining. **In Prep**.

43. Kwon, S. Y.; Blum, J. D.; Carvan, M. J.; Basu, N.; Head, J. A.; Madenjian, C. P.; David, S. R., Absence of Fractionation of Mercury Isotopes during Trophic Transfer of Methylmercury to Freshwater Fish in Captivity. *Environ. Sci. Technol.* **2012,** *46*, (14), 7527-7534.

44. Kwon, S. Y.; Blum, J. D.; Chirby, M. A.; Chesney, E. J., Application of mercury isotopes for tracing trophic transfer and internal distribution of mercury in marine fish feeding experiments. *Environ. Toxicol. Chem.* **2013,** *32*, (10), 2322-2330.

45. Kwon, S. Y.; Blum, J. D.; Nadelhoffer, K. J.; Timothy Dvonch, J.; Tsui, M. T.-K., Isotopic study of mercury sources and transfer between a freshwater lake and adjacent forest food web. *Sci. Total Environ.* **2015,** *532*, (0), 220-229.

46. Tsui, M. T. K.; Blum, J. D.; Finlay, J. C.; Balogh, S. J.; Nollet, Y. H.; Palen, W. J.; Power, M. E., Variation in Terrestrial and Aquatic Sources of Methylmercury in Stream Predators as Revealed by Stable Mercury Isotopes. *Environ. Sci. Technol.* **2014,** *48*, (17), 10128-10135.

47. Tsui, M. T. K.; Blum, J. D.; Kwon, S. Y.; Finlay, J. C.; Balogh, S. J.; Nollet, Y. H., Sources and Transfers of Methylmercury in Adjacent River and Forest Food Webs. *Environ. Sci. Technol.* **2012,** *46*, (20), 10957-10964.

48. Tsui, M. T. K.; Blum, J. D.; Finlay, J. C.; Balogh, S. J.; Kwon, S. Y.; Nollet, Y. H., Photodegradation of methylmercury in stream ecosystems. *Limnol. Oceanogr* **2013,** *58*, (1), 13-22.

49. Gehrke, G. E.; Blum, J. D.; Slotton, D. G.; Greenfield, B. K., Mercury Isotopes Link Mercury in San Francisco Bay Forage Fish to Surface Sediments. *Environ. Sci. Technol.* **2011,** *45*, (4), 1264-1270.

50. Balogh, S. J.; Tsui, M. T. K.; Blum, J. D.; Matsuyama, A.; Woerndle, G. E.; Yano, S.; Tada, A., Tracking the Fate of Mercury in the Fish and Bottom Sediments of Minamata Bay, Japan, Using Stable Mercury Isotopes. *Environ. Sci. Technol.* **2015**.

51. Sherman, L. S.; Blum, J. D., Mercury stable isotopes in sediments and largemouth bass from Florida lakes, USA. *Sci. Total Environ.* **2013,** *448*, (0), 163-175.

52. Marvin-DiPasquale, M.; Agee, J. L.; Kakouros, E.; Kieu, L. H.; Fleck, J. A.; Alpers, C. N., The effects of sediment and mercury mobilization in the South Yuba River and Humbug Creek confluence area, Nevada County, California; concentrations, speciation, and environmental fate; Part 2, Laboratory experiments. *Open-File Report - U. S. Geological Survey* **2011,** *1*.

53. Hammerschmidt, C.; Fitzgerald, W., Bioaccumulation and Trophic Transfer of Methylmercury in Long Island Sound. *Arch. Environ. Contam. Toxicol.* **2006,** *51*, (3), 416-424.

54. USEPA *Method 1630: Methyl Mercury in Water by Distillation, Aqueous Ethylation, Purge and Trap, and CVAFS*; U.S. Environmental Protection Agency, Office of Water, Office of Science and Technology, Engineering and Analysis Division: Washington, D.C., 2001.

55. Demers, J. D.; Blum, J. D.; Zak, D. R., Mercury isotopes in a forested ecosystem: Implications for air-surface exchange dynamics and the global mercury cycle. *Global Biogeochem. Cycles* **2013,** *27*, (1), 222-238.

56. Blum, J. D.; Bergquist, B. A., Reporting of variations in the natural isotopic composition of mercury. *Anal. Bioanal. Chem.* **2007,** *388*, (2), 353-359.

57. Kwon, S. Y.; Blum, J. D.; Chen, C. Y.; Meattey, D. E.; Mason, R. P., Mercury Isotope Study of Sources and Exposure Pathways of Methylmercury in Estuarine Food Webs in the Northeastern US. *Environ. Sci. Technol.* **2014,** *48*, (17), 10089-10097.

58. Masbou, J.; Point, D.; Sonke, J. E., Application of a selective extraction method for methylmercury compound specific stable isotope analysis (MeHg-CSIA) in biological materials. *J. Anal. At. Spectrom.* **2013,** *28*, (10), 1620-1628.

59. Cooke, C. A.; Hintelmann, H.; Ague, J. J.; Burger, R.; Biester, H.; Sachs, J. P.; Engstrom, D. R., Use and Legacy of Mercury in the Andes. *Environ. Sci. Technol.* **2013,** *47*, (9), 4181-4188.

60. Biswas, A.; Blum, J. D.; Bergquist, B. A.; Keeler, G. J.; Xie, Z. Q., Natural Mercury Isotope Variation in Coal Deposits and Organic Soils. *Environ. Sci. Technol.* **2008,** *42*, (22), 8303-8309.

61. Sonke, J. E.; Schafer, J.; Chmeleff, J.; Audry, S.; Blanc, G.; DuprÈ, B., Sedimentary mercury stable isotope records of atmospheric and riverine pollution from two major European heavy metal refineries. *Chem. Geol.* **2010,** *279*, (3-4), 90-100.

62. Rytuba, J. J.; Hothem, R. L.; Brussee, B. E.; Goldstein, D.; May, J. *Environmental assessment of water, sediment, and biota collected from the Bear Creek watershed, Colusa County, California*; 2013-1070; Reston, VA, 2015; p 91.

63. Bouse, R. M.; Fuller, C. C.; Luoma, S.; Hornberger, M. I.; Jaffe, B. E.; Smith, R. E., Mercury-Contaminated Hydraulic Mining Debris in San Francisco Bay. *San Francisco Estuary and Watershed Science* **2010,** *8*, (1).

64. Singer, M. B.; Aalto, R.; James, L. A.; Kilham, N. E.; Higson, J. L.; Ghoshal, S., Enduring legacy of a toxic fan via episodic redistribution of California gold mining debris. *Proceedings of the National Academy of Sciences* **2013**.

65. Tsui, M. T. K.; Finlay, J.; Balogh, S.; Nollet, Y., In Situ Production of Methylmercury within a Stream Channel in Northern California. *Environ. Sci. Technol.* **2010,** *44*, (18), 6998-7004.

66. Tsui, M. T. K.; Finlay, J. C.; Nater, E. A., Mercury Bioaccumulation in a Stream Network. *Environ. Sci. Technol.* **2009,** *43*, (18), 7016-7022.

67. Chasar, L. C.; Scudder, B. C.; Stewart, A. R.; Bell, A. H.; Aiken, G. R., Mercury Cycling in Stream Ecosystems. 3. Trophic Dynamics and Methylmercury Bioaccumulation. *Environ. Sci. Technol.* **2009,** *43*, (8), 2733-2739.

68. Nichols, S. J.; Silverman, H.; Dietz, T. H.; Lynn, J. W.; Garling, D. L., Pathways of Food Uptake in Native (Unionidae) and Introduced (Corbiculidae and Dreissenidae) Freshwater Bivalves. *Journal of Great Lakes Research* **2005,** *31*, (1), 87-96.

69. Pyke, G. H., A review of the biology of Gambusia affinis and G. holbrooki. *Reviews in Fish Biology and Fisheries* **2005,** *15*, (4), 339-365.

70. Moyle, P. B., *Inland fishes of California*. Univ of California Press: 2002.

71. Gantner, N.; Hintelmann, H.; Zheng, W.; Muir, D. C., Variations in Stable Isotope Fractionation of Hg in Food Webs of Arctic Lakes. *Environ. Sci. Technol.* **2009,** *43*, (24), 9148-9154.

72. Perrot, V.; Pastukhov, M. V.; Epov, V. N.; Husted, S. r.; Donard, O. F. X.; Amouroux, D., Higher Mass-Independent Isotope Fractionation of Methylmercury in the Pelagic Food Web of Lake Baikal (Russia). *Environ. Sci. Technol.* **2012,** *46*, (11), 5902-5911.

73. Chandan, P.; Ghosh, S.; Bergquist, B. A., Mercury Isotope Fractionation during Aqueous Photoreduction of Monomethylmercury in the Presence of Dissolved Organic Matter. *Environ. Sci. Technol.* **2015,** *49*, (1), 259-267.

74. Chow, A. T.; Dahlgren, R. A.; Harrison, J. A., Watershed sources of disinfection byproduct precursors in the Sacramento and San Joaquin Rivers, California. *Environ. Sci. Technol.* **2007,** *41*, (22), 7645-7652.

75. Domagalski, J. L.; Alpers, C. N.; Slotton, D. G.; Suchanek, T. H.; Ayers, S. M., Mercury and methylmercury concentrations and loads in Cache Creek basin, California, January 2000 through May 2001. *Scientific Investigations Report* **2004**, 56.

76. Sherman, L. S.; Blum, J. D.; Keeler, G. J.; Demers, J. D.; Dvonch, J. T., Investigation of Local Mercury Deposition from a Coal-Fired Power Plant Using Mercury Isotopes. *Environ. Sci. Technol.* **2011,** *46*, (1), 382-390.

77. Gratz, L. E.; Keeler, G. J.; Blum, J. D.; Sherman, L. S., Isotopic Composition and Fractionation of Mercury in Great Lakes Precipitation and Ambient Air. *Environ. Sci. Technol.* **2010,** *44*, (20), 7764-7770.

78. Chen, J.; Hintelmann, H.; Feng, X.; Dimock, B., Unusual fractionation of both odd and even mercury isotopes in precipitation from Peterborough, ON, Canada. *Geochim. Cosmochim. Acta* **2012,** *90*, (0), 33-46.

79. Sherman, L. S.; Blum, J. D.; Nordstrom, D. K.; McCleskey, R. B.; Barkay, T.; Vetriani, C., Mercury isotopic composition of hydrothermal systems in the Yellowstone Plateau volcanic field and Guaymas Basin sea-floor rift. *Earth Planet. Sci. Lett.* **2009,** *279*, (1-2), 86-96.

80. Brigham, M. E.; Wentz, D. A.; Aiken, G. R.; Krabbenhoft, D. P., Mercury Cycling in Stream Ecosystems. 1. Water Column Chemistry and Transport. *Environ. Sci. Technol.* **2009,** *43*, (8), 2720-2725.

81. Ward, D. M.; Nislow, K. H.; Folt, C. L., Bioaccumulation syndrome: identifying factors that make some stream food webs prone to elevated mercury bioaccumulation. *Ann. N. Y. Acad. Sci.* **2010,** *1195*, (1), 62-83.

82. Marvin-DiPasquale, M.; Lutz, M. A.; Brigham, M. E.; Krabbenhoft, D. P.; Aiken, G. R.; Orem, W. H.; Hall, B. D., Mercury Cycling in Stream Ecosystems. 2. Benthic Methylmercury Production and Bed Sediment-Pore Water Partitioning. *Environ. Sci. Technol.* **2009,** *43*, (8), 2726-2732.

83. Gray, J. E.; Hines, M. E., Biogeochemical mercury methylation influenced by reservoir eutrophication, Salmon Falls Creek Reservoir, Idaho, USA. *Chem. Geol.* **2009,** *258*, (3), 157-167.

84. Lustig, L. K.; Busch, R. D., *Sediment transport in Cache Creek drainage basin in the Coast Ranges west of Sacramento, California*; Professional Paper 562-A. Survey, U. S. G.: 1967.

85. Suchanek, T. H.; Richerson, P. J.; Zierenberg, R. A.; Eagles-Smith, C. A.; Slotton, D. G.; Harner, E. J.; Osleger, D. A.; Anderson, D. W.; Cech, J. J.; Schladow, S. G.; Colwell, A. E.; Mount, J. F.; King, P. S.; Adam, D. P.; McElroy, K. J., THE LEGACY OF MERCURY CYCLING FROM MINING SOURCES IN AN AQUATIC ECOSYSTEM: FROM ORE TO ORGANISM. *Ecological Applications* **2008,** *18*, (sp8), A12-A28.

86. Stoor, R. W.; Hurley, J. P.; Babiarz, C. L.; Armstrong, D. E., Subsurface sources of methyl mercury to Lake Superior from a wetland,Äìforested watershed. *Sci. Total Environ.* **2006,** *368*, (1), 99-110.

87. Buckman, K. L.; Marvin-Di Pasquale, M.; Taylor, V. F.; Chalmers, A.; Broadley, H. J.; Agee, J.; Jackson, B. P.; Chen, C. Y., Influence of a chlor-alkali superfund site on mercury bioaccumulation in periphyton and low-trophic level fauna. *Environ. Toxicol. Chem.* **2015,** *34*, (7), 1649-1658.

88. Yin, R.; Feng, X.; Wang, J.; Bao, Z.; Yu, B.; Chen, J., Mercury isotope variations between bioavailable mercury fractions and total mercury in mercury contaminated soil in Wanshan Mercury Mine, SW China. *Chem. Geol.* **2012,** *336*, (Special Issue), 80-86.

89. Schaefer, J. K.; Yagi, J.; Reinfelder, J. R.; Cardona, T.; Ellickson, K. M.; Tel-Or, S.; Barkay, T., Role of the bacterial organomercury lyase (MerB) in controlling methylmercury accumulation in mercury-contaminated natural waters. *Environ. Sci. Technol.* **2004,** *38*, (16), 4304-4311.

90. Marvin-DiPasquale, M.; Agee, J.; McGowan, C.; Oremland, R. S.; Thomas, M.; Krabbenhoft, D.; Gilmour, C. C., Methyl-mercury degradation pathways: A comparison among three mercury-impacted ecosystems. *Environ. Sci. Technol.* **2000,** *34*, (23), 4908-4916.

5.4 Supporting Information

Figure 5.S1: Regional map of Cache Creek, Yolo Bypass and the Yuba River.

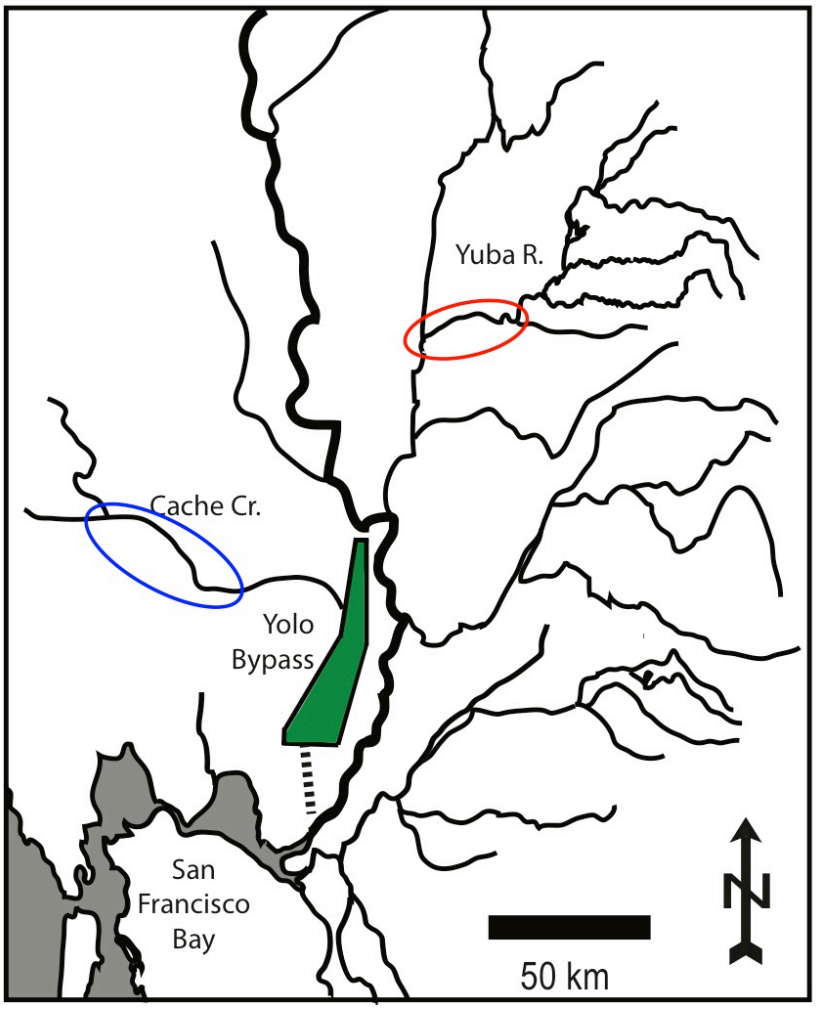

Figure 5.S2: Cache Creek Sampling Locations and Collection Details

Sampling Year	Biota	Feeding Behavior	Cache Creek Sampling Sites			
	Common Name (*scientific ID*)		Reg. Park	Rumsey	Guinda	Capay
2013	Hellgrammite (*Megaloptera*)	Predator (Engulfer)		X		
	Stonefly Larva (*Perlidae*)	Predator (Engulfer)				X
	Damselfly Larva (*Coenagrionidae)*	Predator (Engulfer)				X
	Net Spinning Caddisfly Larva (*Hydropsychidae*)	Collector/Filterer		X		X
	Mayfly Larva (*Heptageniidae & Ephemerellidae spp.*)	Collector/Gatherer or Scraper		X		
	Asian Clam (*Corbicula fluminea*)	Collector/Filterer		X		
2014	Damselfly Larva (*Coenagrionidae)*	Predator (Engulfer)	X	X	X	
	Mixed Dragonfly Larva (*Libellulidae and Gomphidae*)	Predator (Engulfer)	X	X	X	
	Creeping Waterbug Larva (*Naucoridae*)	Predator (Piercer)	X	X	X	
	Burrowing Mayfly Larva (*Ephemeridae*)	Collector/Gatherer				X
	Aquatic Worm (*Oligochaeta*)	Collector/Gatherer				X
	Asian Clam (*Corbicula fluminea*)	Collector/Filterer	X	X	X	X
	Red Swamp Crayfish (*Procambarus clarkia*)	Omnivore			X	X
	Mosquitofish (*Gambusia affinis*)	Omnivore	X		X	X
	Speckled Dace (*Rhinichthys osculus*)	Forager/Omnivore		X		
	Filamentous Algae (*Spyrogyra and Hydrodictyon*)	n/a	X	X	X	X

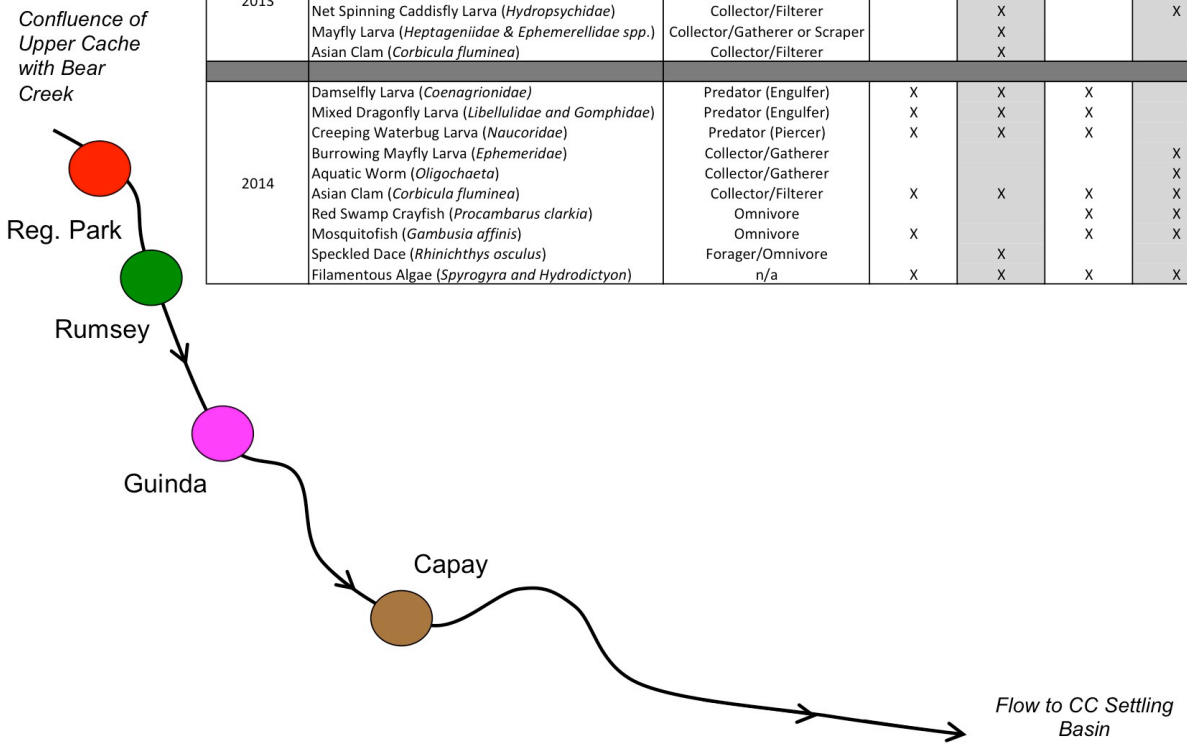

Figure 5.S3: Yolo Bypass Wetland Sampling Locations and Collection Details

Sampling Year	Biota	Feeding Behavior	Yolo Bypass		
	Common Name (*scientific ID*)		Upper	Permanent Wetland 2	Lower
2013	Damselfly Larva (*Coenagrionidae)*	Predator (Engulfer)	X		
	Mixed Dragonfly Larva (*Libellulidae and Gomphidae*)	Predator (Engulfer)	X		
	Backswimmers (*Notonectidae*)	Predator (Piercer)			X
	Midge Larva (*Chironomidae*)	Collector/Gatherer			X
	Red Swamp Crayfish (*Procambarus clarkia*)	Omnivore	X		X
	Mosquitofish (*Gambusia affinis*)	Omnivore	X		X
2014	Damselfly Larva (*Coenagrionidae)*	Predator (Engulfer)	X	X	
	Mixed Dragonfly Larva (*Libellulidae and Gomphidae*)	Predator (Engulfer)		X	
	Dragonfly Larva (*Aeshnidae*)	Predator (Engulfer)		X	
	Water Scavenger Beetle (*Hydrophilidae*)	Predator (Engulfer)		X	
	Creeping Waterbug Larva (*Naucoridae*)	Predator (Piercer)		X	
	Backswimmers (*Notonectidae*)	Predator (Piercer)	X	X	
	Red Swamp Crayfish (*Procambarus clarkia*)	Omnivore	X		
	Fairy shrimp (*Linderiella occidentalis*)	Filterer	X		
	Mississippi Silversides (*Medinia beryllina*)	Planktivore	X		
	Mosquitofish (*Gambusia affinis*)	Omnivore	X	X	

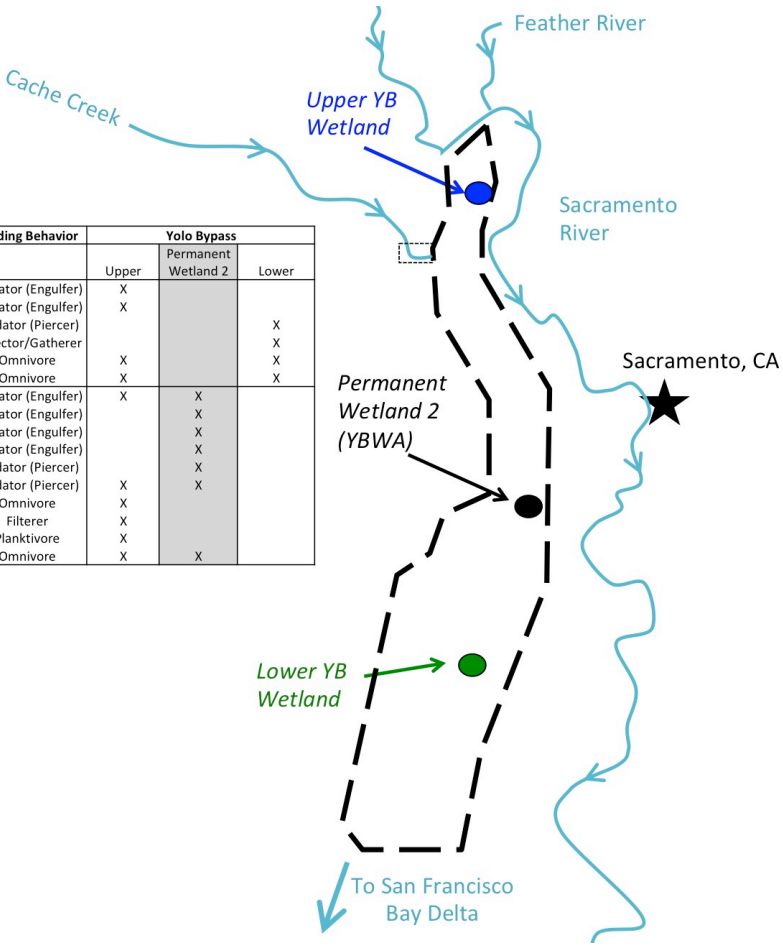

Figure 5.S4: Hg Isotopic Composition of all sediment from the region.
Diamonds represent Cache Creek sediment (colors denote sediment size fraction: filled = <63um, half filled = 1mm-63um, empty = <1mm) and checkered diamonds are from Bear Creek. Circles represent Yolo Bypass (colors denote wetland: blue = upper, black = PW2, green = lower) and squares represent the Yuba and Feather Rivers (orange for Yuba River and yellow for Feather River).[42]

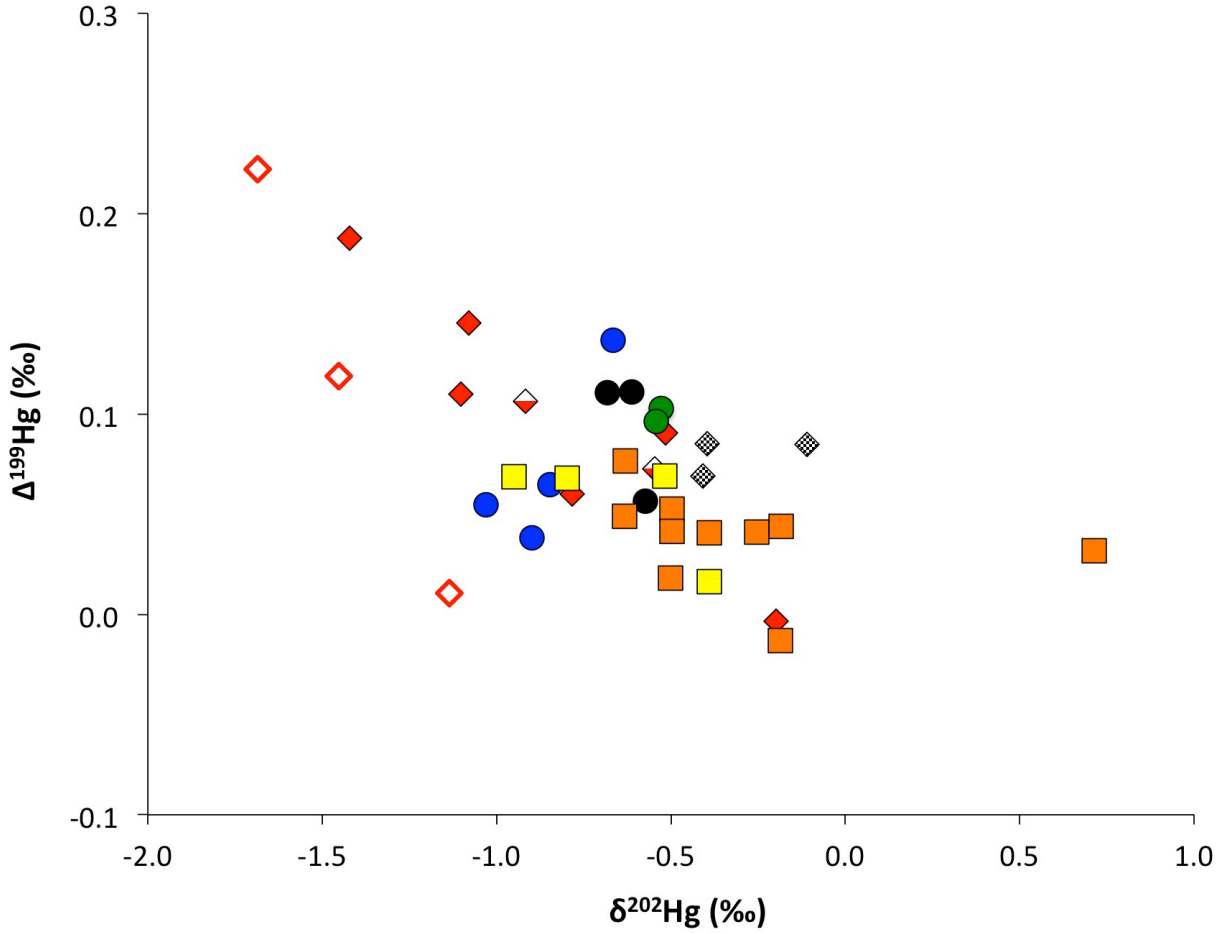

Figure 5.S5: $\Delta^{201}Hg$ vs. $\Delta^{199}Hg$ for Cache Creek biota.
Sediment is plotted as black, white and gray diamonds for comparison but these samples are not included on the linear regression for all biota.

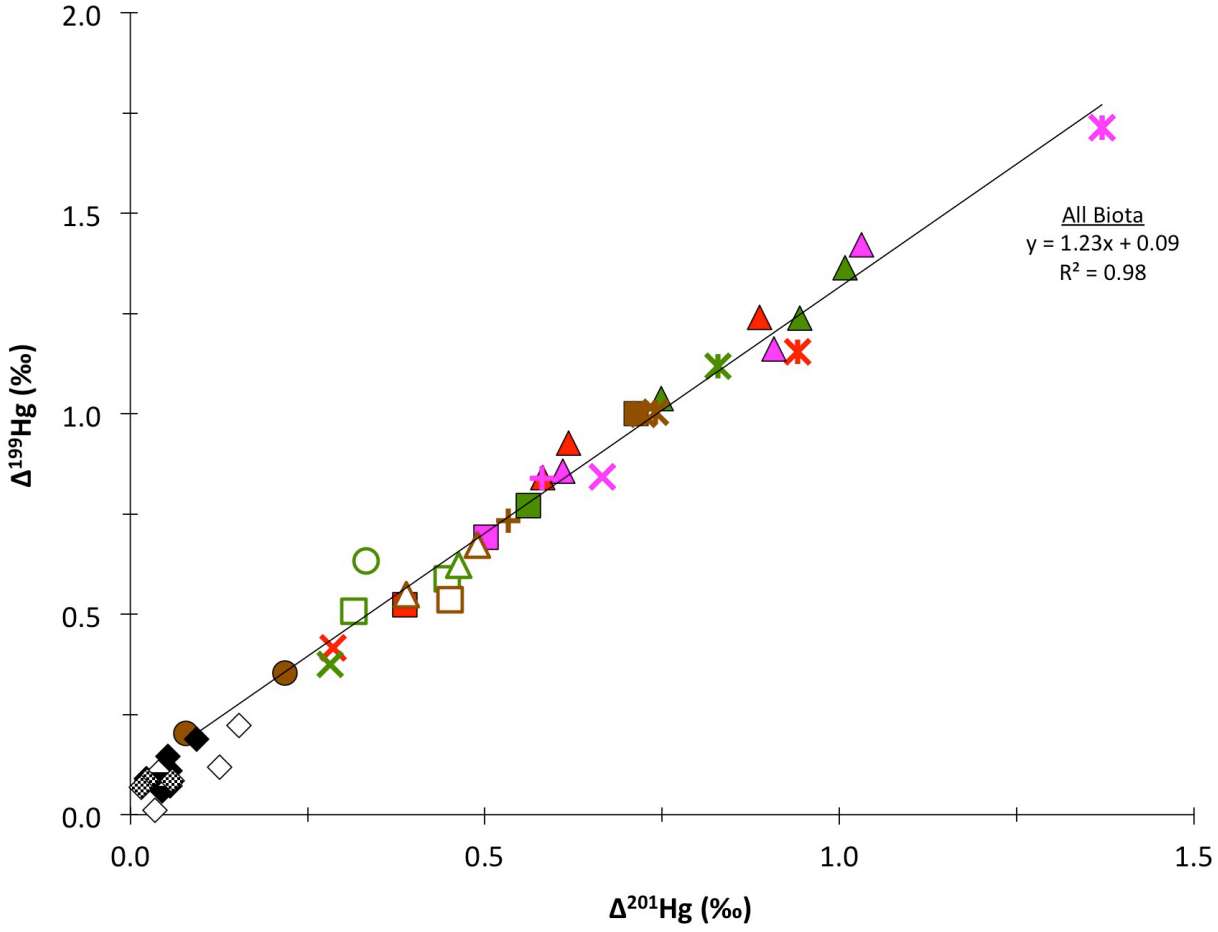

Figure 5.S6: $\Delta^{201}Hg$ vs. $\Delta^{199}Hg$ for Yolo Bypass biota.
Sediment from each wetland is included as black, blue or green diamonds but not used for the regression of all biota.

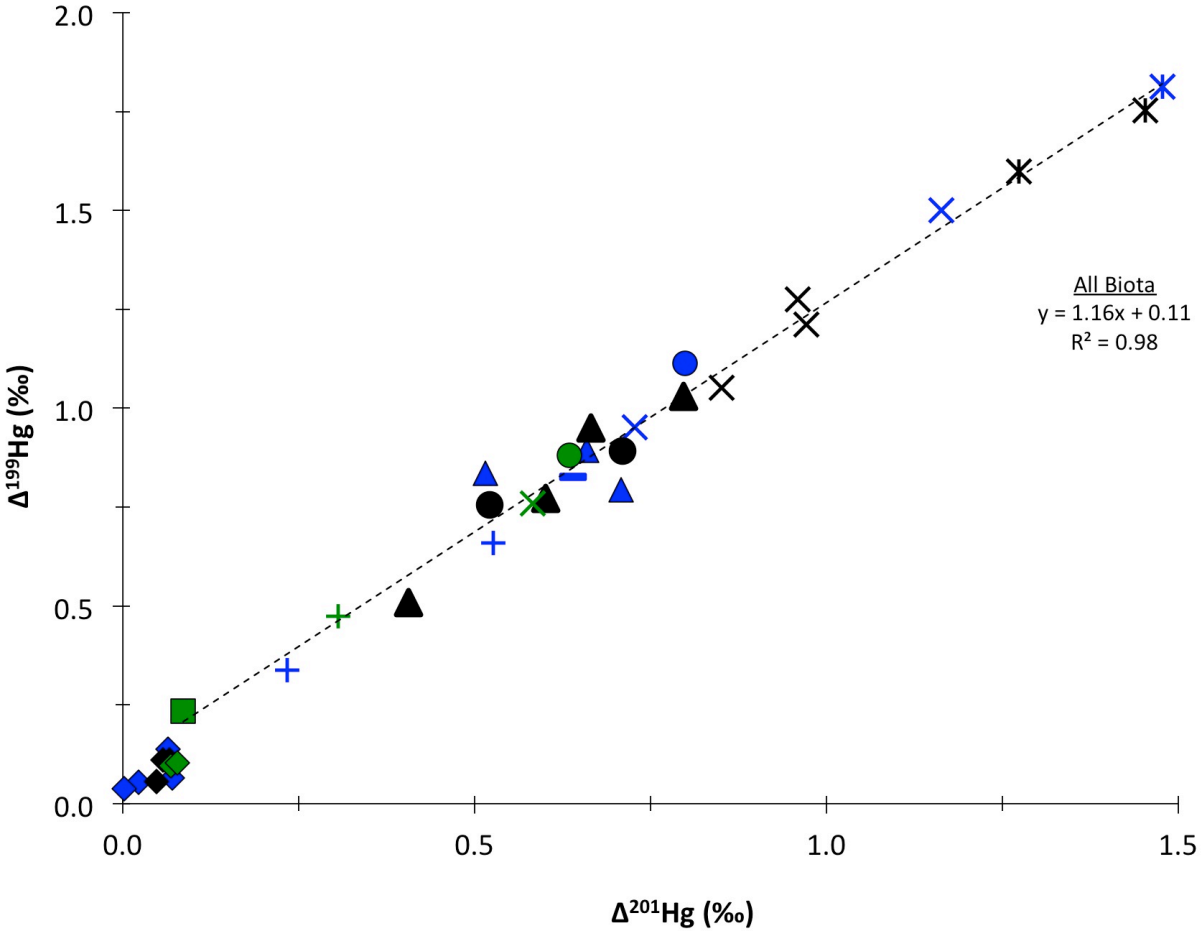

Table 5.S1: THg, MMHg, and Hg isotope values for all sediment from Cache Creek, Bear Creek and Yolo Bypass

Water Body	Site, Location	Sample Type	MMHg	THg	%MMHg	$\delta^{204}Hg$	$\delta^{202}Hg$	$\delta^{201}Hg$	$\delta^{200}Hg$	$\delta^{199}Hg$	$\Delta^{204}Hg$	$\Delta^{201}Hg$	$\Delta^{200}Hg$	$\Delta^{199}Hg$
		km	dw ng/g	dw ng/g	%	‰	‰	‰	‰	‰	‰	‰	‰	‰
Bear Creek	Bar	*unsieved, ground*		23683		-0.14	-0.11	-0.06	-0.03	0.06	0.02	0.02	0.02	0.08
		unsieved, ground		26052		-0.67	-0.40	-0.24	-0.20	-0.01	-0.08	0.06	0.00	0.09
	Terrace	*unsieved, ground*		467600		-0.64	-0.41	-0.29	-0.20	-0.03	-0.03	0.02	0.01	0.07
Cache Creek	Rumsey, Floodplain	*unsieved, ground*		1480.8		-1.71	-1.13	-0.82	-0.57	-0.28	-0.02	0.04	0.00	0.01
	Rumsey Bar	*<1mm, ground*		87.2		-2.14	-1.45	-0.97	-0.70	-0.25	0.03	0.13	0.03	0.12
		1mm-63um, ground		173.4		-1.39	-0.92	-0.65	-0.40	-0.12	-0.03	0.04	0.06	0.11
		<63um, unground	0.89	97.6	0.9%	-1.30	-0.78	-0.54	-0.42	-0.14	-0.13	0.05	-0.02	0.06
		<63um, unground	0.89	1060.0	0.1%	-0.31	-0.20	-0.14	-0.11	-0.05	-0.01	0.01	-0.02	0.00
		<63um, unground	0.89	584.8	0.2%	-2.20	-1.42	-0.98	-0.68	-0.17	-0.08	0.09	0.03	0.19
	Capay Bar	*<1mm, ground*		503.3		-2.55	-1.69	-1.11	-0.81	-0.20	-0.03	0.15	0.03	0.22
		1mm-63um, ground		327.8		-0.75	-0.55	-0.35	-0.26	-0.07	0.06	0.06	0.01	0.07
		<63um, unground	0.98	830.5	0.1%	-0.87	-0.51	-0.36	-0.27	-0.04	-0.11	0.02	-0.01	0.09
		<63um, unground	0.98	3867.7	0.0%	-1.70	-1.10	-0.77	-0.58	-0.17	-0.05	0.06	-0.02	0.11
		<63um, unground	0.98	158.0	0.6%	-1.61	-1.08	-0.76	-0.52	-0.13	0.00	0.05	0.02	0.15
Yolo Bypass	Upper Wetland	*<63um, unground*	2.89	56.7	5.1%	-1.24	-0.85	-0.57	-0.40	-0.15	0.02	0.07	0.02	0.06
		<1mm, ground		61.8		-1.07	-0.67	-0.44	-0.29	-0.03	-0.07	0.06	0.04	0.14
		<1mm, ground		35.8		-1.55	-1.03	-0.75	-0.54	-0.20	-0.01	0.02	-0.02	0.05
		<1mm, ground		37.4		-1.41	-0.90	-0.67	-0.46	-0.19	-0.07	0.00	-0.01	0.04
	Permanent Wetland 2 (PW2)	*<1mm, ground*		130.4		-0.94	-0.61	-0.40	-0.30	-0.04	-0.03	0.06	0.00	0.11
		<1mm, ground		116.3		-0.99	-0.68	-0.45	-0.33	-0.06	0.02	0.07	0.02	0.11
		<1mm, ground		182.4		-0.87	-0.57	-0.38	-0.27	-0.09	-0.01	0.05	0.01	0.06
	Lower Wetland	*<63um, unground*	2.50	253.7	1.0%	-0.78	-0.54	-0.34	-0.25	-0.04	0.03	0.07	0.02	0.10
		<1mm, ground		225.5		-0.86	-0.53	-0.32	-0.25	-0.03	-0.07	0.08	0.01	0.10

Table 5.S2: THg, MMHg and Hg Isotope Values for All Aquatic Organisms

Water Body	Location	Sampling Year	Sample Type	MMHg	THg	%MMHg	$\delta^{204}Hg$	$\delta^{202}Hg$	$\delta^{201}Hg$	$\delta^{200}Hg$	$\delta^{199}Hg$	$\Delta^{204}Hg$	$\Delta^{201}Hg$	$\Delta^{200}Hg$	$\Delta^{199}Hg$
				dw ng/g	dw ng/g	%	‰	‰	‰	‰	‰	‰	‰	‰	‰
Cache Creek	Regional Park	2014	Damselfly Larva (*Coenagrionidae)*	390.9	401.5	97%	-1.48	-0.95	0.17	-0.47	1.00	-0.06	0.89	0.01	1.24
			Mixed Dragonfly Larva (*Libellulidae and Gomphidae*)	472.9	497.8	95%	-1.41	-0.93	-0.12	-0.46	0.61	-0.03	0.58	0.01	0.84
			Creeping Waterbug Larva (*Naucoridae*)	463.0	531.6	87%	-1.60	-1.04	-0.16	-0.48	0.66	-0.05	0.62	0.04	0.93
			Asian Clam (*Corbicula fluminea*)	359.4	843.2	43%	-1.30	-0.86	-0.26	-0.41	0.31	-0.01	0.39	0.02	0.52
			Filamentous Algae (*Spyrogyra and Hydrodictyon*)	78.4	220.1	36%	-0.46	-0.34	0.03	-0.19	0.33	0.04	0.29	-0.02	0.42
			Mosquitofish (*Gambusia affinis*)	560.6	682.5	82%	-1.29	-0.87	0.28	-0.43	0.93	0.02	0.94	0.01	1.15
	Rumsey	2013	Net Spinning Caddisfly Larva (*Hydropsychidae*)	59.0	129.5	46%	-1.65	-1.07	-0.36	-0.54	0.32	-0.06	0.45	0.00	0.59
			Hellgrammite (*Megaloptera*)	182.7	218.4	84%	-1.54	-1.06	-0.33	-0.49	0.36	0.04	0.46	0.04	0.62
			Asian Clam (*Corbicula fluminea*)	138.7	334.4	41%	-1.12	-0.72	-0.23	-0.29	0.33	-0.04	0.32	0.07	0.51
			Mayfly Larva (*Heptageniidae & Ephemerellidae spp.*)	45.2	120.2	38%	-1.21	-0.70	-0.20	-0.37	0.46	-0.16	0.33	-0.02	0.63
		2014	Damselfly Larva (*Coenagrionidae)*	254.7	252.8	100%	-1.54	-1.01	0.25	-0.49	1.11	-0.03	1.01	0.02	1.36
			Mixed Dragonfly Larva (*Libellulidae and Gomphidae*)	220.9	271.2	81%	-1.45	-0.96	0.22	-0.45	1.00	-0.01	0.94	0.03	1.24
			Creeping Waterbug Larva (*Naucoridae*)	231.1	272.3	85%	-1.67	-1.07	-0.06	-0.52	0.77	-0.08	0.75	0.02	1.04
			Asian Clam (*Corbicula fluminea*)	417.3	666.0	63%	-0.85	-0.58	0.13	-0.28	0.63	0.00	0.56	0.01	0.77
			Filamentous Algae (*Spyrogyra and Hydrodictyon*)	7.2	36.6	20%	-1.73	-1.15	-0.58	-0.58	0.08	-0.01	0.28	0.00	0.37
			Speckled Dace (*Rhinichthys osculus*)	375.4	428.7	88%	-1.34	-0.86	0.18	-0.41	0.90	-0.05	0.83	0.02	1.12
	Guinda	2014	Damselfly Larva (*Coenagrionidae)*	411.8	454.0	91%	-1.42	-0.90	0.36	-0.43	1.20	-0.08	1.03	0.02	1.42
			Mixed Dragonfly Larva (*Libellulidae and Gomphidae*)	379.4	395.1	96%	-1.51	-1.01	-0.15	-0.49	0.60	0.00	0.61	0.02	0.86
			Creeping Waterbug Larva (*Naucoridae*)	502.7	588.1	85%	-1.67	-1.10	0.08	-0.55	0.88	-0.03	0.91	0.00	1.16
			Asian Clam (*Corbicula fluminea*)	604.3	888.9	68%	-0.99	-0.69	-0.02	-0.34	0.52	0.04	0.50	0.01	0.69
			Filamentous Algae (*Spyrogyra and Hydrodictyon*)	83.2	139.2	60%	-1.33	-0.91	-0.02	-0.46	0.61	0.03	0.67	-0.01	0.84
			Mosquitofish (*Gambusia affinis*)	588.6	774.0	76%	-1.28	-0.82	0.76	-0.36	1.51	-0.07	1.37	0.05	1.71
			Red Swamp Crayfish (*Procambarus clarkia*)	396.4	409.6	97%	-1.35	-0.82	-0.04	-0.42	0.63	-0.12	0.58	0.00	0.84
	Capay	2013	Stonefly Larva (*Perlidae*)	102.8	104.8	98%	-1.56	-1.03	-0.28	-0.43	0.41	-0.02	0.49	0.09	0.67
			Net Spinning Caddisfly Larva (*Hydropsychidae*)	128.9	165.3	78%	-1.55	-1.10	-0.38	-0.53	0.26	0.10	0.45	0.02	0.54
			Damselfly Larva (*Coenagrionidae)*	220.3	191.4	100%	-1.84	-1.23	-0.54	-0.58	0.24	0.00	0.39	0.04	0.55
		2014	Burrowing Mayfly Larva (*Ephemeridae*)	85.0	151.2	56%	-1.50	-1.02	-0.55	-0.48	0.10	0.02	0.22	0.03	0.35
			Aquatic Worm (*Oligochaeta*)	79.7	222.5	36%	-1.31	-0.81	-0.53	-0.42	0.00	-0.10	0.08	-0.02	0.20
			Asian Clam (*Corbicula fluminea*)	365.2	490.5	74%	-0.28	-0.18	0.57	-0.08	0.95	-0.01	0.71	0.01	1.00
			Filamentous Algae (*Spyrogyra and Hydrodictyon*)	37.6	65.8	57%	-1.11	-0.77	0.14	-0.40	0.80	0.04	0.72	-0.02	1.00
			Mosquitofish (*Gambusia affinis*)	607.7	697.1	87%	-1.49	-0.96	0.02	-0.46	0.76	-0.06	0.74	0.02	1.00
			Red Swamp Crayfish (*Procambarus clarkia*)	294.9	363.8	81%	-1.20	-0.81	-0.08	-0.39	0.53	0.01	0.53	0.02	0.73
Yolo Bypass	Upper	2013	Damselfly Larva (*Coenagrionidae)*	127.5	205.1	62%	-0.41	-0.46	0.17	-0.35	0.72	0.28	0.52	-0.11	0.84
			Mixed Dragonfly Larva (*Libellulidae and Gomphidae*)	233.6	204.1	114%	-0.81	-0.48	0.30	-0.17	0.77	-0.09	0.66	0.07	0.89
			Red Swamp Crayfish (*Procambarus clarkia*)	188.7	162.6	116%	-0.93	-0.52	-0.16	-0.31	0.21	-0.15	0.23	-0.05	0.34
			Mosquitofish (*Gambusia affinis*)	630.3	565.9	111%	-0.54	-0.34	0.47	-0.17	0.87	-0.03	0.73	0.00	0.95
		2014	Damselfly Larva (*Coenagrionidae)*	71.1	74.7	95%	-0.66	-0.35	0.45	-0.18	0.71	-0.14	0.71	0.00	0.79
			Backswimmers (*Notonectidae*)	145.4	167.6	87%	-0.64	-0.39	0.51	-0.17	1.02	-0.06	0.80	0.02	1.11
			Fairy shirmp (*Linderiella occidentalis*)	147.9	165.8	89%	-0.13	-0.10	0.56	-0.03	0.80	0.02	0.64	0.02	0.83
			Mississippi Silversides (*Medinia beryllina*)	113.8	131.2	87%	-0.23	-0.11	1.40	-0.08	1.79	-0.07	1.48	-0.03	1.81
			Mosquitofish (*Gambusia affinis*)	116.7	125.2	93%	-0.13	-0.11	1.08	-0.03	1.47	0.04	1.16	0.02	1.50
			Red Swamp Crayfish (*Procambarus clarkia*)	60.3	67.2	90%	-0.41	-0.30	0.30	-0.12	0.58	0.04	0.53	0.03	0.66
	Permanent Wetland 2	2014	Damselfly Larva (*Coenagrionidae)*	143.6	260.9	55%	-0.46	-0.23	0.23	-0.11	0.45	-0.12	0.41	0.00	0.51
			Mixed Dragonfly Larva (*Libellulidae and Gomphidae*)	133.6	142.5	94%	0.46	0.30	0.89	0.17	1.03	0.01	0.67	0.02	0.95
			Dragonfly Larva (*Aeshnidae*)	189.2	205.6	92%	0.17	0.18	0.93	0.08	1.08	-0.10	0.80	-0.01	1.03
			Water Scavenger Beetle (*Hydrophilidae*)	426.1	523.9	81%	-0.77	-0.47	0.25	-0.22	0.65	-0.07	0.60	0.02	0.77
			Creeping Waterbug Larva (*Naucoridae*)	243.4	297.4	82%	0.15	0.16	0.64	0.10	0.80	-0.09	0.52	0.02	0.76
			Backswimmers (*Notonectidae*)	261.3	296.5	88%	-0.20	-0.14	0.60	-0.05	0.86	0.01	0.71	0.03	0.89
			Mosquitofish (*Gambusia affinis*)	232.7	246.9	94%	0.38	0.26	1.15	0.18	1.34	-0.01	0.96	0.05	1.28
			Mosquitofish (*Gambusia affinis*)	300.5	330.5	91%	0.36	0.23	1.02	0.12	1.11	0.02	0.85	0.01	1.05
	Lower	2013	Backswimmers (*Notonectidae*)	243.7	232.5	105%	-0.33	-0.20	0.48	-0.13	0.83	-0.02	0.63	-0.03	0.88
			Midge Larva (*Chironomidae*)	77.8	131.7	59%	-0.24	-0.13	-0.01	-0.04	0.20	-0.05	0.09	0.02	0.23
			Red Swamp Crayfish (*Procambarus clarkia*)	196.0	167.3	117%	-0.49	-0.34	0.05	-0.16	0.39	0.01	0.31	0.01	0.47
			Mosquitofish (*Gambusia affinis*)	587.4	573.2	102%	-0.26	-0.13	0.48	-0.05	0.73	-0.06	0.58	0.01	0.76

Table 5.S3: Total Hg concentration and Hg Isotope values for all SRMs

For SRMS's, N1 denotes the number of combustion replicates and N2 denotes the total number of isotope measurements during all analytical sessions. Theta denotes the standard deviation of the mean values for process replicates. For UM Almaden, N1 denotes the number of analytical sessions that UM-Almaden was measured and theta represents the SD of mean Hg isotope values for analytical sessions between January 2013 and December 2014 during which the run concentrations were either between 3 and 5 ng/g, or less than 3 ng/g.

Reference Material	N1	N2	THg (dry wt)	1SD	δ^{204}Hg	2σ	δ^{202}Hg	2σ	δ^{201}Hg	2σ	δ^{200}Hg	2σ	δ^{199}Hg	2σ	Δ^{204}Hg	2σ	Δ^{201}Hg	2σ	Δ^{200}Hg	2σ	Δ^{199}Hg	2σ
			ug.g	ug/g	‰	‰	‰	‰	‰	‰	‰	‰	‰	‰	‰	‰	‰	‰	‰	‰	‰	‰
NRC TORT-2	11	23	0.276	0.005	0.00	0.15	0.06	0.08	0.63	0.07	0.09	0.06	0.76	0.04	-0.08	0.06	0.59	0.03	0.06	0.05	0.75	0.04
NIST SRM 1944	6	14	3.51	0.30	-0.68	0.14	-0.45	0.08	-0.35	0.10	-0.21	0.09	-0.11	0.07	-0.01	0.08	-0.01	0.04	0.01	0.06	0.00	0.05
UM-Almaden (3-5 ppb)	100				-0.86	0.07	-0.57	0.05	-0.47	0.05	-0.28	0.04	-0.16	0.04	-0.01	0.06	-0.04	0.03	0.01	0.03	-0.02	0.03
UM-Almaden (<3 ppb)	24				-0.86	0.17	-0.55	0.11	-0.45	0.13	-0.26	0.09	-0.14	0.11	-0.04	0.12	-0.03	0.07	0.02	0.05	0.00	0.09

CHAPTER 6: Conclusions

Mercury (Hg) has been used for centuries in precious metal mining and more recently for industrial processes such as caustic soda production (i.e., the Hg-cell chloralkali process) and Li isotope separation (for thermonuclear weapons production). Inorganic Hg (IHg) has been discharged to aquatic environments during the mining of HgS ores and the use of metallic Hg.[1] Although Hg use has decreased in North America, historical releases of IHg persist in the environment ("legacy Hg"). In aquatic environments, a fraction of IHg can be converted to monomethyl mercury (MMHg) by methylating microbes in low oxygen zones (e.g., in sediment, periphyton or the water column).[2] MMHg bioaccumulates in the food web and the recent realization of its detrimental neurotoxic and developmental effects in humans and wildlife has increased interest in the distribution and biogeochemistry of legacy Hg sources.

It is difficult to differentiate between multiple Hg sources or trace their dispersal and bioaccumulation using total Hg (THg) and MMHg concentration measurements alone. Recent analytical advances have allowed for the measurement of Hg stable isotope ratios in a variety of environmental matrices (soils, sediment, fish, etc.). Natural variations in Hg stable isotope compositions can help differentiate Hg sources and shed new light on Hg transport and biogeochemical transformations in the environment.[3] Identifying and tracing legacy Hg sources is valuable to assist with the remediation of Hg contaminated

environments. Moreover, understanding the transformation of these legacy IHg sources to MMHg may help reduce future MMHg exposures to humans and wildlife.

Throughout this dissertation, variation in Hg stable isotope ratios are used to understand the distribution and transformation of legacy Hg sources. We measured Hg stable isotope ratios in sediment and biota to (1) characterize the isotopic composition of Hg sources from mining and industry, (2) assess the spatial and temporal distribution of these Hg sources and (3) elucidate MMHg formation, degradation and exposure pathways in streams and wetlands contaminated by legacy Hg sources. Below, I provide a brief overview of our key findings and then conclude by considering future directions for Hg isotope research in aquatic ecosystems contaminated by legacy Hg sources.

6.1 Review of Key Findings

6.1.1 Characterizing Legacy Hg Sources

Hg stable isotope ratios can be used to identify Hg sources in sediment, but only if the Hg source is isotopically distinct from uncontaminated sediment in the region. In Chapter 2, we measured the isotopic composition of Hg in sediment directly downstream of the Y12 National Security Facility (Y12) to characterize the isotopic composition of Hg released during its historical use. We found that highly contaminated sediment was isotopically distinct from uncontaminated sediment from a nearby reference stream that contained no Hg point sources. Enabled by this initial finding, we measured sediment along a longitudinal transect downstream of Y12 and were able to identify Y12 derived Hg far downstream (~40 km) of its origin. We further increased the scope of this study by measuring sediment from multiple tributaries of varying size that were nearby but not

downstream of Y12. In larger tributaries, the isotopic composition of sediment reflected the accumulation of background atmospheric and geogenic Hg in the watershed. In small tributaries near Y12, the sediment had anomalous low δ^{202}Hg that we hypothesized was from a local atmospheric Hg source in the region. By characterizing Hg released from Y12 that is stored in local sediment, this study provides a foundation for future Hg isotope research to understand the conversion of this legacy Hg source to MMHg.

6.1.2 Tracing the Spatial and Temporal Distribution of Hg Sources

Building on previous work in San Francisco Bay [4, 5], and utilizing Hg isotope techniques to identify anthropogenic Hg sources (Chapter 2)[6], we investigated the spatial and temporal distribution of Hg sources in SF Bay (Chapter 3).[7] Previously, Gehrke et al.[4] attributed spatial variation in the δ^{202}Hg of SF Bay sediment to different mining sources (Au and Hg mining) that were deposited in the Bay. However, pre-mining sediment was not characterized and the timing of Hg sources entering the Bay was not determined. We used ^{210}Pb dated sediment cores to address these remaining questions. We found that the isotopic composition of pre-mining sediment was consistent with low THg marine sediment measured elsewhere (e.g., [8, 9]). We also observed spatial variation in Hg isotopic compositions in historical (c.1960) sediment, which confirmed that Hg from two distinct mining sources (Hg and Au mining) were deposited in north and south SF Bay prior to 1960.

In Chapters 4 and 5, we moved upstream in the Sacramento River watershed to better characterize legacy Hg and Au mining sources surrounding SF Bay. In Chapter 4, we identified the isotopic composition of Au-mining contaminated sediment in the Yuba Fan,

an anthropogenic sediment deposit alongside the lower Yuba River. Yuba Fan sediment was distinct from pre-mining sediment, and we suggested this Hg source could be traced to downstream floodplains or lowland environments. In Chapter 5, we found highly variable δ^{202}Hg in Hg mining contaminated sediment in Cache Creek. This was consistent with heterogeneity reported in other streams containing Hg mine wastes,[10-12] and suggests it may be challenging to identify and trace distinct Hg sources in sediment downstream of Hg mines. Nonetheless, the Hg isotopic composition of sediment in Yolo Bypass wetlands was indistinguishable from Hg in the Yuba Fan, suggesting the deposition of Au mining derived Hg into Yolo Bypass. Overall, the results in Chapter 4 and 5 generally suggest that sediment Hg isotopic compositions are valuable to identify legacy Hg sources and trace their transport and deposition throughout Sacramento Valley (CA) watersheds.

6.1.3 MMHg Isotopic Composition in Aquatic Food Webs

In Chapters 4 and 5, we began to investigate MMHg formation, degradation and bioaccumulation in stream and wetland environments containing legacy Hg sources (Yuba River, Cache Creek, and Yolo Bypass). The isotopic composition of MMHg is valuable because it reflects the Hg source(s) and the sum of fractionation caused by biogeochemical processes (e.g., methylation and degradation) prior to MMHg entering the food web. Due to the low concentration of MMHg in many environmental matrices, it is difficult to obtain and isolate enough MMHg for direct high precision measurement of its isotopic composition (e.g. [13, 14]). Therefore, in Chapters 4 and 5, we build upon previous work by Tsui et al.[15] to estimate the isotopic composition of MMHg and IHg by analyzing a variety of different aquatic organisms with a range in %MMHg (the percent ratio of MMHg to THg).

In Chapters 4 and 5, we measured THg, MMHg and Hg isotope ratios in a wide range of aquatic organisms. The analysis of a diverse set of biota, particularly in Cache Creek and Yolo Bypass (Chapter 5), provided insight on MMHg sources and potential exposure pathways. There was significant variation in the Hg isotopic composition of organisms that could not be explained by the %MMHg alone. For example, in Cache Creek filamentous algae and clams had a wide range in δ^{202}Hg that we attributed to accumulation of IHg from sediment that is isotopically heterogeneous (δ^{202}Hg range of 1.5‰). In Yolo Bypass, high %MMHg biota had a 1.5‰ range in Δ^{199}Hg, from crayfish who forage near sediment (with low Δ^{199}Hg) to fish who forage at the water surface (with the highest Δ^{199}Hg). We hypothesized that there may be isotopically distinct pools of MMHg in these wetlands (e.g., highly photodegraded MMHg with higher Δ^{199}Hg in the water column).[16] This led to the suggestion that future studies which carefully consider the feeding behavior of different organisms might be able to distinguish between benthic and planktonic MMHg exposure pathways.

Overall we were able to estimate the isotopic composition of MMHg in every location studied in the Sacramento Valley. In the Yuba River (Ch. 4) and Cache Creek (Ch. 5), the pre-photodegraded MMHg (subtracting MDF and MIF from photochemical MMHg degradation) had consistently lower δ^{202}Hg than IHg in sediment (i.e., negative δ^{202}Hg offset). In contrast, in Yolo Bypass wetlands (Ch. 5) pre-photochemically degraded MMHg had higher δ^{202}Hg than IHg (i.e., positive δ^{202}Hg offset). In past studies of lakes, estuaries and the coastal ocean, consistent positive δ^{202}Hg offsets were attributed to net biotic MDF during methylation and degradation.[17-20] Thus, the negative δ^{202}Hg offset in the Yuba River and Cache Creek suggests that net MDF during biotic MMHg formation and degradation is

different than in any previously studied environment. In Chapter 4, we hypothesized that changes in the extent or the pathway of biotic MMHg degradation in the Yuba River could lead to net negative MDF between IHg and MMHg. In Chapter 5, with the additional results from Cache Creek and Yolo Bypass, we hypothesized that biotic MMHg degradation occurs to a lesser extent in streams than in standing water environments. Thus, the combined results of Chapters 4 and 5 suggest a fundamental difference in MMHg degradation in streams compared to wetlands, lakes or coastal ocean environments.

6.2 Future Directions

The results of this dissertation provide interesting avenues for future research to advance the application of Hg isotopes to trace Hg and MMHg. Specifically, additional experimental work to understand Hg isotope fractionation would aid in the comparison of sediment (IHg) and MMHg isotopic compositions (Chapters 4 and 5). For example, throughout this dissertation, we demonstrated that Hg isotope ratios in sediment could identify and trace different legacy Hg sources. However, only a small fraction of Hg in sediment (less than ~5%) is labile and undergoes methylation. The isotopic composition of labile Hg in sediment is unknown and the ability to isolate and measure Hg isotope ratios of this sediment fraction would be valuable. Additionally, estimating the δ^{202}Hg of pre-photodegraded MMHg and its comparison with IHg (Chapter 4 and 5) is reliant on relationships derived from a small number of photochemical MMHg degradation experiments (e.g., [21, 22]). It is not well understood how these experimental relationships may change in different ecosystems (i.e., freshwater, marine, estuarine, etc.) that have different physical conditions (standing vs. flowing water), MMHg concentrations, and types

of DOC or other binding ligands. Thus, future work to identify labile Hg in sediment and expand photochemical degradation studies (with conditions specific to different environments) would strengthen comparisons of IHg and MMHg and advance the interpretation of Hg isotope data in future food web studies.

Despite these caveats, the measurement of Hg stable isotopes in sediment and biota should continue to provide valuable insight on Hg sources and biogeochemistry in aquatic environments. Throughout this work, we demonstrated that Hg isotopes provide a conservative tracer of sediment bound Hg to downstream environments.[6, 7] We also measured Hg isotopes in a variety of different aquatic organisms, with a range of %MMHg, to obtain estimates for the isotopic composition of MMHg in food webs. In the process, we found evidence for multiple MMHg sources and suggested that future work could distinguish between MMHg exposure pathways.[16] By combining sediment and biota Hg isotope measurements, we demonstrated a fundamental difference in MDF between IHg and MMHg in streams (Yuba R. and Cache Cr.)[16, 23] when compared to wetlands (Yolo Bypass) and previously studied lakes,[18] coastal oceans[20] or estuaries.[17, 19] Therefore, future research that combines Hg isotopes in sediment and aquatic organisms, across a range of different environments (i.e., different Hg sources, physical and geochemical characteristics, etc.), should continue to enhance our understanding of Hg biogeochemistry and processes that lead to MMHg bioaccumulation in aquatic food webs.

References

1. Turner, R. R.; Southworth, G. R., Mercury-Contaminated Industrial and Mining Sites in North America: an Overview with Selected Case Studies. In *Mercury Contaminated Sites*, Ebinghaus, R.; Turner, R.; Lacerda, L.; Vasiliev, O.; Salomons, W., Eds. Springer Berlin Heidelberg: 1999; pp 89-112.

2. Hsu-Kim, H.; Kucharzyk, K. H.; Zhang, T.; Deshusses, M. A., Mechanisms Regulating Mercury Bioavailability for Methylating Microorganisms in the Aquatic Environment: A Critical Review. *Environ. Sci. Technol.* **2013,** *47*, (6), 2441-2456.

3. Blum, J. D., Applications of Stable Mercury Isotopes to Biogeochemistry. In Springer-Verlag Berlin Heidelberg: 2011; pp 229-245.

4. Gehrke, G. E.; Blum, J. D.; Marvin-DiPasquale, M., Sources of mercury to San Francisco Bay surface sediment as revealed by mercury stable isotopes. *Geochim. Cosmochim. Acta* **2011,** *75*, (3), 691-705.

5. Yee, D.; Bemis, B.; Hammond, D.; Heim, B.; Jaffe, B.; Rattonetti, A.; van Bergen, S. *Age Estimates and Pollutant Concentrations of Sediment Cores from San Francisco Bay and Wetlands*; Oakland, CA, 2011; pp 45 + Appendices A, B and C.

6. Donovan, P. M.; Blum, J. D.; Demers, J. D.; Gu, B.; Brooks, S. C.; Peryam, J., Identification of Multiple Mercury Sources to Stream Sediments near Oak Ridge, TN, USA. *Environ. Sci. Technol.* **2014,** *48*, (7), 3666-3674.

7. Donovan, P. M.; Blum, J. D.; Yee, D.; Gehrke, G. E.; Singer, M. B., An isotopic record of mercury in San Francisco Bay sediment. *Chem. Geol.* **2013,** *349-350*, (0), 87-98.

8. Mil-Homens, M.; Blum, J.; Canario, J. o.; Caetano, M.; Costa, A. M.; Lebreiro, S. M.; Trancoso, M.; Richter, T.; de Stigter, H.; Johnson, M.; Branco, V.; Cesario, R.; Mouro, F.; Mateus, M.; Boer, W.; Melo, Z., Tracing anthropogenic Hg and Pb input using stable Hg and Pb isotope ratios in sediments of the central Portuguese Margin. *Chem. Geol.* **2013,** *336*, (0), 62-71.

9. Gehrke, G. E.; Blum, J. D.; Meyers, P. A., The geochemical behavior and isotopic composition of Hg in a mid-Pleistocene western Mediterranean sapropel. *Geochim. Cosmochim. Acta* **2009,** *73*, (6), 1651-1665.

10. Wiederhold, J. G.; Smith, R. S.; Siebner, H.; Jew, A. D.; Brown, G. E.; Bourdon, B.; Kretzschmar, R., Mercury Isotope Signatures as Tracers for Hg Cycling at the New Idria Hg Mine. *Environ. Sci. Technol.* **2013,** *47*, (12), 6137-6145.

11. Smith, R. S.; Wiederhold, J. G.; Jew, A. D.; Brown Jr, G. E.; Bourdon, B.; Kretzschmar, R., Small-scale studies of roasted ore waste reveal extreme ranges of stable mercury isotope signatures. *Geochim. Cosmochim. Acta* **2014,** *137*, (0), 1-17.

12. Smith, R. S.; Wiederhold, J. G.; Jew, A. D.; Brown, G. E.; Bourdon, B.; Kretzschmar, R., Stable Hg Isotope Signatures in Creek Sediments Impacted by a Former Hg Mine. *Environ. Sci. Technol.* **2015,** *49*, (2), 767-776.

13. Masbou, J.; Point, D.; Sonke, J. E., Application of a selective extraction method for methylmercury compound specific stable isotope analysis (MeHg-CSIA) in biological materials. *J. Anal. At. Spectrom.* **2013,** *28*, (10), 1620-1628.

14. Epov, V. N.; Rodriguez-Gonzalez, P.; Sonke, J. E.; Tessier, E.; Amouroux, D.; Bourgoin, L. M.; Donard, O. F. X., Simultaneous determination of species-specific isotopic composition of Hg by gas chromatography coupled to multicollector ICPMS. *Anal. Chem.* **2008,** *80*, (10), 3530-3538.

15. Tsui, M. T. K.; Blum, J. D.; Kwon, S. Y.; Finlay, J. C.; Balogh, S. J.; Nollet, Y. H., Sources and Transfers of Methylmercury in Adjacent River and Forest Food Webs. *Environ. Sci. Technol.* **2012,** *46*, (20), 10957-10964.

16. Donovan, P. M.; Blum, J. D.; Singer, M. B.; Marvin-Di Pasquale, M.; Tsui, M. T. K., Comparison of mercury degradation and exposure pathways in streams and wetlands impacted by historical mining. **In Prep**.

17. Gehrke, G. E.; Blum, J. D.; Slotton, D. G.; Greenfield, B. K., Mercury Isotopes Link Mercury in San Francisco Bay Forage Fish to Surface Sediments. *Environ. Sci. Technol.* **2011,** *45*, (4), 1264-1270.

18. Sherman, L. S.; Blum, J. D., Mercury stable isotopes in sediments and largemouth bass from Florida lakes, USA. *Sci. Total Environ.* **2013,** *448*, (0), 163-175.

19. Kwon, S. Y.; Blum, J. D.; Chen, C. Y.; Meattey, D. E.; Mason, R. P., Mercury Isotope Study of Sources and Exposure Pathways of Methylmercury in Estuarine Food Webs in the Northeastern US. *Environ. Sci. Technol.* **2014,** *48*, (17), 10089-10097.

20. Balogh, S. J.; Tsui, M. T. K.; Blum, J. D.; Matsuyama, A.; Woerndle, G. E.; Yano, S.; Tada, A., Tracking the Fate of Mercury in the Fish and Bottom Sediments of Minamata Bay, Japan, Using Stable Mercury Isotopes. *Environ. Sci. Technol.* **2015**.

21. Bergquist, B. A.; Blum, J. D., Mass-dependent and -independent fractionation of Hg isotopes by photoreduction in aquatic systems. *Science* **2007,** *318*, (5849), 417-420.

22. Chandan, P.; Ghosh, S.; Bergquist, B. A., Mercury Isotope Fractionation during Aqueous Photoreduction of Monomethylmercury in the Presence of Dissolved Organic Matter. *Environ. Sci. Technol.* **2015,** *49*, (1), 259-267.

23. Donovan, P. M.; Blum, J. D.; Singer, M. B.; Marvin-Di Pasquale, M.; Tsui, M., Isotopic composition of inorganic mercury and methylmercury downstream of historical gold mining. **In Prep**.